AN EXAMINATION OF THE MECHANISMS OF NEOCORTICAL NETWORK EXCITABILITY IN A MOUSE MODEL OF FRAGILE X SYNDROME

APPROVED BY SUPERVISORY COMMITTEE

Kimberly Huber, Ph.D. (Supervisor)

Jay Gibson, Ph.D. (Supervisor)

Dean Smith, Ph.D.

Steve Cannon, M.D., Ph.D.

Ege Kavalali, Ph.D.

DEDICATION

First and foremost, I would like to thank my mentors, Dr. Jay Gibson and Dr. Kimberly Huber. Together they facilitated my growth as a scientist both technically and analytically, and they remained unfailingly kind and supportive throughout my training. I would also like to thank the members of my graduate committee for numerous helpful discussions and guidance throughout my training. Additionally, I would like to extend my thanks to all the members of the Huber lab, both past and current, for technical assistance and intellectual discussions. Because science is such a highly collaborative discipline, I would be remiss if I did not thank all of labs that provide reagents, animals, or advice that was critically important to the success of this project. Furthermore, I wish to graciously thank my parents, Alanson and Maria Hays, for immeasurable support of all kinds. Their contributions are far too great to quantify here, but their assistance was of utmost importance. I would also like to thank my sisters Sara Sliter-Hays and Amanda Hays who have always supported my pursuits. Finally, I would like to thank my lovely wife, Stephanie Hays. She contributed not only her unending support and love, but also intellectual input and patience to sit through my practice presentations.

AN EXAMINATION OF THE MECHANISMS OF NEOCORTICAL NETWORK EXCITABILITY IN A MOUSE MODEL OF FRAGILE X SYNDROME

by

SETH ALANSON HAYS

DISSERTATION

Presented to the Faculty of the Graduate School of Biomedical Sciences

The University of Texas Southwestern Medical Center at Dallas

In Partial Fulfillment of the Requirements

For the Degree of

DOCTOR OF PHILOSOPHY

The University of Texas Southwestern Medical Center at Dallas

Dallas, Texas

March, 2012

AN EXAMINATION OF THE MECHANISMS OF NEOCORTICAL NETWORK EXCITABILITY IN A MOUSE MODEL OF FRAGILE X SYNDROME

Seth Alanson Hays, Ph.D.

The University of Texas Southwestern Medical Center at Dallas, 2012

Kimberly Huber, Ph.D.

Jay Gibson, Ph.D.

Fragile X Syndrome (FXS) is the most common heritable form of mental retardation. FXS is caused by loss of function mutations in the product of the *Fmr1* gene, the Fragile X Mental Retardation Protein (FMRP). Many FXS patients display symptoms that are indicative of hyperexcitable circuitry, including epilepsy, bursting patterns in their EEG, and sensory hypersensitivity. Similarly, the mouse model of FXS, the *Fmr1* KO mouse, displays a propensity for audiogenic seizures and altered sensory processing, recapitulating many of the

symptoms observed in human patients. An imbalance in excitation to inhibition ratio is thought to underlie many autism spectrum disorders. The hyperexcitability in the *Fmr1* KO may reflect a shift in E/I balance. However, despite the evidence for hyperexcitability, no studies have previously examined basal circuit function in the *Fmr1* KO.

In this study, I report that neocortical networks are hyperexcitable in the *Fmr1* KO. This hyperexcitability is manifest as prolonged persistent activity states, or UP states. UP states are cyclic periods of depolarization that occur synchronously throughout local neocortical neurons. UP states arise from local recurrent connections and are regulated by intrinsic neuronal properties. As such, measurement of UP states provides insight into overall circuit properties.

Furthermore, I observe that the increase in UP state duration in the *Fmr1* KO is intrinsic to neocortical excitatory neurons. Deletion of FMRP in layer 4 or layers 5 and 6 fractionally increases UP state duration, suggesting that the hyperexcitability does not arise from one particular neuronal subtype, but rather all neurons partially contribute to the network hyperexcitation. Disruption of mGluR5 interactions with the scaffolding protein Homer, which results in consitituive mGluR5 signaling, is sufficient to prolong UP states. Futhermore, restoration of Homer-mGluR complexes in the *Fmr1* KO reduces UP state duration to wildtype levels. Pharmacological or genetic reduction of metabotropic glutamate receptor 5 (mGluR5) signaling reduces UP state duration

in the *Fmr1* KO to normal levels, suggesting a potential therapy for Fragile X patients. These data characterize the novel phenotype of hyperexcitable cortical circuitry in the *Fmr1* KO. In addition, this study provides support for an mGluR-Homer dependent mechanism underlying the network hyperexcitability that may be useful in developing additional treatments for FXS.

TABLE OF CONTENTS

PRIOR PUBLICATIONS xiii
LIST OF FIGURES xiv
LIST OF TABLES xvii
LIST OF APPENDICES xviii
LIST OF DEFINITIONS xix
CHAPTER ONE: Fragile X Mental Retardation Protein and the Regulation of Neocortical Network Function 1
Autism is a major neurological disease 1
Fragile X Syndrome, a prevalent genetic form of mental retardation 2
Cytological functions of FMRP 4
Neuronal deficits in the *Fmr1* KO 6
Synaptic changes 7
Intrinsic neuronal changes 10
Circuit level changes 16
Behavioral changes 21
The mGluR theory of Fragile X 25
A Homer theory of Fragile X? 31
Do network excitability changes underlie the pathology of autism? 33
Principles of network function 37
Dynamic network function: The slow oscillation 38
Synaptic and intrinsic properties contribute to network oscillations 43
Motivation for Studies and Summary of Research 46
CHAPTER TWO: Neocortical Rhythmic Activity States in *Fmr1* KO mice are Due to Enhanced mGluR5 Signaling and Involve Changes in Excitatory Circuitry 51
Summary 51

Introduction 52
Materials and Methods 54
Mice 54
Slice preparation 55
UP state recordings and analysis 56
Group I mGluR antagonist and protein synthesis inhibitor pretreatment 58
Recordings in vivo 59
Immunohistochemistry 60
Reagents 61
Results 62
Spontaneously occurring UP states are longer in layer 4 of Fmr1 KO slices 62
UP states are also prolonged in layer 5 64
Rhythmically occurring UP states are longer in Fmr1 KO mice, in vivo . 66
Changes in excitatory circuitry contribute to longer UP states 69
Longer UP states are due to deletion of Fmr1 in cortical excitatory neurons 71
Longer UP states are rescued by genetic reduction mGluR5 signaling ... 73
Longer UP states are rescued by pharmacological blockade of mGluR5 signaling 74
Longer UP states do not depend on recent protein translation 77
Group I mGluR activation increases UP state duration non-differentially 77
Discussion 78
Longer spontaneously occurring UP states in Fmr1 KO mice 79
Comparison with prolonged epileptic bursts in CA3 of Fmr1 KO mice ... 81
Role of group I mGluRs 82
What currents mediate the longer UP states? 83

Implications of longer UP states in Fmr1 KO mice 84
CHAPTER THREE: Disrupted Homer Scaffolds Mediate Abnormal mGluR5 Function in a Mouse Model of Fragile X Syndrome 99
Summary 99
Introduction 100
Materials and Methods 103
Animals 103
Reagents 104
Hippocampal Slice preparation and LTD recordings 104
mGluR signaling in slices and western blotting 105
Coimmunoprecipitation 107
Metabolic labeling of hippocampal slices 107
Neocortical Slice preparation and UP state recordings 108
Audiogenic seizures 110
Behavioral measurements 110
Results 111
Disruption of mGluR5-Homer regulates signaling to translation 111
Deletion of Homer1a rescues mGluR signaling in Fmr1−/y 114
H1a deletion rescues enhanced translation rates in Fmr1−/y 117
Altered LTD is not rescued by deletion of H1a 120
mGluR5-Homer and hyperexcitable neocortical circuits 123
H1a deletion reverses Fmr1−/y behavioral phenotypes 125
Discussion 126
Two mechanisms for mGluR dysfunction in FXS 126
Homer scaffolds coordinate mGluR regulation of translation 127
Altered mGluR5-Homer scaffolds increase translation rates 130
An essential role for FMRP in proper regulation of LTD 132
Altered mGluR5-Homer and neocortical network dysfunction 133

Altered behavior in Fmr1−/y mice is rescued by H1a deletion..... 135
Mechanism of disrupted Homer scaffolds in Fmr1−/y..... 137
CHAPTER FOUR: Further Examination of the Cellular Mechanisms and Relevance of Prolonged UP States in the *Fmr1* KO..... 158
Summary..... 158
Introduction..... 159
Materials and Methods..... 164
Mice..... 164
Slice preparation..... 164
Acute neuronal dissociation..... 166
UP state recordings and analysis..... 167
Intracellular electrophysiology..... 168
Immunohistochemistry..... 170
Audiogenic seizures..... 170
Results..... 171
All cortical layers partially contribute to prolonged UP state duration in the Fmr1 KO..... 171
Specific disruption of mGluR5-Homer interactions causes prolonged UP states..... 174
Reduction of Amyloid Precursor Protein is sufficient to reduce UP state duration..... 175
An examination of intrinsic currents in L5 pyramidal neurons in the Fmr1 KO..... 175
Presumptive mGluR-dependent depolarizing currents are unchanged in the *Fmr1* KO..... 176
H-current is unchanged in the *Fmr1* KO..... 177
Little or no functional Slack current is expressed in neocortical neurons..... 178

Somatic A-type potassium currents are unaltered in the *Fmr1* KO .. 178
Layer 5 pyramidal neurons may be more excitable in the Fmr1 KO 180
Excitatory neocortical deletion of FMRP does not cause audiogenic seizures 181
Discussion 181
Layer-specific contribution of FMRP to network excitability 182
Disrupted mGluR5-Homer interactions results in prolonged UP states 183
Reduction of APP rescues prolonged UP states in the Fmr1 KO 184
Multiple intrinsic currents are unchanged in the Fmr1 KO 186
Cortical neurons are intrinsically hyperexcitable in the Fmr1 KO 189
Audiogenic seizures are not driven by hyperexcitable neocortical circuits 191
CHAPTER FIVE: Concluding Remarks and Recommendations for Future Studies 205
Summary 205
Cortical networks are basally hyperexcitable in the *Fmr1* KO 206
Do synaptic changes underlie prolonged UP states? 209
Are alterations in intrinsic currents responsible for prolonged UP states? 212
Overactive mGluR5 mediates the network hyperexcitability in the *Fmr1* KO 217
Disruption of Homer-mGluR5 scaffolds underlies circuit hyperexcitability 220
Dysfunction of Homer-mGluR5 is the core deficit in network hyperexcitability 222
Conclusions 224

PRIOR PUBLICATIONS

Hays, S.A., Huber, K.M., Gibson, J.R. (2011) Altered neocortical rhythmic activity states in Fmr1 KO mice are due to enhanced mGluR5 signaling and involve changes in excitatory circuitry**.** J Neurosci. 31(40):14223-14234.

Ronesi, J.A., Collins, K.A., **Hays, S.A.**, Tsai, N.-P., Guo, W., Birnbaum, S.G., Hu, J.-H., Worley, P.F., Gibson, J.R., Huber, K.M. (2012) Disrupted mGluR5-Homer scaffolds mediate abnormal mGluR5 signaling, circuit function, and behavior in a mouse model of Fragile X syndrome**.** Nat Neuro. *Electronic publication ahead of print.*

Gibson, J.R., Bartley, A.F., **Hays, S.A.**, Huber, K.M. (2008) Imbalance of neocortical excitation and inhibition and altered UP states reflect network hyperexcitability in the mouse model of Fragile X syndrome. J Neurophysiol. 100:2615-2626.

LIST OF FIGURES

Figure 2.1 Spontaneously occurring persistent activity states, or UP states, are longer in layer 4 of *Fmr1* KO somatosensory cortical slices..... 87
Figure 2.2 Spontaneously occurring UP states are longer in layer 5 89
Figure 2.3 UP states are longer in the *Fmr1* KO *in vivo*..... 90
Figure 2.4 Pharmacologically isolated excitatory circuitry displays longer persistent activity bursts in the *Fmr1* KO..... 91
Figure 2.5 UP states are longer due to deletion of *Fmr1* in neocortical excitatory neurons..... 92
Figure 2.6 Genetic reduction of mGluR5 protein rescues UP state duration in the *Fmr1* KO..... 94
Figure 2.7 Pretreatment with an mGluR5 antagonist rescues UP state duration in *Fmr1* KO slices..... 95
Figure 2.8 MPEP wash-in does not affect UP state duration..... 96
Figure 2.9 Pretreatment with a protein translation inhibitor has no effect on WT and *Fmr1* KO UP state duration 97
Figure 2.10 A group 1 mGluR agonist lengthens UP state duration in both WT and KO slices..... 98
Figure 3.1 Peptide-mediated disruption of mGluR5-Homer scaffolds in WT mouse hippocampus bidirectionally regulates group 1 mGluR signaling to translation initiation and elongation..... 139
Figure 3.2 mGluR5-Homer scaffolds and group 1 mGluR signaling are altered in *Fmr1*-/y mice and rescued by genetic deletion of H1a 141
Figure 3.3 Altered mGluR5-Homer scaffolds in *Fmr1*-/y mediate enhanced basal translation rates and initiation complex formation 143

Figure 3.4 Genetic deletion of Homer1a does not reverse the protein synthesis independence of mGluR-induced LTD or altered protein levels of FMRP target mRNAs 145
Figure 3.5 Disruption of mGluR5-Homer interactions mediates prolonged neocortical UP states in *Fmr1*-/y mice..... 147
Figure 3.6 H1a deletion reduces audiogenic seizures and corrects open field activity in the *Fmr1*-/y mouse..... 149
Supplementary Figure 3.1 Disruption of mGluR5-Homer scaffolds in rat hippocampal slices bidirectionally regulates mGluR signaling to translation initiation and elongation and blocks synthesis of Arc 150
Supplementary Figure 3.2 H1a-mGluR5 interactions are elevated in *Fmr1* KO mice, but total levels of H1a, long Homers, or mGluR5 are unchanged 152
Supplementary Figure 3.3 Effects of the PI3K inhibitor, wortmannin, on protein synthesis rates in WT and *Fmr1* KO hippocampal slices..... 154
Supplementary Figure 3.4 Inhibition of ERK activation in hippocampal slices reduces of abolishes phosphospecific antibody detection of P-ERK, P(S209) eIF4E, and P(65) 4EBP..... 155
Supplementary Figure 3.5 *Fmr1*, H1a, or H1a/*Fmr1* KO do not affect locomotor activity and therefore do not underlie the rescue of open field activity..... 156
Figure 4.1 Deletion of FMRP in layer 4 causes partially prolonged UP states . 192
Figure 4.2 Restoration of FMRP expression in layer 4 at least partially rescues UP state duration..... 193
Figure 4.3 Deletion of FMRP from layers 5 and 6 causes partially prolonged UP states 194
Figure 4.4 Specific disruption of mGluR5-Homer interactions causes prolonged UP states..... 195
Figure 4.5 Presumptive mGluR-dependent depolarizing currents are unchanged in *Fmr1* KO neurons 196

Figure 4.6 Genetic reduction of APP rescues UP state duration in the *Fmr1* KO…… 197
Figure 4.7 Hyperpolarization-activated current is unchanged in layer 5 neurons in the *Fmr1* KO 198
Figure 4.8 Little or no functional sodium-activated potassium current is expressed in layer 5 pyramidal neurons 199
Figure 4.9 A-type and delayed rectifier K+ currents are unchanged in the *Fmr1* KO 200
Figure 4.10 Treatment with 4-AP eliminates the difference in UP state duration between WT and *Fmr1* KO slices 201
Figure 4.11 Layer 5 pyramidal neurons may be intrinsically hyperexcitable in the *Fmr1* KO 202

LIST OF TABLES

Table 3.1 Seizure occurrence and severity in WT, *Fmr1* KO, H1a KO, and H1a/*Fmr1* KO genotypes 157

Table 4.1 Audiogenic seizure incidence and severity in Flox *Fmr1* x *Dlx* Cre mice…. 203

Table 4.2 Audiogenic seizure incidence and severity in Flox *Fmr1* x *Emx1* Cre mice…. 204

LIST OF APPENDICES

Appendix 1 Pharmacological block of fast glutamateric transmission prevents UP states…..... 225

LIST OF DEFINITIONS

4EBP – eIF4E binding protein

5’ TOP – 5’ terminal oligopyrimidine tract

ACSF – artificial cerebrospinal fluid

AGS – audiogenic seizures

AHP – after-hyperpolarization

AMPA – (2-amino-3-(5-methyl-3-oxo-1,2-oxazol-4-yl)propanoic acid)

ANOVA – analysis of variance

APP – Amyloid Precursor Protein

Arc – activity-regulated cytoskeletal protein

ASD – autism spectrum disorder

CamKIIα – calcium/Calmodulin-dependent kinase II alpha

CGG – cytosine guanine guanine

CGP55845 – (2S)-3-(1S)-1-(3,4-Dichlorophenyl)ethylamino-2 hydroxypropyl)(phenylmethyl)phosphinic acid

CNQX – (6-cyano-7-nitroquinoxaline-2,3-dione)

CpG – cytosine prior to guanine

DHPG – (RS)-3,5-dihydroxyphenylglycine

Dlx – Distal-less

DSM-IV – Diagnostic and Statistical Manual of Mental Disorders, 4th edition

DTX – dendrotoxin

E/I – excitation/inhibition ratio

eEF1A – eukaryotic elongation factor 1a

EEG - electroencephalogram

EF2K – elongation factor 2 kinase

eIF4F – eukaryotic initiation factor 4 F

Emx1 – Empty spiracles homeobox 1

ERK – extracellular-signal regulated kinase

EVH1 – Ena-VASP homology domain 1

Flox – flanked by loxP

Fmr1 – Fragile X mental retardation gene

FMRP – Fragile X mental retardation protein

FP – field potential

FS – fast-spiking

FXS – Fragile X Syndrome

GABA – gamma-aminobutyric acid

Gp1 – group 1

GRM5 – mGluR5 gene

H1a – Homer1a

Hz - hertz

I_{KNa} – sodium-dependent potassium current

I_{NaP} – persistent sodium current

IQ – intelligence quotient

KH – K homology domain

KO – knock out

L2/3 – cortical layer 2/3

L4 – cortical layer 4

L5 – cortical layer 5

LTD – long-term depression

LTP – long-term potentiation

LY367385 – (S)-(+)-α-amino-4-carboxy-2-methylbenzeneacetic acid

MeCP2 – methyl CpG binding protein 2

mEPP – miniature endplate potential

mEPSC – miniature excitatory postsynaptic current

mGluR – metabotropic glutamate receptor

mIPSC – miniature inhibitory postsynaptic current

Mnk – MAPK-interacting kinase

MNTB – medial nucleus of the trapezoid body

MPEP – 2-methyl-6-(phenylethynyl)pyridine

mPFC – medial prefrontal cortex

mRNA – messenger ribonucleic acid

mTOR – mammalian target of rapamycin

MTX – Margatoxin

NMDA – *N*-methyl-D-aspartate

p – postnatal day

PI3K – phosphoinositide 3-kinase

PIKE – phosphoinositide-3 kinase enhancer

PPI – paired pulse inhibition

PSD – postsynaptic density

RGG – arginine/glycine rich

RMS – root mean square

S6K – p70 S6 kinase

SatB2 – Special AT-rich sequence-binding protein 2

SHANK – SH3 and multiple ankyrin repeat domains protein

sIPSC – spontaneous inhibitory postsynaptic current

Six3 – Sine oculis homeobox homolog 3

SK – small potassium channel

Slack – sequence like a calcium-activated potassium channel

STDP – spike-timing dependent plasticity

TEA – tetraethylammonium

TRP – transient receptor potential

TTX – tetrodotoxin

WT – wild-type

ZD7288 – 4-Ethylphenylamino-1,2-dimethyl-6-methylaminopyrimidinium chloride

CHAPTER ONE
Introduction

FRAGILE X MENTAL RETARDATION PROTEIN AND THE REGULATION OF NEOCORTICAL NETWORK FUNCTION

Autism is a major neurological disease

Autism is one of the most widespread neurological disorders in the United States, affecting roughly one in one hundred and ten individuals (Baird, Simonoff et al. 2006; Caronna, Milunsky et al. 2008). In addition to the inestimable emotional toll on families, the disease has a massive social impact in the United States, with an approximate cost of $35 billion per year (Ganz 2007). Despite the insights made into the etiology of the disease, autism is still largely diagnosed based on behavioral criteria. Autism spectrum disorder (ASD), as defined by the DSM-IV criteria, is diagnosed by alterations in social interaction, impairments in communication, and stereotyped behavior. Although ASD is qualitatively grouped into one disease, the disorders likely represent a variety of different pathogenic mechanisms. Indeed, many genes have been implicated as risk factors for ASD, suggestive of multiple disease mechanisms (reviewed in (Klauck 2006; Newschaffer, Croen et al. 2007)). Considering the heterogeneity amongst ASDs, identification of a unifying causative feature underlying the disease would be valuable for developing targeted treatments.

Fragile X Syndrome, a prevalent genetic form of mental retardation

One well-defined single gene disease linked to ASD is Fragile X syndrome (FXS). FXS is the single most common form of inherited mental retardation and affects approximately 1:4000 males and 1:8000 females (Bassell and Warren 2008; Garber, Visootsak et al. 2008). This accounts for between one and two percent of all autism diagnoses (Hagerman, Hoem et al. 2010). Although the severity varies, between thirty and fifty percent of FXS patients are also diagnosed with autism (Hagerman, Jackson et al. 1986; Kaufmann, Cortell et al. 2004; Hagerman, Ono et al. 2005). The core deficit observed in patients with FXS is mental retardation, with patient IQs typically ranging from forty to seventy (Merenstein, Sobesky et al. 1996). Additionally, many patients display hypersensitivity to sensory stimuli, particularly tactile and auditory inputs (Miller, McIntosh et al. 1999; Hagerman and Hagerman 2002). FXS is also often comorbid with epilepsy, as up to fifteen percent of FXS patients display seizures (Berry-Kravis 2002; Berry-Kravis, Raspa et al. 2010). An even greater proportion of patients, as many as seventy percent, display abnormal centrotemporal spiking patterns in their EEGs (Sabaratnam, Vroegop et al. 2001; Berry-Kravis 2002). Another hallmark of FXS is the presence of long, thin neuronal spines in several brain regions (Irwin, Patel et al. 2001). This morphology is consistent with immature or underdeveloped spines. In addition to these neurological defects, FXS patients typically display peripheral tissue dysfunction in the form of

prolonged faces, macroorchidsm, and hyperextensible joints (Hagerman and Hagerman 2002).

FXS is caused by the loss of function of the gene product of the *Fmr1* gene, the Fragile X mental retardation protein (FMRP) (Pieretti, Zhang et al. 1991). In the vast majority of cases, silencing of the *Fmr1* gene is caused by the expansion of a CGG repeat (O'Donnell and Warren 2002). In normal individuals, CGG repeat number is between six and sixty. Premutation carriers have between sixty and two hundred copies of the repeat, but FMRP expression is normal. Because this trinoclueotide repeat region is unstable during meosis, premutation carriers may pass expanded repeat region copies to their offspring. The disease manifests when the CGG copy number exceeds two hundred (O'Donnell and Warren 2002). Upon expansion beyond the critical limit, the gene undergoes hypermethylation of CpG island in the 5'-untranslated region, resulting in repression of transcription and thereby absence of FMRP protein (Sutcliffe, Nelson et al. 1992). In rare cases, point mutations within the gene, such as a substitution of isoleucine for asparagine at position 367, can result in severe cases of the disease (De Boulle 1993).

A mouse model of FXS has been developed in order to facilitate study of the disease (Bakker, Verheij et al. 1994). In this model, a neomycin cassette is inserted into exon 5 of the *Fmr1* gene, resulting in absence of FMRP expression. Although the mechanism of FMRP suppression is different, the mouse model

lacks FMRP expression similar to most human patients. In addition, the model recapitulates various important aspects of the disease, including sensory hypersensitivity and thin, immature dendritic spines. These and other phenotypes observed in the mouse model are described in detail below.

Cytological functions of FMRP

FMRP primarily functions as an RNA binding protein (Siomi, Choi et al. 1994; Brown, Jin et al. 2001). It binds to a variety of mRNA molecules, with up to as many as 800 mRNAs as binding partners (Brown, Jin et al. 2001). This accounts for nearly four percent of mRNA transcripts in the mammalian brain, highlighting how alterations in FMRP function could have major consequences (Bassell and Warren 2008). In fact, it is this regulation of so many other gene products that could explain why FXS is one of only a few single gene mental retardation disorders. Whereas other mental retardation disorders may arise from small changes in a number of risk factor genes, the FMRP loss in FXS may indirectly impact enough other genes to cause retardation. FMRP interacts with its partners through various RNA binding motifs (Siomi, Choi et al. 1994; Darnell, Jensen et al. 2001). FMRP contains two tandem KH domains referred to as KH1 and KH2, as well as an RGG domain, all of which are known to bind mRNA. A loop structure known as the "kissing complex" in the target mRNA appears to be the motif necessary for interaction with the KH2 domain (Darnell,

Fraser et al. 2005). The I304N mutation, the point mutation mentioned above that results in a very severe form of FXS, disrupts the KH2 binding domain, highlighting the importance of the interaction of FMRP with its target mRNAs (Siomi, Choi et al. 1994). The RGG box strongly associates with mRNA binding partners through a tertiary structure in the mRNA known as a G-quartet (Darnell, Jensen et al. 2001). The G-quartet is a common motif, with as many as 350,000 predicted occurrences in the human genome (Todd, Johnston et al. 2005). Considering the large number of transcripts that may contain G-quartet sequences and the proportionately small number of transcripts that bind FMRP, there is likely and additional mechanism by which FMRP recognizes and binds the appropriate mRNA targets. Despite its function in binding mRNA, the RGG domain is not necessary for some of FMRP's major functions, such as the regulation of synapse number (Pfeiffer and Huber 2007).

Given its association with mRNA, FMRP occupies a critical position for regulation of its target mRNAs. Indeed, many lines of evidence show a role for FMRP in regulation of protein translation (Bassell and Warren 2008). Because of its dendritic localization and the alterations in spines in the *Fmr1* KO, FMRP has been implicated as a regulator of local protein translation at the synapse. Many of the mRNAs that have been shown to bind to FMRP are synaptic proteins including Arc, CamKIIα, and eEF1A, suggestive of FMRP's function in regulation of synaptic properties (Bassell and Warren 2008).

FMRP can repress translation of mRNA *in vitro* (Li, Zhang et al. 2001). Additionally, several proteins are known to be translated at exaggerated levels in the *Fmr1* KO (Zalfa, Giorgi et al. 2003). FMRP can also reversibly stall polyribosomes, preventing the translation of the associated mRNAs (Darnell, Van Driesche et al. 2011). FMRP is typically thought to act as a translational suppressor; however, some studies have shown that phosphorylation state of FMRP may determine its translational regulation. Dephosphorylated FMRP is triggers translation of target mRNAs, while phosphorylated FMRP suppresses translation (Ceman, O'Donnell et al. 2003). In addition to translation, FMRP is thought to have a role in transport of its mRNA targets to the synapse. Disruption of the ability of FMRP to be transported to the synapse results in altered spine morphology, similar to what is seen with the absence of FMRP (Dictenberg, Swanger et al. 2008).

Neuronal deficits in the *Fmr1* KO

FMRP has a wide range of important functions within the cell. Its regulation of key synaptic proteins puts it in a place to exert a strong effect on neuronal function, and in doing so, ultimately affect behavior. Changes resulting from the loss of FMRP ranging from a synaptic level up to the level of a behaving animal are described below.

Synaptic changes

The absence of gross anatomical changes in the brains of FXS patients suggests that alterations in brain function likely arise from another source (O'Donnell and Warren 2002). Along with changes in intrinsic properties of the neurons, disrupted synaptic function is a likely candidate. FMRP is localized to the synapse and is known to control translation of several synaptic proteins. As such, it is poised to robustly impact the function of synapses. Indeed, FMRP does affect synaptic function in a variety of ways.

One of the major phenotypes observed in both FXS patients and the *Fmr1* KO mouse is the appearance of long, immature spines. Spine morphology abnormalities are a phenomenon observed generally across several types of mental retardation and autism (Marin-Padilla 1972; Kaufmann and Moser 2000). The prevalence of this phenotype even within the *Fmr1* KO varies widely both temporally with development and spatially across brain regions (Comery, Harris et al. 1997; Grossman, Elisseou et al. 2006; Grossman, Aldridge et al. 2010; Levenga, de Vrij et al. 2011). This disparity is not altogether surprising, as it may stem from differences in levels of activity and response to activity both in different brain regions and at different developmental stages. Generally, studies report a greater proportion of thin spines or filopodia, as well as a higher density of spines in the *Fmr1* KO (Comery, Harris et al. 1997; Dölen, Osterweil et al. 2007). Spines are not static structures, but rather exhibit dynamic growth,

maturation, and turnover. The transient nature of the spine phenotype observed in the *Fmr1* KO may be caused by alterations in spine turnover and stability, rather than a baseline increase in number of spines. In support of this, spines on neocortical neurons in the *Fmr1* KO mouse exhibit a higher rate of turnover and more transient protrusions than wildtype (WT) counterparts (Cruz-Martín, Crespo et al. 2010; Pan, Aldridge et al. 2010). This high rate of turnover may prevent the appropriate maturation of spines, leading to the overabundance of immature filopodia observed in the *Fmr1* KO.

Indeed, FMRP has been shown to be directly involved in the pruning, or elimination of spines. Pruning is a necessary step in the activity-dependent conversion of rough map of synaptic connections to a refined system that reinforces the maintained synapses (Segal and Andersen 2000; Tessier and Broadie 2009). As such, FMRP can directly impact information processing by regulating which synaptic contacts are spared and which are pruned. Consistent with the increase in protrusions, *Fmr1* KO neurons in the hippocampus have a higher miniature excitatory postsynaptic current (mEPSC) frequency (Pfeiffer and Huber 2007). This is accompanied by a decrease in synaptic failures in response to minimal stimulation. Together, these data suggest that *Fmr1* KO neurons have an increased number of synaptic contacts. The increase in synaptic contacts can be rescued with the reintroduction of FMRP, suggesting that FMRP is actively involved in pruning synapses. FMRP's effect on synapse elimination relies on the

KH2 domain, suggesting that the mRNA binding function of FMRP is necessary for pruning (Pfeiffer and Huber 2007; Pfeiffer, Zang et al. 2010).

Beyond affecting the number of and maturational state of spines, FMRP exerts control over synaptic function. In layer 4 (L4) of somatosensory cortex, the average EPSC amplitude evoked in fast-spiking (FS) inhibitory neurons when stimulated by a synaptically coupled spiny stellate excitatory neuron is decreased in the *Fmr1* KO (Gibson, Bartley et al. 2008). This phenotype is present at young ages (postnatal day 14 (p14)), and persists at later times (p28), possibly suggesting a permanent deficit. Changes in synaptic strength are not present at FS to spiny stellate connections nor at spiny stellate to spiny stellate connections. This finding may not be surprising, however, considering that each type of synaptic connection likely undergoes different activity-dependent development.

FMRP also plays a critical role in maintaining inhibitory tone in the basolateral amygdala (BLA). In the *Fmr1* KO, principle cells in the BLA receive smaller amplitude spontaneous inhibitory postsynaptic currents (sIPSC) and miniature inhibitory postsynaptic currents (mIPSC), suggesting reduced inhibitory synaptic strength (Olmos-Serrano, Paluszkiewicz et al. 2010). These changes in synaptic strength correlate with some mRNAs that are known to be FMRP targets, including neuroligin-2, an autism-linked protein implicated in synaptic strength, and GABA receptor subunits (Gibson, Huber et al. 2009; Darnell, Van Driesche et al. 2011).

In addition to basal changes in synaptic function, *Fmr1* KO mice exhibit aberrant synaptic plasticity. Long-term depression (LTD), a form of synaptic plasticity driven by synaptic activity, is altered in the *Fmr1* KO. One mechanism of LTD is known to be reliant on synthesis of new proteins at the synapse (Huber, Kayser et al. 2000). This form of LTD, driven by stimulation of group 1 (Gp1) metabotropic glutamate receptors (mGluRs), is enhanced in the *Fmr1* KO (Huber, Gallagher et al. 2002). Furthermore, unlike in WT animals, LTD in the *Fmr1* KO is independent of protein synthesis (Nosyreva and Huber 2006). This corroborates the role of FMRP as a repressor of translation. In contrast to the observed enhancement in LTD, impairments in long-term potentiation (LTP) have been reported in the *Fmr1* KO. This effect of LTP depends on brain area and animal age (Larson, Jessen et al. 2005; Desai, Casimiro et al. 2006). Because plasticity is associated with memory, impairment in the *Fmr1* KO consequently provides a candidate mechanism for altered cognition in FXS.

Intrinsic neuronal changes

In addition to synaptic dysfunction, the changes in intrinsic neuronal properties in the *Fmr1* KO are beginning to be understood. Along with synaptic function, intrinsic excitability changes can also profoundly affect information processing. Alterations in neuronal excitability regulate integration of synaptic

inputs. These properties not only affect the individual neuron, but can have far reaching consequences on the response of the neuronal network.

Although few studies have examined general intrinsic excitability in the *Fmr1* KO, there is some evidence that FMRP does indeed affect intrinsic properties. Input resistance is a neuronal property that represents the sum of open channels, or leakiness, of a cell. Increased input resistance is typically predictive of increased excitability. In L4 spiny stellate cells, input resistance is increased in the *Fmr1* KO compared to WT littermates (Gibson, Bartley et al. 2008). Accompanying this change is an increase in the spiking frequency of KO neurons for a given current injection. Both of these measures suggest an increase in excitability in *Fmr1* KO neurons. Similarly, principal cells in the BLA of the *Fmr1* KO fire more action potentials in response to depolarizing current steps than WT counterparts (Olmos-Serrano, Paluszkiewicz et al. 2010). As mentioned before, these changes could have profound consequences on cognitive processing.

However, other studies have reported no difference in intrinsic properties with the absence of FMRP. In young animals (p10-18), pyramidal neurons in L5 of neocortex do not show any change in input resistance in the *Fmr1* KO (Desai, Casimiro et al. 2006). Additionally, there is no increase in excitability in KO neurons as measured by the propensity to spike in response to current injection (Desai, Casimiro et al. 2006). This could potentially be due to developmental regulation of excitability by FMRP. In a mosaic model of FXS, there is no

significant difference in the input resistance in hippocampal neurons that express FMRP compared to those that do not express FMRP (Hanson and Madison 2007). However, it is important to note that in the mosaic model, WT and KO cells would receive theoretically equivalent synaptic input. If changes in input resistance are not cell autonomous and therefore depend on synaptic input, any alterations in input resistance would not be detected. Also, it is possible that input resistance in hippocampal neurons is not dependent on FMRP.

In addition to general properties of neuronal excitability, recent work has focused on identifying the target proteins that may lead to altered intrinsic properties. Some of the mRNAs bound by FMRP provide intriguing possibilities for how FMRP may regulate intrinsic neuronal properties.

The transcript encoding the voltage-gated potassium channel Kv3.1 is bound by FMRP (Darnell, Jensen et al. 2001). The mRNA for Kv3.1 contains the G-quartet sequence known to be involved in mRNA interaction with FMRP (Strumbos, Brown et al. 2010). Kv3.1 channels produce a rapid repolarizing potassium current that allows cells to maintain spike fidelity at high frequencies. One area of high expression of this channel is the medial nucleus of the trapezoid body (MNTB), an area in the brainstem that receives auditory information (Kaczmarek, Bhattacharjee et al. 2005). Neurons in this structure are tonotopically arranged, and Kv3.1 expression follows a similar gradient. Those neurons that respond to high frequency tones express more Kv3.1 than those that

respond to low frequencies in order to facilitate phase locking to high firing frequencies. In the *Fmr1* KO, gradient Kv3.1 expression is abolished, and Kv3.1 is expressed uniformly across the MNTB, presumably due to loss of FMRP mediated translational control of the transcript (Strumbos, Brown et al. 2010). Correspondingly, the functional gradient of Kv3.1 current is flattened in the *Fmr1* KO. In addition, activity-dependent expression of Kv3.1 is absent, consistent with translational regulation of the Kv3.1 transcript by FMRP. This data shows that loss of FMRP can alter neuronal properties by a changing the expression of one of its target mRNAs. Without proper gradient expression of Kv3.1, it is possible that auditory signal processing would be disrupted. Although not tested directly, these changes in the auditory circuit may be in part responsible for audiogenic seizures that occur in the *Fmr1* KO. Similar to the changes observed in input resistance, a reduction in Kv3.1 current could result in neuronal hyperexcitability.

FMRP also interacts with the mRNA for another voltage-gated potassium channel, Kv4.2. Kv4.2 is encoded by the *KCND2* gene. Functionally, Kv4.2 is the major component of A-type potassium current, a transient, subthreshold current that serves to oppose depolarization (Hoffman 1997; Norris and Nerbonne 2010; Guan, Horton et al. 2011). Kv4.2 regulates dendritic excitability, and like many other FMRP targets, is itself regulated by activity (Tsaur, Sheng et al. 1992). Despite the clear link to FMRP, regulation of Kv4.2 in the *Fmr1* KO

remains contested. One study reports increases in Kv4.2 expression, while a study from a different group reports reduction in Kv4.2 expression (Gross, Yao et al. 2011; Lee, Ge et al. 2011). Both reports used similar brain areas for analysis and similar developmental time points, making it difficult to reconcile the contradictory results. An increase in Kv4.2 expression seems likely, since FMRP is traditionally viewed as a repressor of translation and many proteins are expressed at higher levels in the *Fmr1* KO. Functionally, however, a decrease in Kv4.2 expression is more probable. Seizures and epilepsy are common in the *Fmr1* KO, and they also result from mutations that cause loss of Kv4.2 function and pharmacological block of Kv4.2 (Birnbaum, Varga et al. 2004). On a smaller scale, the hyperexcitability observed in *Fmr1* KO neurons is consistent with a reduction of Kv4.2. Whatever the case, FMRP appears to exert a regulatory function over Kv4.2 expression in some capacity. A-type current reduces dendritic excitability and back propagation of action potentials, thus making it highly important in synaptic integration (Hoffman 1997; Migliore, Hoffman et al. 1999). It is clear that any alterations, whether an increase or decrease, in A-type current could greatly impact neuronal function and thereby cognitive processes.

A third potassium channel has been implicated in FXS, but with a mechanism distinct from Kv3.1 and Kv4.2 (Brown, Kronengold et al. 2010). The sodium-activated potassium channel termed Slack is the gene product of *Slo2.2*. As with other potassium currents, Slack channels serve to oppose inward currents

and thus reduce excitability. One defining characteristic of Slack channels is dependence on intracellular sodium concentration, such that increasing internal sodium will increase Slack open probability (Yang, Desai et al. 2007). Action potentials result in large increases in intracellular sodium, which in turn activates Slack current. As is the case with Kv3.1, Slack is highly expressed in auditory circuits where it is thought to facilitate phase locking of action potentials in high frequency responding neurons (Yang, Desai et al. 2007). Similar to many other proteins, Slack expression levels are modestly increased in the *Fmr1* KO (Brown, Kronengold et al. 2010). Paradoxically, functional Slack current is substantially reduced in MNTB neurons in the *Fmr1* KO. Interestingly, this is reconciled by the finding that FMRP directly interacts with Slack channels to alter channel gating and increase conductance. In excised membrane patches containing Slack, introduction of FMRP to the cytoplasmic face increases the open probability of the channel and nearly eliminates subconductance states (Brown, Kronengold et al. 2010). Direct interaction with channels to alter conductance introduces a radically new role for FMRP in regulation of membrane properties. Although the mechanism is markedly different, this alteration in potassium conductance in neurons of the *Fmr1* KO could strongly affect spike timing and excitability.

While the majority of findings in the *Fmr1* KO are restricted to changes potassium currents, it is very likely that depolarizing currents could be affected as

well. Because expression of most proteins is increased with loss of FMRP, one logical consequence would be the increase in expression of a channel that increases excitability, such as a transient receptor potential (TRP) channel. In addition, considering the link to enhanced mGluR signaling the *Fmr1* KO (described in detail below) and the effect of Gq-signaling on intrinsic depolarizing currents, it is likely that some of these depolarizing currents are enhanced in the *Fmr1* KO (Yoshida, Fransén et al. 2008; Zhang and Seguela 2010). Regardless of the mechanism, alterations in intrinsic currents could have significant effects on circuit function and behavior in the *Fmr1* KO.

Circuit level changes

Although the data is sparse compared to more highly studied functions of FMRP, there is some evidence suggestive of changes in circuit properties in the *Fmr1* KO.

One major feature of network changes in the *Fmr1* KO is disrupted neuronal connectivity. Accompanying the changes in synaptic strength described above are deviations in the number of functional synaptic contacts. This phenomenon has been described in a number of brain regions, suggesting that it may be an overarching consequence of the absence of FMRP. In L4 of the somatosensory cortex, connection probability between FS inhibitory neurons and excitatory spiny stellate neurons is dramatically decreased in the *Fmr1* KO

(Gibson, Bartley et al. 2008). This study also reports a trend towards a decrease in synaptic connection between neighboring excitatory neurons. In addition to reduced within-layer connectivity, *Fmr1* KO mice display a deficit in between layer connections. Photostimulation experiments reveal a decreased response in L4 neurons upon stimulation of L3 neurons from the same barrel column (Bureau, Shepherd et al. 2008). Single connection strength of L3 to L4 projections is unchanged, suggesting that a reduced number of connections is driving alterations in the *Fmr1* KO. In contrast to the reduced connections, medium-range connections may be increased in the *Fmr1* KO. One study shows L5 pyramidal cells with intersomatic distances of 25 to 100 microns in the medial prefrontal cortex of the KO are hyperconnected, suggesting that connectivity changes may have impact beyond immediate local circuitry (Testa-Silva, Loebel et al. 2011). In all three instances, the authors report that the connection deficits are developmentally transient although the synaptic strength changes persist. At older ages, the reduction in connection probability is normalized (Bureau, Shepherd et al. 2008; Gibson, Bartley et al. 2008; Testa-Silva, Loebel et al. 2011). FMRP may be acting during circuit development to regulate connectivity, but even in the absence of FMRP, the circuit is ultimately able to mature normally.

While loss of FMRP throughout the circuit causes reductions in connectivity, these experiments cannot elucidate whether this is a cell-autonomous effect of FMRP or an effect of changes throughout the circuit as a

whole. Using the mosaic *Fmr1* KO mouse, one study has been able to show that the reduction in connectivity is driven by the absence of FMRP in the presynaptic cell, while FMRP in the postsynaptic cell has no effect (Hanson and Madison 2007). This finding is surprising, in that FMRP is typically thought to function at the postsynapse to regulate translation. However, FMRP also regulates motility of the growth cone of axons during development (Antar, Li et al. 2006). It is plausible that FMRP guides initial axonal contacts during development, and this process is disrupted in the *Fmr1* KO. Over the course of maturation, postsynaptic systems refine the contacts in an FMRP-independent mechanism.

Connectivity changes in the *Fmr1* KO have also been observed in the basolateral amygdala. Principle neurons in the BLA have fewer sIPSCs and mIPSCs, indicating that these neurons receive fewer connections from surrounding inhibitory neurons (Olmos-Serrano, Paluszkiewicz et al. 2010). The appearance of the connectivity phenotype in the BLA, a region with fundamentally distinct circuitry, suggests that FMRP may mediate a common mechanism to regulate synaptic connections in many brain regions.

Connectivity, as well as synaptic strength and intrinsic neuronal properties, converge to mediate the response of a circuit to an input. Because of the notable changes in all of these properties in the *Fmr1* KO, a logical consequence would be changes in network dynamics. Indeed, the neocortical network in the *Fmr1* KO is hyperexcitable. Stimulation of the thalamus evokes a

persistent activity state in L4 of neocortex that is driven by recurrent local connections amongst the cortical neurons. This stimulation in the *Fmr1* KO engenders a persistent activity state that is greatly prolonged compared to WT littermates (Gibson, Bartley et al. 2008). Because synaptic input from the thalamus to the cortex is unchanged in the KO, this implies that the prolonged network activation results from hyperexcitability present within the cortical circuitry. It is unclear, however, whether synaptic or intrinsic changes are causing prolonged circuit activation. Spontaneous persistent network activity is enhanced in the *Fmr1* KO, further implicating alterations in network function (Hays, Huber et al. 2011; Ronesi, Collins et al. 2012). The locus and mechanism for enhanced network activity is discussed at length in the following chapters.

Alterations in plasticity mechanisms also impact network function in the *Fmr1* KO. Treatment of hippocampal slices with a GABA antagonist disinhibits the slices and promotes network activity. After allowing time for synaptic plasticity to take place, the hippocampal network in slices from the *Fmr1* KO exhibits prolonged burst discharges reminiscent of epileptic activity patterns (Chuang, Zhao et al. 2005). Slices from WT mice will not undergo the transition to epileptic bursts without concurrent treatment with an mGluR agonist, suggesting that excessive signaling through Gp1 mGluRs is necessary to enhance the network function. This differs from the prolonged persistent activity states observed in the *Fmr1* KO in two distinct ways. First, the hippocampal discharges

result from spontaneous network activity, suggesting that network changes in the *Fmr1* KO may arise from intrinsic neuronal mechanisms independent of local synaptic input. Second, the transition to burst discharges in the hippocampus requires plasticity to take place, whereas the prolonged persistent activity states observed in the cortex represent changes in basal function.

As predicted by synaptic changes and the hyperexcitable intrinsic properties of neurons in the *Fmr1* KO, networks are hyperactive. Epilepsy and altered EEG patterns are commonly observed in FXS patients. The prevalence of epilepsy in FXS patients ranges from ten to twenty percent (Musumeci, Hagerman et al. 1999; Berry-Kravis 2002; Incorpora, Sorge et al. 2002). An even greater proportion of patients have abnormalities in EEG patterns. The irregularities in activity often include focal frontal rhythmic slow waves and most commonly centrotemporal spikes, which are a spike discharge followed by slow waves (Berry-Kravis 2002). The presence of seizures and the stated changes in EEG patterns in FXS are reflective of hyperexcitable networks that occur with the loss of FMRP. Because network function is critically important for information processing, one direct consequence of disruption of network activity is behavioral alterations.

Behavioral changes

Ultimately, synaptic and intrinsic changes would summate and lead to network changes, and network changes could subsequently lead to behavioral changes. Clinically, behavioral changes are the most relevant to FXS. While understanding of neuronal changes is germane to understanding the pathophysiology of Fragile X, amelioration of behavioral deficits in humans is the primary goal of FXS research. Although it is difficult to directly model mental retardation in a rodent, the mouse model displays several behavioral phenotypes that are similar to those observed in patients with FXS.

There are two major non-cognitive behavioral changes that occur in the *Fmr1* KO. First, prepulse inhibition (PPI) of startle response is elevated in the *Fmr1* KO. In this study, the authors show that a weak prestimulus suppresses the response to the startle stimulus to a greater degree in the *Fmr1* KO (Chen and Toth 2001). Although this is a complex response requiring many brain systems, it could be interpreted as an increase in sensory receptivity. This could potentially be driven by a similar mechanism that causes increased persistent activity states in the somatosensory cortex. Corresponding to this phenotype, FXS patients are reported to show exaggerated responses to various sensory inputs (Rogers, Hepburn et al. 2003). Second, *Fmr1* KO mice show increased sensitivity to several seizure modalities. Audiogenic seizures (AGS), or seizures that are triggered by a loud sound, are a common phenotype in *Fmr1* KO mice. AGS

typically occur in sixty percent of *Fmr1* KO mice, while WT littermates essentially do not seize (Musumeci, Bosco et al. 2000; Chen and Toth 2001; Yan, Rammal et al. 2005; Dölen, Osterweil et al. 2007; Musumeci, Calabrese et al. 2007). This phenotype correlates with the sensory hypersensitivity and epilepsy observed in FXS patients and with the enhanced PPI in the *Fmr1* KO. In further support of hyperexcitability, threshold for limbic seizures is lower in the *Fmr1* KO. KO mice require less direct electrical stimulation of the amygdala to cause a seizure compared to WT littermates (Qiu, Lu et al. 2009). Again, the increased propensity for seizures in the *Fmr1* KO is strongly predictive of hyperexcitable circuitry.

The major behavioral deficit associated with FXS is mental retardation, but modeling cognitive dysfunction in rodents can be problematic. However, a number of phenotypes in the *Fmr1* KO recapitulate cognitive deficits observed in patients. In a high level cognitive task, visuospatial discrimination is impaired in the *Fmr1* KO (Krueger, Osterweil et al. 2011). Mice were trained to nose poke a lighted hole to receive a food reward. In the training phase, all five holes were illuminated and resulted in a reward. After training, the test phase consisted of only one lighted hole that resulted in a reward for that particular trial. While *Fmr1* KO mice trained to criterion normally, they made significantly more mistakes than WT littermates during the testing phase (Krueger, Osterweil et al. 2011). Impairments in this task may correlate with mental retardation in patients.

Other behavioral phenotypes are less conclusive because of conflicting results. Studies examining spatial learning in the *Fmr1* KO mice have provided mixed conclusions. Most reports show that acquisition of a water maze task is normal in the KO; nonetheless, there is some evidence that the acquisition phase is altered (Van Dam, D'Hooge et al. 2000). The most consistent finding in the water maze task is impaired reversal learning, or the ability of a mouse to re-learn the position of the platform after it is moved; however, some studies reveal no deficits (Paradee, Melikian et al. 1999; Van Dam, D'Hooge et al. 2000; Eadie, Zhang et al. 2009; Baker, Wray et al. 2010). Presentation of behavioral phenotypes in *Fmr1* KO mice appears to be dependent on the background strain (Dobkin, Rabe et al. 2000).

Because hyperactivity is reported in some FXS patients, open field behavior has been assayed in *Fmr1* KO mice as a behavioral correlate. A larger proportion of time spent in the center of the arena as compared to the edges represents a reduced generalized anxiety. Some studies report that *Fmr1* KO mice spend an increased proportion of time in the center compared to the periphery (Peier, McIlwain et al. 2000; Yan, Rammal et al. 2005; Westmark, Westmark et al. 2011). However, other studies report no change in open field behavior (Mineur, Sluyter et al. 2002; Veeraragavan, Bui et al. 2011). Changes in open field behavior in the *Fmr1* KO are small, and because the behavior is likely

reliant on complex cognitive processes, it is possible that any variations in age or animal strain could cause the discrepancy in results.

FMRP is implicated in neuronal changes in the amygdala, so a logical outcome is changes in fear memory (Zhao, Toyoda et al. 2005; Olmos-Serrano, Paluszkiewicz et al. 2010). Additionally, some FXS patients display propensity for aggression, indicative of amygdalar dysfunction. Classical conditioned fear learning is unchanged in the *Fmr1* KO (Peier, McIlwain et al. 2000). However, *Fmr1* KO mice perform more poorly in a similar fear test that requires greater attention (Zhao, Toyoda et al. 2005).

The most consistent behavioral phenotypes observed in the *Fmr1* KO are propensity for audiogenic seizures and enhanced prepulse inhibition. These phenotypes are clearly indicative of enhanced excitability in neuronal circuitry in the *Fmr1* KO. Indirectly, the other behavioral phenotypes may also be derived from changes in network function. Alterations in network excitability may translate into changes in cognitive processing and consequently to changes in behavior. The wide range of penetrance of behavioral changes observed in the *Fmr1* KO, as well as the dependence on background strain, likely arise from the complexity of the systems involved in behavior. The broad spectrum of penetrance of behavioral deficits in the *Fmr1* KO mice may be reflective of the range of IQs observed in FXS patients (Dykens, Hodapp et al. 1989; Hall, Burns et al. 2008).

The mGluR theory of Fragile X

The major mechanistic theory describing pathogenesis in FXS is the mGluR theory of Fragile X (Bear, Huber et al. 2004). The original derivation of this hypothesis comes from the role of mGluR-dependent protein synthesis in LTD. mGluR-LTD is known to require the synthesis of new proteins in order to persist (Huber, Kayser et al. 2000). FMRP is present at the synapse and binds many synaptically localized mRNA transcripts, and mGluR stimulation drives protein synthesis in synaptoneurosomes (Weiler, Irwin et al. 1997). As such, the authors hypothesized that FMRP could be regulating the synthesis of new proteins downstream of mGluR stimulation at the synapse. The expectation was that changes in FMRP would result in deficits in LTD. Paradoxically, mGluR-dependent LTD in the *Fmr1* KO is enhanced rather than reduced (Huber, Gallagher et al. 2002). This result suggests that while mGluRs stimulate synthesis of new proteins, FMRP is actually working in opposition to mGluRs by preventing translation. Thus, in the case of mGluR-LTD, the consequence of the loss of FMRP is exaggerated mGluR activity. In the simplest case, this could be described by a model in which mGluRs are the gas and FMRP is the brake.

Indeed, a similar mechanism has held true for other outcomes resulting from the loss of FMRP. Many of the phenotypes observed in the *Fmr1* KO are analogous to consequences of mGluR activation. Correspondingly, several *Fmr1* KO phenotypes are ameliorated by reduction of mGluR signaling either

pharmacologically or genetically (Dölen, Osterweil et al. 2007; Dolen and Bear 2008; Dölen, Carpenter et al. 2010). Protein synthesis, an outcome of stimulation of mGluRs, is basally enhanced in the *Fmr1* KO (Dolen, Osterweil et al. 2007; Osterweil, Krueger et al. 2010). Pharmacological antagonism of mGluR5 activity using MPEP, an inverse agonist of the mGluR5 receptor, reduces the enhanced basal protein synthesis in the *Fmr1* KO (Osterweil, Krueger et al. 2010). Additionally, this enhancement in basal protein synthesis can be rescued by genetic reduction of mGluR5 gene dosage, such as in animals that are heterozygous for the *GRM5* allele (Dölen, Osterweil et al. 2007). The absence of one allele is thought to reduce mGluR5 signaling by half. Thus, animals that are *Fmr1* KO have enhanced mGluR5 activation, but animals that are *Fmr1* KO but also heterozygous for *GRM5* have compensatorially normalized mGluR5 activation. Genetic reduction of mGluR5 expression in the *Fmr1* KO background has served to be effective in reverting several phenotypes (Dölen, Osterweil et al. 2007; Repicky and Broadie 2009; Hays, Huber et al. 2011). The aberrant protein synthesis that results in enhanced LTD in the *Fmr1* KO is at least partially rescued by genetic reduction of mGluR5 (Dölen, Osterweil et al. 2007).

A number of interesting phenotypes that may potentially impinge on hyperexcitable circuit function are also rescued in response to blunted mGluR5 signaling in the *Fmr1* KO. Changes in synaptic function and connectivity in the *Fmr1* KO may arise from abnormal spine morphology. Increases in the density of

protrusions on cortical neurons are rescued by genetic reduction of mGluR5 (Dölen, Osterweil et al. 2007). Perhaps even more striking, short term treatments with MPEP can reduce the number of immature filopodia present on cultured neurons (de Vrij, Levenga et al. 2008; Westmark, Westmark et al. 2011). However, chronic MPEP treatment in young *Fmr1* KO mice did not rescue the spine protrusion phenotype (Cruz-Martín, Crespo et al. 2010). These studies examine different brain regions and different developmental ages, using either embryonic hippocampal neurons or young cortical pyramidal neurons in whole animals. The hippocampal neurons show reversal of the phenotype, potentially because very young neurons are more amenable to treatment compared to older neurons. It is also possible that hippocampal neurons contain components needed to respond to MPEP treatment whereas pyramidal neurons do not. These finding provide potential evidence that synaptic changes in the *Fmr1* KO may be rescued by mGluR5 antagonism.

Some network dysfunction in the *Fmr1* KO is also restored upon mGluR5 antagonism. Notably, hippocampal epileptic discharges are reversed by treatment with MPEP (Chuang, Zhao et al. 2005). These bursts arise from plasticity as a result of enhanced glutamatergic signaling. Surprisingly, even after the plasticity to cause the epileptic bursts has taken place, mGluR5 blockade with MPEP prevents further prolonged bursts. This suggests that continued mGluR5 signaling is necessary for the maintenance of epileptic bursts, not just the

induction, possibly by regulating an intrinsic conductance (Bianchi, Chuang et al. 2009). Extending this model to include epilepsy in patients, this may be therapeutically relevant because treatment with an mGluR5 antagonist may be able to revert network hyperexcitability even after it is established. Evidence from this study further upholds the mGluR theory of Fragile X. Both genetic and pharmacological reductions of mGluR5 are sufficient to rescue enhanced persistent network activity states (Hays, Huber et al. 2011). Ultimately, these findings suggest that the hyperexcitability of circuitry in the *Fmr1* KO is likely to be derived from overactive mGluR signaling.

As may be predicted by the rescue of circuit dysfunction, some behavioral phenotypes are also restored by mGluR5 reduction. Remarkably, even high level cognitive tasks are improved by administration of mGluR5 antagonists in the *Fmr1* KO. Altered courtship behavior is rescued with MPEP treatment in the *Drosophila* model of FXS, the *dfmr1* mutant (Choi, McBride et al. 2010). Of note, several of the behavioral phenotypes that are ameliorated by mGluR antagonism are those that are reflective of hyperexcitability. Reduced generalized anxiety observed in the *Fmr1* KO, as measured by time spent in the center of an open field arena, is corrected by treatment with MPEP (Yan, Rammal et al. 2005). Audiogenic seizures are prevented in the *Fmr1* KO after administration of MPEP (Yan, Rammal et al. 2005). In further support of the role of enhanced mGluR5 signaling causing AGS, genetic reduction of mGluR5 is sufficient to partially

reduce seizures (Dölen, Osterweil et al. 2007). These results do implicate overactivation of mGluR5 in seizure generation; however, these data may be potentially misleading. Because WT mice do not have audiogenic seizures, it is not possible to derive whether the anti-epileptic effect of mGluR5 block is through an FMRP dependent mechanism or simply a general depression in excitability. Especially because genetic reduction of mGluR5 signaling does not fully restore AGS to WT levels, MPEP is likely acting partially through another mechanism to reduce seizures. Regardless, these data suggest that overactive mGluR5 signaling are contributing to hyperexcitability in the *Fmr1* KO.

While the effect of mGluR5 reduction on intrinsic properties in the *Fmr1* KO has not been investigated, it is likely that enhanced mGluR5 signaling is changing basal properties of neurons. Many studies have shown that mGluR5 activation causes changes in intrinsic properties. Acute activation of Gp1 mGluRs is sufficient to cause persistent firing in neurons of the entorhinal and anterior cingulate cortex (Yoshida, Fransén et al. 2008; Zhang and Seguela 2010). Consequently, Gp1 mGluR stimulation causes changes within the neuron that support persistent firing, a finding that could be relevant for circuit hyperexcitability. In addition, Kv4.2, a potassium channel altered in the *Fmr1* KO, is also strongly regulated by mGluR signaling. Activation of the kinase ERK through mGluR5 stimulation results in phosphorylation of Kv4.2 channels, which leads to lowered conductance (Hu and Gereau 2003; Hu, Alter et al. 2007). This

reduced potassium conductance results in deficits in repolarization, and therefore enhanced neuronal excitability. Interestingly, Kv4.2 is implicated in pain processing, which is altered in the *Fmr1* KO, suggesting another potential link between mGluR function and phenotypes in the *Fmr1* KO (Price, Rashid et al. 2007). Activation of mGluRs also drives plasticity in layer 5 cortical neurons that results in reduction in SK potassium channels and subsequent reduction of the after-hyperpolarization (AHP) (Sourdet, Russier et al. 2003). This, too, results in enhanced neuronal excitability. Considering the enhancement of neuronal excitability resulting from mGluR activation, it is logical to hypothesize that networks in the *Fmr1* KO will display hyperexcitability.

The mGluR dependent changes in synaptic function and potential changes in intrinsic properties are consistent with the mGluR-dependent hyperexcitability observed in the *Fmr1* KO. A portion of this study focuses on the role of mGluR function in regulation of circuit excitability and function in the *Fmr1* KO. The mGluR theory of Fragile X provides an important framework for experimental design. mGluR5 is particularly amenable for pharmacology because it resides on the surface of the cell. Antagonism of a receptor to treat an autism spectrum disorder would be a novel treatment and a landmark advance in treating neurological disease.

A Homer theory of Fragile X?

Another protein known to directly affect Gp1 mGluR function that has received little attention in terms of FXS is the scaffolding protein Homer. Despite the direct link to mGluR function, relatively few studies have examined the contribution of Homer to FXS. Homer is a postsynaptic scaffolding protein that couples mGluR5 and mGluR1α with other effector proteins (Brakeman, Lanahan et al. 1997). Long Homer proteins contain two motifs that regulate their binding function. An EVH1 domain mediates binding of Homer to its interactors, while a coiled-coil domain regulates dimerization of Homers (Ehrengruber, Kato et al. 2004). There are three mammalian long Homer proteins, Homer1, Homer2, and Homer3, each with different splice variants (Kato, Ozawa et al. 1998; Xiao, Tu et al. 1998). One short splice variant of Homer1, termed Homer1a, is an activity regulated form that is caused by an alternative termination site within the gene. Homer1a (H1a) contains the EVH1 domain, so it retains the ability to interact with effectors, including mGluRs (Ehrengruber, Kato et al. 2004). However, it lacks the coiled-coil motif, rendering it unable to multimerize with other Homers. This confers H1a a unique and opposite function from long Homers. Whereas long Homers promote interaction between mGluRs and other proteins, H1a actually causes the uncoupling of mGluR scaffolding complexes (Kammermeier and Worley 2007). Unexpectedly, rather than reducing mGluR function,

uncoupling causes constitutive, agonist-independent signaling through mGluR5 (Ango, Prezeau et al. 2001).

Either long Homers or H1a, by influencing coupling of mGluRs, may be important for regulating mGluR activity in the *Fmr1* KO. Because uncoupling of mGluR5 results in constitutive signaling, the *Fmr1* KO would be predicted to have reduced Homer-mGluR interactions. Indeed, mGluRs are less associated with long Homers in the *Fmr1* KO (Giuffrida, Musumeci et al. 2005). The reduction in scaffolding is accompanied by a trend toward an increase in association of mGluR5 with H1a. Presumably, this reduction in mGluR coupling could be driving a number of phenotypes in the *Fmr1* KO by causing exaggerated mGluR5 signaling.

There is an inconsistency, however, in the implication of H1a in relation to hyperexcitability in the *Fmr1* KO. Overexpression of H1a actually increases seizure threshold and antagonism of H1a expression prevents this increase, suggesting an inhibitory role for H1a in propagation of seizures (Bockaert, Perroy et al. 2010). The potential mechanism for this effect is H1a-mediated activation of mGluR5 causes enhanced IP3 and subsequent enhanced conductance of BK channels (Sakagami, Yamamoto et al. 2005). However, there is also a strong case for hyperexcitability resulting from H1a expression. The increases in intrinsic neuronal excitability described above may result indirectly from mGluR activation by H1a. In addition, H1a directly interacts with TRPC1, a transient

receptor potential channel, to increase conductance (Yuan, Kiselyov et al. 2003). This would consequently depolarize neurons and lead to increased excitability. These opposing possibilities merit further research into the effect of H1a on excitability. The research presented in this document provides evidence that disruption of Homer-mGluR5 interactions is responsible for network hyperexcitability (Ronesi, Collins et al. 2012). This is a critically important area of research, as Homer may provide another target for directed therapy in FXS patients.

Do network excitability changes underlie the pathology of autism?

Given the heterogeneity observed in autistic disorders, development of a unifying theory has been challenging and often met with controversy. However, one theory in particular has garnered support because it encompasses many of the changes seen across models of ASDs. This theory posits that shifts in excitatory to inhibitory (E/I) ratio underlie many deficits (Rubenstein and Merzenich 2003). One significant manifestation of this hypothesis is that as many as thirty percent of ASD patients exhibit seizures and up to seventy percent have abnormal EEG spike discharges, very similar to the prevalence observed in FXS patients (Lewine, Andrews et al. 1999). This is suggestive of a shift in the E/I balance to favor excitation, resulting in hyperexcitability (Belmonte and Bourgeron 2006).

In addition, there is rich cellular evidence that the E/I ratio is altered in a variety of ASD models. Interestingly, although different models may undergo different mechanisms, the change in E/I ratio is consistently affected. One potential mechanism is a reduction in the number of inhibitory neurons, as is observed in a genetic and a pharmacological model of autism (Gogolla, LeBlanc et al. 2009). Reductions in the synaptic strength of inhibitory neurons onto excitatory neurons is reported for a mouse model of neuroligin-2, an autism related gene (Gibson, Huber et al. 2009). Similarly, excitatory drive onto inhibitory neurons is reduced in the *Fmr1* KO, which would also result in reduced net inhibition (Gibson, Bartley et al. 2008). In the mouse model of Rett syndrome, another model of mental retardation, mIPSC amplitude is reduced, again displaying a reduction in inhibitory neuron strength (Chao, Chen et al. 2010). Excitatory synaptic strength is also reduced in the cortical circuit upon deletion of MeCP2, the gene deleted in Rett syndrome (Wood, Gray et al. 2009). However, MeCP2-deleted mice have EEG abnormalities consisting of epileptiform bursts, suggesting that even with reduced excitatory connection strength, the hyperexcitability is dominated by the reduction in inhibition. In a valparoic acid induced model of autism, L5 pyramidal neurons in the cortex are hyperconnected and much more sensitive to stimulation (Rinaldi, Perrodin et al. 2008). As previously described, *Fmr1* KO mice display epileptogenesis in the hippocampus and prolonged thalamically-evoked persistent activity states in

neocortex, both representative of enhanced excitatory function (Chuang, Yan et al. 2004; Gibson, Bartley et al. 2008).

Although the previous examples have shown a shift in E/I balance to favor excitation, a model of Down syndrome has a shift toward hypoexcitability. In this model, inhibitory transmission is increased at least in part due to an increase in GABA release (Kleschevnikov, Belichenko et al. 2012). Although the balance in excitability is shifted away from excitation, this could be equally detrimental to circuit function. This lends credence to E/I ratio theory, because it shows that a shift in E/I balance of either polarity can disrupt circuit function and potentially lead to ASD.

Up to this point, the E/I theory has been simply a synthesis based on great deal of data from autism models and ASD patients. However, a recent report has undertaken the first direct test of the E/I balance theory of autism. The authors use optogenetics to control excitability of circuitry in medial prefrontal cortex (mPFC), a brain structure known both to be involved in social interaction and to be hyperexcitable in autism (Yizhar, Fenno et al. 2011). In WT mice, increases in the excitability of the circuit caused deficits in both conditioned learning and unconditioned social responses. Reduction in excitability of the circuit had no effect. Only a small number of behaviors were tested, so it is possible that deficits in other behavior paradigms may be revealed when the circuit is hypoexcitable. These findings show that hyperexcitability, or an E/I shift to favor

excitation, does indeed result in behavioral phenotypes that mirror autistic-like behaviors. The authors go on to show that by simultaneously increasing excitation and inhibition, thus keeping the E/I ratio equivalent, there are no observed behavioral deficits. This further suggests that it is not simply increased excitability, but rather truly a shift in the balance of E/I within the circuit that is responsible for behavioral dysfunction.

The hypothesis referred to as the "Intense World Theory" of autism further extends changes in E/I balance directly to symptoms observed in ASD patients (Markram, Rinaldi et al. 2007; Markram and Markram 2010). The core of the Intense World Theory describes some circuits that are hyperactive in autism, and how this hyperactivity may result in the aberrant behaviors observed in ASD individuals. Epilepsy is common across ASD, and likely arises from hyperexcitability within circuitry. Many ASD patients are hypersensitive to sensory inputs, possibly reflective of hyperexcitable sensory circuitry. Additionally, emotional problems are common in ASD patients, and the amygdala is hyperexcitable in some models of autism. Changes in the excitability of the circuit could potentially have large effects on cognitive processing, leading to many of the behavioral abnormalities.

Generally, many phenotypes in ASD patients and autism models can be linked to hyperexcitability and a shift in E/I balance. Changes in E/I balance appear to be an over-arching theme in autism, and may serve to unify many

different disorders into one disease. As such, understanding changes in circuit excitability and network function is integrally important in understanding the pathology of autism.

Principles of network function

Networks orchestrate the coding of information and provide a framework in which a limited number of cells can have a synergistically enhanced information processing capacity. One of the many ways in which network function is manifest is in the generation of oscillations. These network oscillations arise from the properties of the neurons within the circuit, and thus can be used as a measure of circuit properties. There are a variety of types of network oscillations, each typically defined by its frequency. Frequencies range from the slow oscillation (less than 1Hz) to high frequency sharp wave ripples (approximately 150Hz). Each of these types of oscillations have been implicated in certain functions, although direct testing is challenging. Network oscillations are hypothesized to be involved in memory and sensory processing; therefore, they provide a potential candidate that may be altered in autism (Marshall, Helgadottir et al. 2006; Sejnowski and Paulsen 2006; Poulet and Petersen 2008; Akam and Kullmann 2010).

There is a dearth of studies directly testing network oscillations in autistic patients or models. However, general EEG properties, one measure of network

function, appear to be changed in many patients with ASD (Berry-Kravis 2002). Additionally, sleep patterns are disrupted in individuals with autism and FXS (Miano, Bruni et al. 2008; Hollway and Aman 2011). Oscillations feature prominently into the EEG during sleep, with the signal mainly dominated by the slow oscillation. Notably, seizures and epileptic EEG patterns often occur during sleep, providing a potential link to the slow oscillation and pathologically hyperactive circuitry (Lewine, Andrews et al. 1999).

Because the slow oscillation arises from E/I balance within circuits, occurs concurrently with epochs of hyperexcitability, and may be linked to sleep, memory, and sensory perception, it encompasses several phenotypes that are altered in autism. Below I describe the slow oscillation, its properties and potential function, as well as pathology associated with it. The remaining chapters provide a description of alterations in the slow oscillation and potential mechanisms giving rise to the disruption of the slow oscillation in the *Fmr1* KO model of mental retardation.

Dynamic network function: The slow oscillation

The slow oscillation was originally extensively characterized in the neocortex by Steriade and colleagues two decades ago (Steriade, Nunez et al. 1993). Since then, a great deal of insight has been gained into the characteristics and underlying mechanisms. As previously mentioned, the slow oscillation is

prominent during sleep, but also occurs spontaneously under anesthesia and in brain slices in *in vitro* preparations (Steriade, Nunez et al. 1993; Sanchez-Vives and McCormick 2000).

The slow oscillation is a nonlinear bimodal system, comprised of two major states: UP states and DOWN states. UP states are cyclic periods of depolarization from resting membrane potential and are accompanied by a concurrent increase in both excitatory and inhibitory synaptic barrages (Sanchez-Vives and McCormick 2000; Haider, Duque et al. 2006). Because neocortical neurons are recurrently connected, the synaptic input during the UP state is primarily due to surrounding neurons (Sanchez-Vives and McCormick 2000). The depolarizing shift in membrane potential causes neurons to be more likely to fire action potentials. Interspersed between UP states are DOWN states, which are periods of quiescence (Steriade, Nunez et al. 1993; Sanchez-Vives and McCormick 2000). DOWN states are characterized by a return to resting membrane potential and a cessation of most synaptic input. UP state duration varies depending on the subject and the preparation, but typically lasts around one second (Bazhenov, Lonjers et al. 2011). The frequency of UP states is not harmonic, but is rhythmic with UP states occurring at a rate between 0.1 and 1 Hz.

Nearly all neocortical neurons participate in the UP state (Steriade, Nunez et al. 1993). Inhibitory neurons and excitatory neurons both participate, and this

is reflected in the synaptic inputs received during an UP state (Contreras and Steriade 1995). Conductance greatly increases during an UP state because of the synaptic barrage of both IPSCs and EPSCs, but the ratio of E/I conductances remains balanced (Sanchez-Vives and McCormick 2000; Haider, Duque et al. 2006). Additionally, changes in E/I balance result in altered duration and frequency of UP states (Compte, Sanchez-Vives et al. 2003). This provides and interesting link to autism, because alterations in E/I ratio could directly impact UP states by shifting the balance of synaptic inputs. In addition to synaptic mechanisms, intrinsic neuronal properties strongly play into the generation of UP states (McCormick, Shu et al. 2003). The contribution of both synaptic and intrinsic components is described in detail below.

The onset of UP states is temporally precise and nearly synchronous throughout the cortex, with neurons typically becoming depolarized within tens of milliseconds of each other (Sanchez-Vives and McCormick 2000; Volgushev, Chauvette et al. 2006). Layer 5 is thought to generate the UP states, followed by propagation throughout other layers (Chauvette, Volgushev et al. 2010). It is hypothesized that UP states arise from stochastic synaptic events, and because L5 large pyramidal neurons receive many synapses, they are statistically the most likely to drive an UP state. Other cortical layers contain the necessary components to sustain UP states, because stimulation in other layers can cause

generation and propagation of UP states even without an intact L5 (Sanchez-Vives and McCormick 2000).

UP states are clearly observed in intact brain, but are intrinsic to the neocortex. Cortical slabs which have been physically separated from the rest of the brain, as well as isolated slices of neocortex, spontaneously generate a rhythm similar to the slow oscillation (Sanchez-Vives and McCormick 2000; Timofeev, Grenier et al. 2000). These isolated cortical preparations retain most of the characteristics of the slow oscillation, suggesting that UP and DOWN states can be maintained in isolated cortical circuitry. However, the thalamus has a modulatory role in regulating the slow oscillation in the cortex (MacLean, Watson et al. 2005; Rigas and Castro-Alamancos 2009).

Slow waves are known to group other rhythms together, possibly by affecting the excitability of the cells generating the faster oscillation (Steriade 2006). Spindles, delta, beta, and gamma oscillations all occur in phase with the slow oscillation (Steriade 2006). This property of grouping other rhythms may allow the slow oscillation to control the coherence of signals within the circuit. Activity that is coherent with the oscillation is amplified, while out of phase signals are attenuated (Schroeder and Lakatos 2009). This allows the network to preferentially respond to in-phase signals. This coherence filtering also confers the network with the ability to switch between multiple streams of information by changing phase. In the somatosensory cortex, sensory selection is thought to

work through a similar mechanism (Schroeder and Lakatos 2009; Akam and Kullmann 2010). Coherence-based processing relies on the ability excitability of the neurons within the network to be regulated by the oscillation. Indeed, the slow oscillation does control the excitability of neurons within the network through changes in membrane potential (Steriade, Nunez et al. 1993; Steriade 2006). Membrane potential oscillations that make up the slow oscillation change the responsiveness of neurons within the cortex (Hasenstaub, Sachdev et al. 2007). Because network function weighs heavily on processing, one mechanism for alterations in sensation in autism could potentially occur through disruption of the slow oscillation.

The effects of the cortical slow oscillation are not spatially restricted to the neocortex and can cause changes in excitability in diverse brain regions. UP states in the cortex are able to influence excitability in the hippocampus and the cerebellum (Isomura, Sirota et al. 2006; Roš, Sachdev et al. 2009). The widespread effects of the cortical slow oscillation obviate the importance of this rhythm and illustrate how changes in the slow oscillation could have far-reaching consequences for a variety of cognitive processes.

Determining the function of the slow oscillation has been difficult. Because the slow oscillation is derived from a number of different factors, direct specific manipulation is challenging. To date, the most direct test showed that potentiation of the slow oscillation during sleep improves declarative memory in

humans (Marshall, Helgadottir et al. 2006). However, given the importance of the slow oscillation in sensory processing and memory, this topic merits further research.

To understand dysfunction in networks, it is necessary to understand the underpinnings of the generation of network oscillations. The core components that regulate network properties are synaptic function and intrinsic neuronal properties. The contribution of each factor is detailed below.

Synaptic and intrinsic properties contribute to network oscillations

Synaptic function is integrally important in the generation of rhythms. Neurons within cortical circuits are recurrently connected, and it is these recurrent connections are thought to be the basis for the generation of the slow oscillation. Because of this, electrical stimulation of the neurons drives synaptic activity that turns on activity within the network (Shu, Hasenstaub et al. 2003). Similarly, likely due to the inhibitory neurons within the circuit, stimulation can also turn off activity. Therefore, a single stimulus is sufficient to drive reverberant activity within the circuit because of recurrent connections. Slow oscillatory activity propagates as a wave across the cortex, consistent with synaptic activity driving neighboring neurons into an UP state (Sanchez-Vives and McCormick 2000; Compte, Sanchez-Vives et al. 2003; Steriade 2006). Furthermore, given the highly synchronous nature of state transitions, it is unlikely that intrinsic neuronal

currents are solely responsible for the slow oscillation (Volgushev, Chauvette et al. 2006). Instead, fast synaptic transmission probably plays strongly into regulating the synchronous transition of nearby neurons between UP and DOWN states.

Spike timing dependent plasticity (STDP) may also be important for the generation of spontaneous rhythms. Computational modeling has shown that networks that express STDP exhibit bistable oscillations reminiscent of UP states. (Kang, Kitano et al. 2008). Because several forms of plasticity, including STDP, are dysfunctional in the *Fmr1* KO, network oscillations may be disrupted as a result (Meredith and Mansvelder 2010).

More directly, pharmacology reveals the effect of synaptic currents on UP states. Antagonism of AMPA receptors with CNQX blocks UP states (Appendix 1) (Compte, Sanchez-Vives et al. 2003). Additionally, treatment with drugs that block NMDA receptors also attenuates or abolishes UP states (Steriade, Nunez et al. 1993; Compte, Sanchez-Vives et al. 2003). Further demonstrating the importance of excitatory transmission, glutamate spillover is involved in UP state duration in the PFC (Lambe and Aghajanian 2007). Since many mGluRs are located perisynaptically, this enhancement in duration of the UP state may be through mGluR activation. Inhibitory transmission is important in the slow rhythm as well, as pharmacological manipulation of GABA receptors effects UP state duration (Mann, Kohl et al. 2009). The diverse effects of synaptic current

manipulation highlight the significance of synaptic activity in the generation and regulation of the slow oscillation.

In addition to the synaptic function, intrinsic neuronal properties fundamentally regulate network oscillations. Persistent sodium current (I_{NaP}) contributes to the membrane depolarization during the UP state (Steriade, Nunez et al. 1993). This I_{NaP}, in conjunction with spontaneous action potentials amplified by the recurrent connectivity, is thought to primarily underlie generation of the slow oscillation. Conversely, sodium-dependent potassium currents (I_{KNa}) are thought to promote transition to a DOWN state (Compte, Sanchez-Vives et al. 2003). Sodium build-up during the depolarized UP state causes activation of the I_{KNa} which promotes hyperpolarization and subsequent entry into the DOWN state. Computational modeling experiments also suggest the potassium leak current affects transition between UP and DOWN states (Compte, Sanchez-Vives et al. 2003). Hyperpolarization-activated current (I_H) also factors into UP state generation, as networks lacking this conductance fail to shift to UP states (Kang, Kitano et al. 2004). Thus, oscillatory dynamics are governed in part by the variety of intrinsic conductances membrane properties.

Because of the changes in neuronal excitability that occur with the slow oscillation, unchecked network dynamics can be pathological. Increased excitation within the recurrent circuitry can lead to aberrant activity patterns. As such, slow waves can evolve into epileptiform activity in the cortex (Steriade

2006). As may be predicted from the contribution of synaptic and intrinsic components, either mechanism may be responsible for the conversion to epilepsy. In a simple fashion, increased extracellular potassium can drive epileptic activity, likely through non-synaptic mechanisms (Fröhlich, Bazhenov et al. 2010; Fröhlich, Sejnowski et al. 2010). Synaptic properties can also drive aberrant activity. Imbalance in synaptic strengths resulting in E/I ratio changes can engender shifts in excitability within the network. Modeling studies have shown that homeostatic increases in synaptic strength can result in pathological dynamics in the circuit (Fröhlich, Bazhenov et al. 2008). As synaptic development is dysfunctional in the absence of FMRP, this provides another potential link for pathological network function in the *Fmr1* KO.

Motivation for Studies and Summary of Research

Fragile X Syndrome, caused by loss of function of FMRP, is the most common heritable form of mental retardation (O'Donnell and Warren 2002). Many FXS patients exhibit hallmarks of autism, suggesting a potential underlying component between the disorders (Bassell and Warren 2008; Garber, Visootsak et al. 2008). Seizures and EEG abnormalities, including spike burst discharges, are prevalent among many FXS patients, potentially implicating neuronal circuit hyperexcitability (Musumeci, Hagerman et al. 1999; Berry-Kravis 2002; Berry-Kravis, Raspa et al. 2010). Furthermore, sensory hypersensitivity is commonly

reported among FXS patients (Miller, McIntosh et al. 1999; Hagerman and Hagerman 2002). Since sensory processing relies on network function, this provides additional evidence for circuit property alterations in FXS. The mouse model of FXS, the *Fmr1* KO, displays phenotypes similar to FXS patients, including audiogenic seizures and abnormal sensory processing (Chen and Toth 2001). In the proceeding chapters, I provide evidence that circuit function is indeed disrupted in the *Fmr1* KO, and I describe an mGluR5-dependent mechanism that leads to network hyperexcitability.

A great deal of research has gone into identifying synaptic and behavioral changes in the *Fmr1* KO. However, there is a major dearth of studies directly addressing changes at a network level. Before this study, the only direct test of basal network dynamics showed that neocortical persistent activity states evoked by thalamic stimulation are prolonged in the *Fmr1* KO (Gibson, Bartley et al. 2008).

In addition to these data, there are three major theoretical lines of evidence suggesting the spontaneous network function may be altered in the *Fmr1* KO. Firstly, in a bottom-up model, synaptic and intrinsic neuronal changes reported in the *Fmr1* KO would likely result in changes in network function. As network oscillations are largely governed by synaptic and intrinsic function, changes in either of these properties would be predictive of changes in network dynamics. Secondly, in a top-down model, behavioral changes in the *Fmr1* KO presumably

arise from network dysfunction. Because cognitive processes obviously underlie behavioral outcomes, then disruptions in behavior are potentially a product of aberrations in network function. Thirdly, imbalance of excitation and inhibition is thought to cause many of the deficits in autism. FXS shares many features with autism, and a shift of E/I ratio would by reflected by changes in network dynamics. Coupled with the initial investigation of circuit excitability, these three lines of reasoning led us to investigate network function in the *Fmr1* KO.

The majority of this project assesses circuit properties using UP states as a measure of network function. UP states are spontaneously occurring rhythmic periods of neuronal depolarization with simultaneous onset in local networks of neurons (Steriade, Nunez et al. 1993; Sanchez-Vives and McCormick 2000). These oscillations arise from the intrinsic properties of the neurons and the synaptic connections between them. As such, properties of the circuit are manifest in the dynamics of the UP states. Although there are limitations to measuring UP states, such as the inability to control specific conductances, they do provide an accurate measure of circuit excitability.

Despite network function being of critical importance in many cognitive processes, it remains a largely unstudied subject in disease models. Disruption of network function could provide insight into some of the symptoms observed in ASD. I sought to determine whether circuit function was disrupted in the *Fmr1* KO. To do so, I primarily recorded spontaneous UP states *in vitro* in brain slices

containing the somatosensory cortex from mice. This preparation allowed for comparison of various genetic manipulations as well as different pharmacological treatments. The UP states provide a general measure of excitability and spontaneous dynamics within the network.

I observed that UP states from the *Fmr1* KO are prolonged compared to WT, consistent with the hypothesis of hyperexcitable circuitry. Prolonged UP states are observed in both *in vitro* preparations and *in vivo* recordings from intact animals. The increase in UP state duration persists into adulthood, suggesting that it is a permanent deficit. Furthermore, I observe that deletion of FMRP from specific cortical layers partially enhances UP state duration. I show that this increase in excitability results from loss of FMRP from excitatory neurons, while loss from inhibitory neurons has no effect.

Considering the mGluR theory of FXS, I tested whether mGluR dysfunction may be contributing to the prolonged UP state phenotype. Indeed, reduction of mGluR5 signaling is sufficient to reduce UP state duration in the *Fmr1* KO to WT levels. Aberrant mGluR5 signaling in the *Fmr1* KO is typically thought to cause phenotypic deficits by driving enhanced protein translation. However, inhibition of protein synthesis does not reduce UP state duration, suggesting acute, non-protein synthesis dependent mGluR5 signaling may also be affected in the *Fmr1* KO. I also observe that Homer-mGluR5 interactions are involved, as disruption of these interactions causes prolonged UP states in a WT

background. Moreover, restoration of long Homer-mGluR complexes in the *Fmr1* KO rescues UP state duration.

I also provide a preliminary intracellular investigation of some currents that may give rise to hyperexcitability within circuits in the *Fmr1* KO. I observe that presumptive mGluR-dependent depolarizing currents are unchanged in the *Fmr1* KO. Furthermore, A-type potassium current, Slack potassium current, and H-current are unchanged in neocortical neurons in the *Fmr1* KO. However, preliminary examination of general properties in L5 neurons of the *Fmr1* KO indicates a shift towards hyperexcitability.

The observations detailed in the proceeding study provide a characterization of network properties in the *Fmr1* KO. Additionally, these findings provide evidence for a mechanism in which disrupted Homer interactions drive enhanced mGluR5 signaling, which gives rise to the hyperexcitability in the neocortical network in the *Fmr1* KO. These data are consistent with an increase in excitability and a shift in E/I ratio to favor excitation. This contributes to the understanding of network function in FXS and provides a potential link to perturbations in E/I ratio as a unifying cause for ASD.

CHAPTER TWO
Results

NEOCORTICAL RHYTHMIC ACTIVITY STATES IN *FMR1* KO MICE ARE DUE TO ENHANCED MGLUR5 SIGNALING AND INVOLVE CHANGES IN EXCITATORY CIRCUITRY

Summary

Despite the pronounced neurological deficits associated with mental retardation and autism, the degree to which neocortical circuit function is altered remains unknown. Here, we study changes in neocortical network function in the form of persistent activity states in the mouse model of Fragile X Syndrome – the *Fmr1* knockout (KO). Persistent activity states, or UP states, in the neocortex underlie the slow oscillation which occurs predominantly during slow wave sleep, but may also play a role during awake states. We show that spontaneously occurring UP states in the primary somatosensory cortex are 38-67% longer in *Fmr1* KO slices. *In vivo*, UP states re-occur with a clear rhythmic component consistent with that of the slow oscillation and are similarly longer in the *Fmr1* KO. Changes in neocortical excitatory circuitry likely play the major role in this alteration as supported by 3 findings: 1) longer UP states occur in slices of isolated neocortex, 2) pharmacologically isolated excitatory circuits in *Fmr1* KO neocortical slices display prolonged bursting states, and 3) selective deletion of *Fmr1* in cortical excitatory neurons is sufficient to cause prolonged UP states whereas deletion in inhibitory neurons has no effect. Excess signaling mediated

by the group 1 glutamate metabotropic receptor, mGluR5, contributes to the longer UP states. Genetic reduction or pharmacological blockade of mGluR5 rescues the prolonged UP state phenotype. Our results reveal an alteration in network function in a mouse model of intellectual disability and autism which may impact both slow wave sleep and information processing during waking states.

Introduction

Fragile X syndrome (FXS) is the most common form of inherited intellectual disability and is caused by loss of function mutations in *FMR1* which encodes the RNA binding protein, FMRP (Verkerk, Pieretti et al. 1991; O'Donnell and Warren 2002). Many of the impairments in FXS such as altered social responses and hypersensitivity to sensory stimuli are reproduced in the FXS mouse model, the *Fmr1* knockout (KO) mouse (Bakker 1994; Miller, McIntosh et al. 1999; Musumeci, Bosco et al. 2000; Hagerman 2002; Nielsen, Derber et al. 2002; Spencer, Alekseyenko et al. 2005; Brennan, Albeck et al. 2006).

It has been hypothesized that altered cortical function mediates the cognitive and behavioral deficits in FXS (Irwin, Patel et al. 2001). In support of this idea, many cellular and synaptic alterations have been observed in cortical structures in FXS patients and in *Fmr1* KO mice (reviewed in (Bassell and Warren 2008; Pfeiffer and Huber 2009)).

Despite these numerous reported deficits, little electrophysiological evidence of alterations in cortical circuit function exists. There is a plasticity phenomenon in *Fmr1* KO mice where hippocampal networks become more excitable and epileptic in response to pharmacological blockade of inhibition (Chuang, Zhao et al. 2005). However, it is unclear how cortical network function under basal conditions is altered in *Fmr1* KO mice. We have reported one such example where persistent activity states, or UP states, are longer in duration in neocortical slices obtained from *Fmr1* KO mice when thalamic stimulation is used to induce the active state (Gibson, Bartley et al. 2008). UP states are depolarized firing states of neurons that are driven by local recurrent excitation and inhibition, and occur synchronously among all neurons in a cortical region (Haider and McCormick 2009; Sanchez-Vives, Mattia et al. 2010). When they occur spontaneously and repeatedly, they underlie the neocortical slow oscillation which is a rhythm (<1 Hz) occurring during slow wave sleep, but they may also be involved in information processing during awake states (Steriade, Timofeev et al. 2001; Timofeev, Grenier et al. 2001; Marshall, Helgadottir et al. 2006; Haider and McCormick 2009; Okun, Naim et al. 2010). Therefore, UP states are a critical aspect of neocortical circuit function, and understanding how and why they are altered in the *Fmr1* KO mouse would provide important information to how baseline neocortical circuit function is altered in Fragile X Syndrome. Such data would also provide specific strategies for treatment.

Questions remain about prolonged UP states in *Fmr1* KO mice. First, while prolonged UP states are observed with thalamic stimulation (Gibson, Bartley et al. 2008), are spontaneous and rhythmic UP states altered and are alterations intrinsic to neocortex? The answer to this is critical for linking prolonged UP states to possible alterations in the slow oscillation rhythm since neocortex has been hypothesized to primarily mediate the slow oscillation (Steriade 1997; Haider and McCormick 2009). Second, are UP states longer in the *Fmr1* KO *in vivo* or is this strictly an *in vitro* slice phenomenon? Third, what is the relative role of changes in excitatory versus inhibitory circuitry? Fourth, what cellular processes lead to prolonged UP states?

We find that spontaneously occurring UP states are longer in the *Fmr1* KO – both *in vitro* and *in vivo* – and that this alteration involves changes in mGluR5 signaling in neocortical excitatory neurons.

Materials and Methods

Mice

Congenic *Fmr1* KO mice on the C57Bl6 background were originally obtained from Dr. Stephen Warren (Emory University) and have been backcrossed onto the C57Bl6/J mice from the UT Southwestern breeding core colony (Bakker 1994). *Grm5* KO (mGluR5 KO) mice were obtained from Dr. Mark Bear (MIT) but were made by another group (Lu, Jia et al. 1997). *Emx1*

Cre mice were obtained from Dr.Takuji Iwasato and Dr. Shigeyoshi Itohara (Iwasato, Datwani et al. 2000; Iwasato, Inan et al. 2008) and *Dlx5/6* Cre mice were obtained from Dr. Marc Ekker and Dr. John Rubinstein (Monory, Massa et al. 2006). Floxed *Fmr1* mice were obtained from Dr. David Nelson (Mientjes, Nieuwenhuizen et al. 2006). All experiments were performed with littermate comparisons. Experimenters were blind to mouse genotype with respect to data depicted in the following figures: 1, 2, 5, 6.

Slice preparation

Mice 3 weeks of age (P18-P24) were deeply anesthetized with Euthasol (pentobarbital sodium and phenytoin sodium solution) and decapitated. The brain was transferred into ice-cold dissection buffer containing (in mM): 87 NaCl, 3 KCl, 1.25 NaH_2PO_4, 26 $NaHCO_3$, 7 $MgCl_2$, 0.5 $CaCl_2$, 20 D-glucose, 75 sucrose and 1.3 ascorbic acid aerating with 95% O_2–5% CO_2. Thalamocortical slices 400 μm were made on an angled block (Agmon and Connors 1991) using a vibratome (Vibratome 1000 Plus). Following cutting, slices were transected parallel to the pia mater to remove the thalamus and midbrain. This transection was not done for the first experiment (see Fig. 1D,E and indicated in corresponding text). Slices were immediately transferred to an interface recording chamber (Harvard Instruments) and allowed to recover for 1 hr in nominal ACSF at 32ºC containing (in mM): 126 NaCl, 3 KCl, 1.25 NaH_2PO_4, 26 $NaHCO_3$, 2 $MgCl_2$, 2 $CaCl_2$, and

25 D-glucose. After this, slices were perfused with a modified ACSF that better mimics physiological ionic concentrations *in vivo* which contained (in mM): 126 NaCl, 5 KCl, 1.25 NaH_2PO_4, 26 $NaHCO_3$, 1 $MgCl_2$, 1 $CaCl_2$, and 25 D-glucose (based on but modified from (Sanchez-Vives and McCormick 2000; Gibson, Bartley et al. 2008)). We used a slightly higher external K^+ concentration to promote active states (5 mM versus 3.5 mM *in vivo*), but this manipulation was probably unnecessary since the use of 3.5 mM external K^+ still results in spontaneously generated UP states (Rigas and Castro-Alamancos 2007). Slices remained in this modified ACSF for 45 minutes and then recordings were performed with the same modified ACSF.

UP state recordings and analysis

Spontaneously generated UP states *in vitro* were extracellularly recorded using 0.5 MΩ tungsten microelectrodes (FHC, Bowdoinham, ME) placed in layer 4 of primary somatosensory cortex. This extracellular monitoring of UP states is a reliable indicator of the synchronous, depolarized state of neuron populations from which the term "UP state" was originally defined (Sanchez-Vives and McCormick 2000; Rigas and Castro-Alamancos 2007). As indicated, some recordings were performed in layer 5. 10 min of spontaneous activity was collected from each slice. For drug wash-on experiments, data was collected for 70 min. Recordings were amplified 10K fold, sampled at 2.5 kHz, and filtered

on-line between 500Hz and 3 kHz. All measurements were analyzed off-line using custom Labview software. For visualization and analysis of UP states, traces were offset to zero, rectified, and low-pass filtered with a 0.2 Hz cutoff frequency. Using these processed traces, the threshold for detection was set at 4x the RMS (root mean square) noise (5x for picrotoxin + CGP55845 experiments in figure 4) , and an event was defined as an UP state if its amplitude remained above the threshold for at least 200 ms. The end of the UP state was determined when the amplitude decreased below threshold for >600 ms. Two events occurring within 600ms of one another were grouped as a single UP state. These criteria best accounted for the simultaneous occurrence and identical durations of UP states in layers 4 and 5 (see Fig. 2). Our main finding of longer UP states in *Fmr1* KO mice (see Fig. 1) was not strictly dependent on these criteria since the same result was obtained with no grouping of events and with different detection thresholds. UP state amplitude was defined based on the filtered/rectified traces and was unitless since it was normalized to the detection threshold. This amplitude may be considered a coarse indicator of the underlying firing rates of neuronal populations. Direct measures of firing rates were not possible because individual spikes could not be resolved except during the quiet periods (the DOWN states). Data are represented by the mean ± SEM and values. Significant differences were determined using t-tests, one-way ANOVA, two-way ANOVA, or three-way ANOVA where appropriate (all performed with GraphPad Prism 5

except for the three-way which was performed with Sigmaplot). Repeated measures ANOVA was also used when appropriate. Bonferroni posttests were performed following ANOVAs. Sample number (n) is slice or mouse number – the latter for *in vivo* experiments. For all slice experiments, a minimum of 4 mice were used per condition, and on average, 4 slices were examined per mouse.

For cumulative distributions of UP state durations, a normalized cumulative distribution was obtained for each experiment (data from one slice or for *in vivo* experiments, from one mouse), where y values were interpolated for pre-determined points of the x-axis. This enabled the calculation of an average and standard deviation based on experiment, where sample number refers to either slice number or mouse number (the latter for *in vivo*). A Kolmogorov-Smirnov test was performed for statistical analysis. This method equalizes the contribution to the distribution made by each experiment.

Autocorrelations were performed on rectified and filtered traces for 300 second and 60 second epochs for slices and *in vivo* recordings, respectively. Autocorrelations were normalized to the variance resulting in a peak of 1 at time zero. To measure rhythmicity, we measured the side-peaks of the autocorrelogram by averaging the two peak-to-trough distances from each side of the peak.

Group I mGluR antagonist and protein synthesis inhibitor pretreatment

As stated above, slices underwent an initial 1 hour incubation in nominal ACSF. Like other experiments, slices were then exposed to the "modified" ACSF for the next 45 minutes, but in experiments using a Group I metabotropic glutamate receptor (mGluR) antagonists, this latter period included the pretreatment with the antagonist in the ACSF. In experiments inhibiting protein synthesis, this latter period included pretreatment with anisomycin (20 μM). The antagonist or anisomycin remained in the ACSF for the remainder of the experiment – including the recording periods. The pretreatment experimental design, as opposed to application while recording, enabled us to examine many more slices in a single experiment since slices were stored and recorded from the same chamber (see *slice preparation* above). More recordings meant that we obtained more accurate UP state duration values (which varied a few hundred ms from one experiment to the next) and meant that we could more readily detect 35-50% changes in UP state duration among the 8 groups compared in the mGluR antagonist experiments (see Fig. 7B). The pre-incubation time was selected because previous studies have shown the mGluR regulated protein synthesis has electrophysiological effects on this time scale. The mGluR antagonists were the mGluR5-selective antagonist, MPEP (10 μM), and the mGluR1-selective antagonist, LY367385 (100 μM).

Recordings in vivo

3-4 week old mice were anesthetized with urethane (1.5g/kg, 20% solution in distilled water) supplemented with isoflurane (1.5%, 1.5 L/min O_2 flow) and placed in a stereotaxic apparatus with anesthetic maintained. A scalp incision was performed and a craniotomy performed at 2 mm posterior to bregma and 2.5 mm lateral to midline. An extracellular recording electrode (same as described for *in vitro*) was inserted into the craniotomy and advanced to approximately layer 4 and layer 5 of cortex as confirmed with lesions observed after brain fixation. At this point, isoflurane application was stopped, and recordings were performed for 20-30 minutes. Health and depth of anesthesia were monitored by body temperature, heart rate, respiratory rate, tail pinch reflex, and by the clear occurrence of cycling between UP and DOWN states. Any indication of a lighter anesthesia plane resulted in additional injection of urethane. Immediately after recording, the mouse was euthanized with an overdose of Euthasol (pentobarbital sodium and phenytoin sodium solution).

Immunohistochemistry

Immunohistochemistry was performed on progeny of Cre (*Emx1* and *Dlx5/6* Cre) and floxed *Fmr1* mice to confirm cell-type specific deletion of *Fmr1*. Mice (P21-P24) were perfused with cold PBS followed by 4% paraformaldehyde (w/v). The brain was removed and resectioned into 80 µm slices. Antigen retrieval was performed by placing the slices into warm 200 mM sodium citrate

and microwaving for 1 min at low power. The slices were blocked for 1 hr at room temperature in PBS with 3% normal goat serum and 0.5% Triton-X. Primary antibodies were dissolved in blocking solution and applied overnight at 4°C. Secondary antibodies were dissolved in blocking solution and applied for 1 hr at room temperature. Primary antibodies used were mouse anti-FMRP (2F5, 1:200, gift from Dr. Jennifer Darnell, Rockefeller University) and rabbit anti-GABA (A2052, 1:1000, Sigma). The specificity of 2F5 has been demonstrated previously (Gabel, Won et al. 2004) and by our comparison of labeling in *Fmr1* KO versus WT tissue. Specificity of A2052 has been demonstrated previously (Stevens, Smith et al. 2010) and in this study, its labeling was consistent with our use of the *DLX5/6* Cre mouse which is GABAergic neuron specific (see Fig. 5, FMRP was deleted only in GABAergic neurons) (Monory, Massa et al. 2006). Secondary antibodies used were goat anti-mouse 555 and goat anti-rabbit 488 (1:250, Sigma).

Reagents

Drugs were prepared as stocks and stored at -20°C and used within two weeks. The mGluR1-selective antagonist (S)-(+)-α-amino-4-carboxy-2-methylbenzeneacetic acid (LY367385,100 μM), the mGluR5-selective antagonist 2-methyl-6-(phenylethynyl)-pyridine hydrochloride (MPEP, 10 μM), the protein

translation inhibitor, anisomycin (20 μM), the GABAB receptor antagonist, CGP55845 (1 μM), and the mixed group I mGluR agonist (RS)-3,5-dihydroxyphenylglycine (DHPG, 10 μM) were purchased from Tocris Bioscience (Ellisville, MO). The GABAA receptor antagonist, picrotoxin (100 μM), was purchased from Sigma. Drugs required 12-18 minutes upon start of application to reach and perfuse the slice at the steady state concentration due to delays in the perfusion system.

Results

Spontaneously occurring UP states are longer in layer 4 of Fmr1 *KO slices*

Spontaneously generated active states, or UP states, were measured in acute neocortical slices obtained from 3-4 week old WT and *Fmr1* KO mice. UP states were measured with extracellular, multi-unit recordings in layer 4, and then analyzed after rectification and lowpass filtering of the recorded traces (Fig 1A; see Methods). Activity in both WT and KO slices sometimes occurred in closely associated bursts that we grouped together as a single UP state in our analysis (Fig. $1A_2$ and $1B_4$; See Methods). UP states in some slice recordings were not observably rhythmic, but in other recordings, were weakly rhythmic. This weak

rhythmicity was observed by autocorrelograms of the rectified, filtered traces (Fig. 1C).

Similar to thalamically-evoked activity states (Gibson, Bartley et al. 2008), the duration of spontaneously occurring UP states observed in *Fmr1* KO slices was increased by 59% compared to WT (Fig. 1D,E; 777±39 vs. 1236±85 ms, $p<0.001$; WT, KO; n=18, 18 slices). While this analysis was performed by detecting discrete UP states (see Methods), the altered spontaneous activity could also be observed by another independent method that did not rely on our detection of UP states - the autocorrelation of the rectified, filtered traces. The width at half height of the autocorrelation function was 54% larger for traces obtained from KO slices (Fig. 1C; 302±25 vs. 466±50 ms, $p<0.05$; WT, KO), consistent with the longer duration UP states in the KO. Slices in these initial experiments contained the thalamus and its connections with neocortex, and therefore it was possible that the thalamus might be playing a role in the longer UP states. This was not the case since all successive experiments were performed with all subcortical regions removed, and UP states were still longer to the same extent (see controls in Figs. 5-8). The abnormally long UP states persist at later ages (7 weeks) since KO slices obtained from older animals, 7-8 weeks of age, also had longer UP states although the difference was not as pronounced (Fig 1F: 489±29 vs. 640±38 ms, $p<0.01$; WT,KO; n=16, 19 slices).

We examined other UP state characteristics in 3 week old slices by adding control data from another experiment (see controls in Fig. 6. n=46, 41). In addition to duration being similarly longer in this larger data set (67% increase; 761±37 vs. 1274±57 Hz, $p<0.001$; WT, KO), we were able to detect an 18% decrease in UP state frequency (Fig. 1G; 0.185±0.011 vs. 0.151±0.013 Hz, $p<0.05$; WT, KO) and a 35% increase in the percent of time spent in the UP state (13.5±0.8 vs. 18.2±1.1 %, $p<0.001$; WT, KO). The number of bursts within an UP state was also increased by 29% (1.68±0.04 vs. 2.16±0.09 bursts, $p<0.001$; WT, KO), but this did not completely account for the 67% increase in duration. We detected no change in the normalized amplitude of UP states as defined by our rectified, filtered traces (5.4±0.4 vs. 6.4±0.5, $p=0.08$; WT, KO; see Methods) which may reflect no change in the underlying intensity of action potential firing that occurs during UP states. In summary, while a number of characteristics of UP states may be altered in *Fmr1* KO slices, the duration increase was the most salient.

UP states are also prolonged in layer 5

On the scale of seconds, UP states occur roughly simultaneously in all layers in a local neocortical circuit, but on the scale of 10-150 milliseconds, differences in onset and duration across layers are observed (Sanchez-Vives and

McCormick 2000; Chauvette, Volgushev et al. 2010). Therefore, it was not clear if the longer UP states we observed in layer 4 of *Fmr1* KO slices represented a more general phenomenon across all layers. With all the layer 4 recordings depicted in figure 1, we simultaneously recorded from layer 5 (Fig. 2A, n=35, 39). Average UP state duration in layer 5 was not different from that recorded in layer 4 in the same slice. Also, layer 5 UP state duration was longer in *Fmr1* KO compared to WT slices (Fig. 2B, 756 ± 34 vs. 1233 ± 83 ms, $p<0.001$; WT, KO). UP states in a single slice vary in duration, and the length of a single UP state in one layer was strongly correlated with the length in the other layer when examining the inter-layer correlation of UP state durations in a single experiment (Fig. 2C; correlation for durations, WT: R=0.83 ± 0.07; KO: R=0.84 ± 0.03; n=6, 8). There is spontaneous unit activity during the quiet states (or DOWN states) in layer 5 as previously reported (Sanchez-Vives and McCormick 2000), and we observed this in both WT and KO slices with no detected differences in spike frequency (Fig. 2A; 0.92 ± 0.12 vs. 0.96 ± 0.09 Hz; WT, KO; n=16, 16).

A cross correlation analysis of the rectified/filtered traces (not durations as in Fig. 2C) was performed on layer 4 and 5 recordings for each slice, and this indicated a high average correlation (R=0.88 ± 0.02 vs. 0.92 ± 0.01, $p<0.05$; WT, KO) and a slight delay in the layer 4 signals relative to layer 5 (12.7 ± 1.4 vs. 13.7 ± 1.5 ms; WT, KO). The delay is consistent with earlier studies indicating that UP states are initiated in layer 5 (Sanchez-Vives and McCormick 2000). While

these data show an increase in correlation in the KO slices, this difference was small. When examining the raw traces from layer 4 and 5, very little correlation was observed suggesting that while the underlying UP state event is synchronous, the precise firing of neurons in layer 4 and 5 is, in general, not synchronous. In summary, while UP states are longer in both layers 4 and 5 of *Fmr1* KO slices, the relative onset and synchrony of UP states in the two layers appear to be normal.

It has been demonstrated that the deep layers (layers 5 and 6), and not the superficial layers, are sufficient to generate UP states (Sanchez-Vives and McCormick 2000). To determine if the longer UP states are intrinsic to particular cortical layers, we repeated layer 5 recordings from slices containing only the deep layers of neocortex. Slices were resectioned by removal of superficial cortex (layers 1-4, Fig. 2D). UP state duration in both WT and *Fmr1* KO resectioned slices was slightly decreased compared to normal slices but UP state frequency remained unchanged suggesting that these slices were still healthy. Resectioned KO slices still had longer UP states in layer 5 (Fig. 2E,F: 549±27 vs. 733±55 ms; WT, KO; n=22, 22). This indicates that longer UP states in layer 5 of the *Fmr1* KO are, to a large extent, intrinsic to deep layer circuitry.

Rhythmically occurring UP states are longer in Fmr1 KO mice, in vivo

To determine if the longer UP states we observe in *Fmr1* KO slices were a physiologically relevant phenomenon, we recorded UP states in somatosensory cortex *in vivo* in anesthetized mice. As in the acute slices, UP states were indeed longer in *Fmr1* KO mice and had similar durations as those observed in acute slices (Figs. 3A,B; 765±112 vs. 1130±112 ms, $p<0.05$; WT, KO; n=9, 11 mice). We observed no change in the frequency of UP states (Fig. 3C; 0.26±0.03 vs. 0.25±0.03 Hz; WT, KO) which is consistent with our *in vitro* findings where the frequency change was less salient than the duration change. Other parameters were unchanged in the KO, such as the amplitude of the UP states as defined by our rectified, filtered traces (16.0±3.3 vs. 14.6±2.0, WT, KO, unitless, see Methods). These results demonstrate that our observations *in vitro* reflect an existing condition *in vivo*.

The UP states *in vivo* probably occurred as part of the slow oscillation which has been previously been clearly observed in anesthetized cats (Steriade, Nunez et al. 1993; Steriade, Nunez et al. 1993) and mice (Fellin, Halassa et al. 2009). Our recordings contained a distinct rhythmic component which was less than 1 Hz, and therefore reminiscent of the slow oscillation. This can be observed in the autocorrelogram of the rectified, filtered traces (Fig. 3D). When we quantified the consistency of the rhythm in our recordings, we found that UP states *in vivo* were more rhythmic compared to those measured in slices. This was first evident by comparing autocorrelograms of the rectified/filtered traces.

The first side-peak of the autocorrelogram was larger from recordings *in vivo* (0.30±0.09/0.41±0.11; WT/KO; n=9, 11) compared to slices (0.14±0.07/0.13±0.07; WT/KO; n=18, 19; 2-way ANOVA, $p<0.001$ for preparation type). The same result was observed for the second, more distant, side-peak as well (0.30±0.09/0.38±0.11 vs. 0.15±0.05/0.15±0.05; *in vivo* vs. slice; $p<0.001$). Side-peaks always occurred in increments greater than 1 second consistent with the frequency of the slow oscillation. We also measured the ratio of the standard deviation to the average period length for each experiment, and this was lower *in vivo* indicating again that UP state re-occurrence was more regular, and hence more rhythmic (0.41±0.14/0.35±0.18 vs. 0.59±0.12/0.57±0.14; *in vivo* vs. slice; $p<0.05$, 2-way ANOVA). Finally, if UP states were occurring randomly and not rhythmically, the period length distribution would be in the form of a decaying exponential (like the classical theory of mEPPs) (Johnston and Wu 1995). *In vivo,* this was not the case since the average distribution of periods was a 2-tailed, single peaked function and not a decaying exponential (data not shown). This, again, was less clear in slices where the WT distribution for periods appeared more weakly 2-tailed, single-peaked, but for the KO, neither a 2-tailed or decaying exponential distribution could be resolved. In summary, our *in vivo* data suggest that the UP state portion of the slow oscillation is lengthened in the *Fmr1* KO mouse.

Changes in excitatory circuitry contribute to longer UP states

To begin to understand the locus of change that causes prolonged UP states in *Fmr1* KO mice, we next tested if neocortical excitatory circuitry alone displays properties that would promote longer activity states. We isolated the role of excitatory circuitry in generating spontaneously active states by pharmacologically blocking $GABA_A$ and $GABA_B$ receptors using the antagonists picrotoxin (100 μM) and CGP55845 (1 μM), respectively. Block of these GABAergic receptors resulted in periodic epochs of persistent activity that were different from normal UP states in both duration and shape (Fig. 4). These active states were longer in the *Fmr1* KO (Fig. 4A,B: 5.2±0.5 vs. 12.1±1.3 sec, $p<0.01$; WT, KO; n=17, 16), suggesting that alterations occurring in excitatory circuitry promote longer activity states. Neither the number of bursts per active state nor the frequency at which active states occurred were detectably different in the KO in the presence of GABA receptor antagonists (bursts/active: 5.4±1.0 vs. 9.0±1.5, $p=0.06$: frequency: 0.026±0.004 vs. 0.022±0.002 Hz, $p=0.44$; WT, KO), but the antagonist treatment itself resulted in more bursts per active state ($p<0.01$) and a much lower frequency of occurrence (~15% of untreated, $p<0.001$) when compared to untreated slices in figure 1G. Treatment had no detectable effect on percent of time in an active state but did increase normalized amplitude for both genotypes (~30%, $p<0.05$). Additional experiments implementing $GABA_A$ receptor block alone (picrotoxin, 100 μM) also resulted in longer active states in

Fmr1 KO slices (2.0±0.2 vs. 2.8±0.3 sec, $p<0.05$; WT, KO; n=15, 14) indicating that changes in $GABA_A$ signaling alone did not play a significant role in longer UP states. In summary, these data support the assertion that alterations in the recurrent excitation process among excitatory neurons play a significant role in prolonged UP state duration in the *Fmr1* KO mouse.

Blocking GABAergic synapses in hippocampal slices causes a slowly occurring induction of very long persistent activity states in the CA3 region – but only in *Fmr1* KO slices and not WT slices (Chuang, Zhao et al. 2005). This plasticity of cell excitability requires group I mGluR activation. The long activity states in CA3 occur intermittently among very short activity states, and hence, the distribution of durations is bimodal. In a subset of slices in this study, neocortical UP states were measured before and during picrotoxin + CGP55845 application (Fig. 4C,D, n=10,10) and before and during picrotoxin application alone (data not shown, n=7,6). In both sets of experiments, drug application quickly lengthened UP state duration in both WT and KO slices to the same extent and after 60 minutes, the distribution of durations in a single experiment were unimodal in distribution. Therefore, our data demonstrate that the effects of inhibitory blockade on network activity states in *Fmr1* KO slices are different in neocortex compared to those observed previously in the hippocampus.

Longer UP states are due to deletion of Fmr1 *in cortical excitatory neurons*

Next, we determined the relevant locus of *Fmr1* deletion that causes longer UP states in *Fmr1* KO mice. To address this question, we compared the effects of *Fmr1* deletion in excitatory neurons versus inhibitory neurons.

To perform excitatory neuron specific deletion, we crossed *Emx1* Cre males with floxed *Fmr1* females. In the *Emx1* Cre mouse line, Cre is expressed only in cortical excitatory neurons (i.e. neocortex and hippocampus) (Iwasato, Datwani et al. 2000; Iwasato, Inan et al. 2008). Using immunohistochemistry, we confirmed that Cre^{+}:$Fmr1^{flox/Y}$ progeny had *Fmr1* deleted only in cortical excitatory neurons while other genotypes showed no *Fmr1* deletion (Fig. 5A). In control mice (Cre^{-}:$Fmr1^{+/Y}$, Cre^{+}:$Fmr1^{+/Y}$, Cre^{-}:$Fmr1^{flox/Y}$), 96% of GABAergic neurons were FMRP+ while 15% of FMRP+ neurons were GABAergic. Since GABAergic and glutamatergic neurons comprise 15% and 85% of all neurons in neocortex, respectively (Gonchar and Burkhalter 1997), these immunohistochemical data are consistent with FMRP expression in both excitatory and inhibitory neurons. In mice undergoing recombination (Cre^{+}:$Fmr1^{flox/Y}$), 98% of GABAergic neurons were FMRP+ and 97% of FMRP+ neurons were GABAergic. In other words, with recombination, only the GABAergic neurons were FMRP+ while the neocortical excitatory glutamatergic

neurons, by inference, were all FMRP-. FMRP expression in other noncortical structures, such as striatum and thalamus, was normal. When we examined UP states among the 4 possible genotypic combinations, we found that slices obtained from mice with deletion of *Fmr1* in cortical excitatory neurons was sufficient to mimic the long UP states of *Fmr1* KO mice (Fig. 5B; Cre^{-}:$Fmr1^{+/Y}$=986±56, Cre^{+}:$Fmr1^{+/Y}$=939±39, Cre^{-}:$Fmr1^{flox/Y}$=776±74, Cre^{+}:$Fmr1^{flox/Y}$=1398±83 ms; $p<0.001$ comparing Cre^{+}:$Fmr1^{flox/Y}$ with any other genotype; n=20, 22, 19, 19). No change in UP state frequency was detected in any genotype.

Next we examined the role of *Fmr1* deletion from inhibitory neurons. We crossed *Dlx5/6* Cre males with floxed *Fmr1* females. In the *Dlx5/6* Cre mouse line, Cre is expressed in GABAergic neurons in the forebrain, and occasionally, in some excitatory neurons in some regions of more ventral neocortex (Dr. John Rubenstein, personal communication; (Monory, Massa et al. 2006)). But somatosensory cortex is dorsal, and therefore Cre expression should be restricted to GABAergic neurons. This was confirmed by immunohistochemistry. In control mice (Cre^{-}:$Fmr1^{+/Y}$, Cre^{+}:$Fmr1^{+/Y}$, Cre^{-}:$Fmr1^{flox/Y}$), 99% of GABAergic neurons were FMRP+ while 14% of FMRP+ neurons were GABAergic – again consistent with expression of FMRP in both excitatory and inhibitory neurons. In mice undergoing recombination (Cre^{+}:$Fmr1^{flox/Y}$), 0% of GABAergic neurons were FMRP+ and 0% of FMRP+ neurons were GABAergic, confirming that FMRP was deleted from all GABAergic neurons (Fig. 5A). Unlike that found for

deletion of *Fmr1* in cortical excitatory neurons, we found that deletion of *Fmr1* in inhibitory neurons had no effect on UP state duration (Fig. 5C; Cre^-:$Fmr1^{+/Y}$=729±50, Cre^+:$Fmr1^{+/Y}$=776±32, Cre^-:$Fmr1^{flox/Y}$=811±49, Cre^+:$Fmr1^{flox/Y}$=791±56 ms; n=20, 19, 21, 22). Therefore, the longer UP states in the *Fmr1* KO are induced by deletion of *Fmr1* in cortical excitatory neurons.

Longer UP states are rescued by genetic reduction mGluR5 signaling

Ample evidence suggests that many phenotypes in *Fmr1* KO mice are due to excess group 1 metabotropic glutamate receptor (mGluR1 or mGluR5) signaling – specifically that mediated by mGluR5 (Huber, Gallagher et al. 2002; McBride, Choi et al. 2005; Yan, Rammal et al. 2005; Dolen, Osterweil et al. 2007; Meredith, de Jong et al. 2010). To test whether excessive activation of mGluR5 contributes to the longer UP states, we bred mGluR5 (*Grm5)* KO mice with *Fmr1* KO mice to produce *Grm5* heterozygous progeny, which has previously been shown to decrease mGluR5 protein to 60% of normal levels, and thereby presumably decreasing the signaling mediated by this receptor (Dolen, Osterweil et al. 2007). Using this strategy, we compared UP state duration between WT and *Fmr1* KO mice on both a *Grm5* WT background and on a *Grm5* heterozygous background. UP states measured on the *Grm5* heterozygous background (*Fmr1*KO/*Grm5*Het mice) had normal duration in KO slices (Fig. 6A,C; 683±57 vs. 1310±64 ms, $p<0.001$, n=29, 23 for WT, KO;

*Fmr1*KO/*Grm5*Het=785±67 ms, $p<0.01$, n=21, when compared to *Fmr1* KO) and in KO mice, *in vivo* (Fig. 6B,D; 579±74 vs. 1205±232 ms, $p<0.01$, n=6, 4 for WT, KO; *Fmr1*KO/*Grm5*Het=785±67 ms, $p<0.05$, n=7, when compared to *Fmr1* KO). This indicated that a reduction of mGluR5 levels in the *Fmr1* KO normalizes, or rescues, UP state duration. The reduction of mGluR5 dosage on a WT background does not cause any change in UP state duration in both slices (*Grm5het*: 828±45 ms, n=16) and *in vivo* (*Grm5het*: 822±46 ms, n=10), indicating that a reduction of mGluR5 levels alone does not affect UP states. No differences in amplitude or frequency of UP states were detected across genotypes. Taken together, this implicates enhanced mGluR5 activation in contributing to longer UP states in neocortical circuits of *Fmr1* KO mice.

Longer UP states are rescued by pharmacological blockade of mGluR5 signaling

To determine whether group I mGluRs play an acute, as opposed to a developmental, role in determining UP state duration, we examined the effects of specific group 1 mGluR antagonists on UP states in WT and *Fmr1* KO slices. Our strategy incorporated a 3 factor design based on 1) genotype, 2) pretreatment with the mGluR5-selective antagonist, MPEP (10 μM), and 3) pretreatment with mGluR1-selective antagonist, LY367385 (100 μM). This resulted in a comparison of UP state duration among 8 different groups (Fig. 7A,B). We measured UP states after 45 minutes of pretreatment and with drug still present.

We found that MPEP, but not LY367385, had a differential effect on UP state duration which indicated that mGluR5 signaling, but not mGluR1 signaling, was acutely altered in *Fmr1* KO slices. This was observed by three-way ANOVA analysis of duration data, which revealed a significant interaction between MPEP treatment and genotype ($p<0.5$) while no interaction was detected between LY treatment and genotype.

Comparisons between individual groups (Bonferroni post-tests) also supported differential acute mGluR5 signaling. While untreated WT and KO slices had different durations (Fig. 7B; 1038±59 vs. 1428±63 ms, $p<0.001$, n=42, 38), no difference was observed for MPEP treated WT and KO slices (935±54 vs. 1076±63 ms, n=32, 44). These same data indicated that MPEP had no detectable effect on UP state duration in WT slices, but decreased UP state duration in KO slices ($p<0.001$). No changes in frequency of UP states were detected with MPEP treatment. Therefore, while mGluR5 signaling does not contribute to UP state duration in WT slices, it does contribute to prolonged duration in KO slices. In summary, these data show that the longer UP state duration phenotype in KO slices is rescued to normal WT durations by acutely blocking mGluR5.

However, we observed that wash-in of MPEP had no effect on UP state duration in either WT or KO slices (Fig. 8A,B; 45min after MPEP treatment; WT: 876±122 vs. 961±100 ms, $p=0.61$, n=13; KO: 1301±89 vs. 1264±82 ms, $p=0.60$, n=13; paired T-test). This is in direct contrast to the reduction in UP state

duration in KO slices that were pretreated with MPEP (Fig.7). One explanation for this difference may lie in the experimental design. In all cases, slices are exposed to the high activity ACSF 45 min before recording. In the experiments in Fig. 8, the MPEP is in the high activity ACSF, and thus would be present in the slice during the induction of increased activity. For wash-in experiments presented in Fig. 8, the slices receive the high activity ACSF for approximately 60 min before the MPEP treatment to allow for a pre-treatment baseline recording to be established. Therefore, the slices have 60 min of high activity before MPEP treatment, and during this time, the circuit may become hyperactive in the KO and may not revert to normal activity with MPEP treatment. This implicates a possible plasticity phenomenon in the generation of prolonged UP states in the KO. However, under basal conditions *in vivo*, UP states are prolonged in the KO, suggesting that the circuit is hyperactive before any plasticity takes place. Because of the contradictory nature of this observation, we could not adequately interpret these results. MPEP treatment followed by *in vivo* recordings could address this discrepancy.

In contrast to MPEP, the selective blockade of mGluR1 signaling with LY367385 had a strong but similar effect on both WT and KO slices. For both genotypes, UP state duration, UP state frequency, and the incidence of slices displaying UP states were reduced by approximately 40-60% ($p<0.05$ for all). However, duration was still longer in the KO (Fig. 7B; LY367385 results: 456±26

and 720±72 ms, $p<0.05$, n=21, 22). Therefore, mGluR1 function strongly regulates UP states, but does so similarly in both WT and *Fmr1* KO slices.

Longer UP states do not depend on recent protein translation

One function of FMRP is to suppress translation of its mRNA targets (Bassell and Warren 2008). Therefore, it has been proposed that without FMRP, as in Fragile X Syndrome, there is excess mGluR5 driven translation which leads to phenotypes of the disease (Bear, Huber et al. 2004; Dolen and Bear 2008). In support of this idea, mGluR5 and translation dependent plasticity is upregulated in *Fmr1* KO mice (Huber, Gallagher et al. 2002; Bear, Huber et al. 2004; Chuang, Yan et al. 2004). Therefore, it is possible that mGluR5 signaling causes longer UP states in KO slices through signaling to translation. If so, inhibiting protein translation would be expected equalize UP state duration among WT and KO slices similar to MPEP. We pre-incubated slices in the translational inhibitor anisomycin (20 μM) for 45 minutes prior to and during recording. This treatment had no effect on UP state duration in either WT or KO slices (Fig. 9) suggesting that at the time scale studied here, longer UP states in *Fmr1* KO mice are not due to mGluR5 dependent protein synthesis, but instead due to a translation independent signaling function of mGluR5.

Group I mGluR activation increases UP state duration non-differentially

In support of the mGluR antagonist studies above, pharmacological enhancement of group I mGluR activity was sufficient to prolong UP state duration in WT and *Fmr1* KO slices. Application of the group I agonist, DHPG (10 μM), increased the duration of UP states in WT slices (Fig. 10A,B; WT untreated: 671.7± 103.2 ms; WT+DHPG 826.8±131.4 ms; $p<0.01$; n=6) and *Fmr1* KO slices (Fig. 10A,B; *Fmr1* KO untreated: 1361±141.1 ms; WT+DHPG: 1639±134.4 ms; $p<0.05$; n=7). The increase in duration for both genotypes were proportionally identical (Fig. 10B), and based on the non-differential affect of mGluR1 antagonists in figure 7, these similar effects of DHPG may be acting through mGluR1 receptors.

We monitored UP states before and after DHPG application in these experiments since, in previous studies, DHPG caused normally quiet hippocampal CA3 region slices to display very long activity bursts interspersed with shorter bursts (bimodally distributed peaks at 0.5 seconds and at 4-10 seconds) (Taylor, Merlin et al. 1995; Chuang, Zhao et al. 2005). We did not observe this type of change in our neocortical slice preparation (Fig. 10A) indicating that different group I mGluR regulated processes are occurring in neocortex.

Discussion

Little is known about circuit dysfunction in *Fmr1* KO mice, or for that matter, in any mouse model of intellectual disability or autism. In this study, we find that spontaneously occurring UP states are longer in the mouse model of Fragile X Syndrome – the *Fmr1* KO mouse. UP states were 62% longer in slices (combining data from Figs. 1C,6,7,8) and 67% longer *in vivo* (combining data from Figs. 3,6) – the latter supporting the physiological relevance of this network functional change. Neocortical excitatory neurons are probably the most significant locus of these changes since, 1) electrophysiological changes causing the longer UP states are intrinsic to neocortex, 2) activity bursts mediated by excitatory circuitry alone are longer in *Fmr1* KO slices, and 3) the specific locus for *Fmr1* deletion that induces longer UP states is neocortical excitatory neurons. Finally, we find that enhanced mGluR5 signaling underlies the longer UP states in *Fmr1* KO slices.

Longer spontaneously occurring UP states in Fmr1 *KO mice*

We have previously demonstrated that UP states in response to thalamic stimulation were longer in *Fmr1* KO mice (Gibson, Bartley et al. 2008). However, it was not clear to what extent this resulted from alterations in thalamic circuitry since interactions between the thalamus and neocortex can affect UP states (Rigas and Castro-Alamancos 2007; Crunelli and Hughes 2010). Here we show that spontaneously occurring and rhythmic UP states are longer in the *Fmr1*

KO mouse. In slices, these UP states are mediated by neocortical circuits, independent of any thalamic pathway stimulation, and independent of the thalamus itself. The results also indicate that longer thalamically evoked UP states in *Fmr1* KO slices are mostly likely due to changes in neocortex and not to changes in thalamic circuitry. Because spontaneously occurring UP states are thought to be the cellular process underlying the slow oscillation during sleep (Steriade, McCormick et al. 1993), our data more directly suggest that the increase in UP state duration and time spent in the UP state (Fig. 1) may impact processes involving the slow oscillation rhythm in Fragile X patients. This possible link is strengthened by our observations of longer UP states *in vivo* which were observed with a clear rhythmic component reminiscent of the slow oscillation.

The *synchrony* of UP states among different neocortical areas relies on long distance projections, but the actual *generation* of UP states depends on local network function (approximately 1 mm radius) since they directly rely on recurrent synaptic excitation and inhibition among neurons in a local neocortical region (Haider and McCormick 2009). Therefore, the longer UP states in *Fmr1* KO mice are probably caused by network changes on this local scale, and more specifically, our study indicates that changes in local excitatory circuits likely play a significant role.

Comparison with prolonged epileptic bursts in CA3 of Fmr1 *KO mice*

Properties of persistent activity states observed in the CA3 region of the hippocampus are also altered in *Fmr1* KO slices (Chuang, Zhao et al. 2005). These activity states are not UP states, but instead are prolonged epileptic bursts which are induced experimentally by group I mGluR agonists in both WT and *Fmr1* KO slices (Taylor, Merlin et al. 1995). Interestingly, they can also be induced with the application of a GABAergic antagonist which, in turn, activates group I mGluRs, but this method of induction only occurs in *Fmr1* KO slices, and not in WT slices (Chuang, Zhao et al. 2005). Our observations of prolonged UP states may have a common link with prolonged bursts in CA3 since both involve prolonged activity states, both depend on changes in group I mGluR signaling, and both appear to be mediated by changes in excitatory neurons. Moreover, longer UP states in the neocortex (Fig. 7), as well as epileptic bursts in the hippocampal slices obtained from *Fmr1* KO mice, are both reduced to normal durations with mGluR5 antagonism (Chuang, Zhao et al. 2005).

However, our findings differ in some key aspects. First, while persistent activity states in hippocampal CA3 slices permit the effective study of the plasticity of neuronal excitability, they are epileptic in nature and require intense pharmacological manipulations for their induction. On the other hand, UP states are widely thought to underlie aspects of neocortical function under normal conditions. Also, they do not require any special induction protocol, but instead,

occur spontaneously as a baseline process. Bursts in CA3 can be induced by GABAergic receptor blockade, but only in *Fmr1* KO slices, while GABAergic receptor blockade similarly increases UP state duration in both WT and KO neocortical slices (Fig. 4). Finally, CA3 bursts require new protein synthesis, whereas prolonged neocortical UP states persist independent of new protein synthesis (Fig. 9).

Together, our data and that of Chuang et al., reveal an mGluR5-mediated hyperexcitability of circuit function in *Fmr1* KO mice that is common to both hippocampus and neocortex. However, such circuit dysfunction is manifest differently in the two brain regions, perhaps due to the anatomy and physiology of the circuit or distinct function or localization of mGluR5 within each brain region.

Role of group I mGluRs

Our study indicates that enhanced mGluR5 signaling acutely leads to longer UP states in *Fmr1* KO slices. Enhanced mGluR5 signaling is not caused by increased mGluR5 protein in *Fmr1* KO mice since protein level is unchanged (Huber, Gallagher et al. 2002; Dolen, Osterweil et al. 2007). Instead it appears that signaling somewhere downstream of mGluR5 activation is enhanced, and while studies have focused on enhanced mGluR-induced protein translation in the *Fmr1* KO (Bear, Huber et al. 2004; Osterweil, Krueger et al. 2010), our data here support enhanced signaling independent of protein translation as well (Fig. 8).

According to this interpretation of our results, the reduction of mGluR5 protein levels through genetics restores normal UP state duration (Fig. 6) by offsetting the increased signaling of individual mGluR5 receptors. Unlike mGluR5 antagonism, mGluR1 antagonism robustly suppressed the duration and frequency of UP states to a similar extent in both WT and *Fmr1* KO slices (Fig. 7B). These data suggest that mGluR1 regulation of UP states is normal in *Fmr1* KO mice. mGluR1 and mGluR5 may regulate UP state duration through a number of mechanisms including modulation of the intrinsic excitability of neocortical neurons or synaptic function within the circuit (Kim, Kim et al. 2003; Young, Chuang et al. 2004; Bianchi, Chuang et al. 2009; Niswender and Conn 2010). To our knowledge, this is the first indication for dysfunction of a specific group 1 mGluR (mGluR5, but not mGluR1) in *Fmr1* KO mice.

What currents mediate the longer UP states?

The detailed mechanism of longer UP states in the *Fmr1* KO mice is unknown. Changes in inhibitory and excitatory circuitry may be involved, but the fact that we saw longer active states when inhibitory synapses were blocked by a GABAergic antagonist (Fig. 4) suggests that a significant component underlying longer UP states in the *Fmr1* KO resides in excitatory circuitry. Measurements of monosynaptic excitatory transmission in acute slices indicate that synaptic excitation among neocortical excitatory neurons is either slightly decreased or

unchanged (Desai, Casimiro et al. 2006; Bureau, Shepherd et al. 2008; Gibson, Bartley et al. 2008), but other studies point to increased spine number in neocortical excitatory neurons suggesting increased excitation (Bagni and Greenough 2005). Therefore, it is unclear the role excitatory synaptic currents play in promoting longer UP states in the *Fmr1* KO mouse. It is also possible that there is an alteration in a nonsynaptic current in excitatory neurons that promotes longer UP states (Brown, Kronengold et al. 2010; Strumbos, Brown et al. 2010). Based on our findings of differential regulation of UP states by mGluR5 (Figs. 6,7), any underlying cellular current will be modulated differentially by mGluR5 when comparing WT and KO neurons. Studies examining single-cell persistent firing in cortical neurons have reported that mGluR5 activation promotes persistent firing through a nonsynaptic membrane current (Yoshida, Fransen et al. 2008; Zhang and Seguela 2010).

Implications of longer UP states in Fmr1 KO mice

Because *Fmr1* KO slices spend 35% more time in the UP state (Fig. 1D), they may be considered to be more active. This implies that the neocortical circuitry may be more excitable in general, thereby affecting neocortical function in many behavioral states. This is consistent with symptoms in Fragile X patients such as overt epilepsy, EEG abnormalities suggestive of epilepsy, and hyper-responsiveness to sensory stimuli (Hagerman, Amiri et al. 1991; Miller, McIntosh

et al. 1999; Musumeci, Hagerman et al. 1999; Rojas, Benkers et al. 2001; Berry-Kravis 2002; Incorpora, Sorge et al. 2002; Castren, Paakkonen et al. 2003; Frankland, Wang et al. 2004). It is also consistent with *Fmr1* KO mice having an increased propensity for audiogenic seizures (Chen and Toth 2001; Nielsen, Derber et al. 2002; Spencer, Serysheva et al. 2006). Therefore, it is possible that the prolonged UP states themselves or the cellular mechanism that causes the longer UP states mediates the hyperexcitability in Fragile X Syndrome.

Thirty percent of children with FXS are diagnosed with autism and 1-2% of autistic children have FXS making *Fmr1* one of the leading genetic causes of autism (Kaufmann, Cortell et al. 2004; Hagerman, Ono et al. 2005). Because of this strong link to autism, it is intriguing that our findings are consistent with the hypothesis that hyperexcitability in neocortical circuits underlie autism (Rubenstein and Merzenich 2003).

UP states have been demonstrated to underlie the slow oscillation which is a neocortical rhythm (<1 Hz) that occurs during the deeper stages of slow wave sleep and anesthesia (Steriade, Nunez et al. 1993; Steriade 1997; Amzica and Steriade 1998). The slow oscillation during slow wave sleep has been proposed to be involved in long-term memory consolidation in neocortex (Marshall and Born 2007; Crunelli and Hughes 2010). In a previous study, we have also demonstrated that inhibition during UP states is less synchronous (Gibson, Bartley et al. 2008). Therefore, it is possible that the prolonged UP states with

less synchronous inhibition may modify the slow oscillation in Fragile X Syndrome which, in turn, could impact memory consolidation. Our study suggests closer scrutiny of the slow oscillation in Fragile X patients is warranted, but to date, while circadian rhythm and sleep problems have been reported in both Fragile X patients and *Fmr1* KO mice (Musumeci, Ferri et al. 1991; Miano, Bruni et al. 2008; Zhang, Fang et al. 2008; Kronk, Bishop et al. 2010), no such data exists.

Figure 2.1. Spontaneously occurring persistent activity states, or UP states, are longer in layer 4 of *Fmr1* KO somatosensory cortical slices.

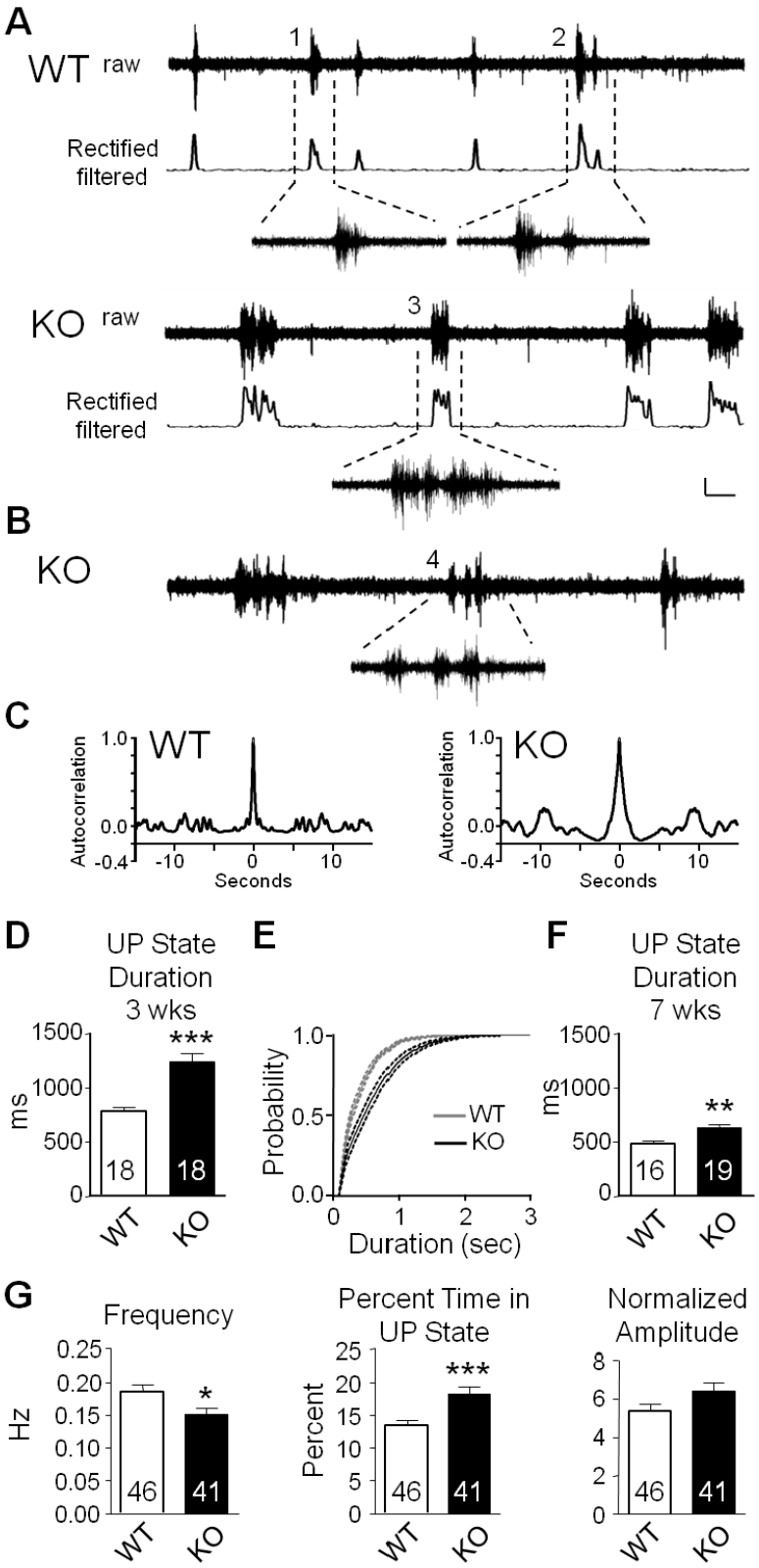

<*Previous page*>

Figure 2.1. Spontaneously occurring persistent activity states, or UP states, are longer in layer 4 of *Fmr1* KO somatosensory cortical slices.
A) Examples of extracellular multi-unit recordings from WT and KO slices demonstrate longer UP states in the KO. The rectified and filtered versions of the traces from which the UP states were analyzed are plotted underneath. Dashed lines indicate shorter epochs of the longer traces which are expanded to show more detail. **B)** In some instances, UP states occurred in the form of closely spaced events, or bursts. These were considered one UP state (numbers 2 and 4 in **A** and **B**; see Methods). **C)** Autocorrelograms from the examples in (**A**) reveal some rhythmic activity, but in general it was weak (See Methods for details of autocorrelograms). **D)** Average UP state duration over all slices was higher in KO slices at 3 weeks of age. **E)** The cumulative distribution of average duration (normalized for each slice and averaged over slices; same data set as **C**, see Methods) was evenly shifted to the right for the KO. Outer dashed lines represent the standard error. **F)** Average UP state duration was still longer at 7 weeks of age. **G)** UP state frequency was decreased and percent of time in the UP state increased. *$p<0.05$, **$p<0.01$, ***$p<0.001$. Scale bars: Vertical in μV: raw traces, 20; rectified, 0.1. Horizontal in ms: long traces, 1500; short traces, 300. Numbers inside bars indicate slice number in all figures except figures 3 and 6D.

Figure 2.2. Spontaneously occurring UP states are longer in layer 5.

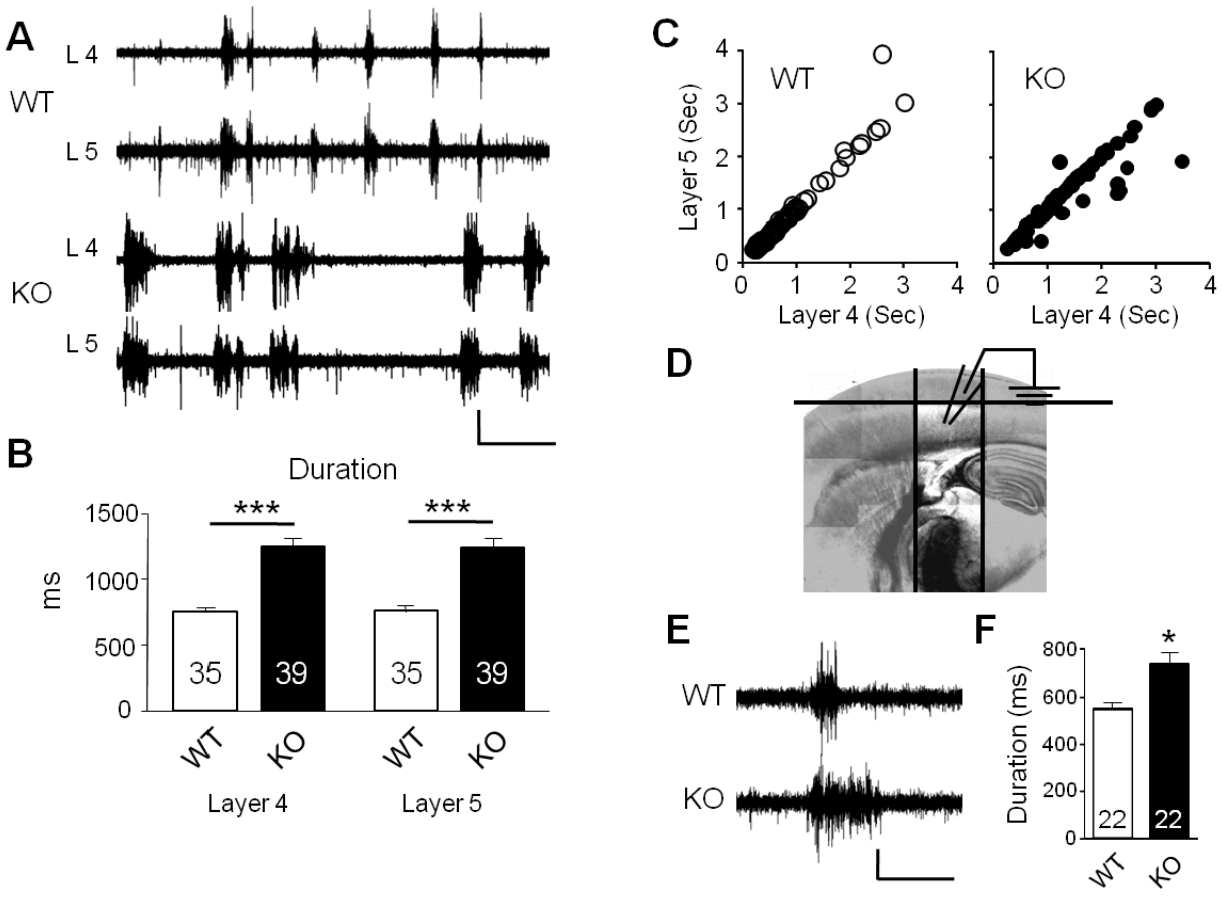

Figure 2.2. Spontaneously occurring UP states are longer in layer 5.
A) Examples of simultaneous multi-unit recordings of layers 4 (L 4) and 5 (L 5) in a WT and a KO slice. **B)** The longer duration phenotype in *Fmr1* KO slices also exists to the same extent in both layers 4 and 5. **C)** Scatter plots depicting UP state durations measured in a single experiment from a WT and a KO slice. Each point represents the duration of a single UP state measured simultaneously in layer 4 and 5. Note the strong correlation. **D)** A picture depicting a slice that was used for recording from deep neocortical layers in isolation. Gray shading indicates regions removed. **E)** UP states recorded in layer 5 of slices containing only deep layers. **F)** Isolated deep layers of neocortex display longer UP states in *Fmr1* KO slices. *$p<0.05$, ***$p<0.001$. Scale bars: 30 µV, 5 sec in (A) and 30 µV, 1 sec in (E).

Figure 2.3. UP states are longer in *Fmr1* KO mice *in vivo*.

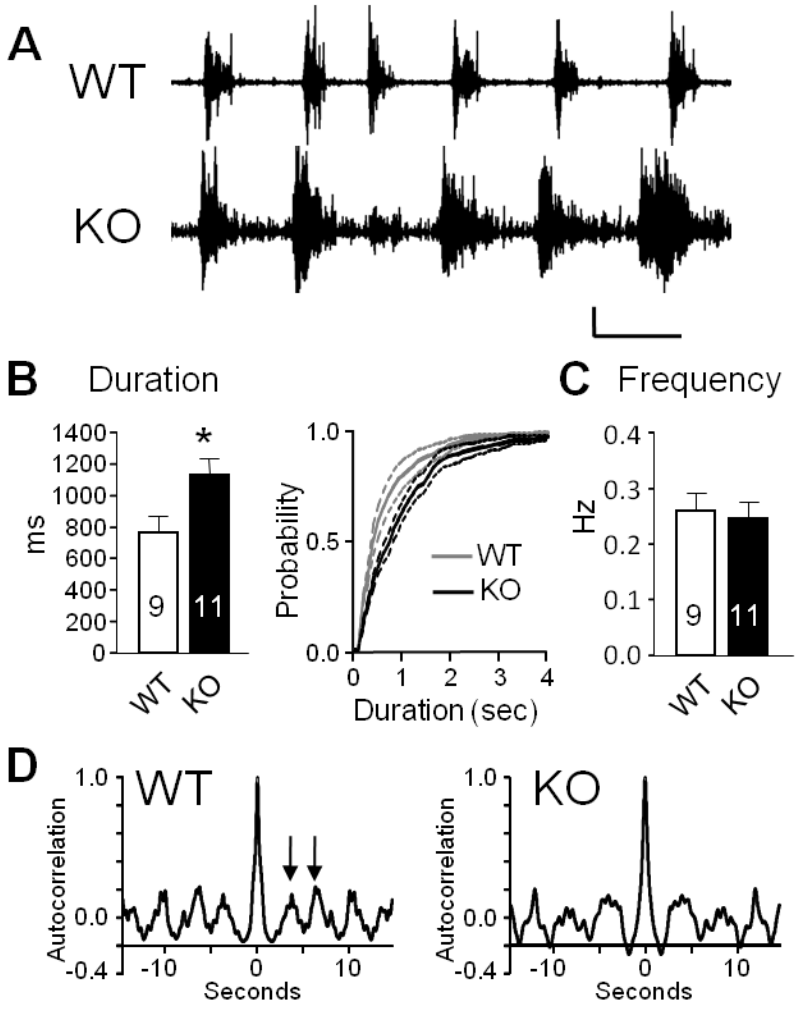

Figure 2.3. UP states are longer in *Fmr1* KO mice *in vivo*.
A) Examples of multi-unit recordings from single WT and KO mice, *in vivo*. **B)** Average duration of UP states is longer in *Fmr1* KO mice (numbers inside bars indicate mouse number). A cumulative histogram (right) indicates an even shift in durations across all animals (normalized for each mouse and averaged over mice; same data set as bar graph to the left, see Methods). Outer dashed lines are standard error. **C)** The frequency of UP states was not detectably different. **D)** Autocorrelations of the filtered, rectified traces depicted in (**A**) reveal a clear rhythmic component of the activity probably reflecting the slow oscillation (See Methods for details of autocorrelograms). Examples of first and second side-peaks are marked by arrows. *$p<0.05$. Scale bars: 50 μV, 3 sec.

Figure 2.4. Pharmacologically isolated excitatory circuitry displays longer persistent activity bursts in *Fmr1* KO slices.

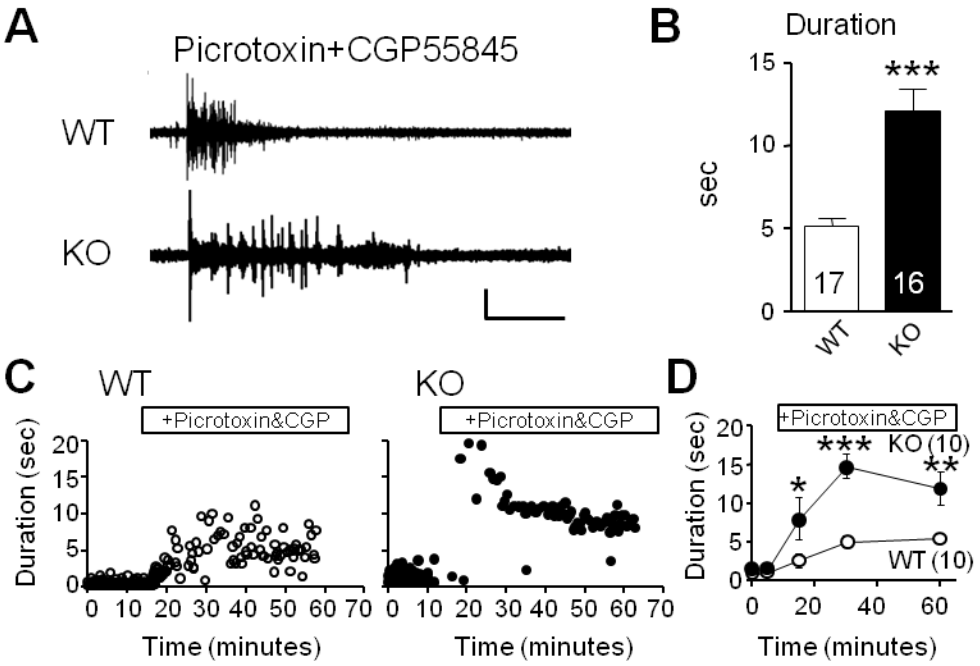

Figure 2.4. Pharmacologically isolated excitatory circuitry displays longer persistent activity bursts in *Fmr1* KO slices.

A) Traces of prolonged bursts of activity collected during application of the $GABA_A$ antagonist, picrotoxin, and the $GABA_B$ receptor antagonist, CGP55845. **B)** The average duration of the bursts was longer in *Fmr1* KO slices. **C)** The time course of the effect of GABA receptor blockade during 2 individual experiments. Antagonists are actually in the bath solution at time zero, but takes 12-18 minutes to reach the slice. Therefore, the upper bars depict the estimated time that the antagonists reach the slice. **D)** Average time course of the effects of GABA receptor blockade. The onset of the effects is not as sharp as individual examples in C because of variability in the time that the antagonists reach the slice preparation. The sample number in **D** is less than that in **B** because only a subset of the slices were monitored before and after antagonist application. *$p<0.05$, **$p<0.01$, ***$p<0.001$. In (**D**), repeated measures ANOVA and Bonferroni corrections were used. Scale bars: 50 μV, 5 sec.

Figure 2.5. UP states are longer due to deletion of *Fmr1* in neocortical excitatory neurons.

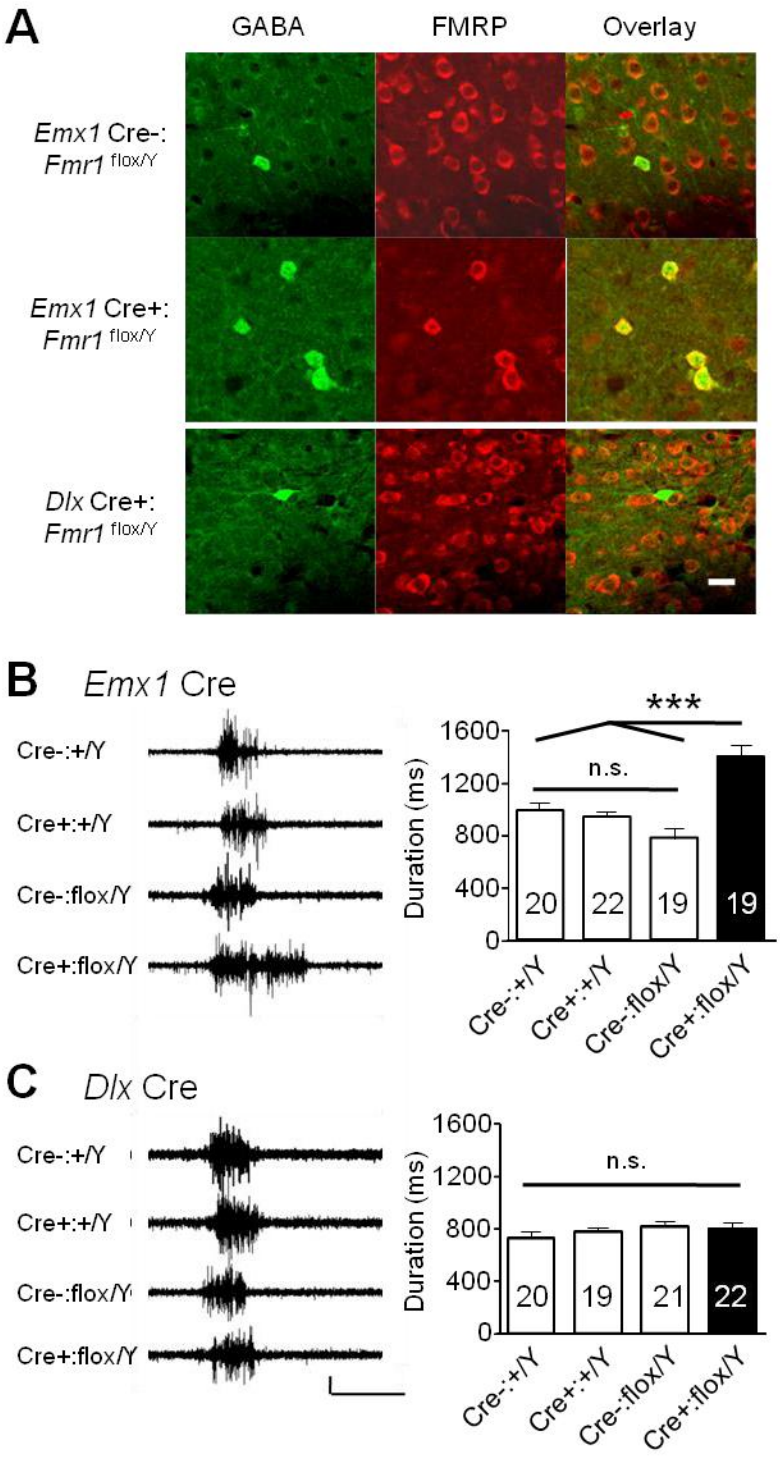

<*Previous page*>

Figure 2.5. UP states are longer due to deletion of *Fmr1* in neocortical excitatory neurons.
A) Immunohistochemistry for GABA (green) and FMRP (red) shows that FMRP is expressed in both inhibitory and excitatory neurons in control animals (top row), FMRP is deleted only in excitatory neurons when recombination occurs in *Emx1* Cre+:floxed *Fmr1* mice (middle row), and FMRP is deleted only in inhibitory neurons when recombination occurs in *Dlx* Cre+:floxed *Fmr1* mice (bottom row). **B)** UP state duration is longer in slices where FMRP was deleted only in cortical excitatory neurons (black bar), thereby recapitulating the phenotype of the constitutive *Fmr1* KO. The large triangular bar indicates that the recombined genotype is different from all of the 3 non-recombinant controls. **C)** Deletion of FMRP in inhibitory neurons did not affect UP state duration (black bar). ***$p<0.001$. n.s. is not significant. Scale bars: 50 μV, 1 sec, applies to both **B** and **C**.

Figure 2.6. Genetic reduction of mGluR5 protein rescues UP state duration in *Fmr1* KO slices.

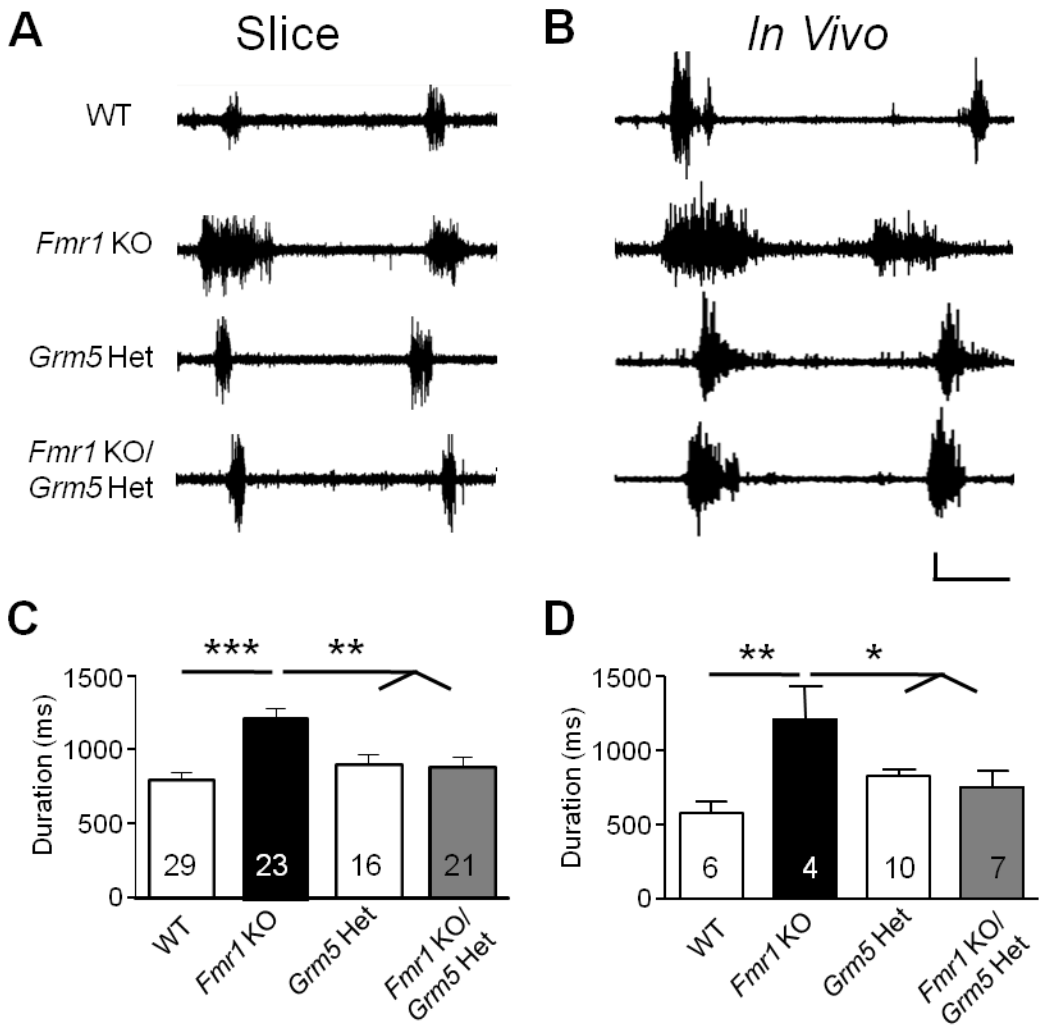

Figure 2.6. Genetic reduction of mGluR5 protein rescues UP state duration in *Fmr1* KO slices.

A,B) Examples of traces from WT and *Fmr1* KO slices (**A**) and mice (**B**, *in vivo*) on a WT *Grm5* background (top 2 traces) and on a heterozygous *Grm5* background (bottom 2 traces). **C,D**) Combination of *Fmr1* KO and *Grm5* heterozygosity (gray) restores UP state duration to WT levels. *Grm5* heterozygosity on a WT background has no effect on UP state duration. The large triangular bar indicates that the KO duration is different from that of both WT and KO on the *Grm5* heterozygous background. *p<0.05, **p<0.01, ***p<0.001. Scale bars: 50 μV, 1 sec.

Figure 2.7. Pretreatment with an mGluR5 antagonist rescues UP state duration in *Fmr1* KO slices.

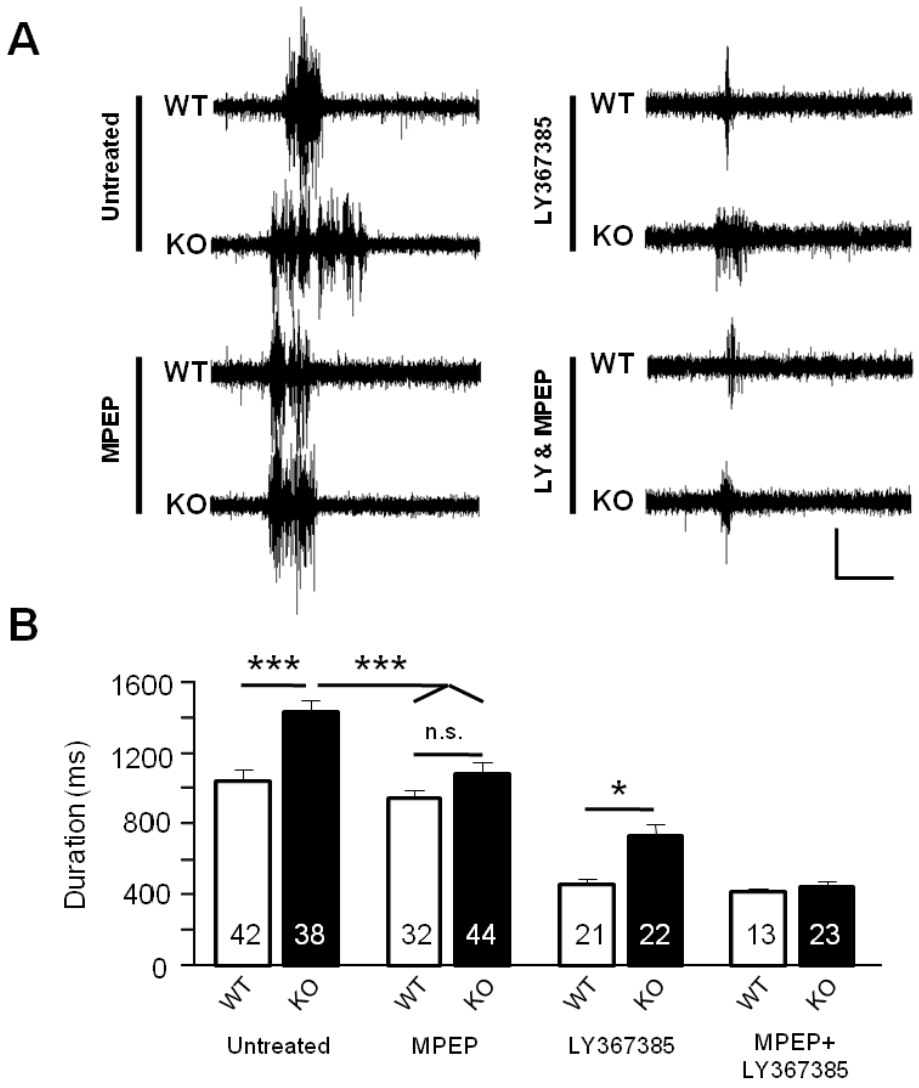

Figure 2.7. Pretreatment with an mGluR5 antagonist rescues UP state duration in *Fmr1* KO slices.

A) Examples of multi-unit recordings from untreated slices and from slices after 45 minute pre-incubation with an mGluR5 selective antagonist (MPEP, 10 μM) or an mGluR1 selective antagonist (LY367385, 100 μM). **B)** Summary of the effects of pretreatment on UP state duration. MPEP rescued the duration phenotype by equalizing the WT and KO UP state durations to normal WT levels. In contrast, while LY367385 significantly decrease duration in both WT and KO slices, UP states were still longer in the KO. The large triangular bar indicates that the untreated KO duration is different from that of both MPEP treated genotypes. **p<0.01, ***p<0.001. n.s. is not significant. Scale bars: 50 μV, 1 sec.

Figure 2.8. MPEP wash-in does not affect UP state duration

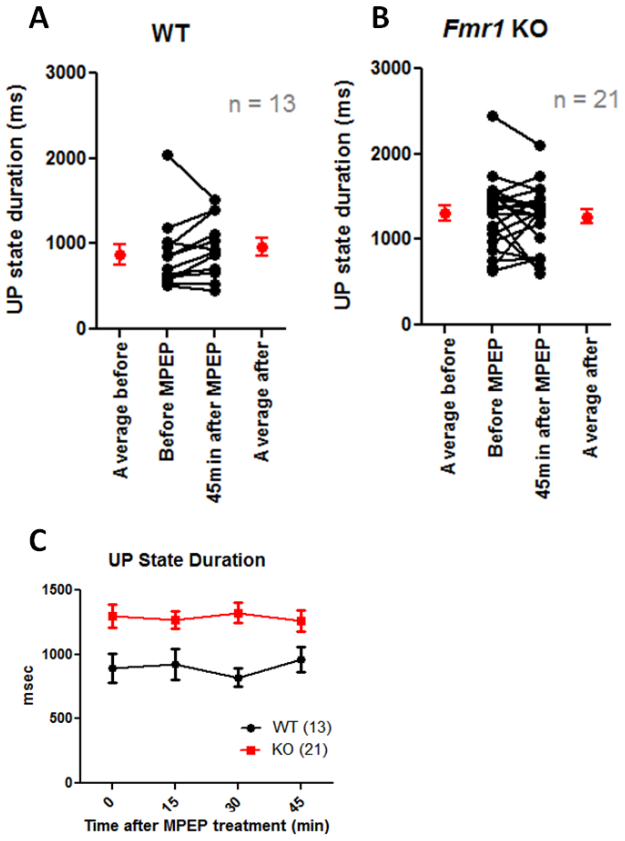

Figure 2.8. MPEP wash-in does not affect UP state duration
A,B) 45 min after MPEP wash-in, duration is unchanged in either WT or *Fmr1* KO slices. Each point represents the average duration over a 5 minute period either before or after MPEP treatment. **C)** UP state duration is stable and unchanged during MPEP wash-in for both genotypes. Average UP state duration measured during a 5 minute period for each time point indicated. N refers to number of slices. A,B T-test. C, Repeated measures ANOVA.

Figure 2.9. Pretreatment with a protein translation inhibitor has no effect on WT or *Fmr1* KO UP state duration.

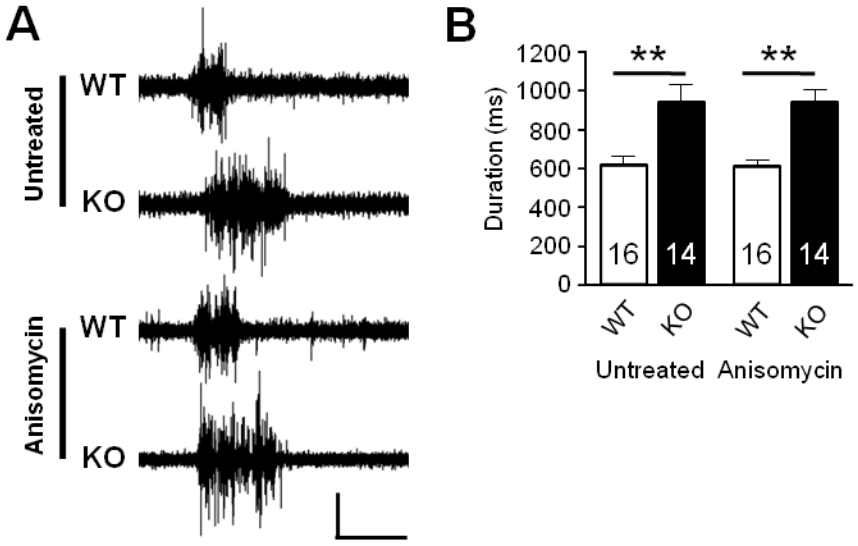

Figure 2.9. Pretreatment with a protein translation inhibitor has no effect on WT or *Fmr1* KO UP state duration.
A) Examples of multi-unit recordings from untreated slices and from slices after 45 minute pre-incubation with anisomycin (20 μM). **B)** While UP state duration was longer in KO slices, durations were not affected by anisomycin treatment. **p<0.01. Scale bars: 50 μV, 1 sec.

Figure 2.10. A group 1 mGluR agonist lengthens UP state duration in both WT and KO slices.

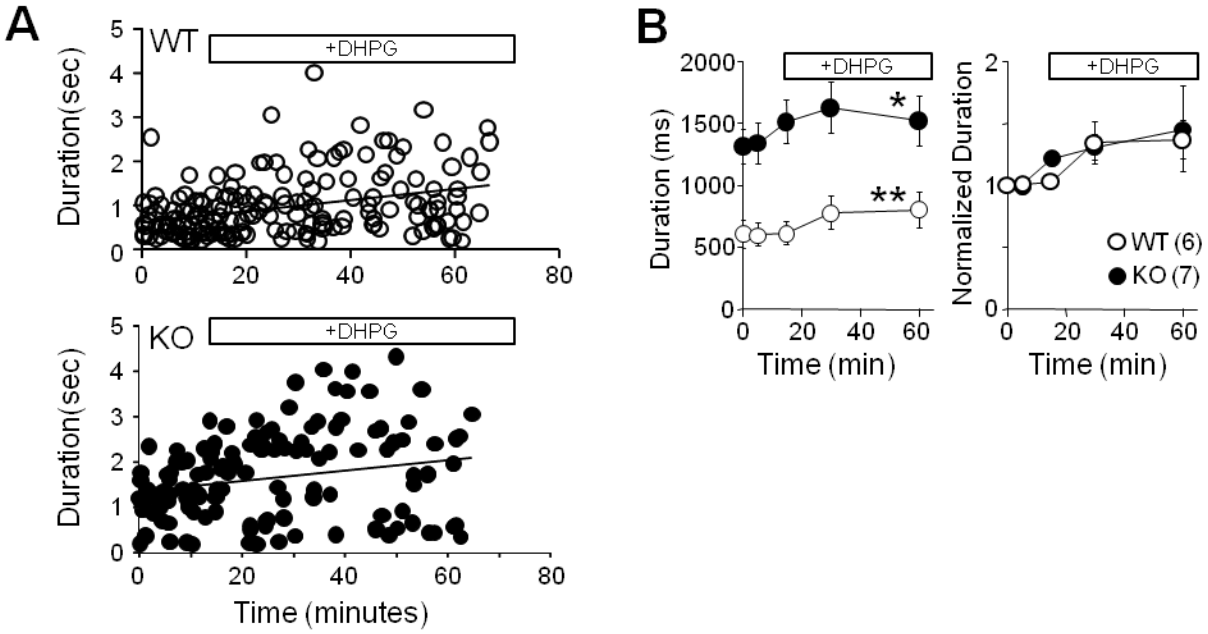

Figure 2.10. A group 1 mGluR agonist lengthens UP state duration in both WT and KO slices.

A) UP state duration plotted as a function of time for 1 WT and 1 KO experiment where DHPG was applied. DHPG is added to ACSF at the 5 minute time point, but the bars above the graphs depict the estimated time that DHPG reaches the slice (same applies to **B**). Trendline indicates timecourse average. **B)** Average time course for DHPG effect on UP state duration over all experiments plotted with raw durations (left) and durations normalized to the 0 minute time point (right). *$p<0.05$, **$p<0.01$. p-values refer to an effect on duration by time (Repeated measures ANOVA).

CHAPTER THREE
Results

DISRUPTED HOMER SCAFFOLDS MEDIATE ABNORMAL MGLUR5 FUNCTION IN A MOUSE MODEL OF FRAGILE X SYNDROME

This chapter contains data that was collected as a collaborative effort between several colleagues. I contributed the UP state data, as well as a portion of the audiogenic seizure data. These data are the most relevant to this study of network function. However, the other data described in this chapter is important in understanding the mechanism of Homer-mGluR scaffold disruption in the *Fmr1* KO.

Summary

Enhanced metabotropic glutamate receptor subunit 5 (mGluR5) function is causally associated with the pathophysiology of fragile X syndrome, a leading inherited cause of intellectual disability and autism. Here we provide evidence that altered mGluR5-Homer scaffolds contribute to mGluR5 dysfunction and phenotypes in the fragile X syndrome mouse model, Fmr1 knockout (Fmr1−/y). In Fmr1−/y mice, mGluR5 was less associated with long Homer isoforms but more associated with the short Homer1a. Genetic deletion of Homer1a restored mGluR5–long Homer scaffolds and corrected several phenotypes in Fmr1−/y mice, including altered mGluR5 signaling, neocortical circuit dysfunction and

behavior. Acute, peptide-mediated disruption of mGluR5-Homer scaffolds in wild-type mice mimicked many Fmr1−/y phenotypes. In contrast, Homer1a deletion did not rescue altered mGluR-dependent long-term synaptic depression or translational control of target mRNAs of fragile X mental retardation protein, the gene product of *Fmr1*. Our findings reveal new functions for mGluR5-Homer interactions in the brain and delineate distinct mechanisms of mGluR5 dysfunction in a mouse model of cognitive dysfunction and autism.

Introduction

Fragile X syndrome (FXS) is the most common inherited form of intellectual disability and a leading genetic cause of autism (Abrahams and Geschwind 2008; Bassell and Warren 2008). FXS is caused by transcriptional silencing of the *FMR1* gene, which encodes fragile X mental retardation protein (FMRP)—an RNA-binding protein that regulates translation of its interacting mRNAs (Bassell and Warren 2008). Most people with FXS show many neurological deficits, including low intelligence quotient, seizures, sensory hypersensitivity, social anxiety, hyperactivity and other characteristics of autism (Berry-Kravis 2002). In the mouse model of FXS, *Fmr1* knockout, plasticity that is dependent on group 1 metabotropic receptor (mGluR1 and mGluR5) stimulation of protein synthesis is enhanced and dysregulated (Lüscher and Huber 2010). These findings motivated the 'mGluR theory of FXS', which posits that altered mGluR-dependent plasticity

contributes to the pathophysiology of the disease (Bear, Huber et al. 2004; Dölen, Osterweil et al. 2007; Dölen, Carpenter et al. 2010). In support of the mGluR theory, many phenotypes in animal models of FXS are reversed by pharmacological or genetic reduction of mGluR5 or downstream signaling pathways (Dölen, Osterweil et al. 2007; Dölen, Carpenter et al. 2010). Notably, a recent report indicates that mGluR5 antagonism can be an effective therapeutic strategy in patients with FXS (Jacquemont, Curie et al. 2011).

Group 1 mGluR activation stimulates *de novo* protein synthesis in neurons, and evidence suggests that FMRP suppresses translation of specific mRNA targets downstream of mGluR activation (Bassell and Warren 2008). In FXS, the loss of an FMRP-mediated 'brake' is proposed to lead to excess mGluR5-driven translation of many FMRP target mRNAs, which in turn leads to an excess of mGluR-dependent plasticity (Bear, Huber et al. 2004; Dölen, Carpenter et al. 2010). Although mGluR5 antagonism rescues many phenotypes associated with FXS, it is unknown whether these phenotypes are due to excess mGluR5-driven translation.

Other evidence suggests there may be altered mGluR5 function that is upstream of translation in *Fmr1−/y* brains. Although total mGluR5 levels are normal in *Fmr1−/y* forebrain, there is less mGluR5 in the postsynaptic density (PSD) fraction and an altered balance of mGluR5 association with short and long isoforms of the postsynaptic scaffolding protein Homer (Giuffrida, Musumeci et

al. 2005). The N-terminal EVH1 (Ena-VASP homology) domain of Homer proteins binds the intracellular C-terminal tail of group 1 mGluRs (mGluR5 and mGluR1a) and affects their trafficking, localization and function (Shiraishi-Yamaguchi and Furuichi 2007). Long, constitutively expressed forms of Homer (Homer1b, 1c, 2 and 3) multimerize through their C-terminal coiled-coil domains and localize mGluRs to the PSD through interactions with SHANK (SH3 and multiple ankyrin repeat domains protein), as well as linking mGluRs to signaling pathways through Homer interactions with phosphoinositide-3 kinase enhancer (PIKE), elongation factor 2 kinase (EF2K) and the inositol-1,4,5-trisphosphate receptor (Shiraishi-Yamaguchi and Furuichi 2007; Park, Park et al. 2008). Homer1a (H1a), a short, activity-inducible form of Homer, lacks the coiled-coiled domain and cannot multimerize with other Homers. Consequently, H1a disrupts mGluR5–long Homer complexes, alters mGluR signaling and causes constitutive, agonist-independent activity of mGluR1 and mGluR5 (Ango, Prezeau et al. 2001).

In *Fmr1−/y* mice, mGluR5 is less associated with the long Homer isoforms and more associated with H1a (Giuffrida, Musumeci et al. 2005). We hypothesized that the altered balance in mGluR5 interactions with Homer isoforms contributes to the mGluR5 dysfunction and pathophysiology of FXS. To test this hypothesis, we crossed *Fmr1−/y* mice with mice selectively lacking the *H1a* isoform of *Homer1* (*H1a−/−*) and determined whether *H1a* deletion restored

mGluR5 function and Homer interactions, as well as neurophysiological and behavioral phenotypes of *Fmr1−/y* mice. In addition, we determined whether acute peptide-mediated disruption of mGluR5-Homer scaffolds in wild-type (WT) mice mimics phenotypes of *Fmr1−/y* mice. Our results indicate that altered Homer isoform interactions are responsible for much, but not all, of the mGluR5 dysfunction and pathophysiology of FXS. Specifically, *H1a* deletion did not rescue the protein synthesis independence of mGluR-dependent long-term synaptic depression (mGluR-LTD) or altered translation of FMRP target mRNAs. The latter results support an essential role for FMRP in translational control of its known target mRNAs and mGluR-LTD. Our results provide new evidence for altered mGluR5-Homer scaffolds in *Fmr1* knockout phenotypes and implicate different mechanisms of mGluR5 dysfunction in distinct phenotypes. Modulation and restoration of mGluR5-Homer interactions may represent a new therapeutic strategy for FXS and related cognitive and autistic disorders.

Materials and Methods

Animals

Congenic *Fmr1* KO mice on the C57/BL6/J background were originally obtained from Dr. Steven Warren (Emory University). Homer1a specific KO mice were generated as described (Hu, Park et al. 2010). All mouse lines were backcrossed onto the C57/Bl6J mice from the UT Southwestern mouse breeding

core facility. All experiments were performed on littermate controls and blind to mouse genotype.

Reagents

Drugs were prepared as stocks and stored at -20°C and used within two weeks. TatmGluR5CT and tat-mGluR5MU (5 μM) were synthesized at the UT Southwestern Protein Chemistry Technology Center. The mixed group I mGluR agonist (RS)-3,5-dihydroxyphenylglycine (DHPG), U0126 and wortmannin were purchased from Tocris Bioscience (Ellisville, MO). Cycloheximide was purchased from Sigma.

Hippocampal Slice preparation and LTD recordings

Acute hippocampal brain slices were prepared from 4-6 wk old Long Evans Hooded rats (Charles River Laboratories, Wilmington, MA, USA), wildtype (WT), *Fmr1* knockout (*Fmr1* KO), Homer1a knockout (H1a-KO), or *Fmr1/Homer1a* double knockout (*Fmr1;H1a* KO) littermates as described previously (Ronesi and Huber 2008). Animals were anesthetized with sodium pentobarbital (50 mg/kg) delivered intraperitoneally and sacrificed by decapitation. The brain was removed and immediately transferred to an ice-cold dissection buffer containing (mM): 212 sucrose, 2.6 KCl, 26 NaHCO3, 1.25 NaH2PO4, 5 MgCl2, 0.5 CaCl2, 10 D-glucose, and brought to pH 7.4 by aerating

with 95% O2–5% CO2. All slice dissection, recording, and incubation solutions were continuously aerated with 95% O2–5% CO2. Transverse slices of 400 μm thickness were made in dissection buffer using a vibratome (Leica VT 1000S), and CA3 was removed immediately after sectioning. Slices recovered for at least four hours at 30°C on a polyester mesh (Netwell inserts; Costar; #64711-00) that was submerged in artificial cerebrospinal fluid (ACSF) containing (mM): 124 NaCl, 5 KCl, 2 CaCl2, 1 MgCl2, 26 NaHCO3, 1.25 NaH2PO4, and 10 D-glucose, and aerated to pH 7.4. LTD recordings were performed as described (Ronesi and Huber 2008). Briefly, slices were transferred to a submersion recording chamber, perfused with ACSF at 2.5-3.5 ml/min at 30+/-1°C. Field potentials (FP) were recorded extracellularly with a glass electrode (1 MΩ) filled with ACSF placed in the stratum radiatum of CA1. FPs were evoked with a concentric bipolar tungsten stimulating electrode (FHC, Bowdoinham, ME) placed in the Schaffer collateral pathway. Test stimuli (200 μsec; 10-30 μA) were delivered every 30 sec to evoke a stable FP baseline at approximately 50% of the maximum FP amplitude. LTD group data plotted in Fig. 3 represents average ± SEM. Significant differences between groups were determined using independent t-test comparing LTD magnitude at one hour after DHPG application between control and cycloheximide conditions for each genotype.

mGluR signaling in slices and western blotting

Slices were prepared exactly as for LTD experiments. Isolated CA1 hippocampal slices (CA3 cut off) were maintained in a static incubation chamber in ACSF at 30°C and aerated with 95% O2–5% CO2. For peptide preincubation experiments, hippocampal slices were preincubated in a static incubation chamber in ACSF containing 5 μM tatmGluR5CT or MU for 4 hours prior to DHPG treatment. Immediately after DHPG treatment (100 μM, 5 min), slices were quick frozen on dry ice and stored at -80°C. Slices were homogenized in lysis buffer containing 65.2 mM Tris, 150 mM NaCl, 1% Triton X-100, 0.1% SDS, 2 mM EDTA, 50 mM NaH2PO4, 10 mM Na4P2O7, protease inhibitor cocktail (Calbiochem), phosphatase inhibitor cocktail 1 and 2 (Sigma), pH 7.4. Protein concentration was determined using a BCA colorimetric protein assay (Pierce), and lysates were resolved on SDS-PAGE (10%) and transferred to nitrocellulose. Membranes were blocked in 5% nonfat dry milk and incubated with the following antibodies (Cell Signaling) according to the manufacturer's instructions: phospho-Thr56 EF2, total-EF2, phospho- Thr 389 p70S6K, total-ERK, eIF4G, eIF4E, Homer (Sc- 8921; Santa Cruz), mGluR5 (Millipore), β3 tubulin, Arc (Synaptic Systems). Blots were washed and incubated in appropriate HRP-conjugated secondary antibody (1:5000; MP Biomedical, Aurora, OH). Bands were detected using enhanced chemiluminescence, and densitometry was performed with Image J. To obtain group data, in each animal, levels of P-EF2 or P-p70S6K or Arc in DHPG treated slices were normalized to levels in untreated slices and averaged

across animals. N = # animals per condition and is plotted on each bar. Significant differences were determined using t-tests (for determining effects of mGluR5CT peptide) or 2 way ANOVA with Bonferroni posttests for tests of the effects of *Fmr1* and *H1a* genotype. Group data is presented in the figures as mean ±SEM. *p< 0.05; **p< 0.01; ***p<0.001.

Coimmunoprecipitation

Hippocampi were lysed in coimmunoprecipitation buffer (50 mM Tris, pH 7.4, 120 mM NaCl, 0.5% NP40), and protein was tumbled overnight at 4°C with 1 μg of antibody (either Homer (Santa Cruz, D-3), Homer1a (Santa Cruz, M-13) or eIF4G (Cell Signaling)). Protein A/G agarose bead slurry (Thermoscientific) was added for one additional hour and the beads were then washed with co-i.p. buffer. Protein was extracted with SDS sample buffer and resolved on 10% SDS-PAGE.

Metabolic labeling of hippocampal slices

Hippocampal slices were prepared as described for electrophysiology. For these experiments only the most ventral slices 3 per hippocampus were used since basal protein synthesis rates differ between dorsal and ventral hippocampal slices. Slices recovered for 3.5 hours in ACSF at 32°C, and then incubated in actinomycin D (25 μM) for 30 min. Where indicated, 20 μM U0126, or 100 nM wortmannin was added at this step. For radiolabeling, slices were incubated in 10

μCi/ml 35S-Met/Cys (express protein labeling mix, Perkin Elmer) for one hour. Slices were lysed on ice in homogenization buffer (10 mM HEPES pH 7.4, 2 mM EDTA, 2 mM EGTA, 1% Triton X-100, protease inhibitors (cocktail III), protein was precipitated in 10% trichloroacetic acid for 10 min, and samples were spun at 13,000Xg for 10 min. The pellet was washed in ice-cold ddH2O and dissolved in 1 N NaOH overnight. Samples were neutralized with HCl and counted in scintillation fluid. Sample cpm were normalized to protein concentration and the amount of ^{35}S-Met/Cys in the incubation ACSF. For experiments with mGluR5-Homer disrupting peptides, slices were reincubated in ACSF containing 5 μM tatmGluR5CT or MU for 4 hours prior to actinomycin incubation.

Neocortical Slice preparation and UP state recordings

For UP state experiments in neocortical slices, mice were deeply anesthetized and decapitated. The brain was transferred into ice-cold dissection buffer containing (mM): 87 NaCl, 3 KCl, 1.25 NaH2PO4, 26 NaHCO3, 7 MgCl2, 0.5 CaCl2, 20 D-glucose, 75 sucrose and 1.3 ascorbic acid aerating with 95% O2–5% CO2. Thalamocortical slices 400 μm were made on an angled block (Agmon and Connors 1991) using a vibratome (Vibratome 1000 Plus). Following cutting, slices were transected parallel to the pia mater to remove the thalamus and midbrain. Slices were immediately transferred to an interface recording chamber (Harvard Instruments) and allowed to recover for 1 hr in ACSF at 32ºC containing

(mM): 126 NaCl, 3 KCl, 1.25 NaH2PO4, 26 NaHCO3, 2 MgCl2, 2 CaCl2, and 25 D-glucose. For UP state recordings, 45 min prior to the beginning of recording session, slices in the interface chamber were perfused with an ACSF which mimics physiological ionic concentrations *in vivo*, containing (mM): 126 NaCl, 5 KCl, 1.25 NaH2PO4, 26 NaHCO3, 1 MgCl2, 1 CaCl2, and 25 D-glucose. To allow time for the tatmGluR5 peptides to permeate the slices, the peptide-containing ACSF was perfused onto the slices in the interface chamber for 4 hr prior to recording and was supplemented with 10 μM HEPES pH7.4, 0.05% BSA, and 5 μM of the appropriate peptide. The peptide-BSA containing ACSF was not oxygenated directly, but slices were oxygenated in the interface recording chamber. Spontaneously generated UP states were recorded using 0.5 MΩ tungsten microelectrodes (FHC, Bowdoinham, ME) placed in layer 4 of somatosensory cortex. 10 min of spontaneous activity was collected from each slice. Recordings were amplified 10K fold and filtered on-line between 500Hz and 3KHz. All measurements were analyzed off-line using custom Labview software. Traces were rectified and lowpass filtered at 0.2Hz. The threshold for detection was set at 4x the RMS noise. An event was defined as an UP state if its amplitude remained above the threshold for at least 200 ms. The end of the UP state was determined when the amplitude decreased below threshold for >600 ms. Two events occurring within 600ms of one another were grouped as a single UP

state. Data plotted in the figures represents the mean ± SEM. Significant differences were determined using a two-way ANOVA with Bonferroni posttests.

Audiogenic seizures

In order to evaluate audiogenic seizures, mice were placed in a plastic chamber (30 x 19 x 12cm) containing a 120 decibel siren (GE 50246 personal security alarm) and covered with a Styrofoam lid. A 120 dB siren was presented to mice for 5 minutes. Mice were videotaped and scored for behavioral phenotype: 0=no response, 1=wild running, 2=tonic-clonic seizures, 3=status epilepticus/death as described (Dölen, Osterweil et al. 2007). Data were analyzed with a 2 way ANOVA and Bonferroni post hoc multiple comparison tests.

Behavioral measurements

Open Field Activity: Mice were placed individually into the periphery of a novel open field environment (44 cm x 44 cm, walls 30 cm high) in a dimly lit room and allowed to explore for 5 min. The animals were monitored from above by a video camera connected to a computer running video tracking software (Ethovision 3.0, Noldus, Leesburg, Virginia) to determine the time, distance moved and number of entries into two areas: the periphery (5 cm from the walls) and the center (all areas excluding the periphery). The open field arenas were wiped and allowed to dry between mice. Time in the center was used as a

measure of anxiety. Data were analyzed with a 2 way ANOVA and Bonferroni post hoc multiple comparison tests.

Locomotor Activity: Mice were placed individually into a new, plastic mouse cage (18 cm x 28 cm) which was located inside a dark Plexiglas box. Movement was monitored by 5 photobeams in one dimension (Photobeam Activity System, San Diego Instruments, San Diego, CA) for 2 hours, with the number of beam breaks recorded every 5 min. Data were analyzed with an ANOVA with genotype and time as the dependent variables.

Results

Disruption of mGluR5-Homer regulates signaling to translation

To investigate whether the altered mGluR5-Homer scaffolds contribute to the mGluR5 dysfunction in Fmr1−/y mice, we determined whether disruption of mGluR5-Homer scaffolds with a peptide in WT mice mimics mGluR5 signaling alterations in the Fmr1−/y mice. The rationale for this approach is based on data that H1a-bound mGluR5, which is increased in the Fmr1−/y, is functionally equivalent to mGluR5 that cannot interact with any Homer isoform (Tu, Xiao et al. 1998; Xiao, Tu et al. 1998; Ango, Prezeau et al. 2001). To disrupt mGluR5-Homer, we incubated acute hippocampal slices from WT mice in a cell-permeable (Tat-fused) peptide containing the proline-rich motif (PPXXF) of the mGluR5 C-terminal tail that binds the EVH1 domain of Homer, mGluR5CT

(YGRKKRRQRRR-ALTPPSPFR) (Tu, Xiao et al. 1998; Mao, Yang et al. 2005; Ronesi and Huber 2008). MGluR5CT reduced mGluR5-Homer interactions to 41 ± 6% of that observed in slices with no peptide treatment (n = 3 mice; P = 0.003) as determined by coimmunoprecipitation of mGluR5 and Homer (Fig. 1a). Notably, mGluR5CT peptide treatment roughly mimicked the 50% decrease in mGluR5–long Homer interaction observed in Fmr1−/y hippocampal lysates. As a control, slices were incubated in a peptide with a mutated Homer binding motif, mGluR5MU (YGRKKRRQRRR-ALTPLSPRR) (Tu, Xiao et al. 1998; Mao, Yang et al. 2005). MGluR5MU peptide had no effect on mGluR-Homer by comparison with slices with no peptide treatment (103 ± 8% of untreated; n = 3; Fig. 1a).

Fmr1−/y mice show a deficit in stimulation of protein synthesis by mGluR1 and mGluR5 that may be a result of altered mGluR5-Homer interactions. Previously, we reported that mGluR5CT peptide-mediated disruption of mGluR5-Homer interactions in rat hippocampal slices inhibits group 1 mGluR activation of the phosphoinositide-3 kinase (PI3K)–mammalian target of rapamycin (mTOR) protein kinase pathway and of translation initiation. However, mGluR5CT does not inhibit mGluR activation of the mitogen-activated protein kinase 1 (ERK) pathway (Ronesi and Huber 2008). Here we observed similar effects in hippocampal slices from WT mice. MGluR5CT peptide incubation blocked activation of PI3K-mTOR pathway in response to the group 1 mGluR agonist (RS)-

3,5-dihydroxyphenylglycine (DHPG; 100 μM; 5 min) as measured by phosphorylation of mTOR on Ser2448 and p70 ribosomal S6 kinase (S6K) on Thr389 (phospho-mTOR: mGluR5MU: 196 ± 27% of basal, n = 8; mGluR5CT: 94 ± 20% of basal, n = 8; $P < 0.01$; phospho-S6K: mGluR5MU: 300 ± 80% of basal, n = 6; mGluR5CT: 114 ± 13% of basal, n = 6; $P < 0.05$; Fig. 1b,c) and had no effect on activation of the ERK pathway as measured by phosphorylation of ERK on Thr202 and Tyr204 (mGluR5MU: 495 ± 117% of basal, n = 4; mGluR5CT: 477 ± 162% of basal, n = 4; not significant; Fig. 1d) (Ronesi and Huber 2008). The mGluR5CT peptide did not affect basal levels of phospho-mTOR, phospho-S6K or phospho-ERK.

Homer and mGluR5 each directly interact with another translational regulatory factor, EF2K (Park, Park et al. 2008). Although phosphorylation of elongation factor 2 (EF2) by EF2K inhibits translation elongation globally, EF2K is required for translational activation of mRNAs such as such as Arc (activity-regulated cytoskeleton-associated protein) and CaMKIIα (calcium/calmodulin-dependent kinase IIα) (Park, Park et al. 2008). A moderate inhibition of elongation globally by EF2K is thought to release translation factors that are then available for translational activation of poorly initiated transcripts. Unexpectedly, mGluR5CT-treated slices showed a robust increase in phosphorylation of EF2 on Thr56 in response to DHPG (590 ± 118% of basal; n = 15 slices, Fig. 1e) in comparison to mGluR5MU-treated slices (294 ± 63% of basal; n = 15; $P < 0.05$).

Similar results were obtained in rat hippocampal slices. The mGluR5CT peptide did not affect basal levels of phospho-EF2. Taken together, our data suggest that Homer interactions facilitate mGluR activation of the PI3K-mTOR pathway to translation initiation, but dampen mGluR-induced phosphorylation of phospho-EF2 and thus restrain inhibition of global elongation rates. Consequently, disruption of mGluR5-Homer would be expected to block mRNA translation by blocking activation of the PI3K-mTOR pathway and translation initiation and enhancing inhibition of elongation to a level that may block elongation of all transcripts, including Arc. Consistent with this model, disrupting mGluR5-Homer interactions in hippocampal slices with mGluR5CT peptide blocked DHPG-induced synthesis of Arc (mGluR5MU: 122 ± 5% of untreated, n = 7; mGluR5CT: 95 ± 7% of untreated, n = 7; Supplementary Fig. 1) and elongation factor 1α (EF1α).

Deletion of Homer1a rescues mGluR signaling in Fmr1−/*y*

mGluR5–long Homer interactions are reduced in *Fmr1−/y* mice, and we hypothesize that this contributes to altered mGluR5 function. If so, then mGluR signaling to translation in *Fmr1−/y* slices may mimic what is observed with mGluR5CT peptide treatment of WT slices (Fig. 1). In support of our hypothesis, DHPG-induced activation of PI3K, mTOR and S6K is deficient in *Fmr1−/y*

hippocampal slices, and ERK activation is unaffected (Ronesi and Huber 2008; Osterweil, Krueger et al. 2010; Sharma, Hoeffer et al. 2010) (Fig. 2b). Furthermore, DHPG-induced phosphorylation of EF2 was enhanced in *Fmr1−/y* slices relative to that in slices from WT littermates (WT: 787 ± 135% of untreated, $n = 7$ mice; *Fmr1−/y*: 1,452 ± 176% of untreated, $n = 6$ mice; Fig. 2c). Notably, these alterations in mGluR signaling parallel what was observed with mGluR5CT peptide treatment of WT slices (Fig. 1). Basal levels of phosphorylated or total EF2 or S6K were unchanged in *Fmr1−/y* slices (Ronesi and Huber 2008). These results indicate that mGluR5 function is not generally enhanced or decreased in *Fmr1−/y* mice, but is changed in a complex way that is mimicked in WT mice by disruption of mGluR5-Homer interactions.

In *Fmr1−/y* mice, mGluR5 is more associated with H1a (Supplementary Fig. 2a) (Giuffrida, Musumeci et al. 2005). Because long Homers compete with H1a for interactions with their effectors, we hypothesized that genetic deletion of *H1a* in *Fmr1−/y* mice may restore normal mGluR5–long Homer interactions and mGluR5 function (Tu, Xiao et al. 1998; Xiao, Tu et al. 1998). To test this idea, we bred *Fmr1−/y* mice with mice with a genetic deletion of *H1a* to create *H1a−/−*; *Fmr1−/y* double knockout mice (Hu, Park et al. 2010). *H1a−/−* mice have normal levels of long Homer isoforms 1, 2 and 3 (Hu, Park et al. 2010). In agreement with previous results, coimmunoprecipitation of long Homer isoforms from *Fmr1−/y* forebrain revealed a reduced association of mGluR5 in comparison

to that in WT littermates (Fig. 2a), whereas coimmunoprecipitation of H1a revealed an increased association with mGluR5 (Supplementary Fig. 2) (Giuffrida, Musumeci et al. 2005). Total levels of mGluR5 and long Homer proteins and of H1a protein and mRNA in *Fmr1−/y* hippocampi were not different from those in WT (Fig. 2a and Supplementary Fig. 2). Genetic deletion of *H1a* restored normal mGluR5-Homer interactions in *Fmr1−/y* mice (n = 4 mice per genotype; Fig. 2a) but did not affect levels of mGluR5, long Homers or their interactions on a WT background (Fig. 2a and Supplementary Fig. 2) (Hu, Park et al. 2010). To determine whether *H1a* deletion restored normal mGluR5 signaling in *Fmr1−/y* mice, we examined mGluR signaling to the mTOR and EF2K translational regulatory pathways. The deficit in mGluR5 signaling to mTOR in the *Fmr1−/y*, as measured by S6K Thr389 phosphorylation (WT: 242 ± 34% of basal, n = 21; *Fmr1−/y*: 135 ± 15%, n = 19; Fig. 2b), was restored in the *H1a−/−*; *Fmr1−/y* (220 ± 28% of untreated, n = 18). Similarly, enhanced mGluR activation of EF2K was rescued to WT levels by *H1a* deletion (*H1a−/−*; *Fmr1−/y*, 826 ± 192% of basal, n = 7; Fig. 2c). *H1a−/−* mice showed normal DHPG-induced phosphorylation of EF2 (796 ± 159% of untreated, n = 6) and S6K (227 ± 34% of treated, n = 14). There was no effect of *Fmr1* or *H1a* genotype on basal levels of phosphorylated or total EF2 or S6K. Furthermore, DHPG treatment did not alter levels of total EF2 or S6K in any genotype (Ronesi and Huber 2008; Sharma, Hoeffer et al. 2010).

H1a deletion rescues enhanced translation rates in *Fmr1−/y*

Although DHPG-induced translation is absent in *Fmr1−/y* mice, basal translation rates in brain are elevated (Bassell and Warren 2008; Dölen, Carpenter et al. 2010; Gross, Nakamoto et al. 2010; Osterweil, Krueger et al. 2010). Enhanced protein synthesis in hippocampal slices was reversed by pharmacological blockade of mGluR5 or of ERK activation, but not by an inhibitor of PI3K or of mTOR (Fig. 3 and Supplementary Fig. 3) (Osterweil, Krueger et al. 2010). Another consequence of mGluR5-H1a interactions is constitutive, or agonist-independent, mGluR5 activity, which may drive translation rates through ERK activation, a pathway that remains intact in *Fmr1−/y* mice and with Homer disruption (Fig. 1d) (Ango, Prezeau et al. 2001; Ronesi and Huber 2008; Osterweil, Krueger et al. 2010). In support of this hypothesis, genetic deletion of *H1a* rescued enhanced translation rates as measured by incorporation of ^{35}S-labeled methionine and cysteine in proteins in hippocampal slices (*Fmr1−/y*: 122 ± 4% of WT, *n* = 14 slices from 7 mice; *H1a−/−*: 102 ± 4% of WT, *n* = 8 slices from 4 mice; double *H1a−/−*; *Fmr1−/y*: 106 ± 6% of WT, *n* = 7 slices from 4 mice; Fig. 3a). Furthermore, mGluR5CT peptide-mediated disruption of mGluR5-Homer in WT slices was sufficient to mimic the enhanced protein synthesis rates observed in *Fmr1−/y* slices (mGluR5CT = 123 ± 6% of mGluR5MU treated, *n* = 16 slices per peptide from

10 mice; P = 0.002; Fig. 3b). In contrast, mGluR5CT had no effect on protein synthesis rates in *Fmr1−/y* slices (mGluR5CT = 106 ± 8% of mGluR5MU treated, n = 14 (mGluR5CT) or 15 (mGluR5MU) slices from 8 mice; P = 0.5; Fig. 3b).

Translation initiation is the rate-limiting step in translation (Proud 2007). To determine whether enhanced translation rates in the *Fmr1−/y* stem from increased initiation, we measured eIF4F translation initiation complexes in hippocampal slices prepared from WT, *Fmr1−/y*, *H1a−/−* and *H1a−/−*; *Fmr1−/y* mice. The eIF4F complex is composed of the 5′ cap binding protein eIF4E, the scaffolding protein eIF4G and the RNA helicase eIF4A (Proud 2007). eIF4F complex assembly can be measured by coimmunoprecipitation of eIF4G and eIF4E and is stimulated by DHPG in WT animals (Banko, Hou et al. 2006). Therefore, we also measured eIF4F complex in DHPG-stimulated slices from each genotype. Consistent with previous reports, eIF4F complex levels were enhanced basally in *Fmr1−/y* slices and no longer stimulated by DHPG (Fig. 3d) (Sharma, Hoeffer et al. 2010). Like ^{35}S-labeled methionine and cysteine incorporation, eIF4F complex levels in *Fmr1−/y* slices were restored to WT levels by *H1a* deletion (Fig. 3d; n = 3 mice per condition). Genetic deletion of *H1a* also rescued the deficit in DHPG-stimulated eIF4F complex assembly in the *Fmr1−/y* (Fig. 3d). These results suggest that elevated protein synthesis rates in *Fmr1−/y* mice are due to enhanced translation initiation that is driven by H1a-bound mGluR5. The deficit in mGluR-stimulated translation initiation in *Fmr1−/y* mice

may be because eIF4F complex levels are saturated basally. Furthermore, mGluR-activation of mTOR is rescued in *Fmr1−/y* mice by *H1a* deletion (see Fig. 2), which may also contribute to restoration of DHPG-induced eIF4F complex assembly (Banko, Hou et al. 2006).

To determine how increased H1a-mGluR5 interactions lead to enhanced signaling to translation downstream of ERK, we examined phosphorylation of initiation factors known to be regulated by ERK in WT and *Fmr1−/y* cortical homogenates and the effects of *H1a* deletion. ERK phosphorylates and activates MAPK-interacting kinase (Mnk), which in turn phosphorylates the cap-binding protein eIF4E on Ser209 (Proud 2007). ERK also phosphorylates eIF4E binding protein (4EBP) at Ser65, a site distinct from mTOR-regulated sites (Thr36 and Thr45) (Herbert, Tee et al. 2002). ERK-dependent phosphorylation of eIF4E and 4EBP (Ser65) is associated with increased translation rates in neurons and other cell types (Kelleher, Govindarajan et al. 2004; Banko, Hou et al. 2006). Consistent with a role for ERK in phosphorylation of these initiation factors in hippocampal slices, phospho-(Ser209)-eIF4E and phospho-(Ser65)-4EBP were strongly reduced or abolished by treatment with U0126, an inhibitor of the upstream kinase that activates ERK (MAP/ERK kinase; MEK) (Supplementary Fig. 4). Phospho-4EBP and phospho-eIF4E levels were enhanced in cortical homogenates from *Fmr1−/y* mice, an effect that was rescued by *H1a* deletion (Fig. 3e). As reported in hippocampal slices (Fig. 1d), phospho-ERK levels were

unchanged in *Fmr1−/y* lysates (Fig. 3e) (Ronesi and Huber 2008; Osterweil, Krueger et al. 2010).

To determine whether mGluR5 activity abnormally drives phosphorylation of ERK, eIF4E and 4EBP (Ser65) in *Fmr1−/y* mice, we treated hippocampal slices from both WT and *Fmr1−/y* mice with the mGluR5 inverse agonist 2-methyl-6-(phenylethynyl)pyridine (MPEP; 10 μM). MPEP treatment did not affect phospho-4EBP or phospho-eIF4E in WT slices. However, in *Fmr1−/y* slices, MPEP reduced phospho-4EBP and phospho-eIF4E by ~50% (Fig. 3f). Unexpectedly, MPEP had no effect on phospho-ERK levels in either WT or *Fmr1−/y* slices. These results support our hypothesis that H1a-mediated mGluR5 activity drives translation initiation through ERK phosphorylation of initiation factors. Because phospho-ERK levels are not affected by *Fmr1* knockout or with MPEP, this suggests that mGluR5 may regulate accessibility or localization of eIF4E or 4EBP with ERK, as opposed to ERK activity *per se*.

Altered LTD is not rescued by deletion of H1a

In WT animals, mGluR-dependent LTD in the CA1 region of the hippocampus requires dendritic protein synthesis of FMRP-interacting mRNAs such as *Arc* and *Mtap1b* (also known as *Map1b*) (Park, Park et al. 2008; Waung, Pfeiffer et al. 2008; Lüscher and Huber 2010). Although mGluR activation induces robust LTD in *Fmr1−/y* mice, mGluR-induced synthesis of Arc and

Map1b is deficient and LTD is independent of new protein synthesis (Park, Park et al. 2008; Lüscher and Huber 2010). From this result, it has been suggested that loss of FMRP-mediated translational suppression leads to enhanced steady-state levels of 'LTD proteins' that allow mGluR-LTD to persist without new protein synthesis (Lüscher and Huber 2010). Consistent with this hypothesis, elevated Map1b and Arc have been reported in *Fmr1*−/*y* neurons (Zalfa, Giorgi et al. 2003; Lüscher and Huber 2010). Alternatively, H1a-bound and constitutively active mGluR5, which drives total protein synthesis rates (Fig. 3), could elevate LTD protein levels and lead to protein synthesis–independent LTD (Osterweil, Krueger et al. 2010).

To distinguish between these possibilities, we determined whether genetic deletion of *H1a* reverses the protein synthesis independence of mGluR-LTD and enhances levels of specific FMRP target mRNAs. To test the protein synthesis dependence of mGluR-LTD, we preincubated slices in the translation inhibitor cycloheximide (60 μM). Although mGluR-LTD was reliably induced with DHPG in *H1a*−/−; *Fmr1*−/*y* mice (81 ± 3% of baseline 60–70 min after DHPG application, n = 11 slices), LTD was not sensitive to cycloheximide (78 ± 1% of baseline, n = 9), and was similar to that in *Fmr1*−/*y* mice (control: 74 ± 4% of baseline, n = 7; cycloheximide: 79 ± 3% of baseline, n = 9; Fig. 4) (Park, Park et al. 2008). LTD was inhibited by cycloheximide treatment in both WT (control: 76 ± 1% of baseline, n = 7; cycloheximide: 92 ± 4% of baseline, n = 8; P = 0.002)

and *H1a*−/− mice (control: 65 ± 5% of baseline, *n* = 6; cycloheximide: 88 ± 5% of baseline, *n* = 6; *P* = 0.01; Fig. 4a,d). These results suggest that the altered mGluR5-Homer scaffolds in *Fmr1*−/*y* mice do not mediate the protein synthesis independence of mGluR-LTD.

To determine whether *H1a* deletion in *Fmr1*−/*y* mice rescues elevated steady state levels of LTD-promoting proteins or other FMRP target mRNAs, we performed western blots of Map1b, Arc and CamKIIα in hippocampal homogenates of WT, *Fmr1*−/*y*, *H1a*−/− and *H1a*−/−; *Fmr1*−/*y* mice (Fig. 4e). Map1b and CamKIIα were elevated in both *Fmr1*−/*y* mice and *H1a*−/−; *Fmr1*−/*y* mice in comparison to WT and *H1a*−/− mice (Fig. 4e), indicating that *H1a* deletion does not restore normal levels of Map1b and CamKIIα in *Fmr1*−/*y* mice. Although we did not detect elevated steady-state protein levels of Arc in hippocampal homogenates from *Fmr1*−/*y* mice, we observed a deficit in DHPG-induced synthesis of Arc in hippocampal slices from *Fmr1*−/*y* mice in comparison to WT (WT: 140 ± 17% of basal or untreated, *n* = 12; *Fmr1*−/*y*: 98 ± 12% of untreated, *n* = 12; Fig. 4f). However, *H1a* deletion did not restore mGluR-induced synthesis of Arc in *Fmr1*−/*y* mice12 (*H1a*−/−; *Fmr1*−/*y*: 91 ± 12% of untreated, *n* = 11). DHPG-induced synthesis of Arc was normal in *H1a*−/− mice (139 ± 11% of untreated, *n* = 11). These results show that altered mGluR5-Homer scaffolds in the *Fmr1*−/*y* mice do not mediate abnormal mGluR-LTD or altered translational control of specific FMRP target mRNAs. Instead, these

results support an essential role for interaction of FMRP with its target mRNAs in mGluR-LTD and translational control of these mRNAs (Supplementary Fig. 6b) (Bassell and Warren 2008; Muddashetty, Nalavadi et al. 2011).

mGluR5-Homer and hyperexcitable neocortical circuits

Humans with FXS and *Fmr1−/y* mice show sensory hypersensitivity, epilepsy and/or audiogenic seizures suggestive of an underlying sensory circuit hyperexcitability (Berry-Kravis 2002; Dölen, Carpenter et al. 2010). We recently discovered synaptic and circuit alterations indicative of hyperexcitability in the somatosensory barrel neocortex of *Fmr1−/y* mice. Neocortical slices of *Fmr1−/y* mice have decreased excitatory drive onto layer 4 fast-spiking interneurons and prolonged thalamically evoked and spontaneously occurring persistent activity, or UP states (Gibson, Bartley et al. 2008; Hays, Huber et al. 2011). UP states represent a normal physiological rhythm generated by the recurrent neocortical synaptic connections and are observed in alert and slow-wave sleep states *in vivo*, as well as in neocortical slice preparations (Sanchez-Vives and McCormick 2000; Haider, Duque et al. 2006). Of note, genetic or pharmacological reduction of mGluR5 in *Fmr1−/y* mice rescues the prolonged UP states in acute slices and *in vivo* (Hays, Huber et al. 2011). To determine whether altered mGluR5-Homer interactions contribute to altered neocortical circuit function and hyperexcitability in *Fmr1−/y* mice, we measured spontaneously occurring UP states in acute slices

from somatosensory barrel cortex using extracellular multiunit recordings (Sanchez-Vives and McCormick 2000). As previously reported, UP states were longer in slices from *Fmr1−/y* mice than in those from WT littermates (WT: 797.4 ± 31.5 ms, *n* = 22 slices; *Fmr1−/y*: 1,212 ± 87.9 ms, *n* = 13; Fig. 5a,b) (Gibson, Bartley et al. 2008; Hays, Huber et al. 2011). In support for a role for altered Homer interactions, UP state duration was shortened to WT levels by *H1a* deletion (*H1a−/−*; *Fmr1−/y*: 872.2 ± 42.1 ms, *n* = 44; Fig. 5a,b). Loss of *H1a* alone did not affect UP states, ruling out general alterations in excitability (*H1a−/−*: 767.7 ± 35.8 ms, *n* = 18).

We next determined whether mGluR5CT peptide-mediated disruption of mGluR5-Homer was sufficient to prolong UP states in WT slices. Preincubation of WT neocortical slices in mGluR5CT peptide increased the duration of UP states in comparison to treatment with mGluR5MU control peptide (WT mGluR5MU: 909.8 ± 103.7 ms, *n* = 13 slices; WT mGluR5CT: 1,408.8 ± 156.4 ms, *n* = 15; Fig. 5c,d). Therefore, acute disruption of mGluR5-Homer complexes is sufficient to mimic the circuit hyperexcitability in *Fmr1−/y* mice. In contrast, mGluR5CT had no effect on the duration of UP states in *Fmr1−/y* slices (*Fmr1−/y* mGluR5MU: 2,014.9 ± 117.9 ms, *n* = 15; *Fmr1−/y* mGluR5CT: 1,819.8 ± 163.8 ms, *n* = 12; Fig. 5c,d), likely because Homer complexes are already disrupted in these mice.

H1a *deletion reverses* Fmr1−/*y behavioral phenotypes*

To determine whether *H1a* deletion rescues any *in vivo* or behavioral phenotypes in *Fmr1*−/*y* mice, we measured the incidence of audiogenic seizures and anxiety as measured using the open field activity test across the four genotypes. We chose these phenotypes because they are robust in the C57/Bl6 strain of *Fmr1*−/*y* mice and sensitive to mGluR5 antagonists (Dölen, Carpenter et al. 2010). Consistent with previous reports, *Fmr1*−/*y* mice showed increased seizure incidence and severity upon exposure to a loud sound relative to WT and *H1a*−/− mice, who exhibited little or no incidence of seizure (seizure score (0–3; 3 being most severe; see Methods): WT, 0.12 ± 0.12; n = 16 mice; *H1a*−/−: 0.04 ± 0.04; n = 24; *Fmr1*−/*y*: 1.6 ± 0.2; n = 39; $P < 0.001$, *Fmr1*−/*y* versus WT or *H1a*−/−; Fig. 6a). *H1a*−/−; *Fmr1*−/*y* mice responded with a reduced incidence and severity of seizure in comparison to *Fmr1*−/*y* littermates (*H1a*−/−; *Fmr1*−/*y* mice, seizure score 1.1 ± 0.2; n = 37; $P < 0.05$, *H1a*−/−; *Fmr1*−/*y* versus *Fmr1*−/*y*, also see Table 3.1). However, *H1a*−/−; *Fmr1*−/*y* mice showed increased seizures in comparison to WT or *H1a*−/− mice ($P < 0.001$; Fig. 6a). Such a partial rescue of the audiogenic seizures by *H1a* deletion is similar to what is observed with genetic reduction of mGluR5 in *Fmr1*−/*y* mice (Dölen, Osterweil et al. 2007).

As previously reported, *Fmr1*−/*y* mice spent more time in the center of a lit open field than WT littermates, which has been interpreted as reduced generalized anxiety in the mice (Fig. 6b; WT, 85 ± 8 s; n = 18 mice; *Fmr1*−/*y*,

138 ± 12; n = 24; $P < 0.01$) (Liu and Smith 2009). *H1a*−/− mice did not differ from WT mice in this behavior (*H1a*−/−, 75 ± 10 s; n = 17). We found that *H1a*−/−; *Fmr1*−/*y* mice behaved like WT mice (*H1a*−/−; *Fmr1*−/*y*, 91 ± 10 s; n = 17), spending significantly less time than *Fmr1*−/*y* mice ($P < 0.01$) in the center of an open arena. There were no differences in locomotor activity between any of the genotypes (Supplementary Fig. 5). Therefore, *H1a* deletion completely rescued the open field activity phenotype, suggesting that altered mGluR5-Homer interactions contribute to altered behavior in *Fmr1*−/*y* mice and may be relevant for altered behaviors in people with FXS.

Discussion

Two mechanisms for mGluR dysfunction in FXS

Here we demonstrate a causative role for reduced Homer scaffolds in mGluR5 dysfunction in a model of human neurological disease. MGluR5 dysfunction in animal models of FXS is well established, and genetic or pharmacological reduction of mGluR5 activity reduces or rescues many disease phenotypes in animal models and most recently in patients (Dölen, Carpenter et al. 2010; Jacquemont, Curie et al. 2011). However, the molecular basis for mGluR5 dysfunction in FXS was essentially unknown. It has been suggested that loss of an FMRP-mediated translational ‘brake’ downstream of mGluR5 leads to enhanced mGluR5 function, but this mechanism cannot account for the deficits in

mGluR5 signaling or translation-independent dysfunction of mGluR5 associated with FXS (Bear, Huber et al. 2004; Ronesi and Huber 2008; Dölen, Carpenter et al. 2010; Hays, Huber et al. 2011).

Our results reveal two mechanisms for mGluR5 dysfunction in *Fmr1−/y* mice. First, an imbalance of mGluR5 interactions from long to short Homer1a isoforms leads to altered mGluR5 signaling, enhanced basal translation rates, neocortical hyperexcitability, audiogenic seizures and open field activity (Supplementary Fig. 6a). Because H1a-bound mGluR5 is constitutively active or agonist independent, our results strongly suggest that the therapeutic action of mGluR5 inverse agonists, such as MPEP, in FXS phenotypes are due, in part, to inhibition of H1a-bound, constitutively active mGluR5 (Ango, Prezeau et al. 2001). Second, our results reveal that disrupted Homer scaffolds in *Fmr1−/y* mice cannot account for altered mGluR-LTD or abnormal translational control of FMRP target mRNAs (Supplementary Fig. 6b) and implicate an essential role for FMRP binding to and translational regulation of specific mRNAs in mGluR-LTD. The discovery that altered Homer scaffolds account for much of the complex dysfunction of mGluR5 in FXS will help to develop alternative, targeted therapies for the disease and provide mechanistic links to other genetic causes of autism.

Homer scaffolds coordinate mGluR regulation of translation

Our data demonstrate new functions of Homer scaffolds in coordination of mGluR-stimulated translation by facilitating activation of the PI3K-mTOR pathway and translation initiation, as well as limiting activation of EF2K and subsequent inhibition of elongation (Ronesi and Huber 2008). Homer links to PIKE, a small GTPase that binds and activates PI3K in response to mGluR activation (Shiraishi-Yamaguchi and Furuichi 2007). The PI3K pathway stimulates mTOR to phosphorylate eIF4E binding protein (4EBP), which in turn releases eIF4E to interact with eIF4G and form the eIF4F translation initiation complex (Proud 2007). Furthermore, mTOR phosphorylates S6K to stimulate translation of 5′ terminal oligopyrimidine tract (5′ TOP) mRNAs that encode ribosomal proteins and translation factors, thus increasing the translational capacity of the cell. MGluR activation of the PI3K-mTOR-S6K pathway was blocked by mGluR5CT, and the deficits in mGluR activation of mTOR and initiation complex (eIF4F) formation in *Fmr1−/y* mice were restored by *H1a* deletion, indicating that Homer scaffolds are key for mGluR-stimulated translation initiation (Ronesi and Huber 2008).

Although somewhat counterintuitive given the fact that mGluRs stimulate translation initiation, mGluRs also stimulate phosphorylation of EF2, which inhibits elongation rate (Park, Park et al. 2008). EF2K and moderate inhibition of elongation are necessary for mGluR-induced synthesis of Arc, as well as mGluR-LTD (Park, Park et al. 2008). Submaximal inhibition of global elongation may

make available rate-limiting factors to translate mRNAs that are poorly initiated and cannot compete effectively for these factors (Scheetz, Nairn et al. 2000). Long Homer interactions limit EF2K activation by mGluRs and thus would be expected to temper mGluR-mediated inhibition of general elongation and, in turn, promote translation of poorly initiated mRNAs (Park, Park et al. 2008). Consequently, disruption of mGluR5-Homer enhances EF2K activity and would be expected to strongly inhibit elongation and block translational activation. Although we did not rescue abnormal mGluR-LTD in *Fmr1−/y* neurons by deletion of *H1a*, in WT slices mGluR5CT peptide treatment blocked mGluR-induced synthesis of Arc and mGluR-LTD (Ronesi and Huber 2008). These results indicate that in WT neurons, where mGluR-LTD requires *de novo* protein synthesis, mGluR5-Homer interactions are necessary to properly stimulate translation and induce LTD.

In *Fmr1−/y* mice there was a deficit in mGluR stimulation of PI3K-mTOR and eIF4F initiation complex formation, whereas EF2K activation was markedly enhanced. These changes would be expected to block mGluR-induced translational initiation and strongly inhibit elongation. mGluR-induced rapid synthesis of many proteins (for example, PSD-95, EF1α, amyloid precursor protein, Arc, CaMKIIα and Map1b) is absent in *Fmr1−/y* mice, which may be mediated, in part, by disrupted mGluR-Homer scaffolds and altered signaling to the translation machinery (Bassell and Warren 2008). Alternatively or in

addition, because FMRP interacts with these mRNAs, it is likely required for mGluR-triggered translational activation of specific target mRNAs (Zalfa, Giorgi et al. 2003; Bassell and Warren 2008). The fact that *H1a* deletion rescues mGluR-mediated translation initiation complex formation but not synthesis of Arc suggests a requirement for both mGluR5-Homer scaffolds and FMRP in mGluR-triggered Arc translation.

Altered mGluR5-Homer scaffolds increase translation rates

Although there is a deficit in mGluR agonist–stimulated translation in *Fmr1−/y* mice, steady-state translation rates and levels of specific proteins are elevated, thus reflecting the complexity of translational control. Because one function of FMRP is to suppress translation of its mRNA targets, an obvious possibility was that the elevated protein synthesis rates and protein levels directly result from loss of FMRP-mediated suppression of mRNA targets (Bassell and Warren 2008; Osterweil, Krueger et al. 2010; Sharma, Hoeffer et al. 2010). In support of this hypothesis, *H1a* deletion does not reverse enhanced protein levels of Map1b and CaMKIIα. However, elevated total protein synthesis rates and translation initiation (eIF4F) complexes were rescued by *H1a* deletion and mimicked in WT mice by mGluR5CT peptide treatment. Thus, increased steady-state translation rates in *Fmr1−/y* tissue are a result of altered mGluR5-Homer scaffolds that are a secondary consequence of FMRP loss. Elevated protein

synthesis rates in *Fmr1−/y* hippocampal slices are reversed by the genetic reduction of mGluR5 (*Grm5*+/−), the mGluR5 inverse agonist MPEP and inhibitors of ERK (Dölen, Carpenter et al. 2010; Osterweil, Krueger et al. 2010). In *Fmr1−/y* cortical lysates, we observed enhanced phosphorylation of translation initiation factors that are downstream of ERK (eIF4E and 4EBP) that was reversed by *H1a* deletion. Furthermore, blocking mGluR5 activity with MPEP strongly reduced phospho-eIF4E and phospho-4EBP in *Fmr1−/y*, but not WT, hippocampal slices. Together these results suggest that H1a-bound and constitutively active mGluR5 in *Fmr1−/y* neurons drives ERK-dependent phosphorylation of eIF4E and 4EBP, which enhances eIF4F initiation complex formation and translation rates (Ango, Prezeau et al. 2001). Because we do not observe an effect of *Fmr1−/y* or MPEP on phospho-ERK levels as detected by western blot, this suggests that mGluR5 either drives ERK activity that is not detectable by phosphorylation at Thr202 and Tyr204 and/or regulates accessibility of eIF4E and 4EBP to ERK.

In contrast to hippocampus, recent results from neocortical synaptoneurosomes of *Fmr1−/y* mice demonstrate a role for PI3K activity in enhanced protein synthesis rates (Gross, Nakamoto et al. 2010). We observed that the PI3K inhibitor wortmannin equalized translation rates between WT and *Fmr1−/y* hippocampal slices, but this was because wortmannin actually increased translation rates in WT, but not *Fmr1−/y*, slices (Supplementary Fig. 3).

Furthermore, elevated basal phosphorylation of PI3K, mTOR and 4EBP (at the mTOR sites) was recently reported in fresh hippocampal lysates of *Fmr1−/y* mice, perhaps as a result of increased PIKE (Osterweil, Krueger et al. 2010; Sharma, Hoeffer et al. 2010). Although we are unable to detect elevated basal activation of the PI3K-mTOR pathway in our slice preparation, persistent activation of downstream effectors of PI3K and mTOR together with constitutive mGluR5-driven ERK may elevate translation rates in *Fmr1−/y* mice (Ronesi and Huber 2008). Phospho-EF2 levels are unchanged in *Fmr1−/y* slices, suggesting that basal or constitutive mGluR5 activity is not sufficient to activate EF2K. The detailed mechanisms by which ERK, PI3K and mTOR, and EF2K contribute to elevated basal protein synthesis rates in *Fmr1−/y* mice requires further study and may differ depending on the brain region, subcellular compartment or preparation.

An essential role for FMRP in proper regulation of LTD

H1a deletion and restoration of mGluR5-Homer scaffolds in *Fmr1−/y* mice did not rescue the protein synthesis independence of mGluR-LTD nor elevated steady-state levels of Map1b and CamKIIα proteins produced from FMRP target mRNAs. This supports the hypothesis that the protein synthesis independence of mGluR-LTD in *Fmr1−/y* mice is a result of loss of FMRP-mediated translational suppression of LTD-promoting proteins, such as MAP1b (Waung, Pfeiffer et al. 2008). Because *H1a* deletion rescued the elevated

incorporation of ^{35}S-labeled methionine and cysteine, but not altered mGluR-LTD and enhanced MAP1b and CaMKIIα levels, this suggests that altered LTD and elevated MAP1b and CamKII are not a result of elevated total protein synthesis rates. Furthermore, the fact that mGluR-triggered Arc synthesis was not rescued by *H1a* deletion supports an essential role for FMRP in mGluR-triggered translational activation of Arc. Recent work has implicated mGluR-triggered dephosphorylation of FMRP in translational activation of FMRP target mRNAs, such as *Dlgap3* (*SAPAP3*) and *Dlg4* (*PSD95*) (Bassell and Warren 2008; Muddashetty, Nalavadi et al. 2011).

Altered mGluR5-Homer and neocortical network dysfunction

Altered neocortical circuit function and hyperexcitability have been predicted to contribute to cognitive disorders and autism (Rubenstein and Merzenich 2003; Uhlhaas and Singer 2006). The epilepsy and electroencephalographic abnormalities observed in people with FXS are indicative of brain hyperexcitability (Berry-Kravis 2002; Dölen, Carpenter et al. 2010). Furthermore, these individuals are hypersensitive to sensory stimuli, and *Fmr1−/y* mice have audiogenic seizures reflecting hyperexcitability of sensory circuits (Berry-Kravis 2002; Dölen, Carpenter et al. 2010). Although UP states are a normal physiological rhythm and are not epileptiform activity, they provide an effective readout of the state of circuit function and excitability (Sanchez-

Vives and McCormick 2000). Furthermore, UP states underlie the slow oscillations that occur during slow wave sleep and are implicated in memory consolidation, as well as sensory processing in waking states (Haider, Duque et al. 2006). Therefore, altered neocortical UP states in the *Fmr1−/y* mouse may be relevant to the sensory processing and cognitive abnormalities in humans with FXS (Gibson, Bartley et al. 2008; Hays, Huber et al. 2011).

Our findings indicate that the longer UP states in *Fmr1−/y* neocortex are mediated by enhanced, likely constitutive, activity of H1a-bound mGluR5 (Hays, Huber et al. 2011). In support of this conclusion, prolonged UP states in the *Fmr1−/y* mouse are reversed by genetic or acute, pharmacological blockade of mGluR5 and genetic deletion of *H1a* (Hays, Huber et al. 2011). Peptide-mediated disruption of mGluR5-Homer interactions prolonged UP states in WT, but not *Fmr1−/y*, slices, which suggests that regulation of Homer scaffolds, by H1a or other means, may regulate neocortical slow oscillations in the normal brain. Of note, H1a is induced in neocortex with sleep deprivation and contributes to the homeostatic increase in slow wave sleep that occurs in response to sleep deprivation (Mackiewicz, Paigen et al. 2008). Consequently, altered UP states, Homer interactions and responses to H1a may contribute to the reported sleep problems in people with FXS.

How does mGluR5 activity lead to longer UP states? Prolonged UP states are not due to mGluR5-driven translation, because the protein synthesis inhibitor

anisomycin does not affect UP state duration in either WT or *Fmr1−/y* slices (Hays, Huber et al. 2011). Therefore, mGluR5 activity likely leads to prolonged UP states through post-translational regulation of the intrinsic excitability and/or synaptic function of neocortical neurons.

Altered behavior in Fmr1−/y mice is rescued by H1a deletion

Genetic reduction of mGluR5 (heterozygosity), or *H1a* deletion, completely rescues neocortical hyperexcitability (for example, long UP states) in *Fmr1−/y* mice, but only partially rescues audiogenic seizures (Dölen, Osterweil et al. 2007; Hays, Huber et al. 2011). This suggests that hyperexcitability in other brain regions, such as the auditory brain stem, also contributes to audiogenic seizures in *Fmr1−/y* mice, through mechanisms independent of mGluR5 and H1a (Brown, Kronengold et al. 2010). Notably, mGluR5 antagonism and *H1a* deletion rescued the increased open field activity in *Fmr1−/y* mice, suggesting that abnormal Homer scaffolds contribute to behavioral symptoms associated with FXS and may represent a new therapeutic target for the disease. In contrast to initial studies, recent reports have failed to rescue some *Fmr1−/y* mouse behaviors by reduction of mGluR5 activity, suggesting mGluR5-independent mechanisms in FXS pathology (Dölen, Osterweil et al. 2007; Dölen, Carpenter et al. 2010; Osterweil, Krueger et al. 2010; Thomas, Bui et al. 2011; Thomas, Bui et al. 2012). Of note, in these studies inhibition of mGluR1 proved efficacious in reducing

some *Fmr1−/y* phenotypes (Thomas, Bui et al. 2011; Thomas, Bui et al. 2012). MGluR1a is a Homer binding protein, and mGluR1a-Homer scaffolds may also be affected in *Fmr1−/y* mice. Alternatively, because of the diverse mRNA targets of FMRP other signaling pathways are likely affected in FXS. However, because mGluR5 antagonism has proven effective in some FXS patients, the understanding of mGluR5 function in the normal brain and its dysfunction in FXS may provide additional and more targeted treatments for the disease and provide insight into autism (Jacquemont, Curie et al. 2011).

For the phenotypes we studied here, *H1a* deletion had no effect in the WT background but only in the *Fmr1−/y* background. This is likely because *H1a* expression is typically low under basal conditions and is strongly induced in response to neuronal activity and experience (Shiraishi-Yamaguchi and Furuichi 2007). The effects of *H1a* induction in WT mice are expected to be mimicked by the mGluR5CT peptide, where we observe effects on mGluR5 signaling, protein synthesis rates, LTD and UP state duration (Ronesi and Huber 2008). In contrast, mGluR5CT peptide has no effect on these measures in *Fmr1−/y* mice (Ronesi and Huber 2008). Therefore, we would expect that experience-dependent *H1a* induction would affect mGluR5 function in WT, but not *Fmr1−/y*, mice. Such insensitivity to experience-induced *H1a* could contribute to deficits in experience-dependent plasticity associated with FXS (Dölen, Osterweil et al. 2007).

Mechanism of disrupted Homer scaffolds in Fmr1−/y

How does loss of FMRP lead to altered mGluR5-Homer scaffolds? Protein levels of long Homers and H1a are unchanged in total homogenates of *Fmr1−/y* hippocampi, and FMRP is not reported to interact with mRNA for any Homer isoforms (Giuffrida, Musumeci et al. 2005; Darnell, Van Driesche et al. 2011). Previous work reported a decrease in tyrosine phosphorylation of long Homer in *Fmr1−/y* forebrain, but it is unknown whether or how this affects interactions with mGluR5 (Giuffrida, Musumeci et al. 2005). Phosphorylation of Homer3 regulates interactions with other Homer effectors (Huang, Huso et al. 2008; Mizutani, Kuroda et al. 2008). Similarly, phosphorylation of mGluR5 at the C-terminal Homer interaction domain reduces the affinity of mGluR5 for Homer (Orlando, Ayala et al. 2009). Therefore, post-translational modification of mGluR5 and/or Homer in *Fmr1−/y* mice may underlie the decreased interactions.

Disrupted or destabilized synaptic scaffolds that affect Homer and/or mGluR5 may also contribute more generally to cognitive disorders and autistic behaviors. Mutations in the Homer binding domain of SHANK3 and the Homer binding protein oligophrenin-1 are implicated in autism and intellectual disability, respectively (Billuart, Bienvenu et al. 1998; Bangash, Park et al. 2011). Expression of a truncated SHANK3 without the Homer binding domain in mice results in degradation of SHANK3 and autistic behaviors in mice. Notably, reduction of long Homers or induction of H1a recapitulates the degradation of

synaptic SHANK3 (Bangash, Park et al. 2011). One possibility is that mGluR5 dysfunction of the kind we describe here may occur in individuals with mutations in SHANK3 or other genes that destabilize Homer scaffolds.

Figure 3.1. Peptide-mediated disruption of mGluR5-Homer scaffolds in WT mouse hippocampus bidirectionally regulates group 1 mGluR signaling to translation initiation and elongation.

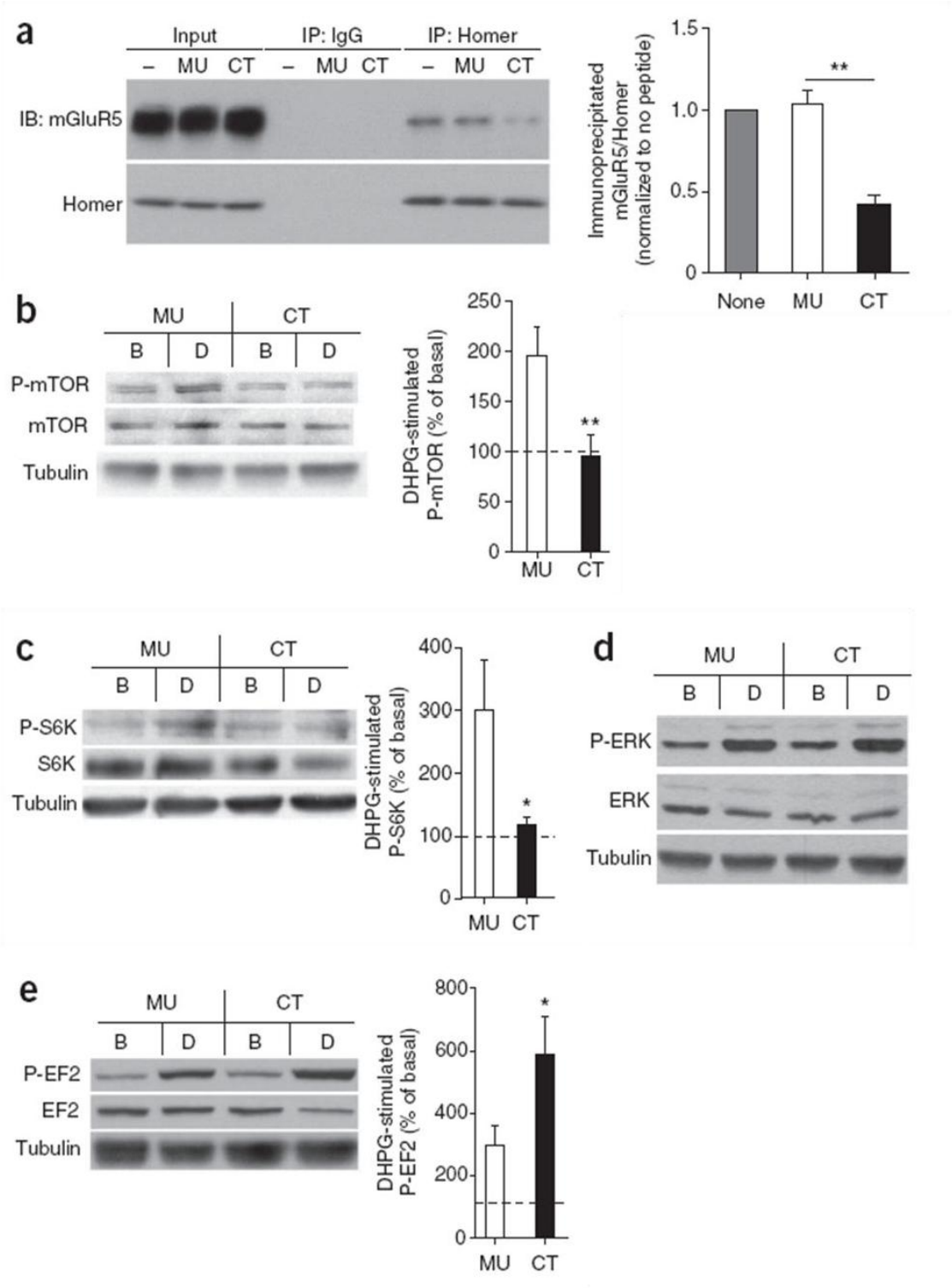

<*Previous page*>

Figure 3.1. Peptide-mediated disruption of mGluR5-Homer scaffolds in WT mouse hippocampus bidirectionally regulates group 1 mGluR signaling to translation initiation and elongation.
(a) Pretreatment of acute hippocampal slices from WT mice with mGluR5CT peptide (CT; 5 h; 5 μM) reduced mGluR5-Homer interactions as determined using coimmunoprecipitation (IP) with a pan-Homer antibody and immunoblotting (IB) for mGluR5. A control peptide, mGluR5MU (MU; 5 h; 5 μM), had no effect on mGluR5-Homer co-IP in comparison to untreated (−) slices. One-half of the input for the co-IP was run on a separate blot (bottom). (b–e) Disruption of mGluR5-Homer interaction altered signaling to translation. Western blots of **(b)** phosphorylation (P-) of mTOR on Ser2448, **(c)** phosphorylation of S6K on Thr389, **(d)** phosphorylation of ERK on Thr202 and Tyr204 and **(e)** phosphorylation of EF2 on Thr56, in the basal (B) condition and DHPG (D) treated hippocampal slices (100 μM; 5 min) from WT mice. Slices were pretreated with the CT or MU peptide as indicated. Left: representative western blots of each phosphorylated and total protein, as well as β-tubulin, in the conditions as indicated. Right: group data for each protein (ratio of phosphorylated/total, normalized to basal, or untreated, slices from the same mouse). n = 4–15 slices per condition from 3–8 mice. *P < 0.05; **P < 0.01; error bars, s.e.m.

Figure 3.2. mGluR5-Homer scaffolds and group 1 mGluR signaling are altered in Fmr1–/y mice and rescued by genetic deletion of H1a.

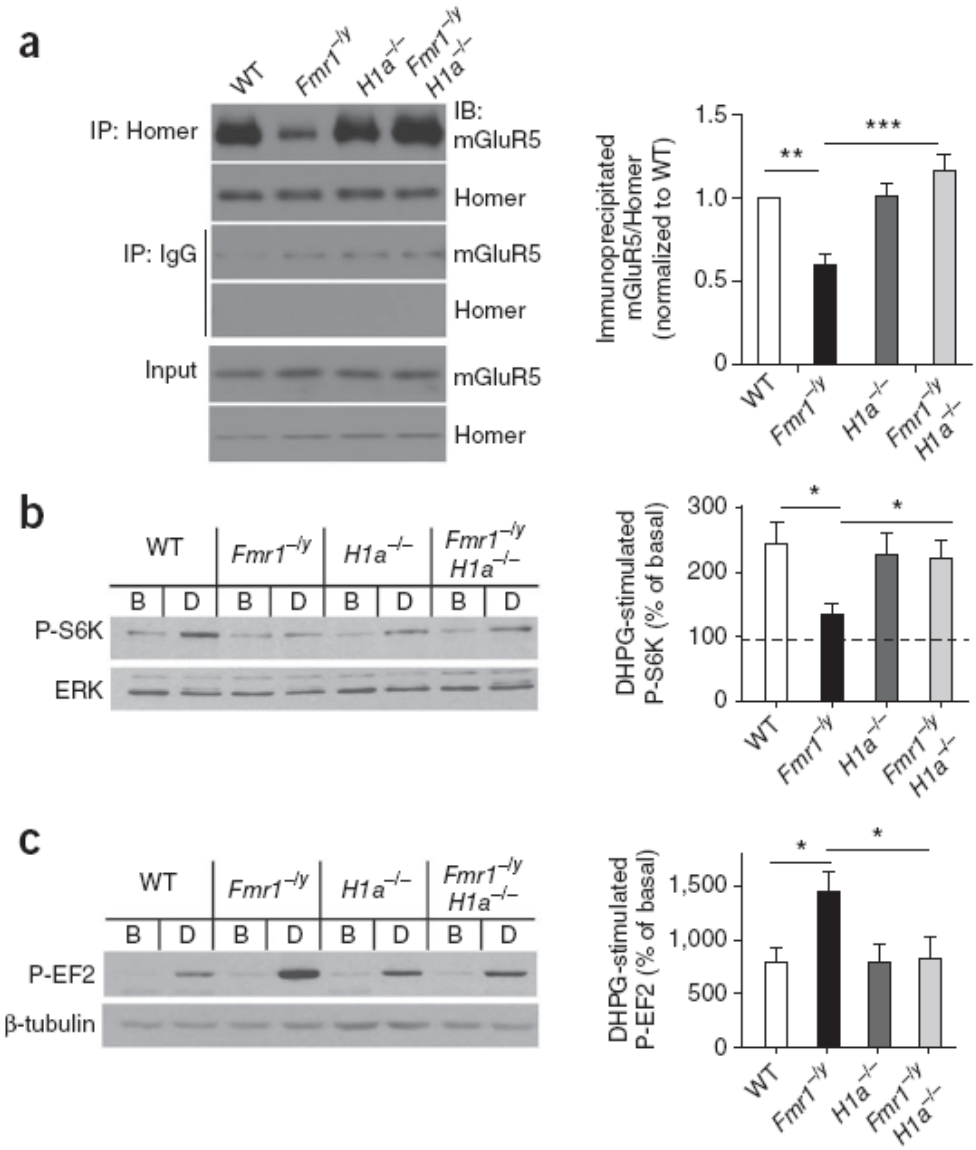

<*Previous page*>

Figure 3.2. mGluR5-Homer scaffolds and group 1 mGluR signaling are altered in Fmr1–/y mice and rescued by genetic deletion of H1a.
(a) Decreased mGluR5–long Homer interactions in the *Fmr1*–/y hippocampus were restored to WT levels in H1a–/–*Fmr1*–/y littermates. mGluR5 coimmunoprecipitation (IP) with Homer was quantified and normalized to immunoprecipitated Homer. Left: representative blots (IB) from one set of littermates reveal a decrease in the amount of mGluR5 that coimmunoprecipitated with Homer in *Fmr1*–/y that was reversed in the H1a–/–*Fmr1*–/y mouse. One-fifth of the input for the IP was run on separate blots and demonstrates normal levels of mGluR5 and Homer across all genotypes. Right: group data from independent co-IPs in four litters reveal a reliable decrease in mGluR5-Homer co-IP (expressed as a ratio of immunoprecipitated mGluR5/Homer) in *Fmr1*–/y mice and rescue by H1a deletion. **(b)** Treatment of acute hippocampal slices from littermates of each of the four genotypes with DHPG (100 μm; 5 min) revealed a deficit in phosphorylation of S6K in *Fmr1*–/y mice that was restored to WT levels in the H1a–/–*Fmr1*–/y. Left: representative western blots of phospho-S6K (P-S6K) and total ERK (loading control) in the basal (B) condition and DHPG (D) treated slices. Right: group data of P-S6K/ERK ratio (normalized to basal levels in untreated slices from the same mouse). n = 14–21 slices per condition from 14–21 mice. **(c)** DHPG-induced EF2 phosphorylation was enhanced in *Fmr1*–/y slices, an effect that was reversed in H1a–/–*Fmr1*–/y. Left: representative western blot of P-EF2 and β-tubulin in the basal (B), or untreated, condition and DHPG (D) treated slices from each genotype. Right: group data for P-EF2/tubulin ratio (normalized to basal levels). n = 6 or 7 slices and mice per genotype. *P < 0.05, **P < 0.01; ***P < 0.001; error bars, s.e.m.

Figure 3.3. Altered mGluR5-Homer scaffolds in *Fmr1–/y* mice mediate enhanced basal translation rates and initiation complex formation.

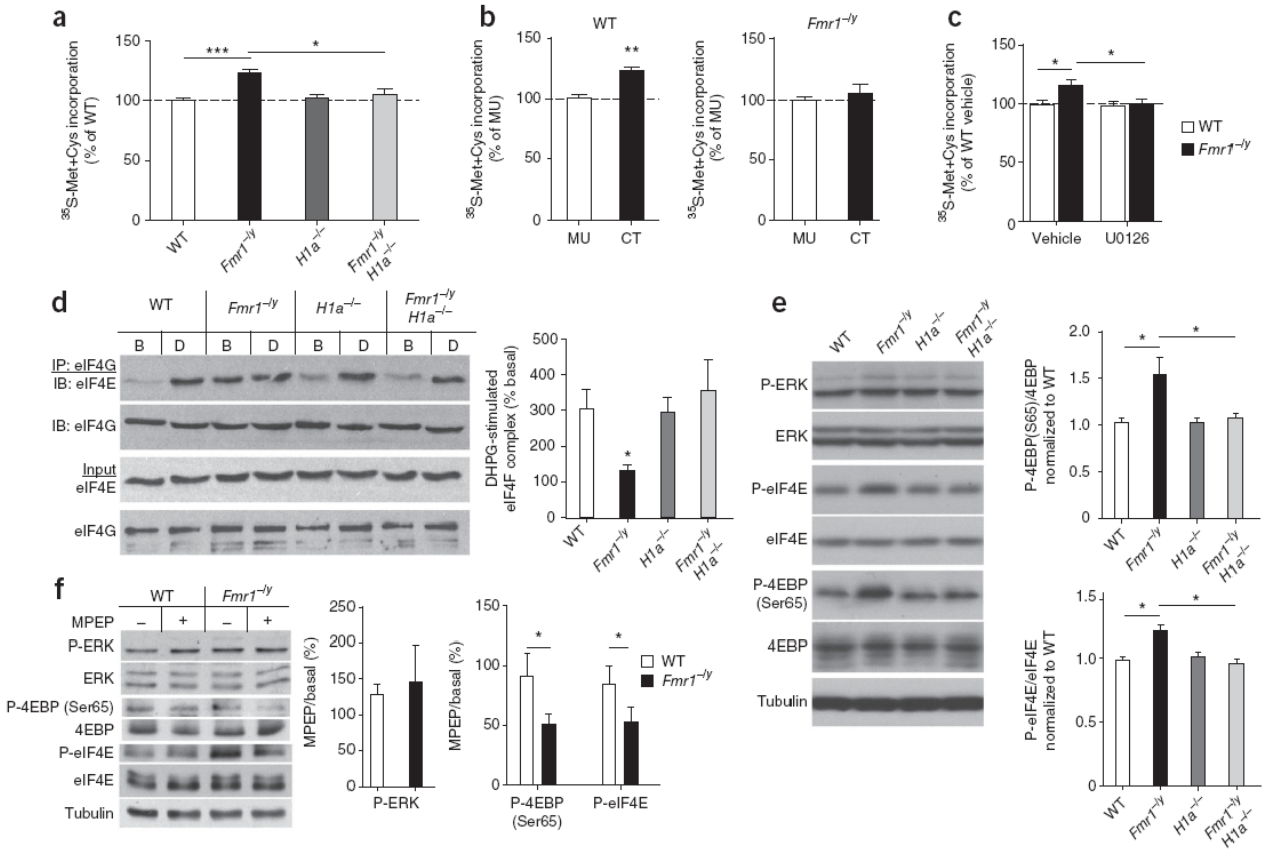

<*Previous page*>

Figure 3.3. Altered mGluR5-Homer scaffolds in *Fmr1–/y* mice mediate enhanced basal translation rates and initiation complex formation.
(a) Acute hippocampal slices from *Fmr1*–/y mice showed elevated protein synthesis rate in comparison to WT littermates as measured by incorporation of ^{35}S-methionine and ^{35}S-cysteine into total protein (n = 14 slices from 7 mice per genotype). Elevated protein synthesis rates in *Fmr1*–/y slices were reversed by H1a deletion (n = 7 slices, 4 mice), whereas H1a deletion alone (n = 8 slices, 4 mice) had no effect. **(b)** Pretreatment of WT hippocampal slices with mGluR5CT (CT; 5 μM; 5 h; n = 16 slices, 4 mice) enhanced incorporation of ^{35}S-methionine and ^{35}S-cysteine in comparison to treatment with mGluR5MU control peptide (MU; n = 16 slices, 4 mice). In contrast, pretreatment of *Fmr1*–/y hippocampal slices (n = 15 slices, 4 mice) with CT peptide had no effect. **(c)** Preincubation of WT or *Fmr1*–/y slices with U0126 (20 μM; 30 min) before ^{35}S-methionine and ^{35}S-cysteine incorporation (n = 12 slices, 6 mice per condition) equalized protein synthesis rates. **(d)** Left: representative immunoblots (IB) of eIF4E coimmunoprecipitating (IP) with eIF4G from hippocampal slices. DHPG (D) induced an increase in eIF4E association with eIF4G, forming the eIF4F translation initiation complex, in WT but not in *Fmr1*–/y littermates despite an elevated level of eIF4F complex under basal (B) conditions. H1a deletion alone had no effect on eIF4F complex levels under basal or DHPG-stimulated conditions, whereas H1a deletion on the *Fmr1*–/y background reversed the enhanced eIF4F complex levels and restored DHPG-induced eIF4F complex formation. Right: quantified group data for eIF4E coimmunoprecipitating with eIF4G (eIF4F complex) in DHPG-treated samples (normalized to the value in basal, or untreated, slices). n = 3 mice per genotype. **(e)** Left: representative western blots of phospho- and total ERK and translation initiation factors that are regulated by ERK (phospho- and total eIF4E and 4EBP) from cortical homogenates in each of four genotypes. Right: quantified group data reveal elevated phospho (P)-4EBP and P-eIF4E in *Fmr1*–/y brains as compared to WT, which is rescued by H1a deletion. P-ERK levels were not different across any genotype (n = 4–6 mice per genotype). (f) Left: representative western blots from acute hippocampal slices prepared from WT and Fmr1–/y mice treated with MPEP (10 μM) or vehicle (H^2O). Right: quantified group data for phosphoproteins in MPEP-treated slices expressed as a percentage of that in basal (untreated) slices reveal a genotypic difference in P-4EBP (Ser65) and P-eIF4E but not P-ERK (n = 2 slices per mouse; 4–8 mice per condition). *P < 0.05; **P < 0.01; ***P < 0.001; error bars, s.e.m.

Figure 3.4. Genetic deletion of Homer1a does not reverse the protein synthesis independence of mGluR-induced LTD or altered protein levels of FMRP target mRNAs.

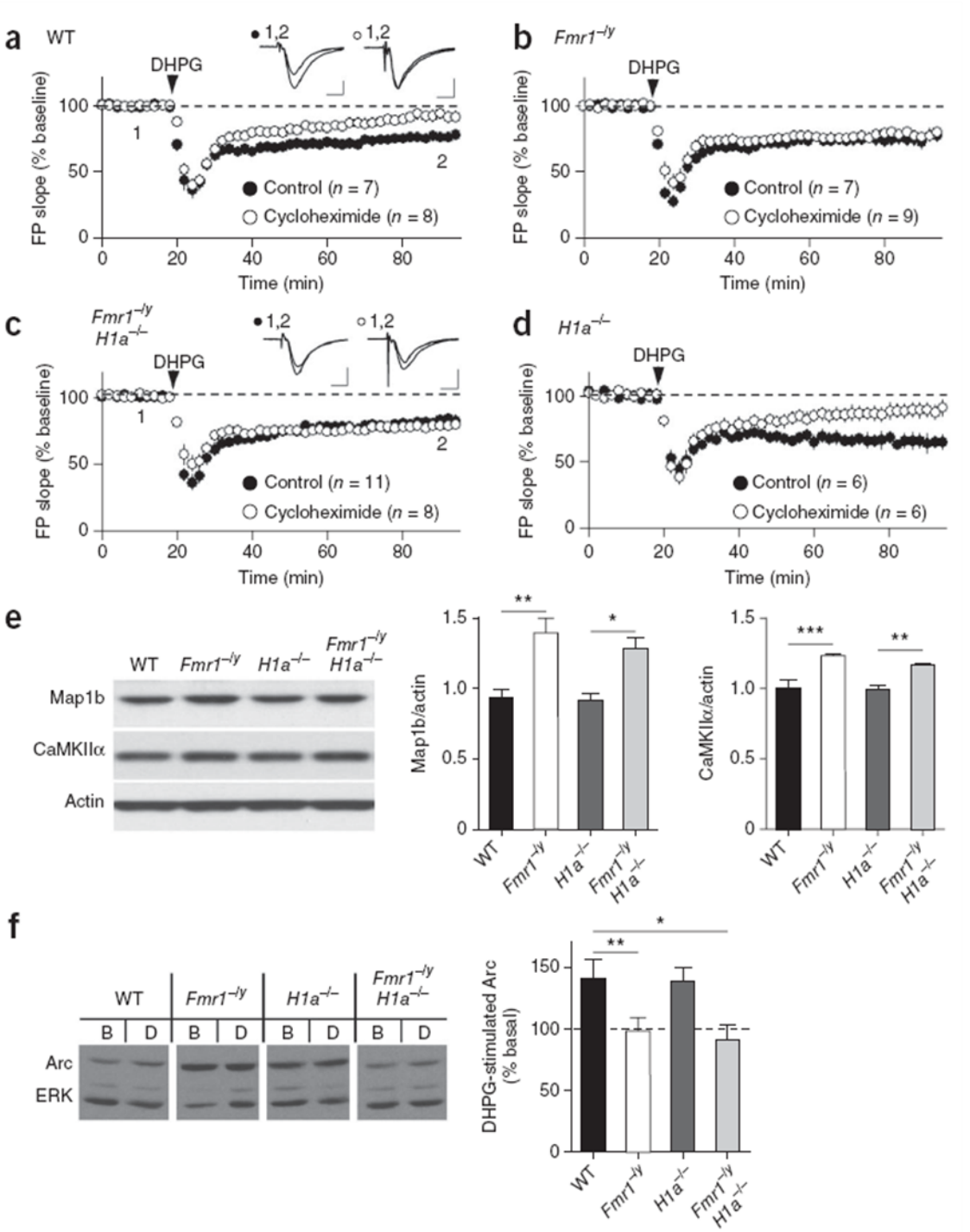

<*Previous page*>

Figure 3.4. Genetic deletion of Homer1a does not reverse the protein synthesis independence of mGluR-induced LTD or altered protein levels of FMRP target mRNAs.

(a) Brief DHPG (100 μM; 5 min) induced long-term depression (LTD) of synaptic transmission in WT hippocampal slices that was reduced by the protein synthesis inhibitor cycloheximide (60 μM; $P < 0.01$). Plotted are group averages of field excitatory postsynaptic potential (FP) slope normalized to pre-DHPG baseline as a function of time. Inset, average of ten FPs taken during the baseline period (1) and 55–60 min after DHPG treatment (2). Scale bars: 0.5 mV, 5 ms. **(b,c)** In *Fmr1*–/y and H1a–/–*Fmr1*–/y mice, DHPG-induced LTD was unaffected by cycloheximide. **(d)** In H1a–/– mice, DHPG-induced LTD was normal and blocked by cycloheximide ($P < 0.05$). n, number of slices. **(e)** Map1b and CaMKIIα were elevated in *Fmr1*–/y mice and were unaffected by H1a deletion. Left: representative western blots of Map1b, CaMKIIα and actin (loading control) from hippocampal homogenates of each genotype. Right: quantified group data of Map1b/actin and CaMKIIα/actin ratios in each genotype. (Map1b/actin ratio: WT, 0.92 ± 0.06; *Fmr1*–/y, 1.4 ± 0.1; H1a–/–, 0.8 ± 0.06; H1a–/–*Fmr1*–/y, 1.28 ± 0.08; CaMKIIα/actin ratio: WT, 1.0 ± 0.04; *Fmr1*–/y, 1.23 ± 0.02; H1a–/–, 1.0 ± 0.03; H1a–/–*Fmr1*–/y, 1.17 ± 0.01; n = 3 or 4 mice per genotype). **(f)** DHPG-induced Arc synthesis was deficient in *Fmr1*–/y mice and was not rescued by H1a deletion. Left: representative western blots of basal (B) Arc levels and DHPG (D)-induced Arc from hippocampal slices of each genotype. Full-length western blots for this figure are shown in Supplementary Figure 10. Group averages reveal a deficit in DHPG-induced Arc synthesis slices taken from *Fmr1*–/y (n = 10 mice) and H1a–/–*Fmr1*–/y (n = 11) mice. DHPG induced Arc synthesis in both WT (n = 12) and H1a–/– (n = 14) littermates. *$P < 0.05$; **$P < 0.01$; ***$P < 0.001$; error bars, s.e.m.

Figure 3.5. Disruption of mGluR5-Homer interactions mediates prolonged neocortical UP states in *Fmr1*–/y mice.

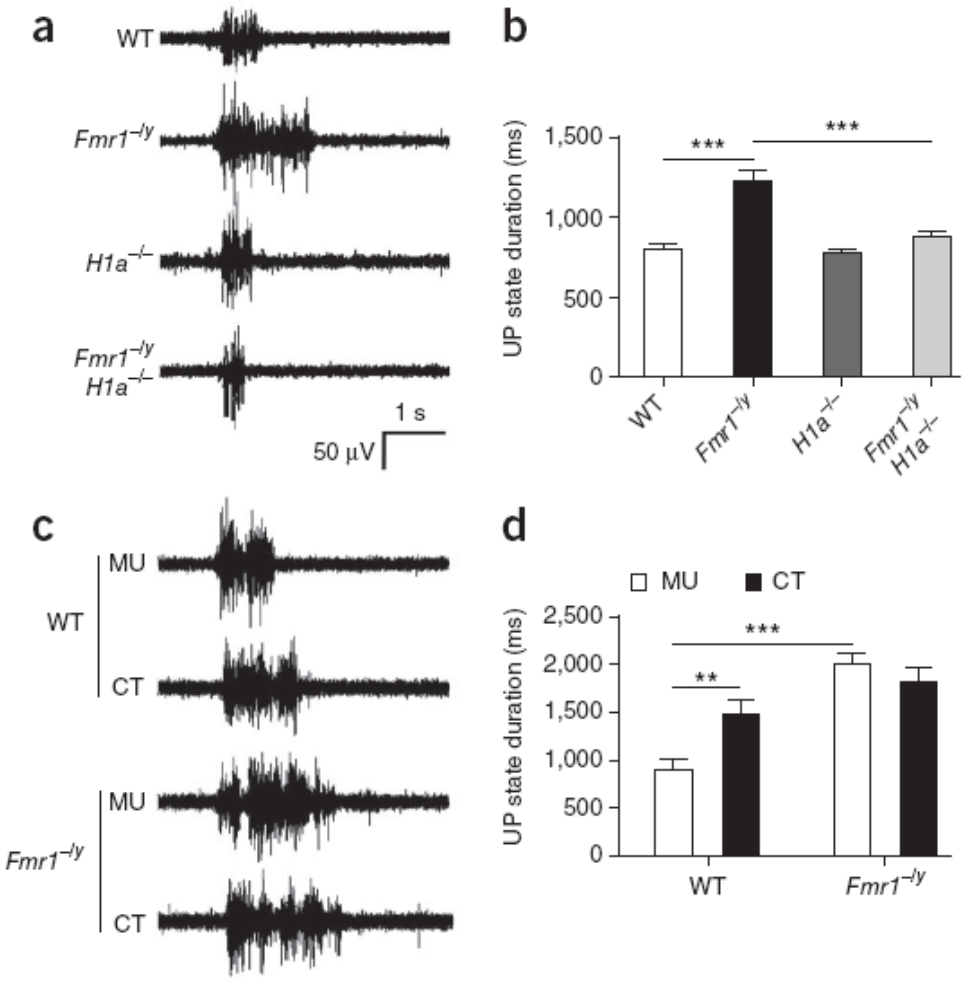

<*Previous page*>

Figure 3.5. Disruption of mGluR5-Homer interactions mediates prolonged neocortical UP states in *Fmr1*–/y mice.
(a,b) Genetic deletion of H1a rescued prolonged UP states in *Fmr1*–/y mice. **(a)** Representative extracellular multiunit recordings of spontaneous, persistent activity or UP states from layer 4 of somatosensory barrel neocortical slices from each genotype. **(b)** Group averages reveal that the UP state duration was prolonged in the *Fmr1*–/y slices (n = 13) in comparison to WT (n = 22). UP state duration in H1a–/–*Fmr1*–/y mice (n = 44 slices) was reduced from that in *Fmr1*–/y mice and was not different from WT. There was no difference between WT and H1a–/– single knockout (n = 18), suggesting that the rescue is dependent on Fmr1 knockout and not a general decrease in excitability due to loss of H1a. **(c)** Representative UP state recordings from WT and *Fmr1*–/y slices treated with the indicated peptide: CT, mGluR5CT; MU, mGluR5MU. **(d)** Pretreatment of WT neocortical slices with CT peptide (4 h; 5 μM; n = 15 slices) to acutely disrupt mGluR5-Homer interactions increased UP state duration in comparison to slices pretreated with MU control (5 μM; n = 13). In contrast, treatment of *Fmr1*–/y slices (n = 12) with CT peptide had no effect on UP state duration in comparison to MU treatment (n = 15). **P < 0.01; ***P < 0.001; error bars, s.e.m.

Figure 3.6. H1a deletion reduces audiogenic seizures and corrects open field activity in the Fmr1–/y mouse.

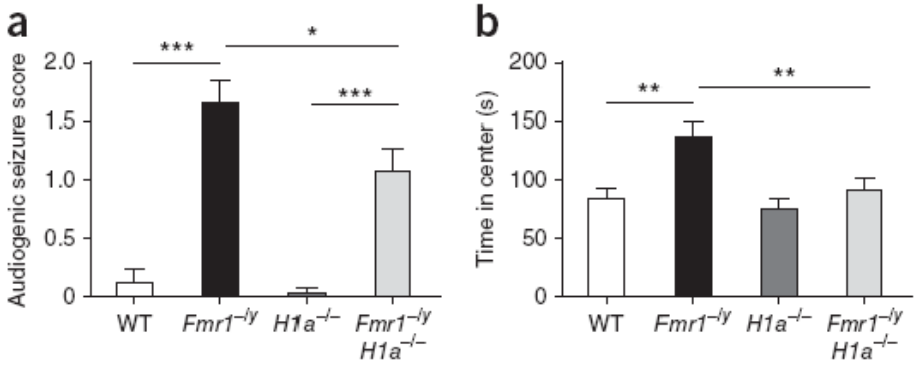

Figure 3.6. H1a deletion reduces audiogenic seizures and corrects open field activity in the Fmr1–/y mouse.

(**a**) Incidence and severity of audiogenic seizures, scored as described in Methods. *Fmr1*–/y mice had an increased seizure score that was reduced in H1a–/–*Fmr1*–/y mice (n = 16, 39, 24 and 37 mice for WT, *Fmr1*–/y, H1a–/– and H1a–/–*Fmr1*–/y, respectively). (**b**) Open field activity, measured as time spent in the center of a lit open arena, was increased in *Fmr1*–/y mice and reversed to WT levels in H1a–/–*Fmr1*–/y mice (n = 18, 24, 17 and 17 mice for WT, *Fmr1*–/y, H1a–/– and H1a–/–*Fmr1*–/y, respectively). *P < 0.05; **P < 0.01; ***P < 0.001; error bars, s.e.m.

Supplementary Figure 3.1. Disruption of mGluR5-Homer scaffolds in rat hippocampal slices bidirectionally regulates mGluR signaling to translation initiation and elongation and blocks synthesis of Arc.

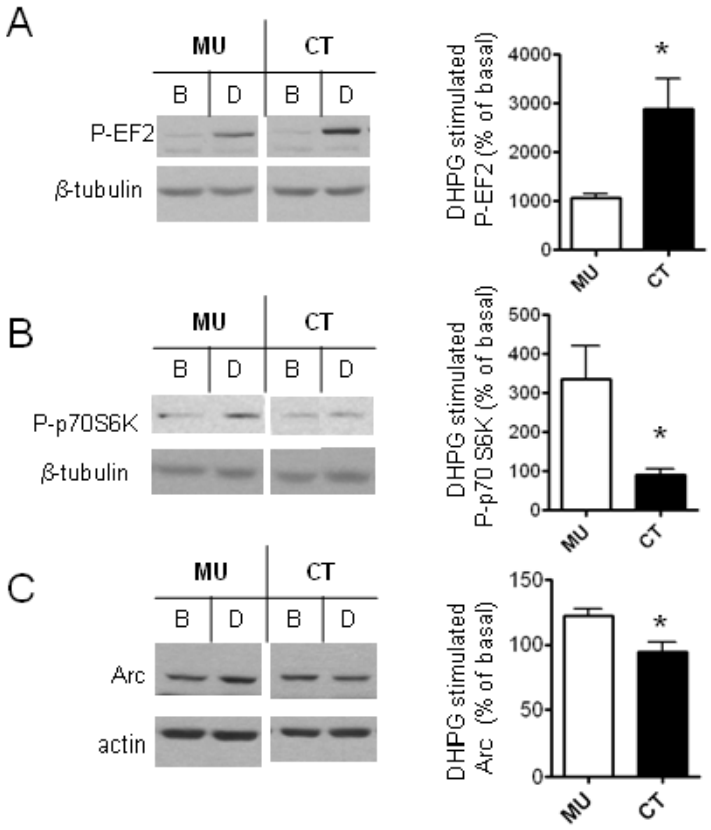

<*Previous page*>

Supplementary Figure 3.1. Disruption of mGluR5-Homer scaffolds in rat hippocampal slices bidirectionally regulates mGluR signaling to translation initiation and elongation and blocks synthesis of Arc. Related to Fig. 1

A. Pretreatment of rat hippocampal slices with a peptide that disrupts mGluR5-Homer interactions (tat-mGluR5CT; CT; 5 hours; 5 μM) results in enhanced DHPG-induced (100 μM; 5 min) phosphorylation of EF2 in comparison to slices treated with a control peptide that does not disrupt mGluR5-Homer interactions (tat-mGluR5MU; MU) (CT; 2876±633% of basal; n = 7 rats; MU; 1060±87% of basal; n = 6). Left: Representative western blot of Thr56 phosphorylated (P)-EF2 and β-tubulin (loading control) in the basal (B), or untreated, condition and DHPG (D) treated slices. Right: To obtain group data for panels **A-C**, in each rat, levels of P-EF2 or P-p70S6K or Arc in DHPG treated slices were normalized a loading control (tubulin or actin) and expressed as a percentage of basal levels (as measured in untreated slices) and averaged across animals. **B.** For a subset of the samples analyzed in panel **A**, DHPG-induced Thr389 phosphorylation of p70S6K was evaluated. MU pretreated slices exhibited robust DHPG- induced phosphorylation of p70S6K, whereas in CT pretreated slices DHPG induced P-p70S6K was blocked (CT; 91±15% of basal, n=5; MU: 337±83% of basal, n=4). **C.** In a separate set of animals, DHPG-induced increases in total Arc protein is blocked with CT peptide (CT: 95±7% of basal, n=7; MU: 122±5% of basal, n=7). *$p < 0.05$.

Supplementary Figure 3.2. H1a-mGluR5 interactions are elevated in *Fmr1* KO mice, but total levels of H1a, long Homers or mGluR5 are unchanged.

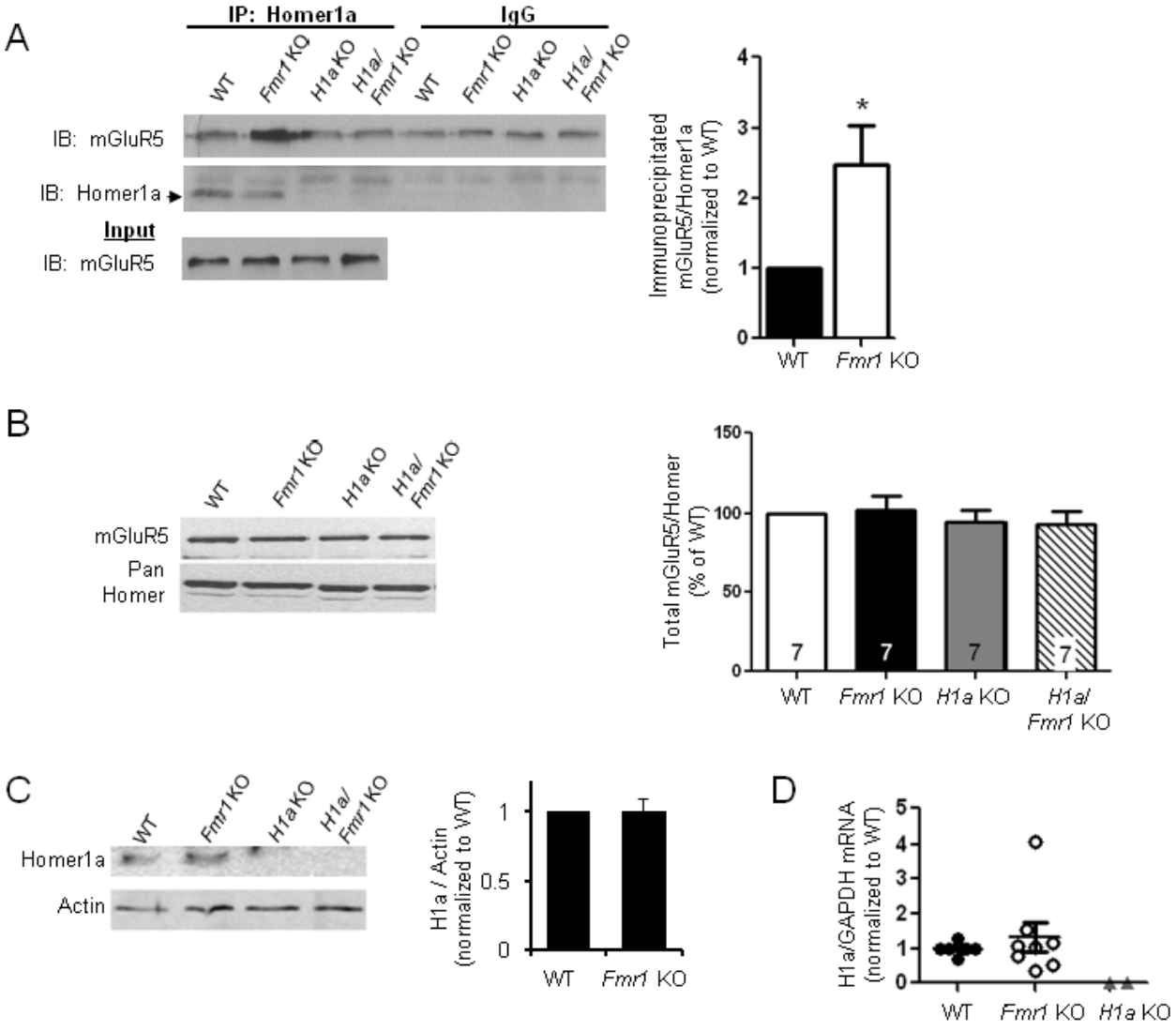

<*Previous page*>

Supplementary Figure 3.2. H1a-mGluR5 interactions are elevated in *Fmr1* KO mice, but total levels of H1a, long Homers or mGluR5 are unchanged. Related to Figure 2.

A. mGluR5-Homer1a interactions are increased in hippocampal homogenates of Fmr1 KO mice. Homer1a was immunoprecipitated from total mouse hippocampal lysate. The level of mGluR5 that coimmunoprecipitated with Homer1a was quantified and normalized to levels of immunoprecipitated Homer1a. Arrowhead indicates specific H1a band that is absent in the H1a KO lysates. There is a low level of mGluR5 that nonspecifically pulls down with goat IgG. Group data from 4 set of littermates reveals an increase in Homer1a/mGluR5 in Fmr1 KO. *$p< 0.05$. **B.** Total mGluR5 and long Homer (with pan-Homer antibody) is normal in WT, *Fmr1* KO, H1a KO and H1a/*Fmr1* KO. **C.** Homer1a protein levels (normalized to actin) are unaffected in total lysates of whole hippocampus of Fmr1 KO mice. **D.** Quantitative RT-PCR hippocampal H1a and GAPDH mRNA reveal there is no change in H1a mRNA levels in Fmr1 KO mice. Note: Homogenates prepared from H1a KO mice demonstrate the specificity of the H1a RT-PCR primers.

Supplementary Figure 3.3. Effects of the PI3K inhibitor, wortmannin, on protein synthesis rates in WT and *Fmr1 KO* hippocampal slices.

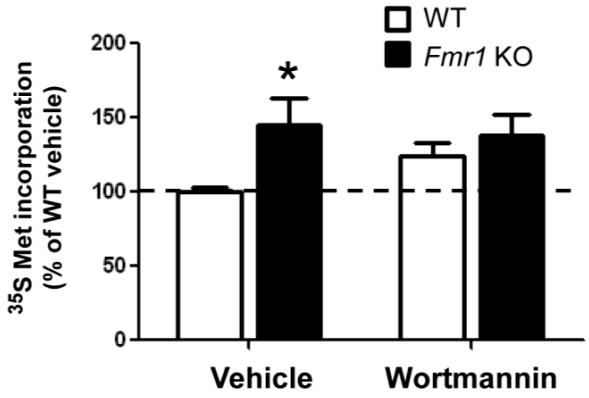

Supplementary Figure 3.3. Effects of the PI3K inhibitor, wortmannin, on protein synthesis rates in WT and *Fmr1 KO* hippocampal slices. Related to Figure 3C.

Acute hippocampal slices from *Fmr1* KO mice display elevated protein synthesis rate in comparison to WT littermates as measured by incorporation of 35S Met/Cys into total protein. Slices from WT or *Fmr1* KO mice were preincubated in the PI3K inhibitor wortmannin (100 nM; 30 min) prior to ^{35}S Met incorporation (n = 12 slices/ 6 mice per condition). Inhibition of PI3K using wortmannin (100 nM) pathway equalizes protein synthesis rates between WT and *Fmr1* KO slices, but this may be due to an increase in protein synthesis rates in WT slices ($p < 0.05$; t-test), as opposed to a decrease of protein synthesis rates in *Fmr1* KO slices.

Supplementary Figure 3.4. Inhibition of ERK activation in hippocampal slices reduces or abolishes phosphospecific antibody detection of P-ERK, P(S209) eIF4E, and P(65) 4EBP.

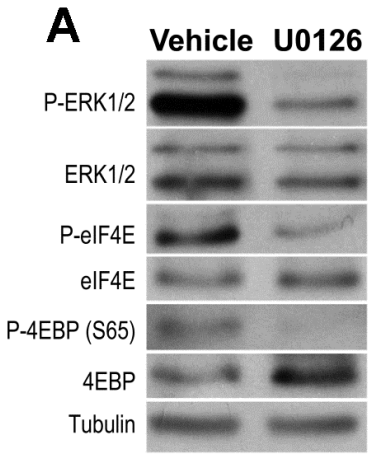

B

	WT		*Fmr1* KO	
MPEP	% of Basal	SEM	% of Basal	SEM
ERK	81	2	106	14
eIF4E	110	9	133	30
4EBP	109	13	116	11

Supplementary Figure 3.4. Inhibition of ERK activation in hippocampal slices reduces or abolishes phosphospecific antibody detection of P-ERK, P(S209) eIF4E, and P(65) 4EBP. Related to Fig. 3.

A. Acute hippocampal slices from WT mice were preincubated in the MEK inhibitor U0126 (20 μM) or vehicle (0.01% DMSO) for 30 min prior to lysis and western blotting. **B.** MPEP treatment of hippocampal slices from WT or *Fmr1* KO mice has no effect on total levels of ERK, eIF4E or 4EBP. Related to Fig. 3F. Acute hippocampal slices were incubated in MPEP (10 μM) or untreated (basal). Total protein levels for ERK, eIF4E, 4EBP were normalized to a loading control (tubulin) on the same blot each for MPEP and untreated slices. Representative blots of this data are shown in Fig. 3F1. (n = 2 slices/mouse; 4- 8 mice/condition).

Supplementary Figure 3.5. *Fmr1*, H1a, or H1a/*Fmr1* KO do not affect locomotor activity and therefore do not underlie the rescue of open field activity.

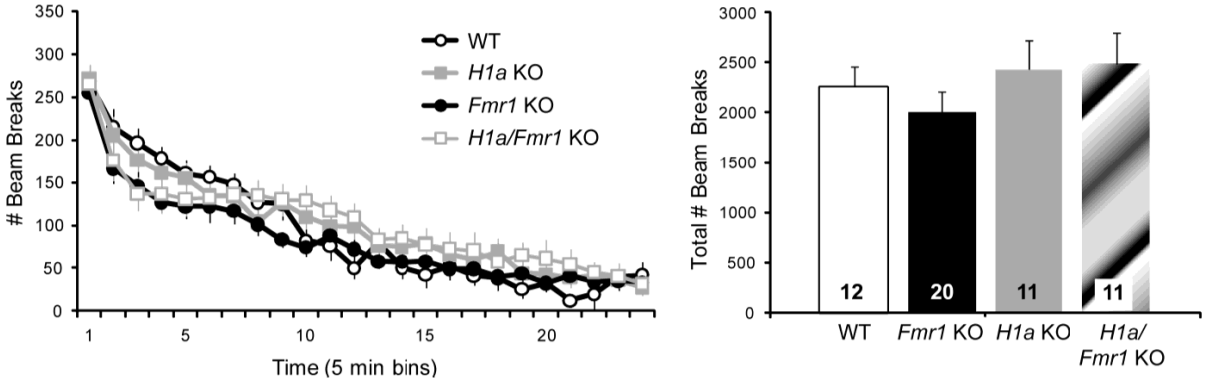

Supplementary Figure 3.5. *Fmr1*, H1a, or H1a/*Fmr1* KO do not affect locomotor activity and therefore do not underlie the rescue of open field activity. Related to Fig. 6.

Locomotor activity, as measured by number of beam breaks per unit time, is unaffected by *Fmr1* KO, H1a KO or H1a/*Fmr1* KO. N = # of mice is indicated on each bar.

Table 3.1. Seizure occurrence and severity in WT, *Fmr1* KO, H1a KO and H1a/*Fmr1* KO genotypes.

	Wild running	Seizure (clonic/tonic)	Status Epilepticus	% Incidence
WT	1/17	1/17	0/17	5.8%
***Fmr1* KO**	29/41	25/41	14/41	61.0%
***H1a* KO**	1/24	0/24	0/24	0.0%
***H1a* KO/*Fmr1* KO**	20/38	13/38	8/38	34.2%*

Table 3.1. Seizure occurrence and severity in WT, *Fmr1* KO, H1a KO and H1a/*Fmr1* KO genotypes. Related to Fig. 6.
* $p < 0.05$ Fisher's Exact test.

CHAPTER FOUR
Preliminary Results

FURTHER EXAMINATION OF THE CELLULAR MECHANISMS AND RELEVANCE OF PROLONGED UP STATES IN THE *FMR1* KO

Summary

Our previous work has identified that UP states are prolonged in the neocortical excitatory circuitry in the *Fmr1* KO. This increase in duration of UP states is driven by enhanced mGluR5 signaling that results from disruption of Homer scaffolds. Here we demonstrate that the prolonged UP state duration is not driven by deletion of FMRP in a specific cortical layer, but rather all layers partially contribute to the hyperexcitability. Furthermore, we provide direct evidence that Homer-mGluR5 disruption is the principle mechanism for increased excitability. We also provide a preliminary assessment of currents that are candidates to drive enhanced network excitability in layer 5 pyramidal neurons. Presumptive mGluR-dependent depolarizing currents, as well as A-type current, H-current, and sodium-dependent potassium current are unchanged in the *Fmr1* KO. However, assessment of general neuronal properties reveals a trend towards an increase in excitability of layer 5 pyramidal neurons in the KO. Additionally, we show that despite increased UP state duration resulting from neocortical excitatory neuron deletion of FMRP, audiogenic seizures are unchanged. These

results provide a framework for understanding the underpinnings of network excitability in the *Fmr1* KO.

Introduction

Fragile X Syndrome is the most common heritable form of mental retardation, affecting approximately 1:2000 males and 1:4000 females (O'Donnell and Warren 2002). In the majority of cases, FXS is caused by loss of function of the gene product of *Fmr1*, the Fragile X mental retardation protein. FXS shares several common features with autism, and many FXS patients are diagnosed with ASD (Hagerman and Hagerman 2002). Shifts in the excitation to inhibition ratio are hypothesized to underlie many deficits in ASD (Rubenstein and Merzenich 2003). Similarly, an imbalance in E/I ratio may cause some of the symptoms of FXS. Suggestive of a disparity in E/I, *Fmr1* KO mice display audiogenic seizures and heightened sensory perception (Chen and Toth 2001). These alterations led us to investigate network properties in the *Fmr1* KO.

Our studies detailed in previous chapters have shown that cortical network excitability is altered in the *Fmr1* KO (Hays, Huber et al. 2011). Specifically, slices from *Fmr1* KO mice display network hyperexcitability in the form of prolonged UP states. UP states are epochs of synchronized depolarization of local networks of neocortical neurons, and can be used as a measure of circuit excitability.

In order to further investigate the currents that are responsible for the network hyperexcitability, I sought to identify the cellular locus of FMRP's function within the circuit. Identifying a particular population of cells in which deletion of FMRP drives prolonged UP states would facilitate the detection of any currents that may be causing circuit hyperexcitability. Previously, I showed that increased UP state duration in the *Fmr1* KO is intrinsic to neocortex (Hays, Huber et al. 2011). Additionally, prolonged UP states result from the loss of FMRP in excitatory neurons. Here, I investigate network function in the presence of various manipulations of FMRP expression in different cortical layers. UP states in the *Fmr1* KO are driven by enhanced mGluR function, and mGluR5 signaling is known to differentially regulate excitability in certain layers. Therefore, I hypothesized that deletion of FMRP from specific layers would have differential effects on UP state duration. However, I find that deletion of FMRP from layer 4 or layer 5 partially increases UP state duration with no differential effects.

I observe that the increase in duration of UP states in the *Fmr1* KO is likely due to excessive mGluR5 activity, as it is rescued by genetic and pharmacological reduction of mGluR5 signaling (Hays, Huber et al. 2011). Additionally, uncoupling of mGluR5 from the scaffold protein Homer causes increased UP state duration. Uncoupling of mGluR5 from long Homers is known to cause mGluR5 to become constitutively active (Ango, Prezeau et al. 2001). *Fmr1* KOs have basally reduced coupling of mGluR5-Homer complexes which

could be driving excessive mGluR signaling, and restoring mGluR-Homer interactions rescues the prolonged UP states (Giuffrida, Musumeci et al. 2005). However, our previous data have been derived from global manipulations of Homer interactions with all its effectors. Here I use a mouse which bears a point mutation the specifically prevents association of mGluR5 and Homer (Cozzoli, Goulding et al. 2009). Disruption of this single specific interaction is sufficient to prolong UP state duration in a gene dosage dependent manner, strongly implicating Homer and mGluR function in regulation of network excitability.

Enhanced mGluR activity gives rise to the network hyperexcitability in the *Fmr1* KO. However, as mGluRs are not themselves ionotropic and therefore cannot directly regulate excitability, we sought to identify the mGluR-dependent current that is motivating enhanced network excitability in the *Fmr1* KO. One potential mechanism for increased network excitability is enhanced depolarizing currents. mGluRs can induce depolarization in cortical neurons, and Homer1a directly interacts with TRP channels to regulate intrinsic depolarizing currents. (Yuan, Kiselyov et al. 2003; Yoshida, Fransén et al. 2008; Zhang and Seguela 2010). I show that presumptive mGluR-dependent depolarizing currents are unchanged in the *Fmr1* KO.

Alternatively, reduced hyperpolarizing currents could equally lead to network hyperexcitability. Several candidate hyperpolarizing currents have been identified as potentially being altered in the *Fmr1* KO. A-type potassium current

is a subthreshold current that opposes depolarization. Kv4.2 protein controls the major component of A-type current, and Kv4.2 is expressed in the neocortex (Serôdio and Rudy 1998; Chen, Yuan et al. 2006; Norris and Nerbonne 2010). A-type current is suppressed by mGluR5 activation and Kv4.2 expression may be reduced in the *Fmr1* KO (Hu, Alter et al. 2007; Gross, Yao et al. 2011). Both cases would lead to a deficit in repolarization, and therefore potentially to enhanced network excitation. I observe that functional somatic A-type current is unchanged in the *Fmr1* KO. Sodium-dependent potassium current mediated by the Slack channel is reduced in MNTB neurons in the *Fmr1* KO (Brown, Kronengold et al. 2010). My preliminary observations suggest that the functional contribution of Slack is minimal and therefore is unlikely to contribute to prolonged UP states.

Although direct examination of the candidates did not identify the conductance responsible for hyperexcitability, I examined general neuronal properties. UP state analysis suggests that layers 4 and 5 contain the alterations giving rise to network hyperexcitability. Our previous studies indicate that excitatory spiny stellate neurons in layer 4 of the neocortex are hyperexcitable (Gibson, Bartley et al. 2008). Here, I provide preliminary evidence that layer 5 excitatory pyramidal neurons show a trend toward enhanced intrinsic excitability, likely mediated by an increase in input resistance.

Corresponding to circuit hyperexcitability, *Fmr1* KO mice display a propensity for audiogenic seizures and prolonged UP state duration (Chen and Toth 2001; Yan, Rammal et al. 2005). Neocortical deletion of FMRP from excitatory neurons recapitulates the prolonged UP states observed in the *Fmr1* KO, while deletion from inhibitory neurons has no effect on network function (Hays, Huber et al. 2011). I sought to determine whether increases in UP state duration directly correlate to audiogenic seizures. Despite the increase in UP state duration, neocortical deletion of FMRP from excitatory or inhibitory neurons has no effect on propensity for audiogenic seizures, thereby implicating subcortical structures in seizure generation in the *Fmr1* KO.

Here, I provide various lines of evidence that give insight into the locus and cellular alterations underlying circuit dysfunction in the *Fmr1* KO. I observe that neurons throughout all cortical layers partially contribute to the increase in UP state duration in the *Fmr1* KO. Specific disruption of the interaction of Homer and mGluR5 is sufficient to cause these prolonged UP states. Additionally, general increases in neuronal excitability potentially give rise to the network hyperexcitability. Furthermore, increases in neocortical network hyperexcitability do not directly correlate to epileptogenesis. These results support the hypothesis that mGluR5 dysfunction resulting from altered Homer interactions gives rise to prolonged UP states in the *Fmr1* KO and provide

additional insight into the mechanism and relevance of the regulation of circuit function by FMRP.

Materials and Methods

Mice

Congenic *Fmr1* KO mice on the C57BL6 background were originally obtained from Dr. Stephen Warren (Emory University) and have been backcrossed onto the C57Bl6/J mice from the UT Southwestern breeding core colony (Bakker 1994). Tg(Satb2-cre)MO23Gsat/Mmcd (*SatB2* Cre) mice were obtained as frozen embryos from Mutant Mouse Regional Resource Centers and generated in the UT Southwestern Transgenic Core Facility. Tg(Six3-cre69)Frty (*Six3* Cre) mice were obtained from Dr. Yasuhide Furuta (Liao and Xu 2008). *Emx1* Cre mice were obtained from Dr.Takuji Iwasato and Dr. Shigeyoshi Itohara (Iwasato, Datwani et al. 2000; Iwasato, Inan et al. 2008) and *Dlx5/6* Cre mice were obtained from Dr. Marc Ekker and Dr. John Rubinstein (Monory, Massa et al. 2006). Floxed *Fmr1* and Fmr1 conditional ON (cON) mice were obtained from Dr. David Nelson (Mientjes, Nieuwenhuizen et al. 2006). All experiments were performed with littermate comparisons. Experimenters were blind to mouse genotype.

Slice preparation

Mice 3 weeks of age (P18-P24) were deeply anesthetized with Euthasol (pentobarbital sodium and phenytoin sodium solution) and decapitated. The brain was transferred into ice-cold dissection buffer containing (in mM): 87 NaCl, 3 KCl, 1.25 NaH2PO4, 26 NaHCO3, 7 MgCl2, 0.5 CaCl2, 20 D-glucose, 75 sucrose and 1.3 ascorbic acid aerating with 95% O2–5% CO2. Thalamocortical slices 400 μm were made on an angled block (Agmon and Connors 1991) using a vibratome (Vibratome 1000 Plus). Following cutting, slices were transected parallel to the pia mater to remove the thalamus and midbrain. Slices were immediately transferred to an interface recording chamber (Harvard Instruments) and allowed to recover for 1 hr in nominal ACSF at 32ºC containing (in mM): 126 NaCl, 3 KCl, 1.25 NaH2PO4, 26 NaHCO3, 2 MgCl2, 2 CaCl2, and 25 D-glucose. After this, slices were perfused with a modified ACSF that better mimics physiological ionic concentrations in vivo which contained (in mM): 126 NaCl, 5 KCl, 1.25 NaH2PO4, 26 NaHCO3, 1 MgCl2, 1 CaCl2, and 25 D-glucose (based on but modified from (Sanchez-Vives and McCormick 2000; Gibson, Bartley et al. 2008)). We used a slightly higher external K+ concentration to promote active states (5 mM versus 3.5 mM in vivo), but this manipulation was probably unnecessary since the use of 3.5 mM external K+ still results in spontaneously generated UP states (Rigas and Castro-Alamancos 2007). Slices remained in this modified ACSF for 45 minutes and then recordings were performed with the same modified ACSF.

Acute neuronal dissociation

Acute neuronal dissociation was performed as previously described (Guan, Horton et al. 2011). Briefly, neocortical slices, prepared as described above, were stored in nominal ACSF at room termperature containing (in mM): 126 NaCl, 3 KCl, 1.25 NaH2PO4, 26 NaHCO3, 2 MgCl2, 2 CaCl2, and 25 D-glucose until dissociation. Slices were microdissected to remove superficial layers, leaving only layers 5 and 6 intact. Remaining tissue was transferred into nominal ACSF supplemented with 1.2mg/mL Sigma protease XIV (Sigma Aldrich) and incubated at 32°C for 25-30 min. After incubation, the tissue was washed twice with HBSS + FBS, and then twice with wash ACSF containing (in mM): 140 sodium isethionate, 2 KCl, 4 MgCl2, 0.1 CaCl2, 23 D-glucose, 15 HEPES. Tissue was then triturated with a 1mL pipet in recording ACSF containing (in mM): 140 sodium isethionate, 3 KCl, 1 MgCl2, 1.9 CaCl2, 12 D-glucose, 10 HEPES, 0.001 TTX, 3 TEA, 0.02 ZD7288, as well as 20 nM DTX and 5 nM MTX to block some delayed rectifier components. The resulting suspension was strained with a cell strainer (Falcon plastics) and transferred immediately onto a poly-D-lysine coated coverslip on the recording stage and allowed to settle for 5 minutes. Recordings were made within 1 hour of dissociation.

UP state recordings and analysis

Spontaneously generated UP states *in vitro* were extracellularly recorded using 0.5 MΩ tungsten microelectrodes (FHC, Bowdoinham, ME) placed in layer 4 of primary somatosensory cortex. This extracellular monitoring of UP states is a reliable indicator of the synchronous, depolarized state of neuron populations from which the term "UP state" was originally defined (Sanchez-Vives and McCormick 2000; Rigas and Castro-Alamancos 2007). As indicated, some recordings were performed in layer 5. 5 or 10 min of spontaneous activity was collected from each slice. Recordings were amplified 10,000-fold, sampled at 2.5 kHz, and filtered on-line between 500Hz and 3 kHz. All measurements were analyzed off-line using custom Labview software. For visualization and analysis of UP states, traces were offset to zero, rectified, and low-pass filtered with a 0.2 Hz cutoff frequency. Using these processed traces, the threshold for detection was set at 5x the RMS (root mean square) noise, and an event was defined as an UP state if its amplitude remained above the threshold for at least 200 ms. The end of the UP state was determined when the amplitude decreased below threshold for >600 ms. Two events occurring within 600ms of one another were grouped as a single UP state. These criteria best accounted for the simultaneous occurrence and identical durations of UP states in layers 4 and 5. Our main finding of longer UP states in *Fmr1* KO was not strictly dependent on these criteria since the same result was obtained with no grouping of events and with

different detection thresholds. UP state amplitude was defined based on the filtered/rectified traces and was unitless since it was normalized to the detection threshold. This amplitude may be considered a coarse indicator of the underlying firing rates of neuronal populations. Direct measures of firing rates were not possible because individual spikes could not be resolved except during the quiet periods (the DOWN states). Data are represented by the mean ± SEM and values. Significant differences were determined using t-tests, one-way ANOVA, or two-way ANOVA where appropriate (all performed with GraphPad Prism 5). Bonferroni posttests were performed following ANOVAs. Sample number (n) is slice number. For all slice experiments, a minimum of 4 mice were used per condition.

For cumulative distributions of UP state durations, a normalized cumulative distribution was obtained for each experiment (data from one slice or for *in vivo* experiments, from one mouse), where y values were interpolated for pre-determined points of the x-axis. This enabled the calculation of an average and standard deviation based on experiment, where sample number refers to slice number. A Kolmogorov-Smirnov test was performed for statistical analysis. This method equalizes the contribution to the distribution made by each experiment.

Intracellular electrophysiology

Either acute slices or acute dissociated neurons were prepared as described above. In slices, recordings were performed in layer 5 pyramidal neurons. In acute dissociation, recordings were performed in presumptive layer 5 pyramidal neurons. Neurons were identified by their morphology, and, when possible, their firing properties. In figure 4.6, slices were stimulated with a bipolar electrode placed approximately 250μm lateral in layer 5. Stimulation intensity began at 100μA and was progressively increased. Pipette resistance typically ranged from 3-7 MΩ. In slices, recordings typically began with a measure of input resistance. Recordings were accepted if series resistance was below 35MΩ. All data were collected and analyzed using custom Labview software (National Instruments). For measurement of general intrinsic properties, H-current, and mGluR-dependent currents, pipette internal contained (in mM): 130 K-gluconate, 6 KCl, 3 NaCl, 10 HEPES, 0.2 EGTA, 4 ATP-Mg, 0.3 GTP-Tris, 14 phosphocreatine-Tris, and 10 sucrose (pH 7.25, 290 mosM). For Slack current measurements, pipette internal contained (in mM): 117.5 KGluc, 12.5 KCl, 5 EGTA, 20 NaCl, 1 MgCl2, 10 HEPES (pH 7.2, 290 mosM). For [0 mM] Na+ experiments, NaCl was substituted for equimolar choline chloride. For A-type current measurements, pipette internal contained (in mM): 85 potassium methylsulfate, 63 KOH, 2 MgCl2, 10 BAPTA, 2 ATP sodium salt, 0.2 GTP sodium salt, 15 creatine phosphate, pH 7.2, 290 mosM.

Immunohistochemistry

Immunohistochemistry was performed to confirm deletion of FMRP. Mice (P21-P24) were perfused with cold PBS followed by 4% paraformaldehyde (w/v). The brain was removed and resectioned into 80 µm slices. Antigen retrieval was performed by placing the slices into warm 200 mM sodium citrate and microwaving for 1 min at low power. The slices were blocked for 1 hr at room temperature in PBS with 3% normal goat serum and 0.5% Triton-X. Primary antibodies were dissolved in blocking solution and applied overnight at 4°C. Secondary antibodies were dissolved in blocking solution and applied for 1 hr at room temperature. The primary antibody against FMRP (2F5, 1:200) was a gift from Dr. Jennifer Darnell. The specificity of 2F5 has been demonstrated previously (Gabel, Won et al. 2004) and by our comparison of labeling in Fmr1 KO versus WT tissue. The secondary antibody used was goat anti-mouse 555 (1:250, Sigma).

Audiogenic seizures

In order to evaluate audiogenic seizures, mice were placed in a plastic chamber (30 x 19 x 12cm) containing a 120 decibel siren (GE 50246 personal security alarm) and covered with a Styrofoam lid. A 120 dB siren was presented to mice for 5 minutes. Mice were videotaped and scored for behavioral phenotype: 0=no response, 1=wild running, 2=tonic-clonic seizures, 3=status

epilepticus/death as described (Dölen, Osterweil et al. 2007). Data were analyzed with a 2 way ANOVA and Bonferroni post hoc multiple comparison tests.

Results

All cortical layers partially contribute to prolonged UP state duration in the Fmr1 KO

In order to identify the locus of the function of FMRP in the cortex, I sought to delete FMRP from particular cortical layers and measure UP states. Mice that express a floxed *Fmr1* gene were crossed to mice that express Cre under the control of the *Six3* promoter. *Six3* expression in the forebrain is restricted to layer 4 of neocortex, and correspondingly, *Six3*-Cre mice show reporter expression restricted to layer 4 (Oliver, Mailhos et al. 1995; Liao and Xu 2008). This floxed *Fmr1* x *Six3* Cre cross resulted in a subset of mice in which FMRP was specifically deleted from layer 4 (Flox *Fmr1*; *Six3* Cre+) as confirmed by immunohistochemistry (Fig. 4.1A). UP states were measured from this genotype and from control littermates (Fig. 4.1B,C). Here "control" refers either WT *Fmr1*; *Six3* Cre- or WT *Fmr1*; *Six3* Cre+ littermates, neither of which have any deletion of FMRP. UP states recorded in layer 4 in slices from Flox *Fmr1*; *Six3* Cre+ animals were prolonged compared to control littermates (Fig. 4.1C; 775±51 vs. 996±60 ms, $p<0.05$; Control, Flox *Fmr1*; *Six3* Cre+; n=25, 16 slices).

A similar increase in duration was observed in layer 5 even though FMRP expression is normal (743±54 vs. 970±69 ms, $p<0.05$; Control, Flox *Fmr1*; *Six3* Cre+; n=24, 16 slices). However, the UP states in these animals are not as long as those observed previously in full *Fmr1* KO mice, suggesting that deletion of FMRP in layer 4 partially contributes to the prolonged UP states in the *Fmr1* KO.

Conversely, the *Six3* Cre mice were crossed to another line that expresses a conditional "ON" *Fmr1* (cON *Fmr1*) gene. In these mice, Cre excises a neomycin cassette from the *Fmr1* gene and allows transcription. Without the presence of Cre, expression is of FMRP is less than 40% of normal levels (David Nelson, personal communication, Fig4.2B), essentially rendering cON *Fmr1* mice without Cre comparable to the *Fmr1* KO. This 40% reduction in expression is sufficient to cause prolonged UP state duration similar to that previously observed in the *Fmr1* KO. When Cre is present, FMRP expression is restored to normal levels. The cross of *Six3* Cre mice to cON *Fmr1* mice results in WT *Fmr1*; Six3 Cre+, which have fully WT FMRP expression, cON *Fmr1*; *Six3* Cre+, which have WT expression of FMRP in layer 4 but no expression elsewhere, and cON *Fmr1*; *Six3* Cre-, which have no expression of FMRP throughout the cortex. FMRP expression was confirmed with immunohistochemistry (Fig. 4.2A). Layer 4 recordings demonstrate that animals which express FMRP only in layer 4 have reduced UP state duration compared to KO-expression littermates, but no difference from WT-expression littermates (Fig. 4.2C; 860±100 vs. 898±127 vs.

1288±73 ms, p<0.05; WT *Fmr1*; *Six3* Cre+, cON *Fmr1*; *Six3* Cre+, cON *Fmr1*; *Six3* Cre-; n=6, 12, 16 slices). Duration is similar in layer 5 (data not shown; 870±91 vs. 913±145 vs. 1342±102 ms, p<0.05; WT *Fmr1*; *Six3* Cre+, cON *Fmr1*; *Six3* Cre+, cON *Fmr1*; *Six3* Cre-; n=6, 11, 10 slices). This may suggest that restoration in layer 4 is sufficient to rescue UP state duration. However, these results are preliminary and require further verification. Furthermore, the remaining 40% expression level of FMRP in neurons which do not express Cre may also complicate interpretation of this data.

To further investigate the layer-specific role of FMRP in network excitability, FMRP was deleted from deep layers of neocortex while leaving expression in superficial layers intact. To this end, floxed *Fmr1* mice were crossed to *SatB2* Cre mice. *SatB2* expression is restricted primarily to layers 5 and 6 in the neocortex (Britanova, de Juan Romero et al. 2008). The cross of floxed *Fmr1* x *SatB2* Cre results in mice in which FMRP is deleted from greater than 80% of cells in layers 5 and 6 (Flox *Fmr1*; SatB2 Cre+), and control littermates (WT *Fmr1*; Cre- or WT *Fmr1*; Cre+) in which FMRP expression is normal as confirmed by immunohistochemistry (Fig. 4.3A). UP state duration is increased to a similar degree in both L4 and L5 in slices from Flox *Fmr1*; *SatB2* Cre+ slices compared to control littermates (Fig. 4.3C; Layer 4: 696±41 vs. 950±65 ms, p<0.01; WT *Fmr1*; *SatB2* Cre+, Flox *Fmr1*; *SatB2* Cre+; n=13, 11 slices; Layer 5: 715±43 vs. 946±65 ms, p<0.01; WT *Fmr1*; *SatB2* Cre+, Flox

Fmr1; *SatB2* Cre+; n=13, 10 slices). Similar to the L4 deletion, deletion from L5/6 does not cause UP states to be prolonged to the magnitude observed in the full *Fmr1* KO, suggesting a partial contribution from deep layers to prolonged UP state duration.

Specific disruption of mGluR5-Homer interactions causes prolonged UP states

Although previous data suggests that global uncoupling of Homer scaffolds results in prolonged UP states, disruption of the interaction of mGluR5 and Homer has not been directly linked to altered excitability. Here, network excitability is assayed in a mouse in which the *Grm5* gene contains point mutation of a phenylalanine to arginine at site 1128 (mGluR5FR), which exclusively disrupts interaction of mGluR5 and Homer while leaving Homer binding to other partners intact (Cozzoli, Goulding et al. 2009). UP states were recorded in slices from wildtype mice (WT), mice with one copy of the mutant allele of mGluR5 (FR Het), or two copies of the mutant allele (FR Homo). UP states were prolonged in slices from the FR Homo compared to WT (Fig. 4.4A; 809±45 vs. 1315±59 ms, $p<0.001$; WT, FR Homo; n=21, 26 slices). Additionally, UP states were longer in the FR Het (1079±58 ms, vs. WT $p<0.01$; vs. FR Homo $p<.01$, n=22 slices) compared to the WT, but significantly shorter than the FR Homo, suggesting that overactive mGluR5 has a dose-dependent effect on UP state duration.

Reduction of Amyloid Precursor Protein is sufficient to reduce UP state duration

Another protein that provides a unique mechanistic link to mGluR dysfunction in the *Fmr1* KO is Amyloid Precursor Protein (APP). APP expression is regulated by FMRP (Westmark and Malter 2007). Furthermore, increased APP levels promote seizures and reduction of APP levels is anti-epileptic (Westmark, Westmark et al. 2009; Westmark, Westmark et al. 2011). Given the role of APP in excitability and the altered APP levels in the *Fmr1* KO, I tested whether genetic reduction of APP levels was sufficient to reduce UP state duration in the *Fmr1* KO. Mice were bred to produce progeny that were heterozygous for APP in the *Fmr1* KO background. Genetic reduction of APP in the *Fmr1* KO does reduce UP state duration to normal levels (Fig. 4.5A; 931±55 vs. 597±30 ms, $p<0.001$; *Fmr1* KO, *Fmr1* KO; APP Het; n=22, 13 slices). Furthermore, APP heterozygosity on the *Fmr1* WT background reduces UP state duration compared to WT animals, suggesting that the rescue is dependent on FMRP and not due to a general reduction in excitability (581±31 vs. 530±31 ms, $p<0.001$; WT, APP Het; n=17, 13 slices).

An examination of intrinsic currents in L5 pyramidal neurons in the Fmr1 KO

One mechanism by which UP states may be prolonged in the *Fmr1* KO is by alterations in intrinsic currents. Either enhanced depolarizing current or

decreased hyperpolarizing current or both may lead to circuit hyperexcitation. Several candidate currents were investigated in the *Fmr1* KO to evaluate if they are altered and if this could contribute to prolonged UP states.

I. Presumptive mGluR-dependent depolarizing currents are unchanged in the *Fmr1* KO

Because enhanced mGluR function drives prolonged UP states in the Fmr1 KO, and mGluRs can cause depolarizing currents, intrinsic mGluR-dependent currents were measured in slices from a mosaic Fragile X mouse model. These mosaic mice have one X chromosome that expresses both GFP and FMRP, and the other X chromosome lacks both GFP and FMRP. Because of X inactivation, half of the cells will be GFP+; *Fmr1* WT and the other half will be GFP-; *Fmr1* KO (Fig. 4.6A) (Hanson and Madison 2007). This allows visual identification of WT and KO cells and facilitates simultaneous measurements from pairs of neighboring cells. Extracellular stimulation in the presence of fast synaptic blockers (in μM, 20 DNQX, 50 APV, 100 Picrotoxin, 1 CGP55845) was used to evoke presumptive mGluR-induced intrinsic currents in pairs of WT and KO cells in L5 of neocortex. No current was evoked without the addition of the glutamate uptake inhibitor TBOA (100 μM, data without TBOA not shown), suggesting that the evoked current was indeed due to glutamate. Presumptive mGluR-intrinsic currents were unchanged between WT and KO cells. Because

WT and KO cells were recorded in pairs, to account for the inherent variability of extracellularly evoked currents raw peak current data was normalized to WT (Fig. 4.6C, one sample t-test, 1 vs. 1.12±0.14 unitless; p=0.41; WT, KO; n=22 pairs). Addition of Gp1 mGluR antagonists reduced or prevented induction of the current in most cases, suggesting this current was likely dependent on Gp1 mGluRs (data not shown). The lack of a difference in mGluR-dependent current between WT and *Fmr1* KO neurons indicates that this current is not contributing to the network hyperexcitability.

II. H-current is unchanged in the *Fmr1* KO

The hyperpolarization activated cation current (Ih) confers stability to membrane potential by opposing hyperpolarization and depolarization, and thus contributes to regulation of excitability (Robinson and Siegelbaum 2003). Alterations in Ih function are linked to epilepsy, and presumably network hyperexcitability (Ludwig, Budde et al. 2003; Strauss, Kole et al. 2004). Ih attenuates dendritic inputs in layer 5 neurons in neocortex (Berger, Larkum et al. 2001). Additionally, this channel is known to be regulated by mGluR5, making it a candidate to be altered in the *Fmr1* KO (Brager and Johnston 2007). Given the potential role in network excitability, Ih was measured in L5 pyramidal neurons in WT and *Fmr1* KO slices. Ih current was isolated by a -30mV step from a holding potential of -60mV. Maximal current was measured as the difference between the

initial peak and the steady state sag. The magnitude of Ih is unchanged in neurons from the *Fmr1* KO, suggesting that it is not involved in prolonged UP states (Fig. 4.7B; 97.3±6.4 vs. 105.4±12.9 pA, p=0.55; WT, KO; n=36, 28 cells).

III. Little or no functional Slack current is expressed in neocortical neurons

Because UP states are a neocortical phenomenon, we wished to test whether Slack-mediated potassium current is reduced in the somatosensory cortex of *Fmr1* KO animals. Potassium currents were measured in L5 neurons in WT mice. Recordings were made with an internal that contained either [20mM] Na+ or [0 mM] Na+. If there were a significant sodium-dependent potassium component, the potassium current measured in [20mM] Na+ would be larger than that measured with the [0mM] Na+ internal. Preliminary analysis shows that peak potassium currents were not different with either internal, suggesting that Slack contributes very little to the total potassium current in these neurons (Fig. 4.8B). Because absence of intracellular sodium did not reduce the total potassium current, we conclude the there is negligible functional Slack conductance in layer 5 pyramidal cells, therefore making it unlikely to contribute to longer UP states.

IV. Somatic A-type potassium currents are unaltered in the *Fmr1* KO

Considering the possible link between Kv4.2 and FMRP, we wished to test A-type currents in the *Fmr1* KO (Gross, Yao et al. 2011; Lee, Ge et al. 2011). Because A-type current is transient, space clamp error makes measurement difficult (Hoffman 1997). To overcome this problem, deep layers of neocortex from WT or *Fmr1* KO mice were acutely dissociated to shear off the majority of the neuronal processes. Patch-clamp recordings were performed immediately afterwards on the remaining somas. A-type current was isolated using a previously described voltage protocol (Guan, Horton et al. 2011). Briefly, a voltage step from -40mV to +10mV isolates delayed rectifier and A-type currents. This is subsequently subtracted from a similar second step that contains a 150ms prestep to -70mV. The prestep inactivates A-type current, leaving only delayed rectifier current. Subtracting the second step from the first results in primarily isolated A-type current. The resulting current was confirmed as A-type current because it is abolished by 5mM 4-AP (data not shown). In contrast to the change predicted by altered Kv4.2 protein levels, there is no difference in somatic A-type current in WT compared to *Fmr1* KO neurons (Fig. 4.9B; 497±33 vs. 592±40 pA, p=0.56; WT, KO; n=32, 39 cells). Delayed rectifier currents were also unchanged (Fig. 4.9D; 311±23 vs. 318±21 pA, p=0.89; WT, KO; n=35, 42 cells). Input resistance is unchanged between WT or KO dissociated neurons (data not shown, 2088±173 vs. 1694±234 MΩ, p=0.19; WT, KO; n=36, 42 cells). These results suggest that it is unlikely that A-type current contributes to prolonged UP states.

However, treatment with 5mM 4-AP, a blocker of several voltage-dependent potassium currents including A-type current, equalizes UP state duration in WT and *Fmr1* KO slices (Fig. 4.10A; 681±42 vs. 651±24 ms, p=0.54; WT, KO; n=16, 16 slices). Although they contrast with intracellular measurements, these results may suggest that A-type current is involved in prolonged UP states in the *Fmr1* KO.

Layer 5 pyramidal neurons may be more excitable in the Fmr1 KO

Because none of our initial candidate currents were changed in the *Fmr1* KO, I sought to broadly assay excitability of L5 neurons. Increases in intrinsic excitability of neurons in the *Fmr1* KO could directly result in prolonged UP states. Various parameters were measured using whole-cell recordings in L5 neocortical neurons in slices from WT and *Fmr1* KO mice. Resting membrane potential was unchanged (Fig. 4.11A; -63±1 vs. -64±1 mV, p=0.26; WT, KO; n=36, 29 cells). Input resistance measured at -60 mV showed a strong trend toward an increase in the *Fmr1* KO (Fig. 4.11B; 237±13 vs. 280±21 MΩ, p=0.07; WT, KO; n=36, 28 cells). At -50 mV, input resistance was significantly increased in the KO (Fig. 4.11C; 531±47 vs. 755±61 pA, p<0.01; WT, KO; n=31, 24 cells). An increase in input resistance typically results in increased excitability. Consequently, the f/I curve showed a strong trend toward increased excitability in the *Fmr1* KO; however, the difference was not significant (Fig. 4.11D; 60 pA

step: 2.85±0.25 vs. 3.48±0.27 action potentials, p=0.09; WT, KO; n=35, 29 cells). This increase in intrinsic excitability in L5 neurons may contribute to network hyperexcitability.

Excitatory neocortical deletion of FMRP does not cause audiogenic seizures

Deletion of FMRP from neocortical excitatory neurons, but not inhibitory neurons, recapitulates increased UP state duration similar to that observed in the *Fmr1* KO (Hays, Huber et al. 2011). This suggests that absence of FMRP from excitatory neurons is sufficient to cause hyperexcitability within the neocortical circuit. To attempt link hyperexcitable networks to epilepsy in the *Fmr1* KO, I tested whether neocortical deletion of FMRP is sufficient to confer vulnerability to audiogenic seizures. As expected, neocortical deletion of FMRP from inhibitory neurons, which does not caused prolonged UP states, did not increase susceptibility to AGS (13.3% incidence in Flox *Fmr1*; *Dlx* Cre+, Table 4.1). However, deletion of FMRP from neocortical excitatory also does not result in vulnerability to AGS, even though it does cause prolonged UP states (7.7% incidence in Flox *Fmr1*; *Emx1* Cre+, Table 4.2). These results fail to link seizures to prolonged UP states, suggesting enhanced neocortical excitation does not directly lead to seizures in the *Fmr1* KO.

Discussion

Layer-specific contribution of FMRP to network excitability

In order to identify the alterations that lead to prolonged UP states, it is necessary to find a population of cells that contribute to the phenotype. Our previous studies have shown that prolonged UP states are intrinsic to excitatory neurons within neocortex (Hays, Huber et al. 2011). I sought to determine if a certain population of neurons was driving the prolonged UP states, or if all neurons partially contributed. To this end, I examined the effect of deletion of FMRP from specific cortical layers. Deletion of FMRP from either layer 4 or layers 5 and 6 resulted in a modest, but significant increase in duration of UP states. The increase in duration was not as large in magnitude as observed in the full *Fmr1* KO from previous experiments. Instead, layer specific deletion resulted in a partial shift toward the prolonged UP states observed in the KO, suggesting that all neurons within the circuit partly contribute to hyperexcitability. Additionally, if FMRP is deleted in one layer, UP state duration is increased throughout all layers of neocortex even if they express FMRP. Because UP states are driven by recurrent connections amongst local networks of neurons, this may not be surprising. Because UP states are by definition network events, FMRP deletion may lead to cell-autonomous changes in excitability but the function of FMRP within the circuit is non-cell-autonomous. Since small changes throughout each neuron in the circuit likely give rise to prolonged UP states, it may prove

difficult to identify any small changes in currents that are driving network hyperexcitability.

Disrupted mGluR5-Homer interactions results in prolonged UP states

Our previous studies have shown that global disruption of Homer scaffolds is sufficient to prolong UP state duration, presumably by causing constitutive signaling through mGluR5 (Ronesi, Collins et al. 2012). Additionally, re-associating Homer scaffolds in the *Fmr1* KO reduces prolonged UP states. However, because both of these lines of evidence rely on global manipulations of Homer interactions, they could not directly link Homer-mGluR5 interactions to network hyperexcitability. As such, the alterations in UP state duration may have been due to Homer associations with other effector proteins. Using the mGluR5FR mouse model, we provide the first direct evidence of Homer-mGluR5 interactions in regulating network function (Cozzoli, Goulding et al. 2009). Our data reveal that specific disruption of Homer-mGluR5 interactions is indeed sufficient to cause prolonged UP states. The duration of UP states observed in the mGluR5FR homozygote is essentially equivalent to that previously measured in the *Fmr1* KO.

This provides two intriguing insights into the pathophysiology of FXS. First, it suggests that mGluR5-mediated increases in network excitability are at a maximal level in the *Fmr1* KO. In the mGluR5FR Homo, all mGluR5 receptors

signal constitutively, resulting in maximal activation. Therefore, because mGluR5 signaling is responsible for the increased UP state duration in the Fmr1 KO (see chapter 2), mGluR5 signaling must also be maximal in the *Fmr1* KO. This is supported by our previous finding that further disruption of global Homer interactions in the *Fmr1* KO does not cause any additional increase in UP state duration (Ronesi, Collins et al. 2012). Although it is possible to increase UP state duration with an agonist of Gp1 mGluRs, this is likely mediated by mGluR1 (Hays, Huber et al. 2011). Secondly, the mechanism of prolonged UP states in the *Fmr1* KO is entirely driven by Homer-mGluR5 interactions. This is particularly surprising in light of FMRP's regulation of as many as 800 mRNAs (Brown, Jin et al. 2001). Despite translational regulation of a wide range of transcripts, the sole function of FMRP in regulating network excitability is through maintenance of Homer-mGluR interactions. To my knowledge, this, along with our experiments in chapter 3, is the first report of Homer regulation of network function. This finding obviates the importance of further study into Homer-mGluR interactions, as they may solely underlie many other features of FXS.

Reduction of APP rescues prolonged UP states in the Fmr1 KO

Another protein that has links to the *Fmr1* KO and mGluR5 is Amyloid Precursor Protein. FMRP is involved in the translational regulation of APP

(Westmark and Malter 2007). APP and its cleavage products, $A\beta_{1-40}$ and $A\beta_{1-42}$, are increased in the *Fmr1* KO and possibly in autism patients (Sokol, Demao Chen et al. 2006; Westmark and Malter 2007; Bailey, Giunta et al. 2008). This increase in APP levels contributes to epileptogenesis in the *Fmr1* KO, as genetic reduction of APP levels reduces seizure severity (Westmark, Westmark et al. 2011). Conversely, overexpression of APP in the *Fmr1* KO further increases seizure severity (Westmark, Westmark et al. 2009). APP may contribute to hyperexcitability at the network level as well, as clusters of neurons near amyloid plaques are hyperactive (Busche, Eichhoff et al. 2008). I observe that UP state duration is reduced to normal levels when APP is reduced in the *Fmr1* KO background. Understanding the mechanism by which APP contributes to hyperexcitability may facilitate identification of alterations in currents that may give rise to prolonged UP states in the *Fmr1* KO. One possibility is that APP reduction is affecting synaptic connectivity and strength during development, but conditional manipulation of APP would be necessary to test this. An interesting possibility arises from a link to Homer and Shank, a scaffold protein that affects NMDAR function. Treatment with $A\beta_{1-40}$ causes the uncoupling of Homer and Shank (Roselli, Hutzler et al. 2009). This could, in turn, affect network excitability in two ways. First, Homer and Shank disassembly could alter NMDAR currents, which are known to impinge upon UP states, and could directly affect network function (Appendix 1) (Bertaso, Roussignol et al. 2010).

Second, if $A\beta_{1-40}$ causes Homer-Shank interactions to be disrupted, perhaps other Homer interactions may be disrupted as well. If so, dysregulation of $A\beta_{1-40}$ levels in the absence of FMRP may be the driving force behind uncoupled Homer interactions in the *Fmr1* KO and may underlie enhanced mGluR activation. As such, further studies into the consequence of APP increases may yield insight into Homer interactions and therefore mGluR dysfunction in the *Fmr1* KO.

Multiple intrinsic currents are unchanged in the Fmr1 KO

There are two major mechanisms that may lead to the network hyperexcitability and prolonged UP states in the *Fmr1* KO. First, altered synaptic connections change local recurrent connections and give rise to hyperexcitable circuits. This hypothesis has not been explicitly tested. Second, changes in intrinsic currents may cause single neurons to be more excitable, thus summating in network hyperexcitability. The hyperexcitability in individual neurons may be caused by enhancements in depolarizing currents, reductions in hyperpolarizing currents, or both. Here, I tested several currents that are candidates to cause prolonged UP states in the *Fmr1* KO.

The simplest mechanistic explanation for increased excitability is an abundance of depolarizing current, thus increasing the propensity of the neuron to fire. mGluR signaling is enhanced in the *Fmr1* KO, and mGluRs can stimulate persistent firing in cortical neurons (Bear, Huber et al. 2004; Zhang and Seguela

2010). Additionally, Homer1a is increased in the *Fmr1* KO and has been shown to increase constitutive TRPC current (Yuan, Kiselyov et al. 2003). Therefore, mGluR mediated currents were a likely candidate to be responsible for increased excitability. However, no changes in mGluR-mediated intrinsic currents were observed in the *Fmr1* KO. It is very possible that this current is unchanged in the KO, but there are some important caveats to this experiment. Because recordings were made in voltage clamp, it is possible that there was minimal contribution of any voltage-dependent channel at the command voltage. Additionally, the stimulation paradigm used for these experiments may not be sufficient to activate all components necessary for the mGluR-dependent currents. While these experiments do provide some evidence that mGluR currents are unchanged, it would be ideal to measure mGluR-dependent currents in individual neurons during an UP state.

Another candidate to be responsible for increased excitability in the *Fmr1* KO was H-current. This current is regulated by mGluR5, and therefore potentially dysregulated in the *Fmr1* KO (Brager and Johnston 2007). I observed the H-current is unchanged in the *Fmr1* KO, therefore it is unlikely to be involved in prolonged UP states.

The other mechanism for increased neuronal excitability is reduced hyperpolarizing currents, potentially causing the network to remain in an active state for a longer time. The sodium-activated potassium current regulated by the

Slack channel is functionally reduced in the *Fmr1* KO, therefore making it a candidate to be involved in prolonging UP state duration (Brown, Kronengold et al. 2010). Although Slack protein is expressed in some areas of the cortex, I observed very little contribution of Slack to total potassium current (Bhattacharjee, Gan et al. 2002). Given the minor influence of Slack on total current, it is unlikely to be involved in prolonged UP states in the *Fmr1* KO.

The subthreshold A-type potassium current was a strong candidate to be responsible for prolonged UP states. Protein levels of Kv4.2, the major mediator of A-type current, are altered in the *Fmr1* KO (Gross, Yao et al. 2011; Lee, Ge et al. 2011). Furthermore, mGluRs strongly regulate Kv4.2 function through a phosphorylation that greatly reduces conductance (Hu and Gereau 2003; Hu, Alter et al. 2007). Because mGluRs are overactive in the *Fmr1* KO, A-type current may be constitutively supressed, thereby leading to hyperexcitability. I observe that somatic A-type current is unchanged in the *Fmr1* KO. This is in direct opposition to both reports that Kv4.2 expression is altered in the *Fmr1* KO (Gross, Yao et al. 2011; Lee, Ge et al. 2011). However, it is important to note that because I used dissociated neurons for recordings, only somatic current could be examined. Functional expression of A-type current increases with distance from the soma, so it is possible that dendritic A-type currents are suppressed in the *Fmr1* KO (Hoffman 1997). Changes in dendritic A-type current could strongly effect synaptic integration and therefore lead to hyperexcitability.

Additionally, although Kv4.2 accounts for the main component of the A-type current, other channels and accessory proteins contribute (Norris, Foeger et al. 2010; Norris and Nerbonne 2010; Guan, Horton et al. 2011). Even if the Kv4.2 component is reduced, A-type current may be compensatorially normalized by increased function of the other components. Therefore, while I show that somatic A-type current is unchanged in the *Fmr1* KO, it is not possible to rule out contribution of A-type current to prolonged UP states.

In support of this, pharmacological blockade of some voltage-gated potassium currents including A-type current equalizes UP state duration in the *Fmr1* KO. It is important to note that the inhibitor used was 4-AP, which affects many other conductances in addition to A-type current. This is highlighted by the fact that treatment of slices with 4-AP should cause an increase in UP state duration if the effect was simply to block A-type current and enhance excitability. However, treatment results in a reduction in duration of UP states, but a large increase in frequency, suggesting multiple components involved in regulation of UP states are affected by 4-AP. However, this data still provides support that A-type or other voltage-gated potassium currents lead to network hyperexcitability in the *Fmr1* KO.

Cortical neurons are intrinsically hyperexcitable in the Fmr1 KO

Because none of the candidate currents were altered in the *Fmr1* KO, I sought to generally assay excitability of L5 neocortical neurons. Increases in intrinsic excitability could directly lead to prolonged UP states. I observe that input resistance measured at -60mV shows a trend toward an increase and input resistance measured at -50mV is significantly increased. The larger magnitude of increased input resistance in *Fmr1* KO at -50mV may suggest that the change is due to alterations in potassium conductance, as the driving force for potassium is greater at -50mV compared to -60mV. Interestingly, no difference in input resistance was observed between WT and KO dissociated neurons which have no processes, suggesting that the difference in input resistance in neurons recorded in slices may arise from conductance changes in the dendrites. Increases in input resistance correlate with enhanced neuronal excitability. Correspondingly, neurons in the *Fmr1* KO show a trend toward firing more action potentials in response to a given current injection. These measures all suggest that individual neurons in L5 are more excitable in the *Fmr1* KO.

Previous studies have shown that L4 neurons in the *Fmr1* KO have similar increases in input resistance and excitability shifts in the f/I curve (Gibson, Bartley et al. 2008). Together with the L5 excitability data, this may suggest that all neurons throughout the neocortex in the *Fmr1* KO are slightly more intrinsically excitable. This is mirrored in the partial increase in UP state duration in the layer-specific FMRP deletion experiments described above. I posit that

modest increases in intrinsic excitability resulting from deletion of FMRP across layers summate to cause the prolonged UP states observed in the *Fmr1* KO.

Audiogenic seizures are not driven by hyperexcitable neocortical circuits

Audiogenic seizures occur in approximately sixty percent of *Fmr1* KO mice and are hypothesized to result from hyperexcitable circuitry (Musumeci, Bosco et al. 2000; Chen and Toth 2001; Yan, Rammal et al. 2005; Dölen, Osterweil et al. 2007). Because I observe hyperexcitability in neocortical circuitry in the form of prolonged UP states, I sought to link this neocortical excitability to audiogenic seizures. As expected, neocortical deletion of FMRP from inhibitory neurons, which does not cause prolonged UP states, also does confer seizure susceptibility. However, neocortical deletion of FMRP from excitatory neurons does cause prolonged UP states but does not confer propensity for audiogenic seizures. This suggests that audiogenic seizures arise from subcortical structures. Other studies have shown FMRP regulates neuronal function in brainstem auditory structures, so AGS may arise from alterations excitability in these structures (Brown, Kronengold et al. 2010; Strumbos, Brown et al. 2010).

Figure 4.1. Deletion of FMRP from layer 4 causes partially prolonged UP states.

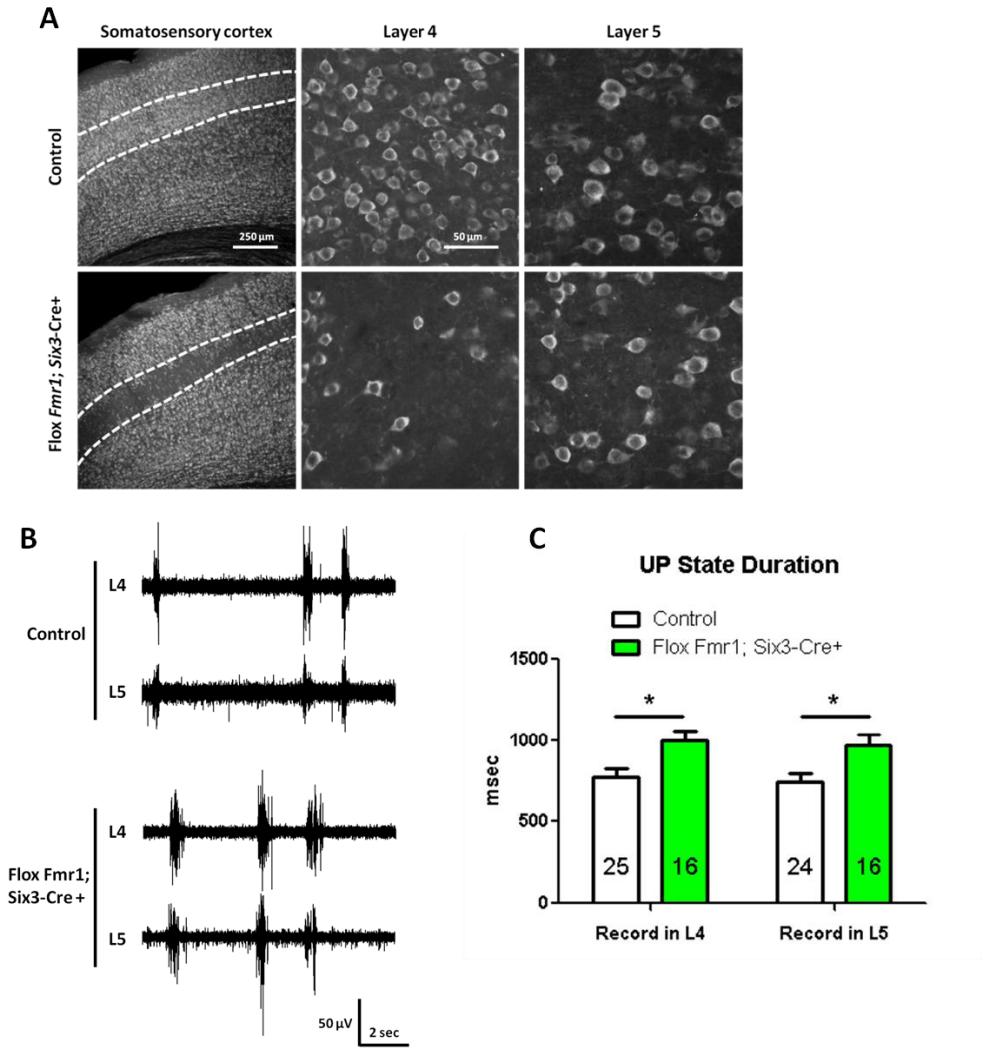

Figure 4.1. Deletion of FMRP from layer 4 causes partially prolonged UP states.

A) Immunohistochemistry for FMRP showing deletion in layer 4. Layer 4 is demarcated by the white dashed lines. FMRP is deleted from greater than 80% of cells in layer 4 with negligible deletion in layer 5. **B)** Representative traces from the groups in **C**. **C)** UP state duration is partially increased in Flox *Fmr1*; *Six3* Cre animals compared to control. A similar increase in duration is observed in both layers 4 and 5. N refers to number of slices. *, $p<0.05$, Two-way ANOVA.

Figure 4.2. Restoration of FMRP expression in layer 4 at least partially rescues UP state duration

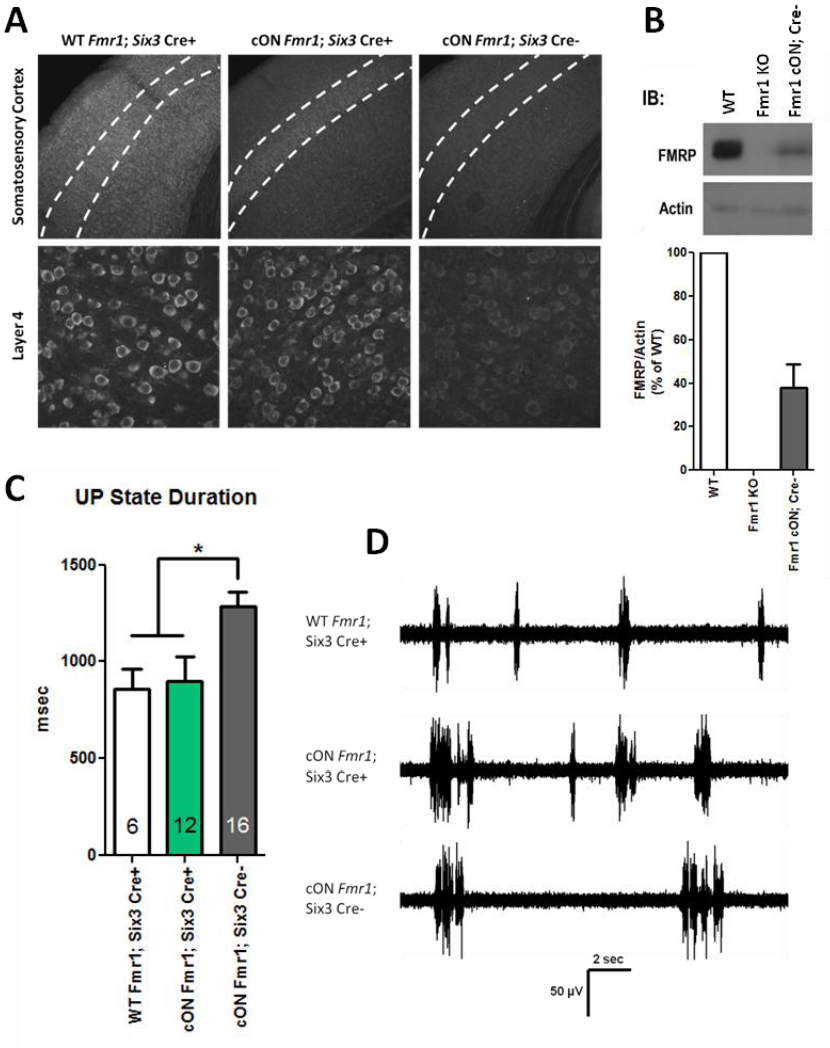

Figure 4.2. Restoration of FMRP expression in layer 4 at least partially rescues UP state duration

A) Immunohistochemistry for FMRP showing deletion in layer 4. Layer 4 is demarcated by dashed white lines. FMRP is reduced in greater than 80% of cells in layer 4 with negligible deletion in layer 5. **B)** FMRP expression levels in *Fmr1* cON animals. *Fmr1* cON animals express approximately 60% less FMRP than WT. FMRP expression for each sample is normalized to actin to control for loading, and then normalized to WT. **C)** UP state duration is partially reduced in Flox *Fmr1*; *Six3* Cre+ animals compared to Flox *Fmr1*; *Six3* Cre-. Similar durations are observed in layer 5. **D)** Representative traces from the groups in **C**. N refers to number of slices. *, $p<0.05$, One-way ANOVA.

Figure 4.3. Deletion of FMRP from layers 5 and 6 causes partially prolonged UP states.

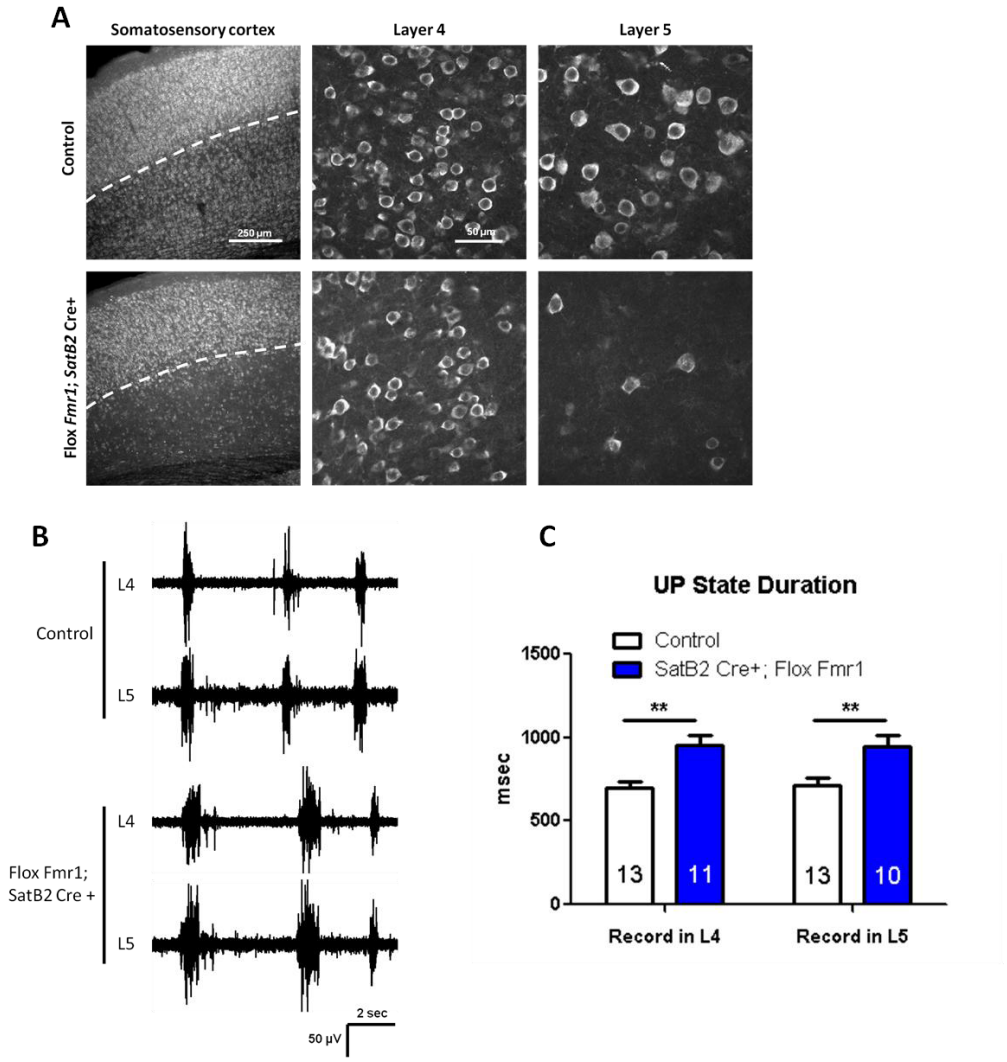

Figure 4.3. Deletion of FMRP from layers 5 and 6 causes partially prolonged UP states.

A) Immunohistochemistry for FMRP showing deletion in deep layers of cortex. The upper boundary of layer 5 is demarcated by the white dashed line. FMRP is deleted from greater than 80% of cells in layers 5 and 6 with less than 20% deletion in superficial layers. . **B)** Representative traces from the groups in **C**. **C)** UP state duration is partially increased in both layers 4 and 5 in Flox *Fmr1*; *SatB2* Cre animals compared to control. N refers to number of slices. **, $p<0.01$, Two-way ANOVA.

Figure 4.4. Specific disruption of mGluR5-Homer interactions causes prolonged UP states.

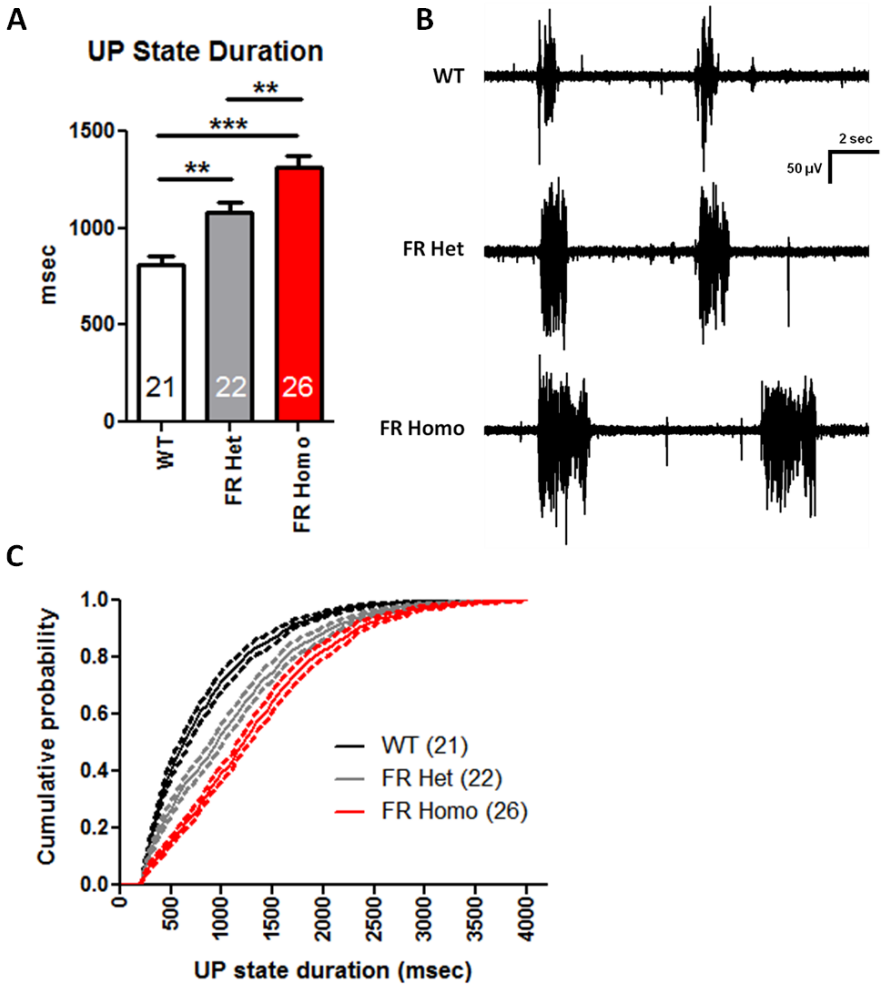

Figure 4.4. Specific disruption of mGluR5-Homer interactions causes prolonged UP states.

A) UP state duration is increased in slices from animals with one copy of the mutant allele (FR Het, gray bar) and further increased in animals with two copies of the mutant allele (FR Homo, blue bar), suggesting that disruption of mGluR5-Homer complexes increases excitability in a dose-dependent manner. **B)** Representative recordings from genotypes in **A**. **C)** The cumulative distribution of average duration (normalized for each slice and averaged over slices, see Methods) was evenly shifted to the right for the FR Het and FR Homo. Outer dashed lines represent the standard error. N refers to number of slices. **, $p<0.01$, ***, $p<0.001$, one-way ANOVA with Bonferroni post-tests.

Figure 4.5. Genetic reduction of APP rescues UP state duration in the *Fmr1* KO

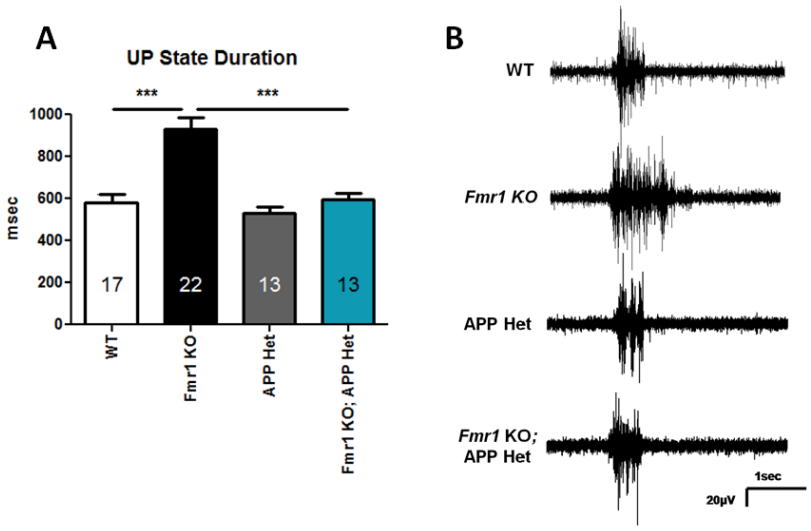

Figure 4.5. Genetic reduction of APP rescues UP state duration in the *Fmr1* KO

A) Reduction of APP gene dosage in the Fmr1 KO reduced UP state duration to WT levels (blue bar). Reduction of APP in a WT has no effecct on duration (gray bar). **B)** Representative traces from the groups in **A**. N refers to number of slices. ***, $p<0.001$, Two-way ANOVA.

Figure 4.6. Presumptive mGluR-dependent depolarizing currents are unchanged in *Fmr1* KO neurons.

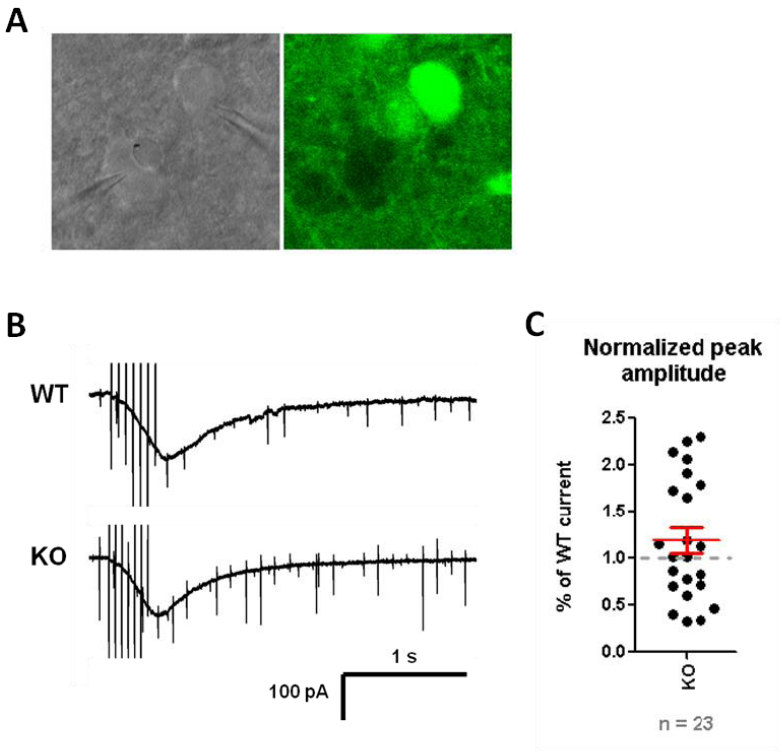

Figure 4.6. Presumptive mGluR-dependent depolarizing currents are unchanged in *Fmr1* KO neurons.

A) Image depicting 2 simultaneously patch-clamped layer 5 pyramidal neurons in the somatosensory cortex of an *Fmr1* mosaic mouse. The left panel is DIC and the right panel is GFP expression reporting FMRP. The left neurons is KO and GFP- and the right neuron is WT and GFP+. **B)** Representative mGluR-dependent currents evoked from lateral stimulation in the cortex. **C)** Peak mGluR-dependent current is unchanged in KO neurons. Peak current amplitude was normalized to the WT neuron from each pair. N refers to umber of cell pairs. One sample t-test.

Figure 4.7. Hyperpolarization-activated current is unchanged in layer 5 neurons in the *Fmr1* KO.

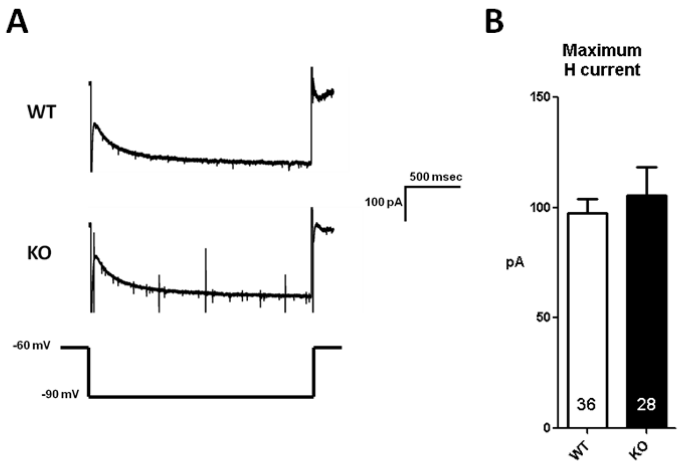

Figure 4.7. Hyperpolarization-activated current is unchanged in layer 5 neurons in the *Fmr1* KO.

A) Example traces of H-current from WT and KO neurons. Current was evoked by a -30mV step from a -60mV holding potential. Maximal current was measured as the difference between the initial peak to the steady state current. B) Maximal H-current is not different between WT and *Fmr1* KO neurons. N refers to number of cells. T-test.

Figure 4.8. Little or no functional sodium-activated potassium current is expressed in layer 5 pyramidal neurons.

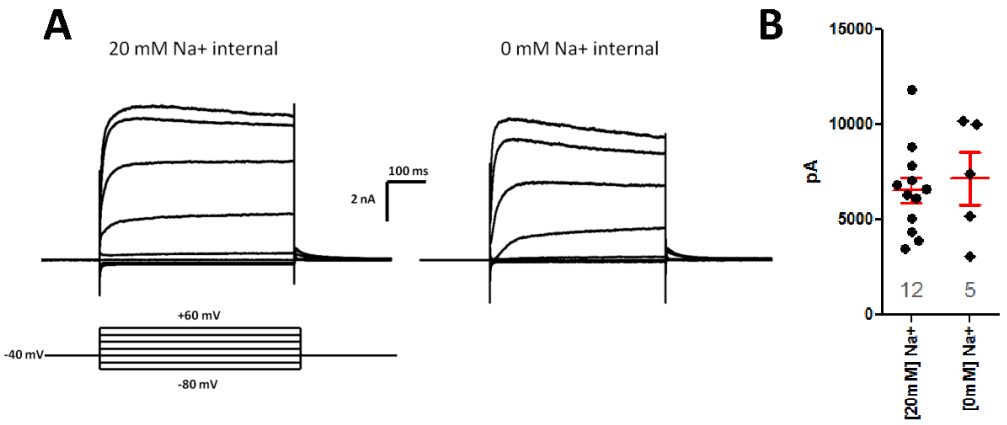

Figure 4.8. Little or no functional sodium-activated potassium current is expressed in layer 5 pyramidal neurons.

A) Example traces of total potassium currents measured in a WT layer 5 pyramidal neuron. Current was evoked by 20mV steps from -80mV to +60mV. As indicated, recordings were made with either 20mM or 0mM internal sodium concentration. B) Preliminary results suggest that there is no difference in K+ current with either 20mM or 0 mM Na+. Data shown are for the step to +60mV. This indicates that there is little or no sodium-activated potassium current expressed in these neurons. N refers to the number of cells.

Figure 4.9. A-type and delayed rectifier K+ currents are unchanged in the *Fmr1* KO.

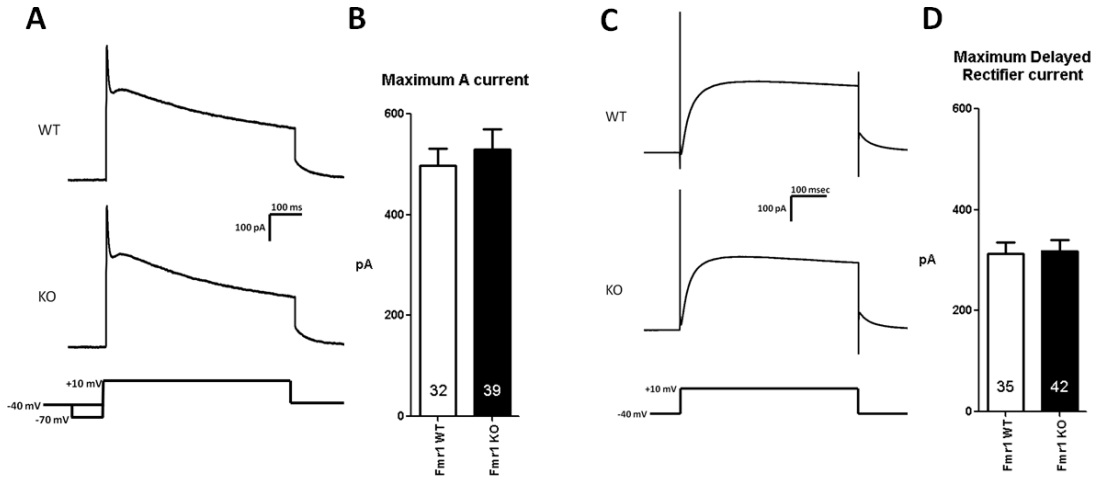

Figure 4.9. A-type and delayed rectifier K+ currents are unchanged in the *Fmr1* KO.

A) Representative recordings of A-type current from WT and *Fmr1* KO neurons. The initial transient peak is the maximum A-type current. A-type current was derived the subtraction of a -30mV prepulsed step from a +50mV step as described in the text. **B)** Maximum A-type current is unchanged in the *Fmr1* KO. **C)** Representative traces illustrating delayed rectifier current. **D)** Maximum delayed rectifier current is unchanged in *Fmr1* KO neurons compared to WT. N refers to number of cells. T-test.

Figure 4.10. Treatment of with 4-AP eliminates the difference in UP state duration between WT and *Fmr1* KO slices.

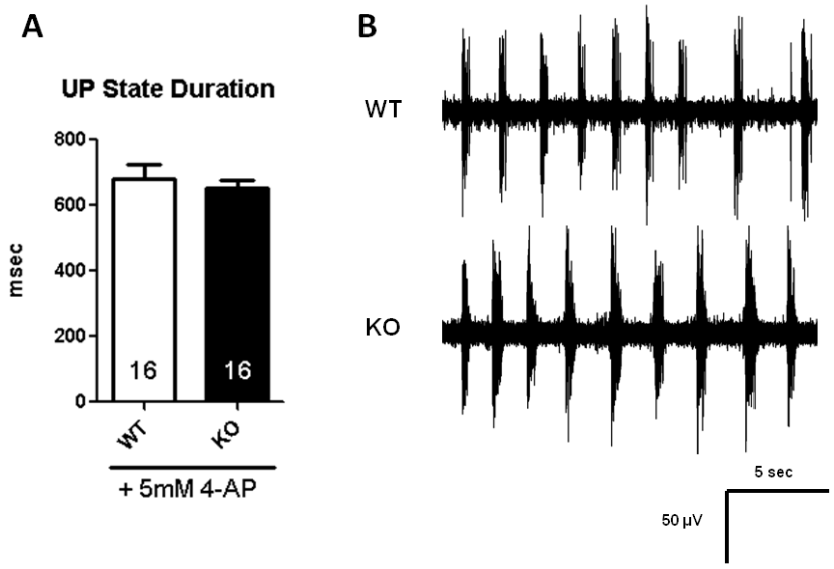

Figure 4.10. Treatment of with 4-AP eliminates the difference in UP state duration between WT and *Fmr1* KO slices.
A) Treatment of WT and *Fmr1* KO slices with 5mM 4-AP, a non-specific blocker of many voltage-gated channels including Kv4.2, abolishes the difference in UP state duration. **B)** Example traces from WT and *Fmr1* KO slices after 5mM 4-AP treatment. N refers to number of slices. T-test.

Figure 4.11. Layer 5 pyramidal neurons may be intrinsically hyperexcitable in the *Fmr1* KO.

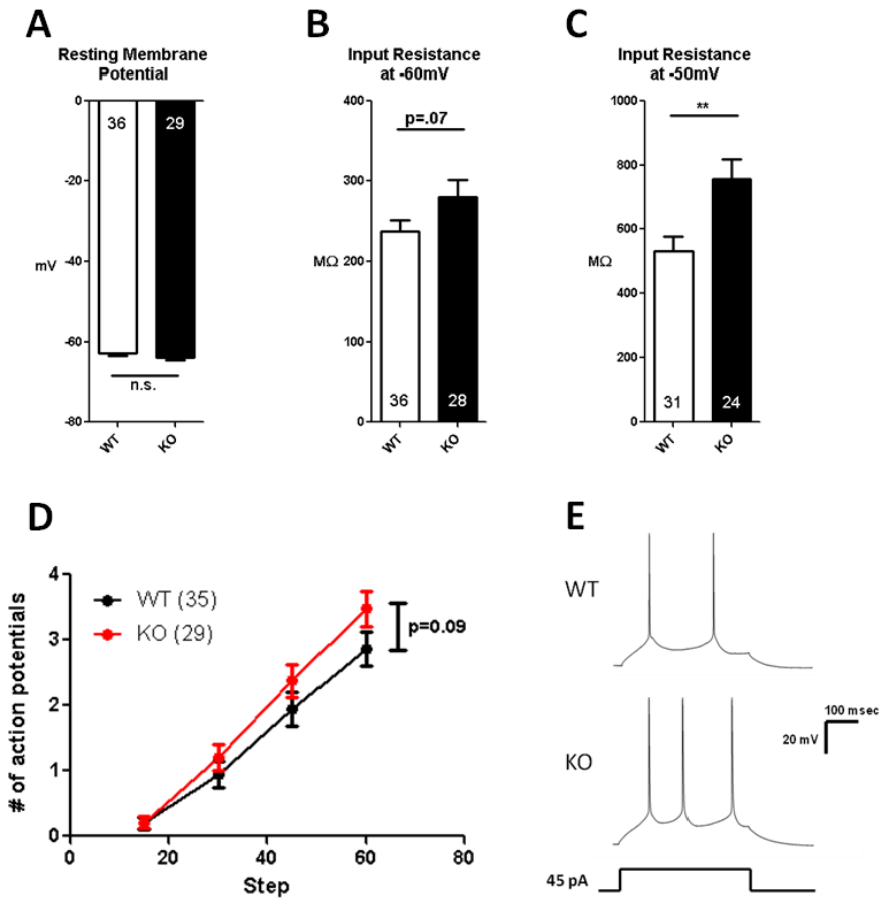

Figure 4.11. Layer 5 pyramidal neurons may be intrinsically hyperexcitable in the *Fmr1* KO.

A) Resting membrane potential is unchanged in the *Fmr1* KO. **B)** Input resistance at -60mV shows a trend toward an increase. **C)** Input resistance measured at -50mV is significantly increased in the *Fmr1* KO compared to WT. **D)** Frequency/input curve showing a trend toward increased excitability in *Fmr1* KO neurons. **E)** Representative recordings from WT and KO neurons showing spikes for a 45 pA current step. N refers to the number of cells. **, $p<0.01$. **A**, **B**, **C**; T-test. **D**; Repeated measures ANOVA.

Table 4.1. Audiogenic seizure incidence and severity in Flox *Fmr1* x *Dlx* Cre mice.

	Wild Running	Seizure (clonic/tonic)	Status Epilepticus	Seziure Incidence
WT *Fmr1*; *Dlx* Cre-	2/17	2/17	2/17	11.7%
WT *Fmr1*; *Dlx* Cre+	1/17	1/17	1/17	5.8%
Flox Fmr1; *Dlx* Cre-	0/18	0/18	0/18	0.0%
Flox *Fmr1*; *Dlx* Cre+	2/15	2/15	2/15	13.3%

Table 4.1. Audiogenic seizure incidence and severity in Flox *Fmr1* x *Dlx* Cre mice.

Incidence refers to seizure incidence compared to WT *Fmr1*;*Dlx* Cre-. Fisher's exact test

Table 4.2. Audiogenic seizure incidence and severity in Flox *Fmr1* x *Emx1* Cre mice

	Wild Running	Seizure (clonic/tonic)	Status Epilepticus	% Incidence
WT *Fmr1*; *Emx1* Cre-	1/15	0/15	0/15	0.0%
WT *Fmr1*; *Emx1* Cre+	1/10	1/10	0/10	0.0%
Flox Fmr1; *Emx1* Cre-	0/9	0/9	0/9	0.0%
Flox *Fmr1*; *Emx1* Cre+	3/13	1/13	1/13	7.7%

Table 4.2. Audiogenic seizure incidence and severity in Flox *Fmr1* x *Emx1* Cre mice

Incidence refers to seizure incidence compared to WT *Fmr1*;.*Emx1* Cre-. Fisher's exact test

CHAPTER FIVE
Discussion

CONCLUDING REMARKS AND RECOMMENDATIONS FOR FUTURE STUDIES

Summary

The studies described in this manuscript characterize and provide a mechanistic framework for prolonged UP states, a novel phenotype in the *Fmr1* KO. To this end, I show that prolonged UP states result from the loss of FMRP from excitatory neurons in the neocortex. Additionally, no specific cortical layer drives the increased duration, but rather all cells within the circuit partially contribute to the hyperexcitability. I also show that enhanced mGluR5 signaling is causing prolonged UP states in the *Fmr1* KO; however, enhanced protein translation is not responsible for the longer duration. Furthermore, disruption of Homer-mGluR5 interactions is sufficient to increase UP state duration, presumably due to enhancement of mGluR5 signaling. Disrupted Homer scaffolds are responsible for prolonged UP states in the *Fmr1* KO, and re-association of Homer complexes is sufficient to reduce network hyperexcitability to normal levels. I also provide preliminary evidence that several intrinsic currents are unchanged in the *Fmr1* KO, but general properties of excitatory neurons in neocortical layer 5 display a shift toward increased excitability. These data provide insight into the novel phenotype of network hyperexcitability and

generally into the pathophysiology of Fragile X syndrome. Additionally, this study provides support for the hypothesis that an imbalance of E/I ratio may underlie many deficits observed in autism.

Cortical networks are basally hyperexcitable in the *Fmr1* KO

Several lines of evidence are predictive of an imbalance in E/I ratio in FXS. FXS patients display hypersensitivity to sensory stimuli, and in many cases, abnormal EEG patterns and epilepsy (Musumeci, Hagerman et al. 1999; Berry-Kravis 2002; Berry-Kravis, Raspa et al. 2010). *Fmr1* KO mice express similar sensory-related deficits in the form of enhanced prepulse inhibition and audiogenic seizures (Chen and Toth 2001). E/I changes that may underlie these behaviors would also manifest as changes in circuit excitability. This study provides the first evidence that neocortical networks in the *Fmr1* KO are basally hyperexcitable and describes the mechanism underlying this hyperexcitability.

The primary finding from this study is that UP states are prolonged in the *Fmr1* KO. UP states are network events in which local populations of neurons become depolarized and have an increased propensity to fire action potentials. These are driven by recurrent connections between the local neurons. UP states, along with less active epochs termed DOWN states, make up the bimodal system of the slow oscillation. UP states are a network phenomenon, and therefore measurement of UP states reveals properties of circuit function and excitability.

The duration of UP states is prolonged in the *Fmr1* KO compared to WT littermates. These changes are observed both in an *in vitro* slice preparation and with *in vivo* recordings from intact animals. Measurement of UP states was originally motivated by the previous finding that excitatory drive onto inhibitory neurons is decreased in layer 4 of somatosensory cortex (Gibson, Bartley et al. 2008). The net result of this change would be a decrease in inhibition, which would lead to an imbalance in E/I ratio and potentially hyperexcitation of the circuitry. However, pharmacological dissection of the circuit shows that increased UP state duration is intrinsic to excitatory circuitry in the *Fmr1* KO. This result demonstrates that even without any inhibition intact, neocortical networks are hyperexcitable. Therefore, the changes that support network hyperexcitability lie in excitatory neurons, although a contribution from inhibitory neurons cannot be fully ruled out. Furthermore, deletion of FMRP from neocortical excitatory neurons fully recapitulates the prolonged UP states observed in the *Fmr1* KO, while deletion from neocortical inhibitory neurons has no effect. This further confirms that loss of FMRP from excitatory neurons engenders network hyperexcitability and provides unexpected support for the E/I ratio theory of autism (Rubenstein and Merzenich 2003). While the original hypothesis of reduced excitatory drive onto inhibitory neurons causing prolonged UP state was largely ruled out, these findings uncover an alternative mechanism

for altered E/I ratio by changes in excitatory neurons which still ultimately results in network dysfunction.

Another important factor in understanding network dysfunction in the *Fmr1* KO is to identify the source of prolonged UP states. Initial experiments from this study show that the changes are intrinsic to neocortex and inherent in excitatory neurons. Further analysis of neuronal subtypes could provide better insight into the mechanism of hyperexcitability. Two principle models could account for the prolonged UP states. First, a single population of neurons may be hyperexcitable and thereby driving hyperexcitability throughout the circuit. Alternatively, all neurons throughout the circuit may have fractional increases in excitability which ultimately summate into circuit hyperexcitability. Deletion of FMRP from layer 4 partially increases UP state duration to a level greater than a WT but not to the degree observed in the full *Fmr1* KO. A similar magnitude of increase is observed with deletion of FMRP from layer 5 and 6. These findings support a diffuse increase in excitability throughout all neocortical neurons in the *Fmr1* KO. By fitting experimental results, computer modeling could be used to estimate the amount of increased excitability necessary in each neuron to result in prolonged UP states. This may prove useful in determining what alterations are driving longer UP states in the KO.

All manipulations of FMRP throughout this study were done using constitutive genetic models. In all cases, FMRP expression was deleted very

early in development, resulting in a network which developed primarily in the absence of FMRP. The possibility remains that FMRP has a developmental role in regulation of circuit function. Indeed, FMRP is known to regulate synapse formation during development and may also be involved in the critical period (Pfeiffer and Huber 2007; Harlow, Till et al. 2010). Any changes in connectivity resulting from early deletion of FMRP could strongly impact circuit function at later stages. This could be tested using conditional expression or deletion of FMRP in conjunction with a Cre recombinase that expresses after circuit development. These experiments would not only contribute to further understanding of network properties in the *Fmr1* KO, but they would determine the feasibility of developing treatments for network dysfunction after development in FXS patients.

This study provides insight into the locus of FMRP's function within the circuit, as well as an analysis of the mGluR5 signaling pathway that mediates the prolonged UP states. The following text describes possible changes that could give rise to the network hyperexcitability observed in the *Fmr1* KO. UP states are a product of the synaptic connections between local circuits and the general intrinsic properties of the neurons within the circuit. Changes in either of these components could lead to longer UP state duration.

Do synaptic changes underlie prolonged UP states?

The first major mechanism which may drive prolonged UP states in the *Fmr1* KO is a change in synaptic connectivity. Because UP states are driven by recurrent connections among local cortical neurons and long range connectivity may serve to synchronize state change, any perturbations in synaptic connectivity would strongly impact the slow oscillation (Volgushev, Chauvette et al. 2006). A number of connectivity changes have been reported in the *Fmr1* KO. Connection frequency between neighboring excitatory neurons is reduced in layer 4 of the somatosensory cortex in the *Fmr1* KO (Gibson, Bartley et al. 2008). This reduction in connectivity between pyramidal neurons may be dependent on FMRP in the presynapse (Hanson and Madison 2007). Additionally, the frequency of connection between an excitatory neuron and a nearby fast-spiking inhibitory neuron is also reduced in this region (Gibson, Bartley et al. 2008). Furthermore, fewer connections exist between layer 2/3 and layer 4 neurons in somatosensory cortex (Bureau, Shepherd et al. 2008). In the mPFC, there is an overabundance of medium-range connections between pyramidal neurons in the *Fmr1* KO (Testa-Silva, Loebel et al. 2011).

Despite the variety of connectivity changes present in the *Fmr1* KO, these are unlikely to underlie the prolonged UP states for two reasons. First, several of the reported connection probability changes in the neocortex are developmentally transient (Bureau, Shepherd et al. 2008; Gibson, Bartley et al. 2008; Testa-Silva, Loebel et al. 2011). While there are deficits in connectivity early in development,

most of these changes are largely normalized at later developmental stages. However, I observe that UP states are prolonged both in early developmental stages and in adulthood. Therefore, because UP states are prolonged even after connectivity is normal, these synaptic connection changes are unlikely to give rise to prolonged UP states. Second, because local recurrent connections drive UP states, longer durations would be caused by increased excitatory connections or reduced inhibitory connections. However, most reports indicate that connections between excitatory neurons are reduced (Bureau, Shepherd et al. 2008; Gibson, Bartley et al. 2008). This reduced connectivity between excitatory neurons would lead to reduced UP state duration, which is the opposite of my observations in the *Fmr1* KO. The increase in medium-range excitatory connections cannot be ruled out as driving the prolonged UP states (Testa-Silva, Loebel et al. 2011). However, medium- and long-range connections are not as important in the generation of the slow oscillation as local connections, but more likely regulate the timing of the shift between states (Volgushev, Chauvette et al. 2006). Excitatory to inhibitory connections are decreased in the *Fmr1* KO (Gibson, Bartley et al. 2008). This would be predicted to cause prolonged UP states, but my studies have shown that prolonged UP states are independent of inhibitory circuitry. Consequently, any alterations in inhibitory neurons likely do not contribute to prolonged UP states.

Because the increase in UP state duration is not developmentally transient, and because the polarity of connection frequency change is opposite that which would cause an increase in duration, changes in connectivity likely do not underlie the prolonged UP states. However, it is possible that changes in connectivity in other layers, such as layer 5, may be influencing UP state duration. This would require a more complete analysis of connections throughout the cortex. While changes in intrinsic current are more likely to cause the prolonged UP states, this is not mutually exclusive with connectivity changes. Both could partially contribute to the phenotype. Although this study cannot fully rule out any contribution of changes in connectivity to alterations in the slow oscillation, I posit that changes in intrinsic current are more likely to underlie network hyperexcitability in the *Fmr1* KO.

Are alterations in intrinsic currents responsible for prolonged UP states?

The second major mechanism which may account for prolonged UP states is an increase in neuronal excitability through changes in intrinsic currents. This, again, could arise from two distinct changes. The simplest explanation for hyperexcitability is an increase in depolarizing currents; however, an equally likely explanation is a decrease in hyperpolarizing current. mGluRs are overactive in the *Fmr1* KO, and mGluR activation can lead to persistent firing in cortical neurons (Yoshida, Fransén et al. 2008; Zhang and Seguela 2010). This

provides a link between increased mGluR signaling and direct regulation of network excitability. Also, Homer1a, which is known to be increased in the *Fmr1* KO, can directly interact with TRP channels and increase conductance (Yuan, Kiselyov et al. 2003). Both of these pathways would lead to increases in mGluR-dependent depolarizing currents in the *Fmr1* KO. However, this study finds that these currents are unchanged and therefore unlikely to be related to prolonged UP states. Another pathway for enhancement of inward current is through NMDARs. Activation of Gp1 mGluRs results in an increase of NMDAR current, and therefore NMDA current may be exaggerated in the *Fmr1* KO (Benquet, Gee et al. 2002). Conversely, NMDAR components may be downregulated in the *Fmr1* KO (Krueger, Osterweil et al. 2011). Although one study reports no change in AMPA/NMDA ratio, this question would be better addressed with direct NMDA measurements both with and without concurrent stimulation of mGluRs (Desai, Casimiro et al. 2006). NMDAR function is necessary for the maintenance of UP states (see Appendix 1), so alterations in NMDAR currents may impact UP state duration in the *Fmr1* KO (Steriade, Nunez et al. 1993; Compte, Sanchez-Vives et al. 2003). Given the possibility for NMDAR change in the *Fmr1* KO and the importance of NMDAR function in UP states, this topic merits further research.

The second pathway for an excitability increase is through downregulation of hyperpolarizing currents. This could cause the circuit to remain in an UP state for a longer duration. Several candidate channels that regulate hyperpolarizing

current are altered in the *Fmr1* KO. Functional data suggests Slack sodium-activated potassium current is reduced in the *Fmr1* KO, but I find little evidence of functional Slack current in layer 5 pyramidal neurons (Brown, Kronengold et al. 2010; Strumbos, Brown et al. 2010). It is therefore unlikely to impact UP state duration. A-type potassium current, mediated primarily by the channel Kv4.2, may also be affected in the *Fmr1* KO. A-type current is strongly suppressed by mGluR activation, and thus could be linked to hyperexcitability in the *Fmr1* KO (Hu and Gereau 2003; Hu, Alter et al. 2007). Furthermore, two studies have reported opposite changes in expression levels of Kv4.2 in the *Fmr1* KO (Gross, Yao et al. 2011; Lee, Ge et al. 2011). In contrast to both, I observe that somatic A-type current in layer 5 pyramidal is unchanged in the *Fmr1* KO, suggesting that the protein level changes do not directly translate to functional changes. Interestingly, block of several voltage-gated potassium currents with 4-AP eliminates the difference in UP state duration between WT and *Fmr1* KO, supporting a role of altered voltage-gated potassium current in the *Fmr1* KO.

Generally, very little is known about intrinsic currents in the *Fmr1* KO. Further analysis of NMDAR or potassium currents in the *Fmr1* KO may provide insight into the mechanism of network hyperexcitability.

General changes in membrane properties could also directly lead to prolonged UP state duration. A previous study showed that excitatory neurons in layer 4 of the somatosensory cortex are hyperexcitable in the *Fmr1* KO (Gibson,

Bartley et al. 2008). In this study, I provide preliminary evidence that layer 5 excitatory neurons are similarly hyperexcitable. This increase is likely a product of higher input resistance observed in these neurons. Together with the layer specific effect of deletion of FMRP on UP state duration, this reveals a locus for the function of FMRP. Deletion of FMRP from layers 4 or 5 and 6 of neocortex partially prolongs UP state duration. Correspondingly, excitatory neurons within layer 4 and 5 of somatosensory cortex are hyperexcitable after deletion of FMRP. This suggests that it is not a certain population of hyperexcitable driving prolonged UP states in the *Fmr1* KO. Instead, loss of FMRP results in modest increases in excitability throughout all neurons within the circuit, which ultimately culminates in network hyperexcitability. Because small increases in excitability likely underlie network changes, it may be difficult to experimentally identify the currents that are responsible. Computer modeling may be a useful tool in determining the network effect of partial increases in excitability. Using the parameters obtained from experimental analysis of layer 4 and 5 excitatory neurons, modeling could determine whether these changes are sufficient to account for the increased UP state duration in the *Fmr1* KO.

Interestingly, UP state duration resulting from deletion of FMRP in layer 4 or layers 5 and 6 appears to be increased to approximately halfway between of the duration observed in WT and full *Fmr1* KO slices. However, in these animals, FMRP is only deleted from approximately 30-40% of the total neurons in the

neocortex. This may suggest that there is a critical limit where a greater number of hyperexcitable cells does not further increase UP state duration. Therefore, UP state duration in an *Fmr1* heterozygous female would be predicted to be increased to nearly that observed in the full *Fmr1* KO. If *Fmr1* heterozygotes do not display some behaviors observed in the *Fmr1* KO, this would be of particular interest in associating increased UP state duration with other phenotypic deficits.

Throughout this study, I relied on extracellular recordings to measure UP state duration. In *in vitro* preparations, UP states are best observed in an interface recording chamber. Unfortunately, this precludes the use of visualized intracellular patch-clamp recording. However, intracellular recordings would greatly increase the power of experiments that could be done to identify altered currents. Development of a technique that would allow voltage-clamp recordings during UP states could be used to assess what currents are active during network oscillations. Additionally, this format would allow testing of whether FMRP is acting in a cell autonomous fashion to cause prolonged UP states. Simultaneous recordings from a WT and KO neuron in the mosaic mouse model would allow measurement of depolarization from baseline, which is one of the criteria for UP states. If the effect is cell autonomous, the KO neuron would remain depolarized longer than the WT neuron, even though the synaptic inputs would be theoretically equivalent. This would provide much more data into the mechanism causing prolonged UP states and greatly assist in uncovering any currents that

may be responsible for network hyperexcitability. Therefore, I recommend that further efforts be put into designing a protocol that would allow visualized patch-clamp recordings during UP states.

Overactive mGluR5 mediates the network hyperexcitability in the *Fmr1* KO

The mGluR theory of Fragile X syndrome has motivated much of the research focused on the disease (Bear, Huber et al. 2004). This theory hypothesizes that increased mGluR signaling in the *Fmr1* KO is responsible for many of the phenotypes. Indeed, this theory has been largely supported by a wide range of studies. Pharmacological antagonism or genetic reduction of mGluR5 rescues many of the deficits observed in the *Fmr1* KO, ranging from protein translation to spine morphology to seizures to learning and memory (Yan, Rammal et al. 2005; Dölen, Osterweil et al. 2007; Choi, McBride et al. 2010; Dölen, Carpenter et al. 2010).

This study provides further support for the mGluR theory of Fragile X. Both pharmacological antagonism and reduction of mGluR5 gene dosage is sufficient to rescue network hyperexcitability in the *Fmr1* KO. Furthermore, genetic reduction of mGluR5 in an *Fmr1* KO reduces UP state duration to normal levels when measured *in vivo*. This suggests that mGluR5 targeted treatments may be therapeutically relevant for FXS patients.

It is not clear how antagonism of mGluR5 rescues UP state duration. As UP states are dependent on a variety of different synaptic and intrinsic components, there are many avenues for mGluR5 reduction to affect network function. Antagonism of mGluR5 can alter spine number, and this may result in changes in connectivity that normalize network function (de Vrij, Levenga et al. 2008; Westmark, Westmark et al. 2011). It seems unlikely that synaptic connections could reorganize on a time scale that would impact network oscillations, as 45 minutes of MPEP treatment reduces UP state duration in the *Fmr1* KO. However, we cannot directly rule out changes in connectivity. A more likely result of mGluR5 antagonism is changes in intrinsic currents that impact neuronal excitability and therefore network function. Signaling through mGluR5 is known to affect a wide variety of currents which could in turn give rise hyperexcitability. Moreover, MPEP treatment in the *Fmr1* KO is sufficient to reduce hyperexcitability in hippocampal networks, presumably by inhibiting the activation of a depolarizing current (Chuang, Zhao et al. 2005; Bianchi, Chuang et al. 2009). The network hyperexcitability in the hippocampus is driven by an mGluR-dependent plasticity, whereas networks are basally more excitable in the neocortex. One interesting possibility is that because network oscillations contribute to plasticity, the cortex may have already undergone the plasticity necessary to prolong UP states simply because the slow oscillation itself promotes plasticity (Steriade 2006). Regardless of the mechanism, the

contribution of mGluR5 is an important finding because this is, to my knowledge, the first study to implicate mGluR5 in basal, spontaneous network excitability, thereby providing more insight into the pathophysiology of FXS. Further studies should focus on elucidating the mechanism of the downstream effectors of mGluR5 that drive prolonged UP states in the *Fmr1* KO, as these represent additional therapeutic targets.

It is controversial whether mGluR5 is hypersensitive or basally hyperactive in the *Fmr1* KO. Protein translation is basally enhanced in the *Fmr1* KO, suggesting that mGluRs are constitutively more active. However, mGluRs are also more responsive to DHPG in the *Fmr1* KO, suggesting that they are hypersensitive. This study cannot directly contribute to understanding which case is relevant, as both cases could conceivably result in network hyperexcitability. If mGluRs are simply more constitutively active, neurons may be basally more excitable, thereby resulting in prolonged UP states. However, because UP states are glutamate driven and last sufficiently long that mGluRs can be stimulated, it is equally possible that the glutamate released with every UP state acts on hypersensitive mGluRs and increases depolarization, thereby causing the network to persist in an UP state for a longer period of time. Treatment with DHPG causes UP states to be prolonged to equal proportions in both WT and KO slices, which would seem to suggest that mGluR5 is not hypersensitive. However, DHPG also stimulates mGluR1 which strongly effects on UP state duration.

Given the strong contribution of mGluR1, it is likely that the increase in UP state duration with DHPG treatment is dominated by mGluR1 with little contribution from mGluR5. Therefore, it would be necessary to use DHPG treatment in combination with mGluR1 antagonism to evaluate the contribution of mGluR5 stimulation.

Disruption of Homer-mGluR5 scaffolds underlies circuit hyperexcitability

A possible mechanism for overactive mGluR5 signaling in the *Fmr1* KO is related to the scaffold protein Homer. Long forms of Homer are scaffold proteins that bind mGluR5 with its postsynaptic effectors (Ehrengruber, Kato et al. 2004). Homer1a is a short form that uncouples mGluR5 complexes, and in doing so drives constitutive mGluR5 signaling (Ango, Prezeau et al. 2001; Ehrengruber, Kato et al. 2004). Previous data suggested that mGluR5 was more uncoupled in the *Fmr1* KO, which corresponds to enhanced mGluR5 signaling (Giuffrida, Musumeci et al. 2005). This study confirms that mGluR5 is more uncoupled, and further demonstrates that mGluR5 is more associated with H1a.

Disruption of global Homer interactions is sufficient to cause prolonged UP states in WT slices. This same disruption in *Fmr1* KO slices has no effect on UP state duration, suggesting that mGluR5-dependent increases in UP state duration are maximal. To confirm that the effect of Homer disruption is through mGluR5, I measured UP states in a model in which a point mutation in mGluR5

specifically disrupts Homer interaction (Cozzoli, Goulding et al. 2009). In animals with two copies of the mutant allele (mGluR5FR), UP state duration was increased to the level observed in the *Fmr1* KO. One copy of the allele caused an intermediate increase in UP state duration, demonstrating a dose dependent effect of mGluR5-Homer interactions. To my knowledge, this is the first report of Homer-dependent regulation of network function. These findings also strongly implicate Homer-mGluR5 interaction in neocortical network hyperexcitability.

Because disruption of Homer-mGluR complexes prolongs UP state duration, and Homer interactions are reduced in the *Fmr1* KO, I sought to test whether promotion of Homer interactions could rescue UP state duration in the *Fmr1* KO. Indeed, deletion of H1a, and therefore promotion of long Homer complexes, in the *Fmr1* KO results in normal UP state duration. This finding further supports disrupted Homer interactions as the core deficit underlying mGluR dysfunction in the *Fmr1* KO.

Two additional experiments could further define the extent of the role of Homer-mGluR interaction. First, concurrent deletion of H1a in the mGluR5FR mutant model could unequivocally demonstrate that H1a-dependent increases in UP state duration in the *Fmr1* KO occur through mGluR5. In this scenario, mGluR5-Homer scaffolds would be disrupted and deletion of H1a could not restore the complexes. Therefore, this manipulation should have no effect on UP state duration. If deletion of H1a in the mGluR5FR mutant rescues UP state

duration, then a secondary effect of H1a was causing prolonged UP states. Second, concurrent deletion of FMRP in the mGluR5FR model would provide an epistasis experiment that would demonstrate that Homer, mGluR5, and FMRP are all acting in the same pathway. In this case, Homer-mGluR interactions would be disrupted. If FMRP serves to cause uncoupling of Homer-mGluR5 complexes leading to hyperexcitability, then deletion of FMRP should not further increase UP state duration in these animals. If Homer-mGluR5 interactions and FMRP regulate network function through different mechanisms, then UP state duration would be further increased in the *Fmr1* KO; mGluR5FR mutant compared to either the *Fmr1* KO or the mGluR5FR mutant. These experiments may ultimately prove useful in solidifying the pathways leading to deficits in the *Fmr1* KO.

Dysfunction of Homer-mGluR5 is the core deficit in network hyperexcitability

FMRP is an RNA binding protein that regulates translation at the synapse (O'Donnell and Warren 2002; Bassell and Warren 2008). Thus, FMRP is poised to have a wide range of effects on neuronal function by affecting any of its numerous bound transcripts. The slow oscillation is derived from a number of factors, and therefore would be prone to dysfunction if any parameters are altered (Steriade, Nunez et al. 1993; Compte, Sanchez-Vives et al. 2003). Considering these two facts, it is truly remarkable that network dysfunction is rescued in the *Fmr1* KO by simply promoting Homer-mGluR5 interactions. Despite the myriad

alterations in the *Fmr1* KO, the only change necessary to cause prolonged UP states is mGluR5 dysfunction resulting from disrupted Homer coupling. UP states are prolonged in the mGluR5FR mutant to the same extent observed in the *Fmr1* KO. This suggests that simple scaffold disruption is sufficient to mimic network hyperexcitability in the *Fmr1* KO. These findings provide evidence that the effect of the loss of FMRP on network function is highly indirect, and that FMRP's only role in regulating network function is to mediate the association of Homer-mGluR5 complexes. Further experiments aimed at determining how FMRP controls Homer-mGluR5 interactions could provide insight into a novel core mechanism of pathophysiology in FXS.

From a network excitability standpoint, the interplay between FMRP, Homer, and mGluR5 offers a unique synthesis of two theories of mental retardation. The mGluR theory of Fragile X postulates that mGluR dysfunction is the core deficit in FXS (Bear, Huber et al. 2004). The E/I balance theory of autism states that an imbalance of excitation an inhibition underlies many phenotypes observed in autism spectrum disorders (Rubenstein and Merzenich 2003). The increase in UP state duration in the *Fmr1* KO is indicative of a shift in E/I ratio to favor excitation. Furthermore, this shift in E/I ratio in the *Fmr1* KO is a result of disrupted Homer-mGluR5 interactions. Thus, the mGluR theory accounts for the E/I shift in FXS, and changes in E/I ratio may manifest as changes in network function and provide a unifying deficit across ASD.

Conclusions

The data provided in this study provide a characterization of neocortical network hyperexcitability in the *Fmr1* KO. The enhancement in excitability manifests as an increase in the duration of UP states. Disruption of Homer-mGluR5 interactions causes enhanced mGluR5 signaling which gives rise to the network hyperexcitability. Alterations in network excitability may lead to several phenotypes in FXS, including seizures and altered sensory perception. The exaggerated network activity in the *Fmr1* KO is indicative of an imbalance of E/I ratio in favor of excitation. A shift in the E/I ratio may underlie pathology in other autism spectrum disorders and therefore altered network function may be a unifying deficit in ASDs.

Appendix 1. Pharmacological block of fast glutamateric transmission prevents UP states

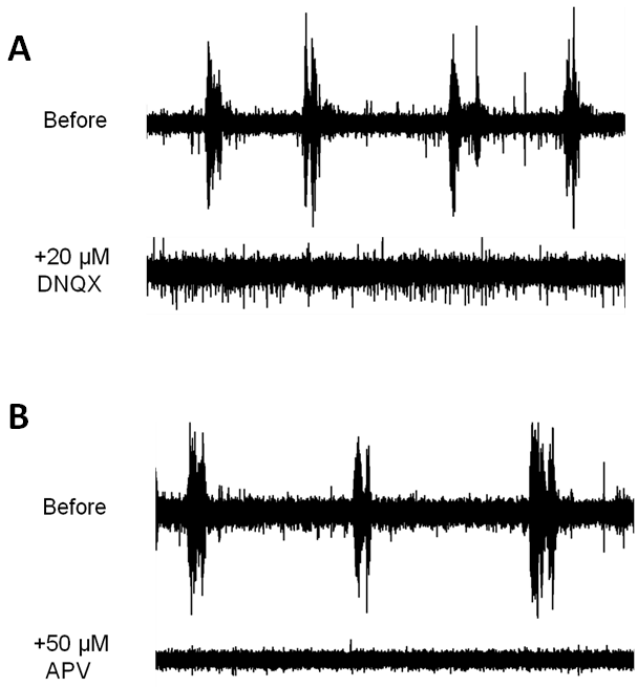

Appendix 1. Pharmacological block of fast glutamateric transmission prevents UP states

A) Treatment of a WT slice with 20 µM DNQX causes the elimination of UP states. **B)** Wash-in of 50 µM APV abolishes UP state activity.

BIBLIOGRAPHY

Abrahams, B. S. and D. H. Geschwind (2008). "Advances in autism genetics: on the threshold of a new neurobiology." Nat Rev Genet **9**(5): 15.

Agmon, A. and B. W. Connors (1991). "Thalamocortical responses of mouse somatosensory (barrel) cortex in vitro." Neuroscience **41**(2-3): 365-379.

Agmon, A. and B. W. Connors (1991). "Thalamocortical responses of mouse somatosensory (barrel) cortexin vitro." Neuroscience **41**(2–3): 365-379.

Akam, T. and D. M. Kullmann (2010). "Oscillations and Filtering Networks Support Flexible Routing of Information." Neuron **67**(2): 308-320.

Amzica, F. and M. Steriade (1998). "Cellular substrates and laminar profile of sleep K-complex." Neuroscience **82**(3): 671-686.

Ango, F., L. Prezeau, et al. (2001). "Agonist-independent activation of metabotropic glutamate receptors by the intracellular protein Homer." Nature **411**(6840): 962-965.

Antar, L. N., C. Li, et al. (2006). "Local functions for FMRP in axon growth cone motility and activity-dependent regulation of filopodia and spine synapses." Molecular and Cellular Neuroscience **32**(1–2): 37-48.

Bagni, C. and W. T. Greenough (2005). "From mRNP trafficking to spine dysmorphogenesis: the roots of fragile X syndrome." Nat Rev Neurosci **6**(5): 376-387.

Bailey, A. R., B. N. Giunta, et al. (2008). "Peripheral biomarkers in Autism: secreted amyloid precursor protein-α as a probable key player in early diagnosis." Int J Clin Exp Med **1**(4): 7.

Baird, G., E. Simonoff, et al. (2006). "Prevalence of disorders of the autism spectrum in a population cohort of children in South Thames: the Special Needs and Autism Project (SNAP)." The Lancet **368**(9531): 210-215.

Baker, K. B., S. P. Wray, et al. (2010). "Male and female Fmr1 knockout mice on C57 albino background exhibit spatial learning and memory impairments." Genes, Brain and Behavior **9**(6): 562-574.

Bakker, C. E., C. Verheij, et al. (1994). "Fmr1 knockout mice: A model to study fragile X mental retardation." Cell **78**(1): 23-33.

Bakker, D. B. (1994). "Fmr1 knockout mice: a model to study fragile X mental retardation. The Dutch-Belgian Fragile X Consortium." Cell **78**(1): 23-33.

Bangash, M A., Joo M. Park, et al. (2011). "Enhanced Polyubiquitination of Shank3 and NMDA Receptor in a Mouse Model of Autism." Cell **145**(5): 758-772.

Banko, J. L., L. Hou, et al. (2006). "Regulation of Eukaryotic Initiation Factor 4E by Converging Signaling Pathways during Metabotropic Glutamate Receptor-Dependent Long-Term Depression." The Journal of Neuroscience **26**(8): 2167-2173.

Bassell, G. J. and S. T. Warren (2008). "Fragile X Syndrome: Loss of Local mRNA Regulation Alters Synaptic Development and Function." Neuron **60**(2): 201-214.

Bassell, G. J. and S. T. Warren (2008). "Fragile X syndrome: loss of local mRNA regulation alters synaptic development and function." Neuron **60**(2): 201-214.

Bazhenov, M., P. Lonjers, et al. (2011). "Non-homogeneous extracellular resistivity affects the current-source density profiles of up–down state oscillations." Philosophical Transactions of the Royal Society A: Mathematical, Physical and Engineering Sciences **369**(1952): 3802-3819.

Bear, M. F., K. M. Huber, et al. (2004). "The mGluR theory of fragile X mental retardation." Trends in Neurosciences **27**(7): 370-377.

Bear, M. F., K. M. Huber, et al. (2004). "The mGluR theory of fragile X mental retardation." Trends Neurosci **27**(7): 370-377.

Belmonte, M. K. and T. Bourgeron (2006). "Fragile X syndrome and autism at the intersection of genetic and neural networks." Nat Neurosci **9**(10): 5.

Benquet, P., C. E. Gee, et al. (2002). "Two Distinct Signaling Pathways Upregulate NMDA Receptor Responses via Two Distinct Metabotropic Glutamate Receptor Subtypes." The Journal of Neuroscience **22**(22): 9679-9686.

Berger, T., M. E. Larkum, et al. (2001). "High I h Channel Density in the Distal Apical Dendrite of Layer V Pyramidal Cells Increases Bidirectional Attenuation of EPSPs." Journal of Neurophysiology **85**(2): 855-868.

Berry-Kravis, E. (2002). "Epilepsy in fragile X syndrome." Developmental Medicine & Child Neurology **44**(11): 724-728.

Berry-Kravis, E. (2002). "Epilepsy in fragile X syndrome." Dev Med Child Neurol **44**(11): 724-728.

Berry-Kravis, E., M. Raspa, et al. (2010). "Seizures in Fragile X Syndrome: Characteristics and Comorbid Diagnoses." American Journal on Intellectual and Developmental Disabilities **115**(6): 461-472.

Bertaso, F., G. Roussignol, et al. (2010). "Homer1a-Dependent Crosstalk Between NMDA and Metabotropic Glutamate Receptors in Mouse Neurons." PLoS ONE **5**(3): e9755.

Bhattacharjee, A., L. Gan, et al. (2002). "Localization of the Slack potassium channel in the rat central nervous system." The Journal of Comparative Neurology **454**(3): 241-254.

Bianchi, R., S.-C. Chuang, et al. (2009). "Cellular Plasticity for Group I mGluR-Mediated Epileptogenesis." The Journal of Neuroscience **29**(11): 3497-3507.

Bianchi, R., S. C. Chuang, et al. (2009). "Cellular plasticity for group I mGluR-mediated epileptogenesis." J Neurosci **29**(11): 3497-3507.

Billuart, P., T. Bienvenu, et al. (1998). "Oligophrenin-1 encodes a rhoGAP protein involved in X-linked mental retardation." Nature **392**(6679): 7.
Birnbaum, S. G., A. W. Varga, et al. (2004). "Structure and Function of Kv4-Family Transient Potassium Channels." Physiological Reviews **84**(3): 803-833.
Bockaert, J., J. Perroy, et al. (2010). "GPCR Interacting Proteins (GIPs) in the Nervous System: Roles in Physiology and Pathologies." Annual Review of Pharmacology and Toxicology **50**(1): 89-109.
Brager, D. H. and D. Johnston (2007). "Plasticity of Intrinsic Excitability during Long-Term Depression Is Mediated through mGluR-Dependent Changes in Ih in Hippocampal CA1 Pyramidal Neurons." The Journal of Neuroscience **27**(51): 13926-13937.
Brakeman, P. R., A. A. Lanahan, et al. (1997). "Homer: a protein that selectively binds metabotropic glutamate receptors." Nature **386**(6622): 5.
Brennan, F. X., D. S. Albeck, et al. (2006). "Fmr1 knockout mice are impaired in a leverpress escape/avoidance task." Genes Brain Behav **5**(6): 467-471.
Britanova, O., C. de Juan Romero, et al. (2008). "Satb2 Is a Postmitotic Determinant for Upper-Layer Neuron Specification in the Neocortex." Neuron **57**(3): 378-392.
Brown, M. R., J. Kronengold, et al. (2010). "Fragile X mental retardation protein controls gating of the sodium-activated potassium channel Slack." Nat Neurosci **13**(7): 819-821.
Brown, M. R., J. Kronengold, et al. (2010). "Fragile X mental retardation protein controls gating of the sodium-activated potassium channel Slack." Nat Neurosci **13**(7): 819-821.
Brown, V., P. Jin, et al. (2001). "Microarray Identification of FMRP-Associated Brain mRNAs and Altered mRNA Translational Profiles in Fragile X Syndrome." Cell **107**(4): 477-487.
Bureau, I., G. M. Shepherd, et al. (2008). "Circuit and plasticity defects in the developing somatosensory cortex of FMR1 knock-out mice." J Neurosci **28**(20): 5178-5188.
Bureau, I., G. M. G. Shepherd, et al. (2008). "Circuit and Plasticity Defects in the Developing Somatosensory Cortex of Fmr1 Knock-Out Mice." J. Neurosci. **28**(20): 5178-5188.
Busche, M. A., G. Eichhoff, et al. (2008). "Clusters of Hyperactive Neurons Near Amyloid Plaques in a Mouse Model of Alzheimer's Disease." Science **321**(5896): 1686-1689.
Caronna, E. B., J. M. Milunsky, et al. (2008). "Autism spectrum disorders: clinical and research frontiers." Archives of Disease in Childhood **93**(6): 518-523.

Castren, M., A. Paakkonen, et al. (2003). "Augmentation of auditory N1 in children with fragile X syndrome." Brain Topogr **15**(3): 165-171.
Ceman, S., W. T. O'Donnell, et al. (2003). "Phosphorylation influences the translation state of FMRP-associated polyribosomes." Human Molecular Genetics **12**(24): 3295-3305.
Chao, H.-T., H. Chen, et al. (2010). "Dysfunction in GABA signalling mediates autism-like stereotypies and Rett syndrome phenotypes." Nature **468**(7321): 7.
Chauvette, S., M. Volgushev, et al. (2010). "Origin of active states in local neocortical networks during slow sleep oscillation." Cereb Cortex **20**(11): 2660-2674.
Chauvette, S., M. Volgushev, et al. (2010). "Origin of Active States in Local Neocortical Networks during Slow Sleep Oscillation." Cerebral Cortex **20**(11): 2660-2674.
Chen, L. and M. Toth (2001). "Fragile X mice develop sensory hyperreactivity to auditory stimuli." Neuroscience **103**(4): 1043-1050.
Chen, X., L.-L. Yuan, et al. (2006). "Deletion of Kv4.2 Gene Eliminates Dendritic A-Type K+ Current and Enhances Induction of Long-Term Potentiation in Hippocampal CA1 Pyramidal Neurons." The Journal of Neuroscience **26**(47): 12143-12151.
Choi, C., S. McBride, et al. (2010). "Age-dependent cognitive impairment in a <i>Drosophila Fragile X model and its pharmacological rescue." Biogerontology **11**(3): 347-362.
Chuang, S.-C., W. Zhao, et al. (2005). "Prolonged Epileptiform Discharges Induced by Altered Group I Metabotropic Glutamate Receptor-Mediated Synaptic Responses in Hippocampal Slices of a Fragile X Mouse Model." J. Neurosci. **25**(35): 8048-8055.
Chuang, S., Q. Yan, et al. (2004). Synaptic activation of Gp1 mGluRs is epileptogenic in hippocampal slices for FMRP knock-out mice. Society for Neuroscience, San Diego, CA.
Chuang, S. C., W. Zhao, et al. (2005). "Prolonged epileptiform discharges induced by altered group I metabotropic glutamate receptor-mediated synaptic responses in hippocampal slices of a fragile X mouse model." J Neurosci **25**(35): 8048-8055.
Comery, T. A., J. B. Harris, et al. (1997). "Abnormal dendritic spines in fragile X knockout mice: Maturation and pruning deficits." Proceedings of the National Academy of Sciences **94**(10): 5401-5404.
Compte, A., M. V. Sanchez-Vives, et al. (2003). "Cellular and Network Mechanisms of Slow Oscillatory Activity (<1 Hz) and Wave Propagations in a Cortical Network Model." Journal of Neurophysiology **89**(5): 2707-2725.

Contreras, D. and M. Steriade (1995). "Cellular basis of EEG slow rhythms: a study of dynamic corticothalamic relationships." The Journal of Neuroscience **15**(1): 604-622.

Cozzoli, D. K., S. P. Goulding, et al. (2009). "Binge Drinking Upregulates Accumbens mGluR5–Homer2–PI3K Signaling: Functional Implications for Alcoholism." The Journal of Neuroscience **29**(27): 8655-8668.

Crunelli, V. and S. W. Hughes (2010). "The slow (<1 Hz) rhythm of non-REM sleep: a dialogue between three cardinal oscillators." Nat Neurosci **13**(1): 9-17.

Cruz-Martín, A., M. Crespo, et al. (2010). "Delayed Stabilization of Dendritic Spines in Fragile X Mice." The Journal of Neuroscience **30**(23): 7793-7803.

Darnell, J. C., C. E. Fraser, et al. (2005). "Kissing complex RNAs mediate interaction between the Fragile-X mental retardation protein KH2 domain and brain polyribosomes." Genes & Development **19**(8): 903-918.

Darnell, J. C., K. B. Jensen, et al. (2001). "Fragile X Mental Retardation Protein Targets G Quartet mRNAs Important for Neuronal Function." Cell **107**(4): 489-499.

Darnell, Jennifer C., Sarah J. Van Driesche, et al. (2011). "FMRP Stalls Ribosomal Translocation on mRNAs Linked to Synaptic Function and Autism." Cell **146**(2): 247-261.

De Boulle, K., Verkerk, Annemieke J.M.H., Reyniers, Edwin, Vits, Lieve, Hendrickx, Jan, Van Roy, Bernadette, Van Den Bos, Feikje, de Graaff, Esther, Oostra, Ben A., Willems, Patrick J. (1993). "A point mutation in the FMR-1 gene associated with fragile X mental retardation." Nature Genetics **3**(1): 5.

de Vrij, F. M. S., J. Levenga, et al. (2008). "Rescue of behavioral phenotype and neuronal protrusion morphology in Fmr1 KO mice." Neurobiology of Disease **31**(1): 127-132.

Desai, N. S., T. M. Casimiro, et al. (2006). "Early postnatal plasticity in neocortex of FMR1 knockout mice." J Neurophysiol **96**(4): 1734-1745.

Desai, N. S., T. M. Casimiro, et al. (2006). "Early Postnatal Plasticity in Neocortex of Fmr1 Knockout Mice." Journal of Neurophysiology **96**(4): 1734-1745.

Dictenberg, J. B., S. A. Swanger, et al. (2008). "A Direct Role for FMRP in Activity-Dependent Dendritic mRNA Transport Links Filopodial-Spine Morphogenesis to Fragile X Syndrome." Developmental cell **14**(6): 926-939.

Dobkin, C., A. Rabe, et al. (2000). "Fmr1 knockout mouse has a distinctive strain-specific learning impairment." Neuroscience **100**(2): 423-429.

Dolen, G. and M. F. Bear (2008). "Role for metabotropic glutamate receptor 5 (mGluR5) in the pathogenesis of fragile X syndrome." J Physiol **586**(6): 1503-1508.
Dölen, G., R. L. Carpenter, et al. (2010). "Mechanism-based approaches to treating fragile X." Pharmacology & Therapeutics **127**(1): 78-93.
Dolen, G., E. Osterweil, et al. (2007). "Correction of fragile X syndrome in mice." Neuron **56**(6): 955-962.
Dölen, G., E. Osterweil, et al. (2007). "Correction of Fragile X Syndrome in Mice." Neuron **56**(6): 955-962.
Dykens, E. M., R. M. Hodapp, et al. (1989). "The Trajectory of Cognitive Development in Males with Fragile X Syndrome." Journal of the American Academy of Child and Adolescent Psychiatry **28**(3): 422-426.
Eadie, B. D., W. N. Zhang, et al. (2009). "Fmr1 knockout mice show reduced anxiety and alterations in neurogenesis that are specific to the ventral dentate gyrus." Neurobiology of Disease **36**(2): 361-373.
Ehrengruber, M., A. Kato, et al. (2004). "Homer/vesl proteins and their roles in CNS neurons." Molecular Neurobiology **29**(3): 213-227.
Fellin, T., M. M. Halassa, et al. (2009). "Endogenous nonneuronal modulators of synaptic transmission control cortical slow oscillations in vivo." Proc Natl Acad Sci U S A **106**(35): 15037-15042.
Frankland, P. W., Y. Wang, et al. (2004). "Sensorimotor gating abnormalities in young males with fragile X syndrome and Fmr1-knockout mice." Mol Psychiatry **9**(4): 417-425.
Fröhlich, F., M. Bazhenov, et al. (2008). "Pathological Effect of Homeostatic Synaptic Scaling on Network Dynamics in Diseases of the Cortex." The Journal of Neuroscience **28**(7): 1709-1720.
Fröhlich, F., M. Bazhenov, et al. (2010). "Maintenance and termination of neocortical oscillations by dynamic modulation of intrinsic and synaptic excitability." Thalamus Relat Syst **3**(2): 10.
Fröhlich, F., T. J. Sejnowski, et al. (2010). "Network Bistability Mediates Spontaneous Transitions between Normal and Pathological Brain States." The Journal of Neuroscience **30**(32): 10734-10743.
Gabel, L. A., S. Won, et al. (2004). "Visual experience regulates transient expression and dendritic localization of fragile X mental retardation protein." J Neurosci **24**(47): 10579-10583.
Ganz, M. L. (2007). "The Lifetime Distribution of the Incremental Societal Costs of Autism." Arch Pediatr Adolesc Med **161**(4): 343-349.
Garber, K. B., J. Visootsak, et al. (2008). "Fragile X syndrome." Eur J Hum Genet **16**(6): 7.
Gibson, J. R., A. F. Bartley, et al. (2008). "Imbalance of Neocortical Excitation and Inhibition and Altered UP States Reflect Network Hyperexcitability in

the Mouse Model of Fragile X Syndrome." J Neurophysiol **100**(5): 2615-2626.
Gibson, J. R., A. F. Bartley, et al. (2008). "Imbalance of neocortical excitation and inhibition and altered UP states reflect network hyperexcitability in the mouse model of fragile X syndrome." J Neurophysiol **100**(5): 2615-2626.
Gibson, J. R., K. M. Huber, et al. (2009). "Neuroligin-2 Deletion Selectively Decreases Inhibitory Synaptic Transmission Originating from Fast-Spiking but Not from Somatostatin-Positive Interneurons." The Journal of Neuroscience **29**(44): 13883-13897.
Giuffrida, R., S. Musumeci, et al. (2005). "A Reduced Number of Metabotropic Glutamate Subtype 5 Receptors Are Associated with Constitutive Homer Proteins in a Mouse Model of Fragile X Syndrome." J. Neurosci. **25**(39): 8908-8916.
Gogolla, N., J. LeBlanc, et al. (2009). "Common circuit defect of excitatory-inhibitory balance in mouse models of autism." Journal of Neurodevelopmental Disorders **1**(2): 172-181.
Gonchar, Y. and A. Burkhalter (1997). "Three distinct families of GABAergic neurons in rat visual cortex." Cereb Cortex **7**(4): 347-358.
Gross, C., M. Nakamoto, et al. (2010). "Excess Phosphoinositide 3-Kinase Subunit Synthesis and Activity as a Novel Therapeutic Target in Fragile X Syndrome." The Journal of Neuroscience **30**(32): 10624-10638.
Gross, C., X. Yao, et al. (2011). "Fragile X Mental Retardation Protein Regulates Protein Expression and mRNA Translation of the Potassium Channel Kv4.2." The Journal of Neuroscience **31**(15): 5693-5698.
Grossman, A. W., G. M. Aldridge, et al. (2010). "Developmental characteristics of dendritic spines in the dentate gyrus of Fmr1 knockout mice." Brain Research **1355**(0): 221-227.
Grossman, A. W., N. M. Elisseou, et al. (2006). "Hippocampal pyramidal cells in adult Fmr1 knockout mice exhibit an immature-appearing profile of dendritic spines." Brain Research **1084**(1): 158-164.
Guan, D., L. R. Horton, et al. (2011). "Postnatal development of A-type and Kv1- and Kv2-mediated potassium channel currents in neocortical pyramidal neurons." Journal of Neurophysiology **105**(6): 2976-2988.
Hagerman, R. (2002). The physical and behavioral phenotype. Fragile X Syndrome: Diagnosis, Treatment, and Research. R. Hagerman and P. Hagerman. Baltimore, The Johns Hopkins University Press**:** 3-109.
Hagerman, R., G. Hoem, et al. (2010). "Fragile X and autism: Intertwined at the molecular level leading to targeted treatments." Molecular Autism **1**(1): 12.

Hagerman, R. J., K. Amiri, et al. (1991). "Fragile X checklist." Am J Med Genet **38**(2-3): 283-287.
Hagerman, R. J. and P. J. Hagerman (2002). Fragile X syndrome: Diagnosis, Treatment, and Research. Baltimore, Maryland, Johns Hopkins University Press.
Hagerman, R. J., A. W. Jackson, et al. (1986). "An analysis of autism in fifty males with the fragile X syndrome." American Journal of Medical Genetics **23**(1-2): 359-374.
Hagerman, R. J., M. Y. Ono, et al. (2005). "Recent advances in fragile X: a model for autism and neurodegeneration." Curr Opin Psychiatry **18**(5): 490-496.
Hagerman, R. J., M. Y. Ono, et al. (2005). "Recent advances in fragile X: a model for autism and neurodegeneration." Current Opinion in Psychiatry **18**(5): 490-496.
Haider, B., A. Duque, et al. (2006). "Neocortical Network Activity In Vivo Is Generated through a Dynamic Balance of Excitation and Inhibition." J. Neurosci. **26**(17): 4535-4545.
Haider, B. and D. A. McCormick (2009). "Rapid neocortical dynamics: cellular and network mechanisms." Neuron **62**(2): 171-189.
Hall, S., D. Burns, et al. (2008). "Longitudinal Changes in Intellectual Development in Children with Fragile X Syndrome." Journal of Abnormal Child Psychology **36**(6): 927-939.
Hanson, J. E. and D. V. Madison (2007). "Presynaptic Fmr1 Genotype Influences the Degree of Synaptic Connectivity in a Mosaic Mouse Model of Fragile X Syndrome." J. Neurosci. **27**(15): 4014-4018.
Harlow, E. G., S. M. Till, et al. (2010). "Critical Period Plasticity Is Disrupted in the Barrel Cortex of Fmr1 Knockout Mice." Neuron **65**(3): 385-398.
Hasenstaub, A., R. N. S. Sachdev, et al. (2007). "State Changes Rapidly Modulate Cortical Neuronal Responsiveness." The Journal of Neuroscience **27**(36): 9607-9622.
Hays, S. A., K. M. Huber, et al. (2011). "Altered Neocortical Rhythmic Activity States in Fmr1 KO Mice Are Due to Enhanced mGluR5 Signaling and Involve Changes in Excitatory Circuitry." The Journal of Neuroscience **31**(40): 14223-14234.
Herbert, T. P., A. R. Tee, et al. (2002). "The Extracellular Signal-regulated Kinase Pathway Regulates the Phosphorylation of 4E-BP1 at Multiple Sites." Journal of Biological Chemistry **277**(13): 11591-11596.
Hoffman, D. A., Magee, Jeffrey C., Colbert, Costa M., Johnston, Daniel (1997). "K+ channel regulation of signal propagation in dendrites of hippocampal pyramidal neurons." Nature **387**(6636): 7.

Hollway, J. A. and M. G. Aman (2011). "Sleep correlates of pervasive developmental disorders: A review of the literature." Research in Developmental Disabilities **32**(5): 1399-1421.

Hu, H.-J., B. J. Alter, et al. (2007). "Metabotropic Glutamate Receptor 5 Modulates Nociceptive Plasticity via Extracellular Signal-Regulated Kinaseâ€“Kv4.2 Signaling in Spinal Cord Dorsal Horn Neurons." The Journal of Neuroscience **27**(48): 13181-13191.

Hu, H.-J. and R. W. Gereau (2003). "ERK Integrates PKA and PKC Signaling in Superficial Dorsal Horn Neurons. II. Modulation of Neuronal Excitability." Journal of Neurophysiology **90**(3): 1680-1688.

Hu, J.-H., J. M. Park, et al. (2010). "Homeostatic Scaling Requires Group I mGluR Activation Mediated by Homer1a." Neuron **68**(6): 1128-1142.

Huang, G. N., D. L. Huso, et al. (2008). "NFAT Binding and Regulation of T Cell Activation by the Cytoplasmic Scaffolding Homer Proteins." Science **319**(5862): 476-481.

Huber, K. M., S. M. Gallagher, et al. (2002). "Altered synaptic plasticity in a mouse model of fragile X mental retardation." Proceedings of the National Academy of Sciences **99**(11): 7746-7750.

Huber, K. M., S. M. Gallagher, et al. (2002). "Altered synaptic plasticity in a mouse model of fragile X mental retardation." Proc Natl Acad Sci U S A **99**(11): 7746-7750.

Huber, K. M., M. S. Kayser, et al. (2000). "Role for Rapid Dendritic Protein Synthesis in Hippocampal mGluR-Dependent Long-Term Depression." Science **288**(5469): 1254-1256.

Incorpora, G., G. Sorge, et al. (2002). "Epilepsy in fragile X syndrome." Brain and Development **24**(8): 766-769.

Incorpora, G., G. Sorge, et al. (2002). "Epilepsy in fragile X syndrome." Brain Dev **24**(8): 766-769.

Irwin, S. A., B. Patel, et al. (2001). "Abnormal dendritic spine characteristics in the temporal and visual cortices of patients with fragile-X syndrome: a quantitative examination." Am J Med Genet **98**(2): 161-167.

Irwin, S. A., B. Patel, et al. (2001). "Abnormal dendritic spine characteristics in the temporal and visual cortices of patients with fragile-X syndrome: A quantitative examination." American Journal of Medical Genetics **98**(2): 161-167.

Isomura, Y., A. Sirota, et al. (2006). "Integration and Segregation of Activity in Entorhinal-Hippocampal Subregions by Neocortical Slow Oscillations." Neuron **52**(5): 871-882.

Iwasato, T., A. Datwani, et al. (2000). "Cortex-restricted disruption of NMDAR1 impairs neuronal patterns in the barrel cortex." Nature **406**(6797): 726-731.

Iwasato, T., M. Inan, et al. (2008). "Cortical adenylyl cyclase 1 is required for thalamocortical synapse maturation and aspects of layer IV barrel development." J Neurosci **28**(23): 5931-5943.

Jacquemont, S., A. Curie, et al. (2011). "Epigenetic Modification of the FMR1 Gene in Fragile X Syndrome Is Associated with Differential Response to the mGluR5 Antagonist AFQ056." Science Translational Medicine **3**(64): 64ra61.

Johnston, D. and S. Wu (1995). Foundations of Cellular Neurophysiology. Cambridge, MA, The MIT Press.

Kaczmarek, L. K., A. Bhattacharjee, et al. (2005). "Regulation of the timing of MNTB neurons by short-term and long-term modulation of potassium channels." Hearing Research **206**(1–2): 133-145.

Kammermeier, P. J. and P. F. Worley (2007). "Homer 1a uncouples metabotropic glutamate receptor 5 from postsynaptic effectors." Proceedings of the National Academy of Sciences **104**(14): 6055-6060.

Kang, S., K. Kitano, et al. (2004). "Self-organized two-state membrane potential transitions in a network of realistically modeled cortical neurons." Neural Networks **17**(3): 307-312.

Kang, S., K. Kitano, et al. (2008). "Structure of Spontaneous UP and DOWN Transitions Self-Organizing in a Cortical Network Model." PLoS Comput Biol **4**(3): e1000022.

Kato, A., F. Ozawa, et al. (1998). "Novel Members of the Vesl/Homer Family of PDZ Proteins That Bind Metabotropic Glutamate Receptors." Journal of Biological Chemistry **273**(37): 23969-23975.

Kaufmann, W. E., R. Cortell, et al. (2004). "Autism spectrum disorder in fragile X syndrome: communication, social interaction, and specific behaviors." Am J Med Genet A **129**(3): 225-234.

Kaufmann, W. E. and H. W. Moser (2000). "Dendritic Anomalies in Disorders Associated with Mental Retardation." Cerebral Cortex **10**(10): 981-991.

Kelleher, R. J., A. Govindarajan, et al. (2004). "Translational Control by MAPK Signaling in Long-Term Synaptic Plasticity and Memory." Cell **116**(3): 467-479.

Kim, S. J., Y. S. Kim, et al. (2003). "Activation of the TRPC1 cation channel by metabotropic glutamate receptor mGluR1." Nature **426**(6964): 285-291.

Klauck, S. M. (2006). "Genetics of autism spectrum disorder." Eur J Hum Genet **14**(6): 7.

Kleschevnikov, A. M., P. V. Belichenko, et al. (2012). "Increased efficiency of the GABAA and GABAB receptor-mediated neurotransmission in the Ts65Dn mouse model of Down syndrome." Neurobiology of Disease **45**(2): 683-691.

Kronk, R., E. E. Bishop, et al. (2010). "Prevalence, nature, and correlates of sleep problems among children with fragile X syndrome based on a large scale parent survey." Sleep **33**(5): 679-687.

Krueger, D. D., E. K. Osterweil, et al. (2011). "Cognitive dysfunction and prefrontal synaptic abnormalities in a mouse model of fragile X syndrome." Proceedings of the National Academy of Sciences **108**(6): 2587-2592.

Lambe, E. K. and G. K. Aghajanian (2007). "Prefrontal cortical network activity: Opposite effects of psychedelic hallucinogens and D1/D5 dopamine receptor activation." Neuroscience **145**(3): 900-910.

Larson, J., R. E. Jessen, et al. (2005). "Age-Dependent and Selective Impairment of Long-Term Potentiation in the Anterior Piriform Cortex of Mice Lacking the Fragile X Mental Retardation Protein." The Journal of Neuroscience **25**(41): 9460-9469.

Lee, Hye Y., W.-P. Ge, et al. (2011). "Bidirectional Regulation of Dendritic Voltage-Gated Potassium Channels by the Fragile X Mental Retardation Protein." Neuron **72**(4): 630-642.

Levenga, J., F. M. S. de Vrij, et al. (2011). "Subregion-specific dendritic spine abnormalities in the hippocampus of Fmr1 KO mice." Neurobiology of Learning and Memory **95**(4): 467-472.

Lewine, J. D., R. Andrews, et al. (1999). "Magnetoencephalographic Patterns of Epileptiform Activity in Children With Regressive Autism Spectrum Disorders." Pediatrics **104**(3): 405-418.

Li, Z., Y. Zhang, et al. (2001). "The fragile X mental retardation protein inhibits translation via interacting with mRNA." Nucleic Acids Research **29**(11): 2276-2283.

Liao, G.-Y. and B. Xu (2008). "Cre recombinase-mediated gene deletion in layer 4 of murine sensory cortical areas." genesis **46**(6): 289-293.

Liu, Z.-H. and C. B. Smith (2009). "Dissociation of social and nonsocial anxiety in a mouse model of fragile X syndrome." Neuroscience Letters **454**(1): 62-66.

Lu, Y. M., Z. Jia, et al. (1997). "Mice lacking metabotropic glutamate receptor 5 show impaired learning and reduced CA1 long-term potentiation (LTP) but normal CA3 LTP." J Neurosci **17**(13): 5196-5205.

Ludwig, A., T. Budde, et al. (2003). "Absence epilepsy and sinus dysrhythmia in mice lacking the pacemaker channel HCN2." EMBO J **22**(2): 9.

Lüscher, C. and K. M. Huber (2010). "Group 1 mGluR-Dependent Synaptic Long-Term Depression: Mechanisms and Implications for Circuitry and Disease." Neuron **65**(4): 445-459.

Mackiewicz, M., B. Paigen, et al. (2008). "Analysis of the QTL for sleep homeostasis in mice: Homer1a is a likely candidate." Physiological Genomics **33**(1): 91-99.
MacLean, J. N., B. O. Watson, et al. (2005). "Internal Dynamics Determine the Cortical Response to Thalamic Stimulation." Neuron **48**(5): 811-823.
Mann, E. O., M. M. Kohl, et al. (2009). "Distinct Roles of GABAA and GABAB Receptors in Balancing and Terminating Persistent Cortical Activity." The Journal of Neuroscience **29**(23): 7513-7518.
Mao, L., L. Yang, et al. (2005). "The Scaffold Protein Homer1b/c Links Metabotropic Glutamate Receptor 5 to Extracellular Signal-Regulated Protein Kinase Cascades in Neurons." J. Neurosci. **25**(10): 2741-2752.
Marin-Padilla, M. (1972). "Structural abnormalities of the cerebral cortex in human chromosomal aberrations: a Golgi study." Brain Research **44**(2): 625-629.
Markram, H., T. Rinaldi, et al. (2007). Intense World Syndrome.
Markram, K. and H. Markram (2010). "The Intense World Theory ? a unifying theory of the neurobiology of autism." Frontiers in Human Neuroscience **4**.
Marshall, L. and J. Born (2007). "The contribution of sleep to hippocampus-dependent memory consolidation." Trends Cogn Sci **11**(10): 442-450.
Marshall, L., H. Helgadottir, et al. (2006). "Boosting slow oscillations during sleep potentiates memory." Nature **444**(7119): 610-613.
Marshall, L., H. Helgadottir, et al. (2006). "Boosting slow oscillations during sleep potentiates memory." Nature **444**(7119): 4.
McBride, S. M., C. H. Choi, et al. (2005). "Pharmacological rescue of synaptic plasticity, courtship behavior, and mushroom body defects in a Drosophila model of fragile X syndrome." Neuron **45**(5): 753-764.
McCormick, D. A., Y. Shu, et al. (2003). "Persistent Cortical Activity: Mechanisms of Generation and Effects on Neuronal Excitability." Cereb. Cortex **13**(11): 1219-1231.
Meredith, R. M., R. de Jong, et al. (2010). "Functional rescue of excitatory synaptic transmission in the developing hippocampus in Fmr1-KO mouse." Neurobiol Dis.
Meredith, R. M. and H. D. Mansvelder (2010). "STDP and Mental Retardation: Dysregulation of Dendritic Excitability in Fragile X Syndrome." Front Synaptic Neurosci **2**(10).
Merenstein, S. A., W. E. Sobesky, et al. (1996). "Molecular-clinical correlations in males with an expanded FMR1 mutation." American Journal of Medical Genetics **64**(2): 388-394.

Miano, S., O. Bruni, et al. (2008). "Sleep phenotypes of intellectual disability: a polysomnographic evaluation in subjects with Down syndrome and Fragile-X syndrome." Clin Neurophysiol **119**(6): 1242-1247.
Miano, S., O. Bruni, et al. (2008). "Sleep phenotypes of intellectual disability: A polysomnographic evaluation in subjects with Down syndrome and Fragile-X syndrome." Clinical Neurophysiology **119**(6): 1242-1247.
Mientjes, E. J., I. Nieuwenhuizen, et al. (2006). "The generation of a conditional Fmr1 knock out mouse model to study Fmrp function in vivo." Neurobiol Dis **21**(3): 549-555.
Migliore, M., D. A. Hoffman, et al. (1999). "Role of an A-Type K⁺ Conductance in the Back-Propagation of Action Potentials in the Dendrites of Hippocampal Pyramidal Neurons." Journal of Computational Neuroscience **7**(1): 5-15.
Miller, L. J., D. N. McIntosh, et al. (1999). "Electrodermal responses to sensory stimuli in individuals with fragile X syndrome: A preliminary report." American Journal of Medical Genetics **83**(4): 268-279.
Miller, L. J., D. N. McIntosh, et al. (1999). "Electrodermal responses to sensory stimuli in individuals with fragile X syndrome: a preliminary report." Am J Med Genet **83**(4): 268-279.
Mineur, Y. S., F. Sluyter, et al. (2002). "Behavioral and neuroanatomical characterization of the Fmr1 knockout mouse." Hippocampus **12**(1): 39-46.
Mizutani, A., Y. Kuroda, et al. (2008). "Phosphorylation of Homer3 by Calcium/Calmodulin-Dependent Kinase II Regulates a Coupling State of Its Target Molecules in Purkinje Cells." The Journal of Neuroscience **28**(20): 5369-5382.
Monory, K., F. Massa, et al. (2006). "The endocannabinoid system controls key epileptogenic circuits in the hippocampus." Neuron **51**(4): 455-466.
Muddashetty, Ravi S., Vijayalaxmi C. Nalavadi, et al. (2011). "Reversible Inhibition of PSD-95 mRNA Translation by miR-125a, FMRP Phosphorylation, and mGluR Signaling." Molecular cell **42**(5): 673-688.
Musumeci, S. A., P. Bosco, et al. (2000). "Audiogenic seizures susceptibility in transgenic mice with fragile X syndrome." Epilepsia **41**(1): 19-23.
Musumeci, S. A., G. Calabrese, et al. (2007). "Audiogenic seizure susceptibility is reduced in fragile X knockout mice after introduction of FMR1 transgenes." Experimental Neurology **203**(1): 233-240.
Musumeci, S. A., R. Ferri, et al. (1991). "Epilepsy and fragile X syndrome: a follow-up study." Am J Med Genet **38**(2-3): 511-513.
Musumeci, S. A., R. J. Hagerman, et al. (1999). "Epilepsy and EEG Findings in Males with Fragile X Syndrome." Epilepsia **40**(8): 1092-1099.

Musumeci, S. A., R. J. Hagerman, et al. (1999). "Epilepsy and EEG findings in males with fragile X syndrome." Epilepsia **40**(8): 1092-1099.
Newschaffer, C. J., L. A. Croen, et al. (2007). "The Epidemiology of Autism Spectrum Disorders*." Annual Review of Public Health **28**(1): 235-258.
Nielsen, D. M., W. J. Derber, et al. (2002). "Alterations in the auditory startle response in Fmr1 targeted mutant mouse models of fragile X syndrome." Brain Res **927**(1): 8-17.
Niswender, C. M. and P. J. Conn (2010). "Metabotropic glutamate receptors: physiology, pharmacology, and disease." Annu Rev Pharmacol Toxicol **50**: 295-322.
Norris, A. J., N. C. Foeger, et al. (2010). "Interdependent Roles for Accessory KChIP2, KChIP3, and KChIP4 Subunits in the Generation of Kv4-Encoded IA Channels in Cortical Pyramidal Neurons." The Journal of Neuroscience **30**(41): 13644-13655.
Norris, A. J. and J. M. Nerbonne (2010). "Molecular Dissection of IA in Cortical Pyramidal Neurons Reveals Three Distinct Components Encoded by Kv4.2, Kv4.3, and Kv1.4 α-Subunits." The Journal of Neuroscience **30**(14): 5092-5101.
Nosyreva, E. D. and K. M. Huber (2006). "Metabotropic Receptor-Dependent Long-Term Depression Persists in the Absence of Protein Synthesis in the Mouse Model of Fragile X Syndrome." Journal of Neurophysiology **95**(5): 3291-3295.
O'Donnell, W. T. and S. T. Warren (2002). "A decade of molecular studies of fragile X syndrome." Annu Rev Neurosci **25**: 315-338.
O'Donnell, W. T. and S. T. Warren (2002). "A decade of moleular studies of Fragile X syndrome." Annual Review of Neuroscience **25**(1): 315-338.
Okun, M., A. Naim, et al. (2010). "The subthreshold relation between cortical local field potential and neuronal firing unveiled by intracellular recordings in awake rats." J Neurosci **30**(12): 4440-4448.
Oliver, G., A. Mailhos, et al. (1995). "Six3, a murine homologue of the sine oculis gene, demarcates the most anterior border of the developing neural plate and is expressed during eye development." Development **121**(12): 4045-4055.
Olmos-Serrano, J. L., S. M. Paluszkiewicz, et al. (2010). "Defective GABAergic Neurotransmission and Pharmacological Rescue of Neuronal Hyperexcitability in the Amygdala in a Mouse Model of Fragile X Syndrome." The Journal of Neuroscience **30**(29): 9929-9938.
Orlando, L. R., R. Ayala, et al. (2009). "Phosphorylation of the homer-binding domain of group I metabotropic glutamate receptors by cyclin-dependent kinase 5." Journal of Neurochemistry **110**(2): 557-569.

Osterweil, E. K., D. D. Krueger, et al. (2010). "Hypersensitivity to mGluR5 and ERK1/2 Leads to Excessive Protein Synthesis in the Hippocampus of a Mouse Model of Fragile X Syndrome." The Journal of Neuroscience **30**(46): 15616-15627.

Osterweil, E. K., D. D. Krueger, et al. (2010). "Hypersensitivity to mGluR5 and ERK1/2 leads to excessive protein synthesis in the hippocampus of a mouse model of fragile X syndrome." J Neurosci **30**(46): 15616-15627.

Pan, F., G. M. Aldridge, et al. (2010). "Dendritic spine instability and insensitivity to modulation by sensory experience in a mouse model of fragile X syndrome." Proceedings of the National Academy of Sciences **107**(41): 17768-17773.

Paradee, W., H. E. Melikian, et al. (1999). "Fragile X mouse: strain effects of knockout phenotype and evidence suggesting deficient amygdala function." Neuroscience **94**(1): 185-192.

Park, S., J. M. Park, et al. (2008). "Elongation Factor 2 and Fragile X Mental Retardation Protein Control the Dynamic Translation of Arc/Arg3.1 Essential for mGluR-LTD." Neuron **59**(1): 70-83.

Peier, A. M., K. L. McIlwain, et al. (2000). "(Over)correction of FMR1 deficiency with YAC transgenics: behavioral and physical features." Human Molecular Genetics **9**(8): 1145-1159.

Pfeiffer, B. E. and K. M. Huber (2007). "Fragile X Mental Retardation Protein Induces Synapse Loss through Acute Postsynaptic Translational Regulation." The Journal of Neuroscience **27**(12): 3120-3130.

Pfeiffer, B. E. and K. M. Huber (2009). "The state of synapses in fragile X syndrome." Neuroscientist **15**(5): 549-567.

Pfeiffer, B. E., T. Zang, et al. (2010). "Fragile X Mental Retardation Protein Is Required for Synapse Elimination by the Activity-Dependent Transcription Factor MEF2." Neuron **66**(2): 191-197.

Pieretti, M., F. Zhang, et al. (1991). "Absence of expression of the FMR-1 gene in fragile X syndrome." Cell **66**(4): 817-822.

Poulet, J. F. A. and C. C. H. Petersen (2008). "Internal brain state regulates membrane potential synchrony in barrel cortex of behaving mice." Nature **454**(7206): 881-885.

Price, T. J., M. H. Rashid, et al. (2007). "Decreased Nociceptive Sensitization in Mice Lacking the Fragile X Mental Retardation Protein: Role of mGluR1/5 and mTOR." The Journal of Neuroscience **27**(51): 13958-13967.

Proud, C. G. (2007). "Signalling to translation: how signal transduction pathways control the protein synthetic machinery." Biochem J **403**(2): 18.

Qiu, L.-F., T.-J. Lu, et al. (2009). "Limbic Epileptogenesis in a Mouse Model of Fragile X Syndrome." Cerebral Cortex **19**(7): 1504-1514.

Repicky, S. and K. Broadie (2009). "Metabotropic Glutamate Receptor-Mediated Use-Dependent Down-Regulation of Synaptic Excitability Involves the Fragile X Mental Retardation Protein." J Neurophysiol **101**(2): 672-687.

Rigas, P. and M. A. Castro-Alamancos (2007). "Thalamocortical Up states: differential effects of intrinsic and extrinsic cortical inputs on persistent activity." J Neurosci **27**(16): 4261-4272.

Rigas, P. and M. A. Castro-Alamancos (2009). "Impact of Persistent Cortical Activity (Up States) on Intracortical and Thalamocortical Synaptic Inputs." Journal of Neurophysiology **102**(1): 119-131.

Rinaldi, T., C. Perrodin, et al. (2008). "Hyper-connectivity and hyper-plasticity in the medial prefrontal cortex in the valproic acid animal model of autism." Frontiers in Neural Circuits **2**.

Robinson, R. B. and S. A. Siegelbaum (2003). "Hyperpolarization-activated cation currents: From Molecules to Physiological Function." Annual Review of Physiology **65**(1): 453-480.

Rogers, S. J., S. Hepburn, et al. (2003). "Parent Reports of Sensory Symptoms in Toddlers with Autism and Those with Other Developmental Disorders." Journal of Autism and Developmental Disorders **33**(6): 631-642.

Rojas, D. C., T. L. Benkers, et al. (2001). "Auditory evoked magnetic fields in adults with fragile X syndrome." Neuroreport **12**(11): 2573-2576.

Ronesi, J. A., K. A. Collins, et al. (2012). "Disrupted Homer scaffolds mediate abnormal mGluR5 function in a mouse model of fragile X syndrome." Nat Neurosci.

Ronesi, J. A. and K. M. Huber (2008). "Homer Interactions Are Necessary for Metabotropic Glutamate Receptor-Induced Long-Term Depression and Translational Activation." J. Neurosci. **28**(2): 543-547.

Ronesi, J. A. and K. M. Huber (2008). "Metabotropic Glutamate Receptors and Fragile X Mental Retardation Protein: Partners in Translational Regulation at the Synapse." Sci. Signal. **1**(5): pe6-.

Roš, H., R. N. S. Sachdev, et al. (2009). "Neocortical Networks Entrain Neuronal Circuits in Cerebellar Cortex." The Journal of Neuroscience **29**(33): 10309-10320.

Roselli, F., P. Hutzler, et al. (2009). "Disassembly of Shank and Homer Synaptic Clusters Is Driven by Soluble Î²-Amyloid₁₋₄₀ through Divergent NMDAR-Dependent Signalling Pathways." PLoS ONE **4**(6): e6011.

Rubenstein, J. L. and M. M. Merzenich (2003). "Model of autism: increased ratio of excitation/inhibition in key neural systems." Genes Brain Behav **2**(5): 255-267.

Rubenstein, J. L. R. and M. M. Merzenich (2003). "Model of autism: increased ratio of excitation/inhibition in key neural systems." Genes, Brain and Behavior **2**(5): 255-267.
Sabaratnam, M., P. G. Vroegop, et al. (2001). "Epilepsy and EEG findings in 18 males with fragile X syndrome." Seizure : the journal of the British Epilepsy Association **10**(1): 60-63.
Sakagami, Y., K. Yamamoto, et al. (2005). "Essential roles of Homer-1a in homeostatic regulation of pyramidal cell excitability: a possible link to clinical benefits of electroconvulsive shock." European Journal of Neuroscience **21**(12): 3229-3239.
Sanchez-Vives, M. V., M. Mattia, et al. (2010). "Inhibitory modulation of cortical up states." J Neurophysiol **104**(3): 1314-1324.
Sanchez-Vives, M. V. and D. A. McCormick (2000). "Cellular and network mechanisms of rhythmic recurrent activity in neocortex." Nat Neurosci **3**(10): 1027-1034.
Sanchez-Vives, M. V. and D. A. McCormick (2000). "Cellular and network mechanisms of rhythmic recurrent activity in neocortex." Nat Neurosci **3**(10): 1027-1034.
Scheetz, A. J., A. C. Nairn, et al. (2000). "NMDA receptor-mediated control of protein synthesis at developing synapses." Nat Neurosci **3**(3): 6.
Schroeder, C. E. and P. Lakatos (2009). "Low-frequency neuronal oscillations as instruments of sensory selection." Trends in Neurosciences **32**(1): 9-18.
Segal, M. and P. Andersen (2000). "Dendritic spines shaped by synaptic activity." Current Opinion in Neurobiology **10**(5): 582-586.
Sejnowski, T. J. and O. Paulsen (2006). "Network Oscillations: Emerging Computational Principles." The Journal of Neuroscience **26**(6): 1673-1676.
Serôdio, P. and B. Rudy (1998). "Differential Expression of Kv4 K+ Channel Subunits Mediating Subthreshold Transient K+ (A-Type) Currents in Rat Brain." Journal of Neurophysiology **79**(2): 1081-1091.
Sharma, A., C. A. Hoeffer, et al. (2010). "Dysregulation of mTOR Signaling in Fragile X Syndrome." The Journal of Neuroscience **30**(2): 694-702.
Shiraishi-Yamaguchi, Y. and T. Furuichi (2007). "The Homer family proteins." Genome Biology **8**(2): 206.
Shu, Y., A. Hasenstaub, et al. (2003). "Turning on and off recurrent balanced cortical activity." Nature **423**(6937): 288-293.
Siomi, H., M. Choi, et al. (1994). "Essential role for KH domains in RNA binding: Impaired RNA binding by a mutation in the KH domain of FMR1 that causes fragile X syndrome." Cell **77**(1): 33-39.

Sokol, D. K., Demao Chen, et al. (2006). "High Levels of Alzheimer Beta-Amyloid Precursor Protein (APP) in Children With Severely Autistic Behavior and Aggression." Journal of Child Neurology **21**(6): 444-449.
Sourdet, V., M. Russier, et al. (2003). "Long-Term Enhancement of Neuronal Excitability and Temporal Fidelity Mediated by Metabotropic Glutamate Receptor Subtype 5." The Journal of Neuroscience **23**(32): 10238-10248.
Spencer, C. M., O. Alekseyenko, et al. (2005). "Altered anxiety-related and social behaviors in the Fmr1 knockout mouse model of fragile X syndrome." Genes Brain Behav **4**(7): 420-430.
Spencer, C. M., E. Serysheva, et al. (2006). "Exaggerated behavioral phenotypes in Fmr1/Fxr2 double knockout mice reveal a functional genetic interaction between Fragile X-related proteins." Hum Mol Genet **15**(12): 1984-1994.
Steriade, M. (1997). "Synchronized activities of coupled oscillators in the cerebral cortex and thalamus at different levels of vigilance." Cereb Cortex **7**(6): 583-604.
Steriade, M. (2006). "Grouping of brain rhythms in corticothalamic systems." Neuroscience **137**(4): 1087-1106.
Steriade, M., D. A. McCormick, et al. (1993). "Thalamocortical oscillations in the sleeping and aroused brain." Science **262**(5134): 679-685.
Steriade, M., A. Nunez, et al. (1993). "Intracellular analysis of relations between the slow (< 1 Hz) neocortical oscillation and other sleep rhythms of the electroencephalogram." J Neurosci **13**(8): 3266-3283.
Steriade, M., A. Nunez, et al. (1993). "A novel slow (< 1 Hz) oscillation of neocortical neurons in vivo: depolarizing and hyperpolarizing components." J Neurosci **13**(8): 3252-3265.
Steriade, M., A. Nunez, et al. (1993). "A novel slow (< 1 Hz) oscillation of neocortical neurons in vivo: depolarizing and hyperpolarizing components." J. Neurosci. **13**(8): 3252-3265.
Steriade, M., I. Timofeev, et al. (2001). "Natural waking and sleep states: a view from inside neocortical neurons." J Neurophysiol **85**(5): 1969-1985.
Stevens, H. E., K. M. Smith, et al. (2010). "Fgfr2 is required for the development of the medial prefrontal cortex and its connections with limbic circuits." J Neurosci **30**(16): 5590-5602.
Strauss, U., M. H. P. Kole, et al. (2004). "An impaired neocortical Ih is associated with enhanced excitability and absence epilepsy." European Journal of Neuroscience **19**(11): 3048-3058.
Strumbos, J. G., M. R. Brown, et al. (2010). "Fragile X Mental Retardation Protein Is Required for Rapid Experience-Dependent Regulation of the Potassium Channel Kv3.1b." The Journal of Neuroscience **30**(31): 10263-10271.

Strumbos, J. G., M. R. Brown, et al. (2010). "Fragile X mental retardation protein is required for rapid experience-dependent regulation of the potassium channel Kv3.1b." J Neurosci **30**(31): 10263-10271.
Sutcliffe, J. S., D. L. Nelson, et al. (1992). "DNA methylation represses FMR-1 transcription in fragile X syndrome." Human Molecular Genetics **1**(6): 397-400.
Taylor, G. W., L. R. Merlin, et al. (1995). "Synchronized oscillations in hippocampal CA3 neurons induced by metabotropic glutamate receptor activation." J Neurosci **15**(12): 8039-8052.
Tessier, C. R. and K. Broadie (2009). "Activity-dependent modulation of neural circuit synaptic connectivity." Frontiers in Molecular Neuroscience **2**.
Testa-Silva, G., A. Loebel, et al. (2011). "Hyperconnectivity and Slow Synapses during Early Development of Medial Prefrontal Cortex in a Mouse Model for Mental Retardation and Autism." Cerebral Cortex.
Thomas, A., N. Bui, et al. (2012). "Group I metabotropic glutamate receptor antagonists alter select behaviors in a mouse model for fragile X syndrome." Psychopharmacology **219**(1): 47-58.
Thomas, A. M., N. Bui, et al. (2011). "Genetic reduction of group 1 metabotropic glutamate receptors alters select behaviors in a mouse model for fragile X syndrome." Behavioural Brain Research **223**(2): 310-321.
Timofeev, I., F. Grenier, et al. (2000). "Origin of Slow Cortical Oscillations in Deafferented Cortical Slabs." Cerebral Cortex **10**(12): 1185-1199.
Timofeev, I., F. Grenier, et al. (2001). "Disfacilitation and active inhibition in the neocortex during the natural sleep-wake cycle: an intracellular study." Proc Natl Acad Sci U S A **98**(4): 1924-1929.
Todd, A. K., M. Johnston, et al. (2005). "Highly prevalent putative quadruplex sequence motifs in human DNA." Nucleic Acids Research **33**(9): 2901-2907.
Tsaur, M.-L., M. Sheng, et al. (1992). "Differential expression of K+ channel mRNAs in the rat brain and down-regulation in the hippocampus following seizures." Neuron **8**(6): 1055-1067.
Tu, J. C., B. Xiao, et al. (1998). "Homer Binds a Novel Proline-Rich Motif and Links Group 1 Metabotropic Glutamate Receptors with IP3 Receptors." Neuron **21**(4): 717-726.
Uhlhaas, P. J. and W. Singer (2006). "Neural Synchrony in Brain Disorders: Relevance for Cognitive Dysfunctions and Pathophysiology." Neuron **52**(1): 155-168.
Van Dam, D., R. D'Hooge, et al. (2000). "Spatial learning, contextual fear conditioning and conditioned emotional response in Fmr1 knockout mice." Behavioural Brain Research **117**(1–2): 127-136.

Veeraragavan, S., N. Bui, et al. (2011). "The modulation of fragile X behaviors by the muscarinic M4 antagonist, tropicamide." Behavioral Neuroscience;Behavioral Neuroscience **125**(5): 783-790.
Verkerk, A. J., M. Pieretti, et al. (1991). "Identification of a gene (FMR-1) containing a CGG repeat coincident with a breakpoint cluster region exhibiting length variation in fragile X syndrome." Cell **65**(5): 905-914.
Volgushev, M., S. Chauvette, et al. (2006). "Precise Long-Range Synchronization of Activity and Silence in Neocortical Neurons during Slow-Wave Sleep." The Journal of Neuroscience **26**(21): 5665-5672.
Waung, M. W., B. E. Pfeiffer, et al. (2008). "Rapid Translation of Arc/Arg3.1 Selectively Mediates mGluR-Dependent LTD through Persistent Increases in AMPAR Endocytosis Rate." Neuron **59**(1): 84-97.
Weiler, I. J., S. A. Irwin, et al. (1997). "Fragile X mental retardation protein is translated near synapses in response to neurotransmitter activation." Proceedings of the National Academy of Sciences **94**(10): 5395-5400.
Westmark, C. J. and J. S. Malter (2007). "FMRP Mediates mGluR₅-Dependent Translation of Amyloid Precursor Protein." PLoS Biol **5**(3): e52.
Westmark, C. J., P. R. Westmark, et al. (2009). "MPEP reduces seizure severity in Fmr-1 KO mice overexpressing human Abeta." Int J Clin Exp Pathol **3**(1): 56-68.
Westmark, C. J., P. R. Westmark, et al. (2011). "Reversal of Fragile X Phenotypes by Manipulation of AβPP/Aβ Levels in <italic>Fmr1^{KO}</italic> Mice." PLoS ONE **6**(10): e26549.
Wood, L., N. W. Gray, et al. (2009). "Synaptic Circuit Abnormalities of Motor-Frontal Layer 2/3 Pyramidal Neurons in an RNA Interference Model of Methyl-CpG-Binding Protein 2 Deficiency." The Journal of Neuroscience **29**(40): 12440-12448.
Xiao, B., J. C. Tu, et al. (1998). "Homer Regulates the Association of Group 1 Metabotropic Glutamate Receptors with Multivalent Complexes of Homer-Related, Synaptic Proteins." Neuron **21**(4): 707-716.
Yan, Q. J., M. Rammal, et al. (2005). "Suppression of two major Fragile X Syndrome mouse model phenotypes by the mGluR5 antagonist MPEP." Neuropharmacology **49**(7): 1053-1066.
Yang, B., R. Desai, et al. (2007). "Slack and Slick KNa Channels Regulate the Accuracy of Timing of Auditory Neurons." The Journal of Neuroscience **27**(10): 2617-2627.
Yizhar, O., L. E. Fenno, et al. (2011). "Neocortical excitation/inhibition balance in information processing and social dysfunction." Nature **477**(7363): 7.
Yoshida, M., E. Fransen, et al. (2008). "mGluR-dependent persistent firing in entorhinal cortex layer III neurons." Eur J Neurosci **28**(6): 1116-1126.

Yoshida, M., E. Fransén, et al. (2008). "mGluR-dependent persistent firing in entorhinal cortex layer III neurons." European Journal of Neuroscience **28**(6): 1116-1126.

Young, S. R., S. C. Chuang, et al. (2004). "Modulation of afterpotentials and firing pattern in guinea pig CA3 neurones by group I metabotropic glutamate receptors." J Physiol **554**(Pt 2): 371-385.

Yuan, J. P., K. Kiselyov, et al. (2003). "Homer Binds TRPC Family Channels and Is Required for Gating of TRPC1 by IP3 Receptors " Cell **114**(6): 777-789.

Zalfa, F., M. Giorgi, et al. (2003). "The Fragile X Syndrome Protein FMRP Associates with BC1 RNA and Regulates the Translation of Specific mRNAs at Synapses." Cell **112**(3): 317-327.

Zhang, J., Z. Fang, et al. (2008). "Fragile X-related proteins regulate mammalian circadian behavioral rhythms." Am J Hum Genet **83**(1): 43-52.

Zhang, Z. and P. Seguela (2010). "Metabotropic Induction of Persistent Activity in Layers II/III of Anterior Cingulate Cortex." Cerebral Cortex **20**(12): 2948-2957.

Zhang, Z. and P. Seguela (2010). "Metabotropic Induction of Persistent Activity in Layers II/III of Anterior Cingulate Cortex." Cereb Cortex.

Zhao, M.-G., H. Toyoda, et al. (2005). "Deficits in Trace Fear Memory and Long-Term Potentiation in a Mouse Model for Fragile X Syndrome." The Journal of Neuroscience **25**(32): 7385-7392.